Single amino acid substitutions in lipase A affect its production and secretion by *Bacillus subtilis*

Inaugural-Dissertation

zur Erlangung des Doktorgrades
der Mathematisch-Naturwissenschaftlichen Fakultät
der Heinrich-Heine-Universität Düsseldorf

vorgelegt von

Pia Skoczinski

aus Dormagen

Düsseldorf, August 2016

aus dem Institut für Molekulare Enzymtechnologie

der Heinrich-Heine-Universität Düsseldorf

Gedruckt mit der Genehmigung der

Mathematisch-Naturwissenschaftlichen Fakultät der

Heinrich-Heine-Universität Düsseldorf

Referent: Prof. Dr. Karl-Erich Jaeger
Korreferent: Prof. Dr. Holger Gohlke

Tag der mündlichen Prüfung: 07.11.2016

Erklärung

Hiermit versichere ich, dass ich die vorgelegte Dissertation selbstständig verfasst habe und keine anderen als die angegebenen Quellen, Darstellungen und Hilfsmittel benutzt wurden. Alle Textstellen, die sinngemäß anderen Werken oder sonstigen Quellen entnommen worden sind, sind jeweils unter genauer Angabe der Quelle als Entlehnung gekennzeichnet.

Die Dissertation wurde in der vorgelegten oder ähnlicher Form noch bei keiner anderen Institution eingereicht. Ich habe bisher keine erfolglosen Promotionsversuche unternommen.

Düsseldorf, den

Pia Skoczinski

Danksagung

Hiermit möchte ich mich recht herzlich bei all denjenigen bedanken, die mich in den letzten Jahren unterstützt und zur Entstehung dieser Arbeit beigetragen haben.

Zunächst gilt besonderer Dank Herrn Prof. Karl-Erich Jaeger, der mir meine Promotion am Institut für Molekulare Enzymtechnologie ermöglicht und mir dieses äußerst interessante Projekt überlassen hat. Vielen Dank für stetige Anregungen und hilfreiche, konstruktive Diskussionen.

Herrn Prof. Dr. Holger Gohlke danke ich ebenfalls für hilfreiche Anregungen und für die freundliche Übernahme des Korreferats.

Danke an das *CLIB-Graduate Cluster Industrial Biotechnology* für das Promotionsstipendium. Vielen Dank an Frau Dr. Sonja zu Meyer-Berstenhorst, Frau Dr. Jessica Hilbig, Frau Dr. Jennifer Pahlke und Frau Dr. Martina Holz für die hervorragende Koordination und die ständige Hilfsbereitschaft.

Meinen Lipase-Kooperationspartnerinnen, im Rahmen des *CLIB-Graduate Cluster Industrial Biotechnology,* Anuseema Bhadauriya (CPCLAB, Heinrich-Heine-Universität Düsseldorf) und Marianne Schulte (ICS-6, FZ Jülich) danke ich für die konstruktive und angenehme Zusammenarbeit.

Ebenfalls möchte ich mich bei Frau Dr. Susanne Wilhelm für die andauernde Hilfsbereitschaft bedanken.

Vielen Dank an alle Mitarbeiter des Instituts für Molekulare Enzymtechnologie für das hervorragende Arbeitsklima welches stets durch Freundlichkeit und Hilfsbereitschaft geprägt war.

Danke an die Mitarbeiter der AG *Bacterial Enzymology* unter der Leitung von Dr. Filip Kovacic und der AG *Bacterial Cell Factories* unter der Leitung von Dr. Andreas Knapp. Insbesondere bedanke ich mich bei Florian Bleffert, Peter Dollinger, Dr. Stephan Thies und Alexander Bollinger für die hilfreichen wissenschaftlichen Diskussionen und die freundschaftliche Unterstützung während meiner Promotion.

Bei unserer ehemaligen Laborantin Martina Paul und meiner ehemaligen Praktikantin Swetlana Davydov bedanke ich mich für die tolle experimentelle Unterstützung.

Großer Dank geht an meine ehemalige Masterstudentin Kristina Volkenborn für ihre großartige Hilfe bei den Signalpeptid-*Screenings* und Mutagenesen.

Ganz besonders bedanke ich mich bei Dr. Alexander Fulton und Dr. Andreas Knapp.

Danke Alex für deine jahrelange Unterstützung, unermüdliche Geduld und deine andauernde Diskussionsbereitschaft (obwohl das nicht immer ganz einfach für dich war), du warst ein toller Lehrer.

Auch dir Andreas danke ich für deine Unterstützung und die unzähligen konstruktiven Diskussionen die wir fast täglich seit sechs Jahren führen, wir haben Ideen entwickelt, herumgesponnen, manche waren genial andere weniger, aber wir haben immer was gelernt, es lebe das Tag-Team.

Vielen, vielen Dank an meine Familie und an meine Freunde. Danke Mama, danke Papa, danke Flo, danke Myri, danke Jenny, danke Lisa, ohne euch hätte ich das nicht geschafft und wäre nicht da wo ich heute bin. Ihr seid die Besten, ich liebe euch.

Veröffentlichungen im Rahmen der Promotion

Publikationen

Skoczinski P., Volkenborn K., Fulton A., Knapp A. and Jaeger K.-E. Single amino acid substitutions affect homologous production and secretion of lipase A by *Bacillus subtilis* (in preparation).

Fulton A., Frauenkron-Machedjou J., Skoczinski P., Wilhelm S., Zhu L., Schwaneberg U. and Jaeger K.-E. (2015). Exploring the protein stability landscape: *Bacillus subtilis* lipase A as a model for detergent resistance. *ChemBioChem*. 16: 930-936.

Poster

Huesgen K., Ripphahn M., Davydov S., Skoczinski P., Knapp A. and Jaeger K.-E. Production and secretion of enzymes for biomass breakdown by *Bacillus subtilis* (2016). BACELL, Paris, Frankreich.

Skoczinski P., Huesgen K., Knapp A., Fulton A. and Jaeger K.-E. Is there a perfect match? Systematic analysis of signal peptide – enzyme combinations for efficient secretion of lipase A from *Bacillus subtilis* (2015). 8th International Conference on Gram-Positive Microorganisms, Montecatini Terme, Italien.

Skoczinski P., Huesgen K., Fulton A., Knapp A., Funken H. and Jaeger K.-E. Systematic mutational analysis of lipase secretion in *Bacillus subtilis* (2014). Jahrestagung der Vereinigung für Allgemeine und Angewandte Mikrobiologie (VAAM), Dresden.

Vorträge

Skoczinski P., Huesgen K., Knapp A., Fulton A. and Jaeger K.-E. Single amino acid substitutions affect production and secretion of lipase by *Bacillus subtilis* (2016). BACELL, Paris, Frankreich.

Skoczinski P., Huesgen K., Knapp A., Fulton A., Funken H. and Jaeger K.-E. Systematic mutational analysis of lipase secretion in *Bacillus subtilis* (2014). 5th annual CLIB-GC/iGRASPseed symposium “From Gene to Protein and Beyond”, Düsseldorf.

Content

List of Figures

List of Tables

Abbreviations

A. dest	Aqua destillata; destilled water
Amp	Ampicillin
APS	Ammonium persulfate
ATP	Adenosine triphosphate
bp	Base pair
BSA	Bovine serum albumin
CEC	Cation Exchange Chromatography
C-terminus	Carboxy terminus
°C	Degree Celsius
DMSO	Dimethylsulfoxide
DNA	Deoxyribonucleic acid
DNAse	Deoxyribonuclease
dNTP	Deoxyribonucleosidetriposphate
EC	Enzyme commission number
EDTA	Ethylendiamintetraacetic acid
ELISA	Enzyme linked immunosorbent assay
EtBr	Ethidium bromide
EtOH	Ethanol
ev	Empty vector
Fig.	Figure
fw	Forward
g	Gram
g	Gravitational acceleration
h	Hour
HIC	Hydrophobic Interaction Chromatography
His-tag	A repetitive sequence of six histidine residues
kb	Kilobases
IPTG	Isopropyl β-D-1-thiogalactopyranoside
kDa	Kilodalton
Km	Kanamycin
l	Liter
LB	Lysogeny Broth
Lip	Lipase
LipA	*B. subtilis* lipase A
M	Molarity (mol/l)
m	Milli
µ	Micro
min	Minutes
mRNA	Messenger RNA
MTP	Microtiterplate
n	Nano
NaDoc	Sodium deoxycholate
nm	Nanometer
N-terminus	Amino terminus
NTA	Nitrilotriacetic acid
O.D.	Optical density
PAGE	Polyacrylamide gel electrophoresis
PBS	Phosphate buffered saline
PDB	Protein Data Base
PCR	Polymerase chain reaction
P_{HpaII}	Constitutive promoter
*p*NPP	*para*-Nitrophenyl palmitate
PVDF	Polyvinylidine fluoride
RT-qPCR	quantitative real time PCR
rev	Reverse
rpm	Rounds per minute
RNA	Ribonucleic acid
RT	Room temperature
S	Supernatant
SDM	Site directed mutagenesis
SDS	Sodium dodecyl sulfate
SP	Signal peptide
SSM	Site saturation mutagenesis
SRP	Signal recognition particle
Tab.	Table
Tat	Twin arginine translocation
TBS	Tris buffered saline
TEMED	Tetramethylethylenediamine
TCA	Trichloracetic acid
U	Units
UniProt	Universal Protein Resource
v/v	Volume per volume
w/v	Weight per volume
WC	Whole cells

1. Introduction

1.1. Microbial enzymes in industrial applications

Industrial production processes for the generation of chemicals and pharmaceuticals often include chemical product synthesis, as for example the total synthesis of acetylsalicylic acid, well known as Aspirin® (Markenregister DE 36433). Such chemical syntheses are often performed under harsh conditions as high temperature, low pH and high pressure, also these syntheses result in low catalytic efficiency and lack enantiomeric specificity for synthesis of chiral molecules (Adrio & Demain, 2014). These disadvantages have been overcome with the use of microbial enzymes, which function as so called biocatalysts. Biocatalysts allow reaction performance with less energy and increased velocity. The enzyme-substrate complex can form the metastable transition state decreasing the activation energy. For industrial processes this means, certain biochemical or biological reactions can be outperformed more effectively towards conventional chemical methods regarding stereo- and regioselectivity of the reaction. Furthermore, biocatalysts have the advantage to act under mild reaction conditions and do not need functional group protection of substrates resulting in cost reduction, cutting down waste disposal and energy costs (Adrio & Demain, 2014; Gong *et al.*, 2012).

Therefore microbial enzymes are currently widely used in several industrial applications with leading use in food industry, animal feed stuff industry and in production of washing agents (Maurer *et al.*, 2013). The most abundant enzyme classes in these fields are proteases, amylases and lipases (Maurer *et al.*, 2013). The possibility to select and genetically optimize enzymes specifically regarding the desired properties (Cheng & Schwaneberg, 2015; Porter *et al.*, 2016), as well as the use of whole cell biotransformations (Bräutigam *et al.*, 2007; Li *et al.*, 2014) lead to the upcoming of about 150 industrial processes including microbial enzymes or microbial whole cell biocatalysts (Adrio & Demain, 2014).

To comply the demand of microbial enzymes for these various applications several bacteria have been established as so called microbial cell factories, not only for new protein or enzyme identification (Murphy, 2012) but also for homologous and heterologous enzyme production (Westers *et al.*, 2004b). Besides the well-established *Escherichia coli*, as a Gram-negative host for high level heterologous gene expression and protein production, the

Gram-positive soil bacterium *Bacillus subtilis* has become an attractive alternative cell factory. In addition to that, *B. subtilis* provides a well-established and characterized lipase LipA that is commonly used as a model lipase for engineering of this industrial relevant class of biocatalysts (see 1.5 for details).

1.2. Classification and definition of lipases

The enzyme class of hydrolases (EC 3) comprises enzymes cleaving covalent bonds by consumption of water. Enzymes of the carboxylester hydrolases subgroup (EC 3.1.1) specifically act on carboxylesters and include esterases (EC 3.1.1.1) as well as lipases (EC 3.1.1.3) which are both able to hydrolyze and transesterify ester bonds. Here, lipases also named triacylglycerol hydrolases are known to act on lipids which means they catalyze the hydrolysis and synthesis of esters formed from glycerol and long-chain fatty acids (Fig. 1.1) (Ali *et al.*, 2012; Jaeger & Reetz, 1998).

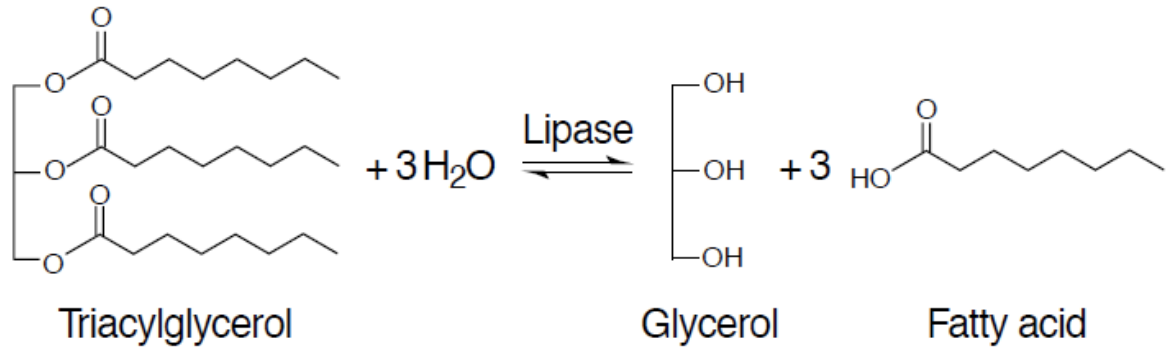

Fig. 1.1 Hydrolysis and synthesis of triacylglycerol.
(Jaeger & Reetz, 1998) A triacylglycerol can be hydrolyzed into glycerol and long chain fatty acids or synthesized from these compounds.

Due to the increasing number of newly identified and isolated carboxyl hydrolases, a further classification based on the nucleotide and amino acid sequence similarities as well as 3D structures was established (Arpigny & Jaeger, 1999). This way, eight families of carboxylester hydrolases, also referred to as lipolytic enzymes, were differentiated, with family I, the family of „true lipases“, representing the largest cluster of categorized lipases with six subfamilies (Arpigny & Jaeger, 1999).

Originally, lipases were defined based on their activation at the lipid-water interface. This interfacial activation describes the enzyme activation after exceeding the critical micelle concentration of the substrate in solution. This indicates that lipases do not follow the

classical Michaelis-Menten kinetics and prefer the hydrolysis of hydrophobic lipids (Eggert, 2001; Jaeger & Reetz, 1998). With the elucidation of the first 3D structure of the human pancreas lipase (Winkler *et al.*, 1990) and the lipase of *Rhizomucor miehei* (Brady *et al.*, 1990) the process of interfacial activation was explained by reorientation of the amphiphilic lid structure, which covers the active site of the lipase, at the lipid-water interface (Brzozowski *et al.*, 1991). This definition based on interfacial activation is not true for all lipases, as for example the cutinase of *Fusarium solani pisi* and the here studied lipase LipA of *Bacillus subtilis.* These two neither show activation at the lipid-water interface nor carry a lid-structure covering the catalytic triad in aqueous solution (Lesuisse *et al.*, 1993; van Pouderoyen *et al.*, 2001) Also the lipases from *Burkholderia glumae* and *Pseudomonas aeruginosa* are exceptions, indeed carrying a lid structure but not following interfacial activation (Jaeger *et al.*, 1993; Noble *et al.*, 1993). This inconsistence leads to a revised lipase definition independent from interfacial activation and the presence of a lid-structure, but based on the fatty acid-chain length of the triacyglyceride. Today, lipases are defined as carboxylester hydrolases, which in contrast to esterases are able to hydrolyze hydrophobic triacylglycerides with more than nine carbon atoms (Funke, 2005; Verger, 1997).

1.3. Structure and catalytical mechanism of lipases

The resolution of the three dimensional structure of lipases (Brady *et al.*, 1990; Pauwels *et al.*, 2006; Winkler *et al.*, 1990) revealed the existence of a characteristic common folding pattern, the α/β-hydrolase fold (Fig. 1.2) (Ollis *et al.*, 1992). The core in this folding pattern consists of a central β-sheet region out of eight single β-sheets (β1-β8) (Fig. 1.2). This β-sheet core is surrounded by six α- helices (αA-αF) (Fig. 1.2). Lipases are structurally similar to serine proteases and also show similarities in the active site. This consists of the polar serine, aspartic or glutamic acid and the positively charged histidine. The nucleophilic serine is located at the C-terminal end of β-sheet β5 in a highly conserved pentapeptide, G-X-S-X-G (Ollis *et al.*, 1992) (Fig. 1.2). This lipase consensus motif forms a characteristic β-turn-α-motif, the nucleophilic elbow. This γ-turn called structure exhibits energetically unfavored torsion angles in the peptide backbone, leading to an exposed position of the catalytic serine (Jaeger & Reetz, 1998). Here, it can be charged and is able to interact with the substrate (Jaeger & Reetz, 1998; Ollis *et al.*, 1992). The catalytic active acid and histidine are located in

the turn structures at the C-terminus of the β-sheets β7 and β8. As mentioned above, some lipases exhibit an α-helical structure that covers the catalytic triad like a lid (Brady *et al.*, 1990; Pauwels *et al.*, 2006; Winkler *et al.*, 1990).

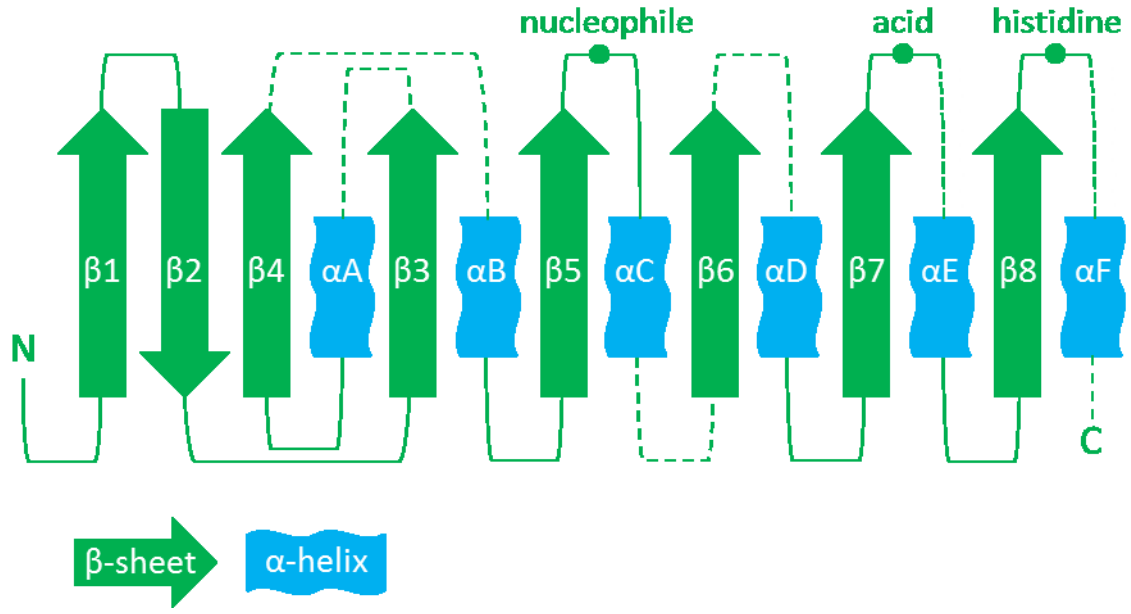

Fig. 1.2 Secondary structure topology of the canonical α/β-hydrolase fold.
Modified according to (Van Pouderoyen *et al.*, 2001). The canonical α/β-hydrolase fold consists of eight β-sheets (green arrows) and six α-helices (blue banners).

Substrate binding induces a conformational change of the lipase and leads to a reorientation of the lid (Cambillau & Tilbeurgh, 1993). This way, the active site is exposed and able to bind and hydrolyze the substrate (Cambillau & Tilbeurgh, 1993). The structural similarity of lipases and serine proteases also indicates a similar mechanism of substrate hydrolysis that was proven by structural analyses (Nardini & Dijkstra, 1999). The two-step lipase hydrolysis mechanism is shown in Fig. 1.3. The mechanism starts with the formation of the acyl-enzyme complex by a nucleophilic attack of the activated serine on the carbonyl C-atom of the substrate ester bond (Fig. 1.3A). The catalytic active serine is activated by the hydrophilic histidine abstracting a proton. The emerging positively charge of the histidine is compensated by the negatively charged acid that is also responsible for the suitable arrangement of the histidine ring structure. This way the substrate ester is covalently bound to the serine and a tetrahedral intermediate is formed (Fig. 1.3B). In this transition state, the negatively charged carbonyl oxygen is stabilized by the amino groups of the peptide backbone forming the oxyanion hole. This hole is formed by two amino groups of the peptide backbone of the residue following the catalytic active serine and a second residue at

the end of β-sheet β3 (Kazlauskas, 1994; Lang *et al.*, 1998; Schrag *et al.*, 1997). During the tetrahedral transition state, the proton of the histidine is transferred to the negatively charged oxygen atom of the substrate ester.

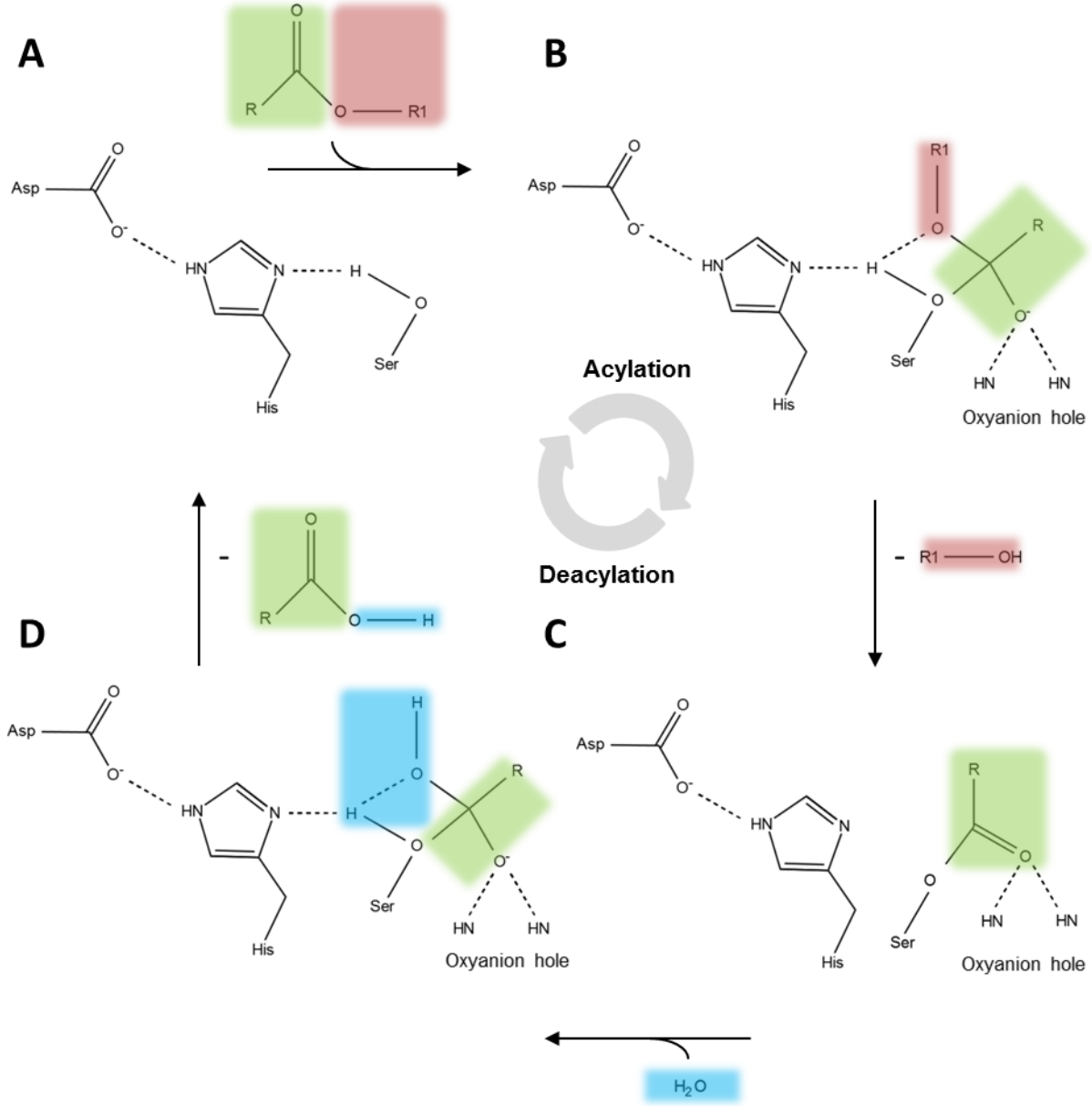

Fig. 1.3 Catalytic mechanism of substrate hydrolysis by lipases.
The amino acid residues of the catalytic triad aspartic acid (or glutamic acid), histidine, serine and the peptide backbone forming the oxyanion hole are illustrated. **A** Residues of the catalytic triad and the addition of the carbonyl ester. **B** The nucleophilic attack of the activated serine on the carbonyl atom of the ester bond leads to the formation of the tetrahedral transition state. This transition state is stabilized by hydrogen bonds with the amino groups of the oxyanion hole residues. **C** The covalently formed intermediate (acyl-enzyme complex) is formed where the fatty acid is bound to the active serine. **D** The second tetrahedral transition state is formed by the addition of water and a similar nucleophilic attack like for the acylation reaction, finally the fatty acid is released to regenerate the initial active form of the enzyme (Cambillau & Tilbeurgh, 1993; Kazlauskas, 1994; Lang *et al.*, 1998; Schrag *et al.*, 1997). R and R1: hydrocarbons. The different functional groups are colored for simplification: Free or bound alcohol group (red), fatty acid (green) and water molecule (blue).

So the alcohol of the substrate ester is released from the intermediate and the substrate acid is covalently bound to the catalytic active serine establishing the acyl-enzyme complex (Fig. 1.3C).

The second step of the reaction includes the regeneration of the enzyme by deacylation. Therefore, the catalytic active histidine abstracts a proton from a water molecule resulting in a hydroxide ion. This ion attacks the carbonyl atom of the covalently bound substrate leading to the formation of a second tetrahedral transition state, also stabilized by the oxyanion hole (Fig. 1.3D). The substrate is released by the transfer of a proton from the positively charged histidine to the negatively charged oxygen atom of the serine, this way regenerating the enzyme to its initial form and providing it for another substrate hydrolysis.

1.4. Lipolytic enzymes of *Bacillus subtilis*

Carboxylester hydrolases (EC 3.1.1), especially lipases (EC 3.1.1.3), have evolved as fundamental enzymes for several processes in industry (Treichel *et al.*, 2009). The demand for lipases with specific properties like stability and activity in organic solvents, ionic liquids or at high temperatures is still increasing (Bornscheuer *et al.*, 2002; Menoncin *et al.*, 2008). Therefore, several novel lipases of microbial origin, fulfilling these properties have been identified and characterized in different *Bacillus* and *Geobacillus* species (Tab. 1.1). Due to the classification based on the primary and tertiary structure similarities (Arpigny & Jaeger, 1999), carboxylester hydrolases from *Bacillus* sp. and *Geobacillus* sp. belong to subfamily 4 and 5 of superfamily I (Arpigny & Jaeger, 1999). These subfamilies show the largest number of relatively small lipases with the smallest characterized one in *Geobacillus thermocatenulatus* (Schmidt-Dannert *et al.*, 1994). Lipases from *Bacillus* and *Geobacillus* species have in common that the first glycine residue in the lipase consensus motif G-X-S-X-G (Ollis *et al.*, 1992) is replaced by an alanine (Tab. 1.1), resulting in a *Bacillus* lipase consensus motif A-H-S-M-G that is detected in all identified *Bacillus* carboxylester hydrolases so far (Tab. 1.1). The lipases from *Geobacillus* species show an additional substitution of the methionine in the A-H-S-M-G motif to glutamine (A-H-S-Q-G) (Tab. 1.1). Psychrophilic, mesophilic and thermophilic lipases were characterized and prefer neutral to alkaline milieu (pH 7-12) with most of them showing pH optima at alkaline pH (Tab. 1.1). All

identified lipases prefer substrates with short (C4) to mid-long (C12) fatty acid chains with a tendency to substrate with a chain length of about eight carbon atoms.

Tab. 1.1 Overview of characterized carboxylester hydrolases from *Bacillus* and *Geobacillus* species.
Modified according to (Eggert, 2001). The characterized carboxylester hydrolases are summarized according to the temperature classification. The organism, the name of the enzyme, the molecular weight, the measured pH and temperature optimum, as well as the substrate specificity mainly towards *p*-nitrophenyl ester (*p*NP) and triacylglycerides (TG) is shown. Also the lipase consensus motif is shown.

organism	enzyme	mol. weight (kDa)	pH optimum	temperature optimum (°C)	substrate specificity	consensus motif	reference
mesophilic lipases							
Bacillus subtilis	lipase A	19.3	10	35-40	*p*NP-C8 TG-C8	A-H-S-M-G	(Dartois *et al.*, 1992; Lesuisse *et al.*, 1993)
	lipase B	19.4	12	35-40	*p*NP-C8 TG-C8	A-H-S-M-G	(Eggert, 2001)
Bacillus pumilus	lipase	19.3	9-10	30	not detected	A-H-S-M-G	(Moeller *et al.*, 1995)
thermophilic lipases							
Bacillus sp. DR90	lipase	26.8	8	75	*p*NP-C4	A-H-S-M-G	(Asoodeh *et al.*, 2014)
Bacillus licheniformis	lipase	19.2	10-11	55	*p*NP-C6-C8	A-H-S-M-G	(Nthangeni *et al.*, 2001)
	esterase	81.3	8-8.5	55	*p*NP-C6-C8	A-H-S-M-G	(Alvarez-Macarie *et al.*, 1999)
psychrophilic lipases							
Bacillus pumilus ArcL5	lipase BpL5	19	9	20	*p*NP-C8	A-H-S-M-G	(Wi *et al.*, 2014)
thermophilic lipases from *Geobacillus* species							
Geobacillus thermo-catenulatus	BTL1	16	7-8	60-70	*p*NP-C10-C12	not detected	(Schmidt-Dannert *et al.*, 1994)
	BTL2	43	8-9	60-70	*p*NP-C10 TG-C4	A-H-S-Q-G	(Rúa *et al.*, 1998; Schmidt-Dannert *et al.*, 1994)
Geobacillus stearothermo-philus L1	lipase	43	9-10	60-65	*p*NP-C8 TG-C3,C12	A-H-S-Q-G	(Kim *et al.*, 2000; Lee *et al.*, 1999)
Geobacillus stearothermo-philus L2	lipase	43	9-10	60-65	*p*NP-C8 TG-C3,C12	A-H-S-Q-G	(Sinchaikul *et al.*, 2001)
Geobacillus thermo-leovorans	lipase	43	7-8	70-75	*p*NP-C6 TG-C8	A-H-S-Q-G	(Lee *et al.*, 1999)

Several of these lipases show properties interesting for their application in industrial processes like the organic solvent-tolerant lipase from *Bacillus* sp. DR90 (Asoodeh *et al.*, 2014) or the lipase BpL5 from an arctic *Bacillus pumilus* strain ArcL5 (Wi *et al.*, 2014). A mutant of this psychrophilic lipase shows an increased activity in the hydrolysis and synthesis of tricaprylin (Wi *et al.*, 2014), a common ingredient in cosmetic products. Nevertheless, the most established, best characterized and engineered lipase from *Bacillus* sp. with biotechnological relevance is the lipase A of *B. subtilis* (Dartois *et al.*, 1992; Eggert, 2001; Lesuisse *et al.*, 1993).

1.5. The model enzyme lipase LipA from *Bacillus subtilis*

The *Bacillus subtilis* lipase LipA, also known as BSLA (Fulton, 2014), with a molecular weight of 19.34 kDa and a length of 181 amino acids (UniProt: P37957) is one of the smallest known `true lipases` (Arpigny & Jaeger, 1999). The resolution of the X-ray crystal structure of LipA (PDB: 1I6W) (Fig. 1.4B) revealed a reduced α/β-hydrolase folding pattern, also known as a `minimal fold` for this class of enzymes (Fig. 1.4A) (Van Pouderoyen *et al.*, 2001). This means that the first two β-sheets β1 and β2, present in the canonical α/β-hydrolase fold (Fig. 1.2) are missing in those lipases, resulting in a β-sheet core region of six β-sheets (β3-β4) surrounded by six α-helices (Fig. 1.4A). Additionally, the α-helices αA, αC and αF are N- and/or C-terminally accompanied by additional 3_{10}-helices. The αE-helix consists of only four amino acids and the αD-helix is substituted by a small 3_{10}-helix (Fig. 1.4A). LipA does not carry a lid structure and shows a surface exposed catalytic triad consisting of the nucleophilic serine at position 77, the aspartic acid at position 133 and the positively charged histidine at position 156 (Van Pouderoyen *et al.*, 2001) (Fig. 1.4B). The catalytic serine is embedded in the lipase consensus motif A-H-S-M-G and located in the γ-turn between the β5-sheet and the αC-helix (Fig. 1.4A). The already mentioned oxyanion hole (1.3), necessary to stabilize the tetrahedral transition state during substrate hydrolysis is formed by the peptide backbone nitrogen atoms of the residues I12 and M78 (Eggert, 2001; van Pouderoyen *et al.*, 2001). Like several other `true lipases` of the lipase superfamily I (Arpigny & Jaeger, 1999), as for example the lipases from *Pseudomonas aeruginosa* (Nardini *et al.*, 2000) and *Burkholderia glumae* (Noble *et al.*, 1993), LipA does not follow the mechanism of interfacial activation at the lipid/water interface (Lesuisse *et al.*, 1993) but nevertheless differs from those in other fundamental characteristics.

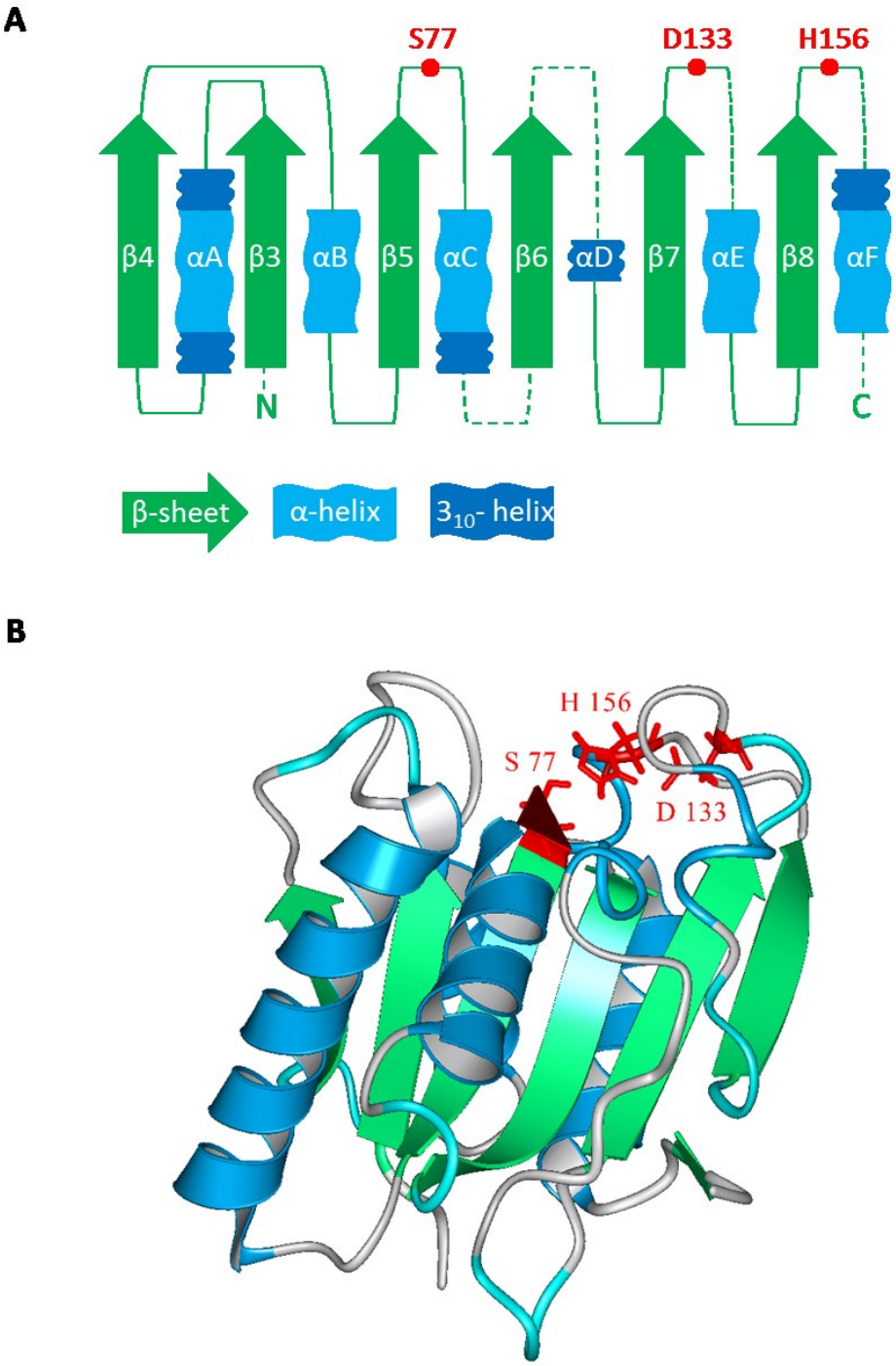

Fig. 1.4 Minimal α/β-hydrolase folding pattern and 3D structure of *B. subtilis* lipase.
Modified according to (Van Pouderoyen *et al.*, 2001). Secondary structures of *B. subtilis* LipA are schematically illustrated in **A** and visualized on the 3D X-ray structure (PDB: 1I6W) in **B**. LipA is lacking the first two β-sheets β1 and β2 of the canonical α/β-hydrolase fold. Therefore, the minimal α/β-hydrolase fold of LipA consists of six β-sheets (green arrows), five α-helices (blue banners) and five 3_{10}-helices (dark blue). The amino acid residues of the catalytic triad are shown and labelled in red.

As already mentioned, LipA does not exhibit an α-helical lid structure that covers the catalytic triad (Fig. 1.4B) (Van Pouderoyen *et al.*, 2001), furthermore its tertiary structure is not stabilized by disulfide bonds, because LipA does not exhibit cysteine residues (Lesuisse

et al., 1993). In contrast to the lipases from *P. aeruginosa* and *B. glumae* (Rosenau *et al.*, 2004), *B. subtilis* LipA does not need a chaperone, a foldase, or a cofactor to fold into its native, active conformation (Lesuisse *et al.*, 1993). LipA is a very hydrophobic protein, composed of 59 % hydrophobic amino acids (UniProt: P37957) with an isoelectric point of 9.7 (Dartois *et al.*, 1992; Lesuisse *et al.*, 1993). LipA was classified as a lipase due to its ability to hydrolyze sn-1 and sn-3 glycerol esters with a preference for esters with mid-long fatty acid chains of eight carbonyl atoms (Lesuisse *et al.*, 1993), but with the additional capability to hydrolyze triacylglycerides (C2-C18) and vinyl esters (C3-C14) independent from their chain length (Eggert, 2001). As an extracellular carboxylester hydrolase, LipA physiologically plays a role in lipid degradation for *B. subtilis* nutrient supply (Antelmann *et al.*, 2001; Kunst *et al.*, 1997). Native LipA is produced during exponential growth of *B. subtilis* reaching its optimum at the end of the logarithmic growth phase (Eggert *et al.*, 2001). Although LipA showed a potential RR/KR signal peptide consensus motif for translocation via the Tat pathway (Tjalsma *et al.*, 2000), proteomic analyses of a Tat component deletion strain revealed that LipA secretion is not mediated by the Tat pathway (Jongbloed *et al.*, 2002). This suggestion of LipA secretion via the general Sec-SRP pathway of *B. subtilis* (see 1.6 for details) was confirmed by the absence of LipA in the culture supernatant of a *B. subtilis* strain reduced in the production of the Sec pathway components SRP and its receptor (Zanen *et al.*, 2006). A second Sec-secreted *B. subtilis* carboxylester hydrolase is the LipA paralogous lipase B (UniProt: Q79F14). These lipases show 68.49 % nucleotide and 73.63 % amino acid sequence identity. Characterization concerning pH and temperature optimum as well as substrate specificity and additives tolerance (Eggert, 2001; Eggert *et al.*, 2000, 2001) revealed similar properties as determined formerly for LipA (Eggert, 2001; Eggert *et al.*, 2001; Lesuisse *et al.*, 1993).

The mentioned properties of LipA, its detailed characterization and the fact of being one of the smallest known lipases makes it a suitable model protein for lipase engineering strategies regarding industrial applications. In chemical industry, chiral compounds are of huge importance and, especially for the production of pharmaceuticals, enantiomerically pure compounds are necessary. For this purpose, lipases can be engineered to substrate specific and enantioselective biocatalysts. The application of directed evolution as such an engineering approach was confirmed using the *B. subtilis* LipA as model protein to improve its enantioselectivity towards meso-1,4-diacetoxy-2-cyclopentene (Funke *et al.*, 2009).

Several other optimization approaches aimed at the experimental and computational identification of amino acid substitutions in *B. subtilis* LipA, representing the class of α/β-hydrolases, to increase its thermostability (Ahmad *et al.*, 2008; Kamal *et al.*, 2011, 2012; Rathi *et al.*, 2016). The most detailed and intensive studies were performed for lipase A tolerance in ionic liquids (Frauenkron-Machedjou *et al.*, 2015) and detergents (Fulton *et al.*, 2015). Here, the effect of each of the 20 natural occurring amino acids on LipA stability was tested to explore the full protein stability landscape as a basic principle for engineering of α/β-hydrolases. Despite its function as a model protein for engineering the biochemical properties of lipases, LipA was also used to study physiological effects during recombinant protein production in the commonly used *E. coli* expression system *E. coli* BL21(DE3) (Rahmen *et al.*, 2015a, b). Therefore, LipA was also used as a model protein for target protein effects on protein production in the microbial cell factory *B. subtilis*.

1.6. *Bacillus subtilis* as a microbial cell factory

As already mentioned (1.1), the demand for suitable production hosts for microbial enzymes and also for other relevant industrial biomolecules is still increasing. The Gram-positive soil bacterium *B. subtilis* has evolved to a commonly used microbial cell factory (Liu *et al.*, 2013; Öztürk *et al.*, 2015). In contrast to the Gram-negative *E. coli* expression host, *B. subtilis* is lacking a second, outer membrane and so secreted microbial enzymes are directly released into the extracellular space (Kang *et al.*, 2014; Schallmey *et al.*, 2004). This results in easy downstream processing and enzyme purification (Heo *et al.*, 2013), because time consuming cell disruption or the formation of `inclusion bodies` known from cytoplasmic enzyme production in *E. coli* is avoided (Mar Carrio *et al.*, 2000). The elucidation of the *B. subtilis* 168 genome sequence (Kunst *et al.*, 1997), the progress in genetic manipulation (Widner *et al.*, 2000) as well as the fact that *B. subtilis* is a non-pathogenic bacterium whose produced biomolecules are `generally recognized as safe` by the FDA (Food and Drug Administration) makes it a prominent expression host for homologous and heterologous proteins and biomolecules. As for example the sugar D-ribose is synthesized in a fed-batch fermentation of *B. subtilis* with 47 g/l (Park *et al.*, 2004) and the heterologous green fluorescent protein GFP is produced yielding 10 g/l (Wenzel *et al.*, 2011). In order to establish and to further improve *B. subtilis* as a microbial cell factory for secretory protein production, several

approaches have been performed to optimize all steps in *B. subtilis* protein biosynthesis (Fig. 1.5). Each of these steps represents a bottleneck in the protein production pipeline from gene expression and mRNA synthesis, to protein translation with simultaneous or subsequent protein translocation and folding as possible occurring proteolysis in the culture supernatant.

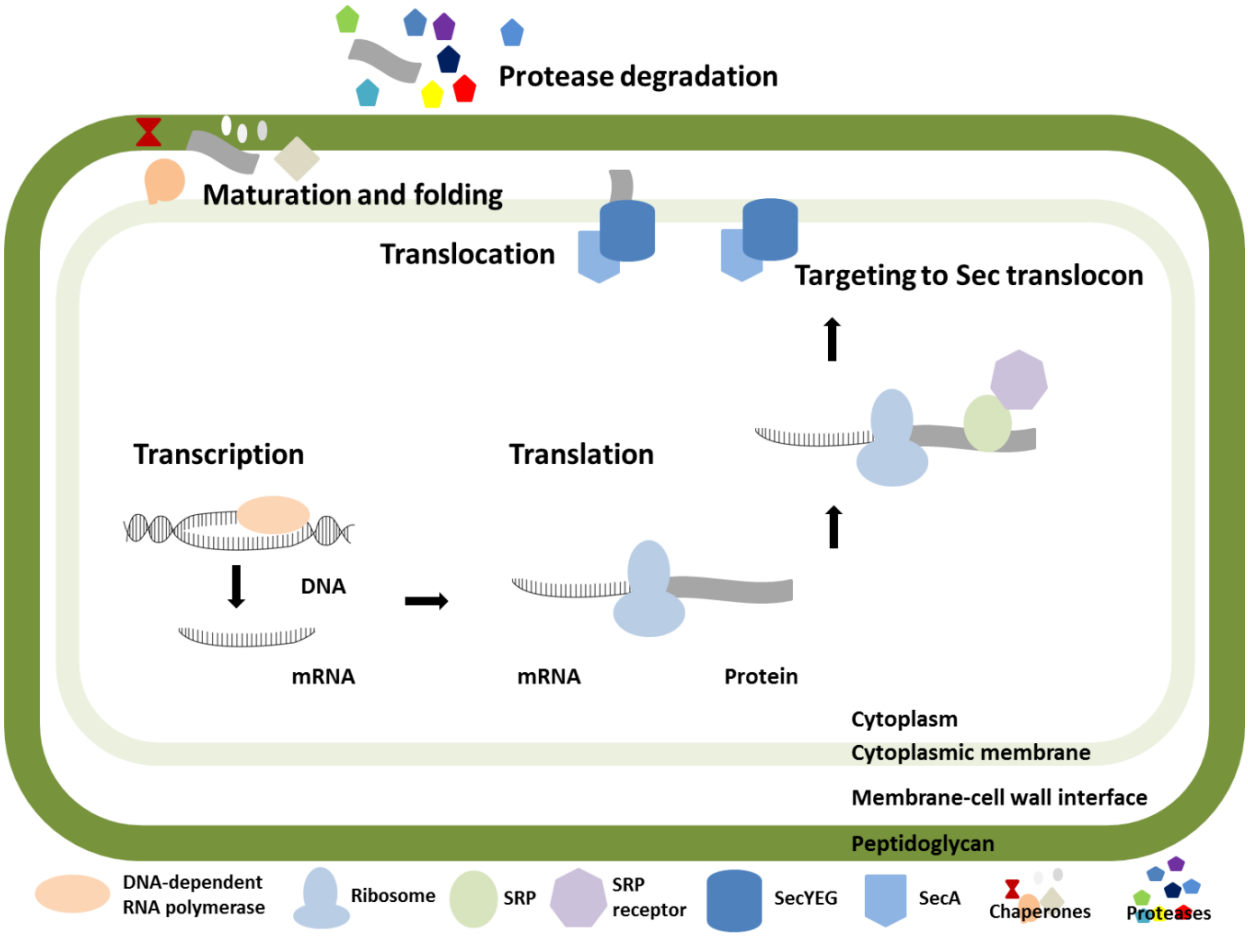

Fig. 1.5 Steps in *B. subtilis* protein production.
Modified according to (Nijland & Kuipers, 2008). The commonly known bottlenecks in *B. subtilis* protein production are shown including transcription, translation, targeting and translocation, subsequent maturation and folding and possible protease degradation in the culture supernatant.

Transcription

Synthesis of mRNA is catalyzed by the DNA-dependent RNA polymerase (RNAP). This RNA polymerase consists of a core enzyme of four subunits (α, α', β, β') and a sigma-factor (σ). The σ-factor is necessary for transcription initiation by promoter recognition and binding and afterwards released from the complex with the core enzyme (Mooney *et al.*, 1998). In contrast to *E. coli* producing only six σ-factors, *B. subtilis* exhibits 17 different σ-factors, necessary for induction and maintenance of the different cellular states of the *B. subtilis* population (Shank & Kolter, 2011). These different σ-factors, including the σ-factor SigA as a

control for permanent gene expression, can recognize different promoters and therefore they can regulate gene expression and mRNA synthesis by altering the composition of the RNA polymerase (Uptain *et al.*, 1997). In general, the promoter region is located -10 to -35 bp upstream of the corresponding transcription start (Mooney *et al.*, 1998). It is composed of the so called Pribnow box at the -10 region, related to the eukaryotic TATA box, a 17 nucleotide spacer sequence and the -35 region (Huang & Helmann, 1998). The Pribnow box shows the consensus 5'TATAAT 3' motif (Pribnow, 1975) and the -35 region shows a 5'TTGACA 3' motif for recognition of the σ-factor SigA (Kazuo & Ogasawara, 2002). The strength of a promoter is dependent on the frequency of transcription initiation, which means the sufficiency of promoter recognition and binding by the corresponding σ-factor (Li *et al.*, 2004). Promoter regions similar to the mentioned consensus sequence recognized by the housekeeping factor SigA show frequent initiation of transcription and are therefore defined as 'strong promoters' (Wang & Roy, 1984). Thus, optimization of promoters by changing their sequences to the respective consensus sequence is a promising target to improve gene expression. This approach was accomplished for the SigA-dependent promoter of the *aprE*-gene, coding for the biotechnological relevant subtilisin E (Henner *et al.*, 1988). A mutant version of this promoter was patented by the biotechnological company Genencor® (now belonging to DuPont™) for high protein production in *B. subtilis* (Nijland & Kuipers, 2008). Also several inducible promoter systems have been established for *B. subtilis*, especially for the production of heterologous proteins. Besides IPTG inducible promoters (Chen *et al.*, 2010; Phan *et al.*, 2012), also auto-inducible promoters (Lee *et al.*, 2010) and sugar inducible promoters (Heravi *et al.*, 2011) have been established and used to fine tune homologous and heterologous gene expression (Liu *et al.*, 2013). Despite the efficient mRNA production by adequate promoters, the mRNA amount also depends on its half-life which is mainly affected by nuclease mediated decay and is crucial for successful gene expression. Decay of mRNA in *B. subtilis* is mediated by the activities of several endo- and exoribonucleases (Liu *et al.*, 2015). *B. subtilis* exhibits four exoribonucleases with 3` to 5` activity (Craven *et al.*, 1992; Luttinger *et al.*, 1996; Oussenko & Bechhofer, 2000; Oussenko *et al.*, 2002) and one exoribonuclease with 5` to 3` activity and also endoribonuclease activity (Even *et al.*, 2005), with the 3` to 5` degrading polynucleotide phosphorylase (PNPase) being the major mRNA turnover enzyme in *B. subtilis* (Deutscher & Reuven, 1991). The major endoribonuclease in *B. subtilis* is the single-stranded RNA

hydrolyzing RNase Y, necessary for initiation of mRNA decay (Shahbabian *et al.*, 2009). Endo- and exoribonuclease mRNA decay is necessary in the bacterial metabolism for recycling of nucleotides and therefore essential for the maintenance and regulation of protein biosynthesis (Liu *et al.*, 2015). Thus, reduction of mRNA decay to improve gene expression by deletion of RNase genes has not been subjected (or published) so far.

Translation

Following transcription, the synthesized mRNA is translated into the protein sequence. This step of translation is composed of three consecutive steps: initiation, elongation and termination (Rocha *et al.*, 1999)**.** The most rate limiting step during translation is the initiation step (De Smit & Van Duin, 1994). Here, first the initiation complex needs to be formed. This complex includes the 30S ribosomal subunit, the mRNA, the formylated Met-tRNA and three initiation factors (De Smit & Van Duin, 1994). Therefore, the free 3'-end of the pyrimidine rich 16S rRNA of the 30S subunit binds to the purine rich shine dalgarno sequence (ribosome binding site) upstream from the coded gene on the mRNA (Rocha *et al.*, 1999). The efficient and suitable binding of the ribosome to the mRNA is dependent on possible mRNA secondary structures that are formed around the ribosome binding site and could impede translation initiation (De Smit & Van Duin, 1994) or by codon bias at the beginning of the translated gene enhancing wobble base pairing of tRNA and mRNA resulting in weak binding (Bulmer, 1988). Elongation, the second step of translation, could then be negatively influenced by mRNA secondary structures as well, leading to ribosome dissociation from the mRNA (De Smit & Van Duin, 1994) and so to a delay of translation. A decrease in translation velocity is known to be caused by rare codons in the mRNA (Curran, 1989; Varenne *et al.*, 1989) or by low tRNA abundance for frequent codons (Osawa & Muto, 1987). This stall in translation is necessary at different stages in translation to provide subsequent efficient folding of the protein (Chaney & Clark, 2015). Termination of translation is mediated by the binding of a so called release factor (RF) (Nakamura *et al.*, 1996). This release factor substitutes the tRNA in the ribosomal complex and recognizes the respective stop codons in the mRNA (RF1: UAA, UAG and RF2: UGA) (Nakamura *et al.*, 1996). Improvement of translation for efficient protein synthesis can be achieved by the use of optimized ribosome binding sites that promote an efficient and strong binding of the ribosome to the mRNA (Nijland & Kuipers, 2008) or by substituting rare codons with optimal codons as it was shown for *E. coli* (Nijland & Kuipers, 2008) to fasten translation. Despite

adapted codon usage often increase protein production in *E. coli*, rare codons can be essential for protein production in *B. subtilis*, because proteins destined to be secreted are synthesized with a N-terminal signal peptide and rare codons in the coding sequence of this peptide facilitate binding of the signal peptide by the signal recognition particle through slowing down translation (Power *et al.*, 2004).

Targeting and translocation

Four distinct translocation pathways for secreted proteins are known in *B. subtilis* (Fu *et al.*, 2007), all mediated by specific signal peptides which are the targeting signal for secretory protein recognition (Tjalsma *et al.*, 2000). The twin-arginine translocation (Tat) pathway for folded proteins (Jongbloed *et al.*, 2000), several ATP-binding cassette (ABC) transporters for bacteriocins and pheromones (Quentin *et al.*, 1999), a pseudopilin export pathway necessary for competence development (Tjalsma *et al.*, 2004) and the major Sec-SRP pathway for export of the largest number of *B. subtilis* secretory proteins (Yamane *et al.*, 2004). Here, the proteins are kept in an unfolded state by the signal recognition particle (SRP). The SRP is a highly conserved ribonucleoprotein complex that can directly bind to secretion-necessary signal peptide of the nascent protein chain emerging from the ribosome (Fu *et al.*, 2007) and so promoting Sec-dependent protein translocation during translation (Van Wely *et al.*, 2001)**.** In contrast to *E. coli*, this cotranslational secretion pathway is the generally used one in *B. subtilis* for unfolded proteins. In *E. coli* the use of the SRP to keep the protein in an unfolded state is linked only to very hydrophobic signal peptides of proteins destined to be inserted into the cytoplasmic membrane (Pool, 2005). Here, the general secretory pathway includes the SecB chaperone for posttranslational protein translocation (Fekkes *et al.*, 1997; Kumamoto & Francetić, 1993). *B. subtilis* exhibits no SecB homologous protein, but the *csaA* gene was identified to be able to complement growth defects of *B. subtilis* strains lacking or deficient in different components (SecA, DnaK, DnaJ) of the translocation machinery (Müller *et al.*, 2000a). The CsaA protein shows chaperone like activities and is able to interact with Sec-dependent secretion precursor protein (Müller *et al.*, 2000a, b) and could therefore be involved in a posttranslational Sec-dependent secretion in *B. subtilis.*

The binding of the SRP to the hydrophobic signal peptide occurs when the synthesized protein is still attached to the ribosome and between 70 and 150 amino acids long (Fekkes & Driessen, 1999). This results in the formation of the ribosome-nascent-chain-SRP complex

(RNC-SRP complex), which is in turn bound by the peripheral membrane associated SRP receptor (Yamane *et al.*, 2004) and transported to the SecYEG translocon in the cytoplasmic membrane (Tjalsma *et al.*, 2004; van Wely *et al.*, 2001). Here, the ATPase SecA necessary for translocation, is peripherally associated to the cytoplasmic membrane and bound by the signal peptide of the translocated protein (Van Wely *et al.*, 2001). The signal peptide and the adjacent protein unloop and are pulled through the SecYEG translocation pore, driven by ATP hydrolysis and by the driving force of the still ongoing translation (Van Roosmalen *et al.*, 2004; Schiebel *et al.*, 1991; van der Wolk *et al.*, 1997). Directly after translocation, the N-terminal signal peptide is hydrolyzed by a Type I signal peptidase SipS or SipT and the translocated protein is released into the membrane-cell wall interface (Tjalsma *et al.*, 2000). The hydrolyzed signal peptide is then subsequently degraded by the signal peptide peptidases SppA or TepA. This degradation is necessary to circumvent the inhibition of further protein translocation by `plugging` the Sec pathway and surrounding membrane areas with leftover signal peptides (Bolhuis *et al.*, 1999). In order to improve cotranslational secretion in *B. subtilis,* former studies assayed fusions of a target protein with Sec-specific N-terminal signal peptides. Despite the saturation mutagenesis of an homologous signal peptide to increase secretion of an heterologous protein in *B. subtilis* (Caspers *et al.*, 2010), screening of so called signal peptide toolboxes is a promising approach to identify an optimal signal peptide for the secreted protein of interest (Brockmeier *et al.*, 2006; Degering *et al.*, 2010). Additionally, the SecATPase was examined as a potential target for optimization. The deletion of 66 amino acids from the C-terminus of SecA resulted in a 1.2-fold increase in the recombinant human interferon-α production (Kakeshita *et al.*, 2010).

Protein maturation, folding and protease degradation

Until the secreted protein reaches the extracellular space of *B. subtilis* in its native and active conformation, it passes the peptidoglycan layer thereby undergoing a quality and conformation control mediated by extracellular chaperones (Fu *et al.*, 2007). The cytoplasmic membrane anchored and extracellularly exposed lipoprotein PrsA acts as such a chaperone and ensures proper protein folding (Kontinen & Sarvas, 1993). Also the cell wall associated extracellular protease WprA can act as a quality control enzyme by proteolysis of malfolded proteins (Kang *et al.*, 2014), despite this it also controls the homeostasis of the membrane-cell wall interface proteases HtrA and HtrB, also degrading poorly folded proteins connected to the secretion stress response (Westers *et al.*, 2004a) and is able to

degrade homologous proteins involved in protein quality control as for example the mentioned PrsA (Krishnappa *et al.*, 2014). *B. subtilis* also harbors two extracellularly thiol-disulfide oxidoreductases BdbB and BdbC for disulfide bond formation which is required for the correct tertiary structure of certain proteins (Fu *et al.*, 2007).

Altogether, *B. subtilis* produces eight extracellular proteases that degrade secreted proteins and represent a limiting factor in heterologous secretory protein production in *B. subtilis* (Westers *et al.*, 2004b).

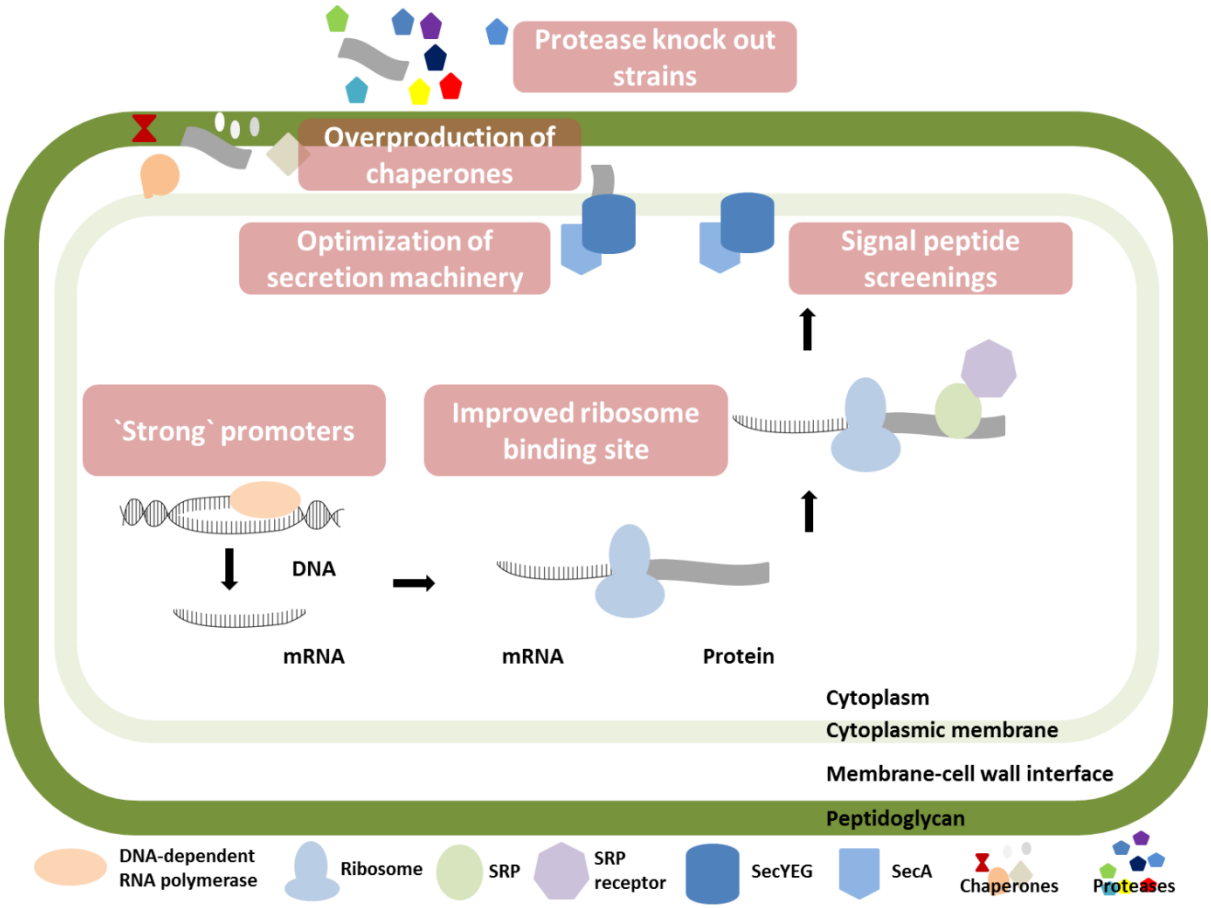

Fig. 1.6 Strategies to optimize protein production in *B. subtilis*.
Modified according to (Nijland & Kuipers, 2008). Summary of the mentioned and explained optimization strategies in chapter 1.6 (references therein).

Deletion of the genes coding for these extracellular proteases (Westers *et al.*, 2004b) together with the overproduction of PrsA (Kontinen & Sarvas, 1993) and the modulation of the thiol-disulfide oxidoreductases BdbB and BdbC (Kouwen *et al.*, 2009a, b) are proven approaches to improve secretory protein production. All mentioned optimization strategies to establish and further improve *B. subtilis* as a microbial cell factory are summarized in Fig. 1.6. These approaches aimed at each step in protein production also representing bottlenecks in homologous and heterologous protein synthesis.

1.7. Target protein effects on production and secretion

Secretory protein production in *B. subtilis* is dependent on the efficiency of the above described steps in the production pipeline (1.6) that are considered as bottlenecks. Enduring optimization of these bottlenecks (Fig. 1.6) leads to the establishment of a *B. subtilis* microbial cell factory producing and secreting proteins in large amounts (Nijland & Kuipers, 2008). The fact of steadily upcoming new optimized expression systems including deletion or overproduction strains, improved promoters or ribosome binding sites (Song *et al.*, 2015) probably indicate that not all influencing parameters for an efficient production have been considered so far, as for example possible effects of the target protein itself. A relatively large number of studies published different effects of the target protein on its production and secretion in bacteria and also eukaryotic cells (Tab. 1.2). These random findings are not based on specific optimization strategies and do not follow any pattern regarding the origin of the coding gene sequence (Gram-negative, Gram-positive or eukaryotic) or the kind of production strategy (homologous or heterologous) (Tab. 1.2), but different specific classes of effects could be determined. For example, mutations within the target protein or the amino acid net charge mainly of the N-terminal part of the protein could negatively influence its secretion (Hausmann *et al.*, 2008; Kajava *et al.*, 2000; Khokhlova & Nesmeyanova, 2003; Kohara *et al.*, 1991; Li *et al.*, 1988; Nijland *et al.*, 2007). Also specific domains and amino acids were identified to interact with components of the translocation machinery thus influencing secretion (Altman *et al.*, 1990; Andersson & von Heijne, 1991; Bensing & Sullam, 2010; Bensing *et al.*, 2012; Duplay & Hofnung, 1988; Feltcher *et al.*, 2013; Hemilä & Sibakov, 1991; Hodak *et al.*, 2006; Khokhlova & Nesmeyanova, 2003; Le Loir *et al.*, 1998; Mallik *et al.*, 2002; Rasmussen & Silhavy, 1987). For amino acid substitutions affecting the secretion of three eukaryotic enzymes into the endoplasmatic reticulum, it was possible to transfer their effects to other homologous proteins (De Jaco *et al.*, 2006). The lipase A from *P. aeruginosa* was subjected to mutagenesis to identify amino acid substitutions that improve its enantioselectivity towards the model substrate 2-methyldecanoic acid.

Tab. 1.2 Overview of analyzed underlying target protein effects on production and secretion in bacteria.
The target proteins are grouped according to the underlying effect on production and secretion in the particular expression host. The protein origin organism and its classification are listed. Where - describes Gram-negative organisms and + describes Gram-positive ones.

effect	target protein	organism	expression host	reference
mutations	*P. aeruginosa* LipA	-	homologous	(Hausmann *et al.*, 2008)
	Clostridium perfringens β-toxin	+	*B. subtilis*	(Nijland *et al.*, 2007)
	E. coli PhoA	-	homologous	(Khokhlova & Nesmeyanova, 2003)
	Homo sapiens Lysozym	eukaryotic	*Saccharomyces cerevisiae*	(Li *et al.*, 1988) (Kohara *et al.*, 1991)
net charge	*E. coli* PhoA	-	homologous	(Kajava *et al.*, 2000)
	Homo sapiens Lysozym	eukaryotic	*Saccharomyces cerevisiae*	(Kohara *et al.*, 1991)
specific domains	*E. coli* MBP	-	homologous	(Duplay & Hofnung, 1988)
	E. coli LamB	-	homologous	(Rasmussen & Silhavy, 1987)
	E. coli Lep	-	homologous	(Andersson & Von Heijne, 1991)
	Streptococcus gordonii GspB	+	homologous	(Bensing & Sullam, 2010)
	Staphylococcus aureus Nuc	+	*Lactococcus lactis*	(Le Loir *et al.*, 1998)
	E. coli β-Lactamase	-	homologous	(Hemilä & Sibakov, 1991)
	Bordetella pertussis FHA	-	*E. coli*	(Hodak *et al.*, 2006)
interaction	*E. coli* LamB	-	homologous	(Altman *et al.*, 1990)
	Streptococcus gordonii GspB	+	homologous	(Bensing *et al.*, 2012)
	Salmonella typhimurium SopB	-	*E. coli*	(Roblin *et al.*, 2013)
	E. coli PhoA	-	homologous	(Khokhlova & Nesmeyanova, 2003)
	Mycobacterium smegmatis Lipoprotein	+	homologous	(Feltcher *et al.*, 2013)
	E. coli λ-Repressorprotein	-	homologous	(Mallik *et al.*, 2002)
transfer	*Homo sapiens* Neuroligin-3 *Homo sapiens* Butyrylcholinesterase *Homo sapiens* Acetylcholinesterase	eukaryotic	homologous	(De Jaco *et al.*, 2006)

LipA variants showing improved enantioselectivity also showed a decrease in secretion efficiency in the homologous host, so indicating an impair in secretion based on the enantioselectivity related amino acid substitution (Hausmann *et al.*, 2008).

Such mutations could also alter the amino acid net charge of the protein and so influencing secretion efficiency or they could strengthen the interaction of the protein with the secretion pathway components like SecA or SecB, as it was shown for *E. coli* mature alkaline phosphatase PhoA (Khokhlova & Nesmeyanova, 2003). Pathogenic Gram-positive bacteria like *Streptococcus gordonii* are known to exhibit a second, accessory Sec system, especially for the secretion of virulence factors (Bensing & Sullam, 2002). The glycoprotein GspB is a virulence factor of *S. gordonii* and needs a so called AST domain (Accessory Sec Transport domain) adjacent to the signal peptide which interacts with the accessory Sec system and is therefore necessary for recognition and transport via this Sec system (Bensing & Sullam, 2010; Bensing *et al.*, 2012). All these findings confirm an influence of the target protein on its production and secretion not only in bacteria but also in eukaryotic cells. Nevertheless, the target protein has so far not been subjected for a detailed optimization approach regarding its production in the respective chosen microbial cell factory.

1.8. Aim of this work

The demand for microbial enzymes as industrial biocatalysts with certain selectivities and activities towards a given substrate is still increasing. To meet this demand, microorganisms are needed that can be easily manipulated on a genetical and physiological level to produce foreign biomolecules as proteins and metabolites with high efficiency. *B. subtilis* is one of those microorganisms designated as 'microbial cell factory'. Intensive analyses in the last years established and further improved *B. subtilis* as such a cell factory for secretory protein production. Nevertheless, there are still problems in protein production complicating a general *B. subtilis* 'microbial cell factory' design, always demanding for adjustment to the target protein for production. Although a possible influence of the target protein itself on its production and secretion is known and could be a reason for non-optimal production in an actually supposed to be optimized expression system, this influence was never analyzed in a detailed and systematic manner. The results from this detailed view on the target protein will provide new global insights regarding the functional properties of the engineered protein but also, which is more fundamental, will challenge the existing optimization strategies for efficient protein production. For this purpose, the well-known and biochemically characterized *B. subtilis* lipase A (LipA) was chosen as a homologous model protein. This allows the elucidation of essential beneficial target protein effects without interfering factors from heterologous protein production like different codon usages. The presented work aims at the first systematic mutational analysis to identify single amino acid and codon substitutions within the target protein beneficial for secretory protein production in *B. subtilis.* This approach can be divided into three steps.

1) Generation of a library covering all possible LipA single amino acid substitutions with about 30,000 *lipA* clones by site saturation mutagenesis that are subsequently screened.
2) Development of a suitable qualitative and quantitative TECAN® robot supported high throughput screening system for lipase detection in the *B. subtilis* culture supernatant.
3) Validation and characterization of identified beneficial single amino acid and codon substitutions and their detailed role in LipA production.

Furthermore, identified beneficial amino acid and codon substitutions will be combined for LipA and also transferred to a second lipase to allow conclusions about the general validity of such approaches.

2. Material and Methods

2.1. Chemicals and enzymes

All used chemicals and enzymes are obtained, unless otherwise noted, in *p.a.* quality from the following companies:

Antibiotics: AppliChem (Darmstadt), Gerbu (Wieblingen)

Chemicals: Sigma-Aldrich (Munich), Carl Roth GmbH (Karlsruhe), BD Germany (Heidelberg)

Enzymes: Thermo Fisher Scientific Germany (Dreieich), lysozyme from Sigma-Aldrich (Munich)

Antibodies: Primary Antibody: polyclonal LipA antibody was generated by Eurogentec (Cologne); Secondary-Antibody: Goat-Anti-Rabbit IgG (H+L)-HRP conjugate was obtained from BioRad Laboratories GmbH (Munich)

2.2. Bacterial strains and plasmids

Tab. 2.1 Overview of used bacterial strains.

strain	genotype	reference
B. subtilis 168	*trpC2*	(Burkholder & Giles, 1947)
B. subtilis TEB1030	*trpC2 his nprE aprE bpf ispI lipA lipB*	(Eggert *et al.*, 2003)
E. coli DH5α	*supE44 Δ(lacZYA-argF) U196 (phi80ΔlacZM15) hsdR17 recA1 endA1 gyrA96 thi-1 relA1*	(Woodcock *et al.*, 1989)
E. coli BL21(DE3)	F^- *ompT gal dcm lon hsdS*$_B$($r_B^- m_B^-$) λ(DE3 [*lacI lacUV5-T7 gene 1 ind1 sam7 nin5*]) [*malB*$^+$]$_{K\text{-}12}$(λ^S)	Novagen, Darmstadt

Tab. 2.2 Overview of used plasmids.

plasmid	genotype	reference
pBSMul1	shuttle vector for *E. coli* and *B. subtilis*, ribosome binding site, P_{HpaII}, secretion (*sslipA*) and purification (C-terminal 6x-His-tag); *colE1 repB Km*^{r} *Amp*^{r}	(Brockmeier, 2006)
pBSMul1*lipAsslipA*	pBSMul1 containing a 568 bp *Eco*RI-*Hin*dIII fragment of *B. subtilis* lipase *lipA*	(Skoczinski, 2012)

plasmid	genotype	reference
pBS*lipAsslipA*	pBSMul1*lipAsslipA* containing a 568 bp *Eco*RI-*Hin*dIII fragment of *B. subtilis* lipase *lipA,* where the *Eco*RI restriction site between *sslipA* and *lipA* was deleted	(Fulton, 2014)
pET-22b (+)	*E. coli* expression vector, ribosome binding site, P_{T7}, secretion (*sspelB*) and purification (C-terminal 6x-His-tag), *lacI pMB1 f1 Amp^r*	Novagen, Darmstadt
pET22*lipAΔss*-his	pET-22b (+) containing *B. subtilis* lipase *lipA* in frame with the N-terminal 6x-His-tag, without signal sequence	(Fulton, 2014)
pET22*lipAΔss*	pET-22b (+) containing a 568 bp *Nde*I-*Hin*dIII fragment of *B. subtilis* lipase *lipA*, without signal sequence	(Röllen, 2012)
pBSMul1*lipA*_SP	pBSMul1*lipAsslipA* containing a 568 bp *Eco*RI-*Hin*dIII fragment of *B. subtilis* lipase *lipA,* where the *Hin*dIII restriction site downstream of *lipA* was deleted and reinserted upstream of *sslipA*	This study
pBSMul1*lipAssvpr*	pBSMul1*lipA*_SP containing a 568 bp fragment of *B. subtilis lipA* and a 110 bp *Hin*dIII-*Eco*RI fragment of the *ssvpr*	This study
pBS*lipBsslipB*	pBSMul1 containing a 632 bp Gibson assembled fragment of *B. subtilis* lipase *lipB* with *sslipB*	This study
pET22*lipBΔss*-his	pET-22b (+) containing a 570 bp *Xba*I-*Xho*I fragment of *B. subtilis* lipase *lipB* in frame with the C-terminal 6x-His-tag, without signal sequence	This study

2.3. Oligonucleotides

All oligonucleotides used in this study were obtained from MWG Eurofins (Ebersberg) or Sigma-Aldrich (Munich) purified, salt free and lyophilized. Primers were dissolved in A. dest. achieving a final concentration of 100 pmol/µl and stored at -20 °C. For PCR reactions the primer stock solutions were diluted 10-fold.

Tab. 2.3 Oligonucleotides used in this study.
Restriction sites or modification sites are underlined. All oligonucleotides used for site saturation mutagenesis of plasmid based *lipA* are listed in the appendix (Tab. 8.1).

primer	sequence 5` to 3`	modifications
lipA		
QC_G13S_fw	ATGGTTCACGGTATTTCGGGGGCATCATTCAAT	G13S
QC_G13S_rev	ATTGAATGATGCCCCCGAAATACCGTGAACCAT	
QC_N48Q_fw	GACAAGACAGGCACACAGTATAACAATGGACCG	N48Q
QC_N48Q_rev	CGGTCCATTGTTATACTGTGTGCCTGTCTTGTC	
QC_P53D_fw	AATTATAACAATGGAGACGTATTATCACGATTT	P53D
QC_P53D_rev	AAATCGTGATAATACGTCTCCATTGTTATAATT	
QC_A105N_fw	GTGACGCTTGGCGGCAACAACCGTTTGACGACA	A105N
QC_A105N_rev	TGTCGTCAAACGGTTGTTGCCGCCAAGCGTCAC	
QC_Y139T_fw	ATGATTGTCATGAATACCTTATCAAGATTAGAT	Y139T
QC_Y139T_rev	ATCTAATCTTGATAAGGTATTCATGACAATCAT	
ssvpr		
Δ*Hin*dIII_Cterm_fw	CCGTCGACGCGGCCGCG	Deletion of *Hin*dIII restriction site
Δ*Hin*dIII_Cterm_rev	CGCGGCCGCGTCGACGG	
*Hin*dIII_Nterm_fw	GCGATTTACATAATAAGCTTAAGGAGGACATATG	Insertion of *Hin*dIII restriction site
*Hin*dIII_Nterm_rev	CATATGTCCTCCTTAAGCTTATTATGTAAATCGC	
vpr_*Hind*III_fw	ATATAAGCTTAAGGAGGATATTATGAAAAAGG	*Hin*dIII
vpr_*Eco*RI_ rev	ATATGAATTCAGCAGCCGGAGCTGC	*Eco*RI
lipB		
GA_*sslipBlipB*_fw	GCGATTTACATAATAAGGAGGACAGGGAATAAACGTGAA AAAAGT	Gibson assembling
GA_*sslipBlipB*_rev	AGATATCGCGGCCGCAGATATTAATTTGTATTGAGGCCTCCG	
*Xba*I_*lipB*_fw	CGCGTCTAGAAAGGAGATATAGTGGAGTCAGTACATAATC	*Xba*I
*Xho*I_*lipB*_rev	GGCCGCCTCGAGATTTGTATTGAGGCCTCCG	*Xho*I
QC_S14G_fw	CTTGTTCATGGAATAGGAGGTGCATCATACAAC	S14G
QC_S14G_rev	GTTGTATGATGCACCTCCTATTCCATGAACAAG	
QC_N49Q_fw	GATAAAACAGGAAACCAGCTAAATAACGGCCCG	N49Q
QC_N49Q_rev	CGGGCCGTTATTTAGCTGGTTTCCTGTTTTATC	
QC_P54D1_fw	AACCTAAATAACGGCGACCAGCTTGCTTCATAT	P54D (GAC)
QC_P54D1_rev	ATATGAAGCAAGCTGGTCGCCGTTATTTAGGTT	

primer	sequence 5` to 3`	modifications
lipB		
QC_P53D2_fw	CAACCTAAATAACGGCGATCAGCTTGCTTCATATG	P54D (GAT)
QC_P53D2_rev	CATATGAAGCAAGCTGATCGCCGTTATTTAGGTTG	
QC_A106N_fw	GTAACGCTTGGAGGGAACAATGGTTTAGTGTCA	A106N
QC_A106N_rev	TGACACTAAACCATTGTTCCCTCCAAGCGTTAC	
QC_S140T_fw	CAAATTGTCATCAATACGTTGTCTCGGTTACAAGG	S140T
QC_S140T_rev	CCTTGTAACCGAGACAACGTATTGATGACAATTTG	

2.4. Media and growth conditions

For application, the LB medium (10 g/l tryptone, 5 g/l yeast extract, 10 g/l NaCl) and LB agar (LB medium with 15 g/l agar) is adjusted to pH 7 with NaOH and autoclaved at 121 °C, 200 kPa for 20 min (Sambrook & Russell, 2001)**.**

Sterile filtered antibiotics and IPTG were added at a temperature of below 60 °C.

Unless otherwise noted, cultivation of *E. coli* was carried out in selective LB medium at 37 °C, 120-130 rpm for 16 h (Tab. 2.5).

Cultivation of *B. subtilis* was carried out in selective LB medium under various cultivation conditions.

Microfermentation in 48-well FlowerPlate® and online biomass measurement

Precultures of *B. subtilis* were incubated in 1,100 µl selective LB medium in 48-well Flowerplates (FlowerPlate® (48 well MTP) without optodes, m2p-labs, Baesweiler) at 37 °C, 1,100 rpm for 16 h (TiMix 5, Edmund Bühler GmbH, Hechingen) sealed with breathable foils (Rotilabo®- cling film for cell cultures, Carl Roth GmbH, Karlsruhe). Expression culture was inoculated to an $O.D._{580\ nm}$ of 0.05 in 1,100 µl selective LB medium in 48-well FlowerPlates® and cultivated at 37 °C, 1,100 rpm for 6 h sealed with breathable foils. For online biomass measurement a replicate of the expression culture inoculated to an $O.D._{580\ nm}$= 0.05 in a 48-well FlowerPlate® (FlowerPlate® (48 well MTP) with O_2 and pH optodes, m2p-lab, Baesweiler) was cultivated in the BioLector® (m2p-labs, Baesweiler) at 37 °C, 1,100 rpm for 24 h sealed with breathable foils.

Tab. 2.4 Biolector®-conditions.
Flowerplate®-Lot. 1311

Temperature setpoint [°C]:	37
Shaking frequency [rpm]:	1,100
MTP type:	MTP-48-FlowerPlate
MTP lot:	1311-hc-Temp37
Filling volume [µL]:	1,100
Plate seal:	breathable foil
Measurement data 1:	FS:1 F:Biomass G:40
Measurement data 2:	FS:2 F:pO2-hc G:51
Measurement data 3:	FS:3 F:pH-hc G:24
Measurement data 4:	Cal.Biomass[OD600 [-]]:FS=1
Measurement data 5:	Cal.pH [-]:FS=3
Measurement data 6:	Cal.pO2 [-]:FS=2

96-well microtiterplate cultivation

Precultures of *B. subtilis* were incubated in 150 µl selective LB medium in 96-well microtiter plates (Greiner Bio-one, Frickenhausen) at 37 °C, 900 rpm for 6 h (TiMix 5, Edmund Bühler GmbH, Hechingen) sealed with breathable foils (Rotilabo®- cling film for cell cultures, Carl Roth GmbH, Karlsruhe). Inoculation of expression culture in 150 µl selective LB medium in 96-well microtiter plates to an $O.D._{580\ nm}$ of 0.05 was performed with the TECAN® robot system freedom evo (Tecan Group Ltd., Männedorf). Expression culture was cultivated at 25 °C, 900 rpm for 16 h sealed with breathable foils.

Unless otherwise noted, all precultures were inoculated from single colonies of selective *B. subtilis* protoplast regeneration agar plates (2.9.3).

Tab. 2.5 Relevant antibiotics used for growth selection.

substrate	final concentration (µg/ml)	organism
ampicillin	100	*E. coli*
kanamycin	50	*B. subtilis*

2.5. Storage of bacterial cultures

1.8 ml of a bacterial culture was stored at -80 °C after the addition of 138 µl DMSO. For storage of *B. subtilis* precultures in microtiter plates 80 % (v/v) sterile glycerol was added to each well to a final concentration of 20 % (v/v) and the plates were stored at -80 °C.

2.6. Isolation of nucleic acids

Isolation of plasmid DNA was performed using the innuPREP Plasmid Mini Kit (Analytik Jena, Jena) according to manufacturer instruction.

For isolation of plasmid DNA from *B. subtilis,* the cells were incubated in the provided resuspension buffer after addition of 100 µg lysozyme at 37°C for 30 min in order to achieve complete cell lysis.

DNA concentration was determined using the NanoDrop 2000C spectrophotometer (Thermo Fisher Scientific Germany, Dreiech) according to manufacturer instructions.

2.7. Agarose gel electrophoresis

(Vogelstein & Gillespie, 1979)

Agarose gel electrophoresis for DNA analysis and DNA isolation was accomplished using 0.5x TBE buffer (17.8 mM Tris, 17.8 mM boric acid, 0.5 mM Na_2-EDTA) and 1 % (w/v) agarose in 0.5x TBE buffer with 0.5 % (v/v) EtBr (1 mg/ml stock solution). The Gene Ruler 1kb Plus DNA ladder (Thermo Fisher Scientific Germany, Dreieich) was applied as a molecular weight standard. Visualization and documentation of EtBr stained DNA was done with the Gel iX Imager (Intas Science Imaging Instruments GmbH, Göttingen).

2.8. *In vitro* recombination of DNA

(Dugaiczyk *et al.*, 1975; Smith *et al.*, 1976)

Hydrolysis, dephosphorylation and ligation reactions were performed using enzymes and buffers from Thermo Fisher Scientific (Dreieich) under conditions recommended by the manufacturer.

Gibson Assembly (Gibson *et al.*, 2009)

The Gibson Assembly was performed by mixing the Gibson Assembly reagent Master Mix (1x isothermal reaction buffer, 0.005 U/µl T5 Exonuclease, 0.03 U/µl Phusion® DNA Polymerase, 5 U/µl Taq DNA Ligase) with 6 µl of a DNA solution containing equimolar amounts of linearized vector (10-100 ng) and insert and incubated at 50 °C for 1 h. *E. coli* DH5α was transformed with 10 µl of a 10-fold diluted reaction mixture (2.9.1; 2.9.2).

The 5x isothermal reaction buffer contains 0.5 M Tris-HCl pH 7.5, 0.01 M $MgCl_2$, 0.2 mM dGTP, 0.2 mM dATP, 0.2 mM dCTP, 0.2 mM dTTP, 0.01 M DTT, 5 % (w/v) PEG 8000 and 1mM NAD.

2.9. Transformation of bacteria

2.9.1. Production and transformation of chemical competent *E. coli*

Modified according to (Hanahan & Harbor, 1983)

500 ml LB medium were inoculated with an overnight *E. coli* culture to an $O.D._{580\ nm}$ of 0.05 and cultivated to an $O.D._{580\ nm}$ = 0.4-0.5 at 37 °C, 120-130rpm. The culture was chilled on ice for 10 min and centrifuged at 4 °C, 2,790 *g* for 10 min. The pellet was resuspended in 35 ml sterile, ice cold FB buffer pH 6.4 (100 mM KCl, 67.5 mM $CaCl_2$, 10 % (w/v) glycerin, 10 mM potassium acetate solution), incubated on ice for 20 min and centrifuged again at 4 °C, 2,790 *g* for 10 min. The pellet was resuspended in 8.5 ml sterile, ice cold FB buffer and split into 100 µl aliquots. The chemical competent cells were stored at -80°C. For transformation plasmid DNA or ligation mixtures were added to the cells, and the suspension was incubated on ice for 20 min, followed by a 90 sec incubation at 42 °C and addition of 700 µl LB medium. After regeneration at 37 °C for 30 min the cells were spread on selective ampicillin agar plates. The plates were incubated at 37 °C for 16 h.

2.9.2. Production and transformation of electrocompetent *E. coli*

Modified according to (Sambrook & Russell, 2001)

500 ml LB medium were inoculated with an overnight *E. coli* culture to an $O.D._{580\ nm}$ of 0.05 and cultivated to an $O.D._{580nm}$= 0.5-0.7 at 37 °C, 120-130 rpm. The culture was chilled on ice for 20 min and centrifuged at 4 °C, 2,790 *g* for 15 min. The pellet was resuspended in 1 volume 10 % (v/v) sterile, ice-cold glycerol and again centrifuged at 4 °C, 2,790 *g* for 15 min. The cells were subsequently resuspended in ½ volume 10 % (v/v) sterile, ice-cold glycerol and centrifuged at 4 °C, 2,790 *g* for 15 min and resupended in 20 ml 10 % (v/v) sterile, ice-cold glycerol. After a last 15 min centrifugation step, the cell pellet was resuspended in 2 ml 10 % (v/v) sterile, ice-cold glycerol, divided into 50 µl aliquots and freezed at -80 °C. For transformation plasmid DNA or ligation mixtures were added and, the suspension was incubated on ice for 20 min. After electroporation using a 2 mm cuvette and program Ec2 (Bio-Budget Technologies GmbH, Krefeld) with the MicroPulser (BioRad Laboratories GmbH, Munich), 1 ml LB medium was added. After regeneration at 37 °C for 30 min, the cells were spread on selective ampicillin agar plates. The plates were incubated at 37 °C for 16 h.

2.9.3. Production and transformation of *B. subtilis* protoplasts

Modified according to (Chang & Cohen, 1979)

5 ml 1x PAB medium (17.5 g/l Bacto Antibiotic medium 3) without antibiotics were inoculated with a *B. subtilis* colony from an overnight culture on LB medium agar plate and cultivated at 37 °C, 120-130 rpm for 16 h. The 5 ml preculture was transferred into 50 ml 1x PAB medium, this main culture was cultivated at 37 °C, 120-130 rpm for 2 h. The cells were subsequently sedimented at RT, 2,790 *g* for 10 min. The pellet was resuspended in 5 ml SMMP medium and transferred into a 15 ml falcon tube. After addition of 400 µl sterile filtered lysozyme (stock concentration 25 mg/ml), the suspension was incubated at 37 °C for 2 h in a rolling tube mixer. The protoplasts containing suspension was transferred into a 50 ml falcon tube and centrifuged at 4 °C, 1,640 *g*, for 15 min. The protoplasts were carefully resuspended in 5 ml SMMP and again centrifuged 4 °C, 1,640 *g*, for 15 min. The protoplasts were carefully resuspended in 5 ml SMMP medium and split into 140 µl aliquots. The aliquots were stored at -80°C. Plasmid DNA was diluted in 2x SMM medium (0.5 M sucrose, 0.02 M maleic acid, 0.02 M $MgCl_2$; pH 6.5 with NaOH) to a final volume of 10 µl and added to the protoplasts. After addition of 420 µl PEG solution (40g PEG 6000 in 50 ml 2x SMM medium), the protoplasts were gently inverted for 2 min. 1.4 ml SMMP medium were added and the protoplasts were centrifuged at RT, 1,250 *g* for 15 min. The supernatant was discarded and the protoplasts were resuspended in 280 µl SMMP and incubated at 30 °C, 350 rpm for 90 min. The transformed protoplasts were spread on selective protoplast regeneration plates, distributed by slewing the plates and incubated at 37 °C for 16 h. SMMP medium contained equal parts of 2x SMM and 4x PAB (70 g/l Bacto Antibiotic medium 3). All media and solutions were solved in A. dest., autoclaved separately at 121 °C, 200 kPa for 20 min and stored at RT. The protoplast regeneration plates contained 200 ml agar (40 g/l), 100 ml K_2HPO_4 (35 g/l) / KH_2HPO_4 (15 g/l), 20 ml $MgCl_2$ (203 g/l), 50 ml Difco casaminoacids (50 g/l), 50 ml yeast extract (100 g/l), 30 ml glucose (200 g/l), 500 ml succinic acid (118 g/l ,pH 7.3 with NaOH). All components for protoplast regeneration plates were solved in A. dest., autoclaved separately at 121 °C, 200 kPa for 20 min and stored at RT. BSA solution was sterile filtered. The components were prewarmed to 60 °C and mixed. BSA and kanamycin in a final concentration of 500 µg/ml (higher concentration necessary due to kanamycin hydrolysis by succinic acid (Jandová & Tichý, 1987)) were added below 60 °C.

2.10. Polymerase chain reaction

2.10.1. Phusion® Standard PCR

Amplification of DNA fragments was performed under standard PCR conditions (Tab. 2.6) in 25 or 50 µl total volume using a PCR reaction mix containing 1x Phusion® GC buffer with 7.5 mM $MgCl_2$, 0.2 mM dNTP Mix, 10-100 ng plasmid DNA or 10 ng genomic DNA, 0.2 pmol/µl primer oligonucleotides, 1 U Phusion® polymerase, 3 % DMSO (v/v).

Tab. 2.6 Phusion® Standard PCR program.
x: annealing temperature dependent on the melting temperature (Tm) of the used primer.

	temperature °C	min	
initial denaturation	98	0.5	
denaturation	98	0.5	30 cycles
annealing	x	0.5	
elongation	72	1	
final elongation	72	10	
hold	15	∞	

2.10.2. QuikChange® PCR

(Edelheit *et al.*, 2009)

QuikChange® PCR was applied for site saturation mutagenesis (SSM) and site directed mutagenesis (SDM). QuikChange® PCR was performed in 25 or 50 µl total volume using a PCR reaction mix containing 1x Phusion® GC buffer with 7.5 mM $MgCl_2$, 0.2 mM dNTP-Mix, 10-100 ng plasmid DNA, 0.2 pmol/µl primer oligonucleotides, 1 U Phusion® polymerase, 3 % DMSO (v/v). The PCR was separated into two steps (Tab. 2.7), with two samples containing either the forward primer or the reverse primer. Both samples were mixed after the first amplification step. So the homologous forward and reverse primers were able to anneal with the template DNA in the first five cycles and not with each other to allow the amplification of a sufficient amount of new template fragments for the annealing in the last 18 cycles.

Tab. 2.7 QuikChange® PCR program.
x: annealing temperature dependent on the melting temperature (T_m) of the used primer.

	temperature °C	min	step I	step II
initial denaturation	98	0.5		
denaturation	98	0.5	5 cycles	18 cycles
annealing	x	0.75		
elongation	72	3.5		
final elongation	72	10		
hold	15	∞		

During a QuikChange® PCR, the whole plasmid is amplified and PCR products carry primer mediated modification while non-modified template DNA remains which makes a *Dpn*I hydrolysis necessary. *Dpn*I recognizes and hydrolyzes methylated template DNA. This ensures a lower contamination with template DNA in the following transformation. 2 µl *Dpn*I were added to 50 µl QuikChange® PCR product and incubated at 37 °C for 16 h. *Dpn*I hydrolysis was inactivated by incubating the sample at 80 °C for 20 min. The *Dpn*I treated QuikChange® PCR product was desalted and concentrated using the PCR purification protocol of the innuPREP DOUBLEpure Kit (Analytik Jena, Jena).

2.11. Isolation of RNA and quantitative real time PCR

B. subtilis TEB1030 with different mutagenesis vectors was cultured in a microfermentation system using a 48-well FlowerPlate® for 6 h (2.4). 500 µl culture ($O.D._{580\ nm}$ of 1-2) was centrifuged at RT, 21,000 *g* for 10 min. The supernatant was discarded and the pellet was resuspended in 100 µl TE buffer (10 mM Tris-HCl, 1 mM EDTA pH 8) containing 2 mg/ml lysozyme. RNA was prepared using the NucleoSpin® RNA Kit (Macherey-Nagel, Düren) following the protocol for RNA preparation from up to 10^9 bacterial cells. Two additional DNA digestion steps were applied. After the Kit recommended on-column DNA digestion a subsequent second on-column DNA digest was performed. 80 µl 8-fold diluted DNase in DNase reaction buffer (RNase-Free DNase Set; Qiagen, Hilden) was added and incubated at RT for 15 min. Afterwards it was continued with step 8 of the RNA preparation protocol. RNA was eluted in 47 µl RNase/DNase free water and 6 µl 6-fold diluted DNase in DNase reaction buffer (Ambion DNA-free™ DNA Removal Kit; Thermo Fisher Scientific Germany, Dreieich) was added and incubated at 37 °C for 30 min. This third DNA digest was inactivated by adding 5 µl of the Ambion DNA-free™ DNA Removal Kit inactivation buffer. After incubation at RT for 2 min and centrifugation at 21,000 *g* for 2 min, the supernatant containing the isolated RNA was taken off. RNA concentration was determined using the NanoDrop 2000C spectrophotometer (Thermo Fisher Scientific Germany, Dreieich) according to manufacturer instructions. cDNA synthesis of 1,000 ng RNA was performed with the Maxima First Strand cDNA Synthesis Kit for RT-qPCR Kit (Thermo Fisher Scientific Germany, Dreieich) as recommended. The primer pairs listed in Tab. 2.8, generated with the Primer3 tool and 50 ng cDNA or 50 ng of RNA (NoRT-controls) were applied for RT-qPCR

using the Maxima SYBR/ROX qPCR Master Mix (Thermo Fisher Scientific Germany, Dreieich) as recommended. Gene expression analysis was performed using the REST 2009 software (Qiagen, Hilden). *B. subtilis* TEB1030 expressing wild-type *lipA* (wt*lipA*) was analyzed as a reference point in parallel. To give information about the reliability and reproducibility of given RT-qPCR data, the relative change of normalized *lipA* transcript amount among all wt*lipA* expression was determined using the REST 2009 software (Qiagen, Germany). 33 replicates were therefore analyzed as two technical replicates and revealed a standard error in wt*lipA* transcript amount of 0.6 or 1.2 (lower and upper standard error). Therefore, a cutoff value was determined. Only changes in transcript amount lower than 0.4 or larger than 2.2 with a p-value < 0.05 (calculated by REST2009) were defined as significantly changed. The same analysis was performed for *B. subtilis* TEB1030 expressing wt*lipB*. Six biological replicates were analyzed as two technical replicates leading to a standard error of wt*lipB* transcript amount of 0.7 or 2 (lower and upper standard error) determining a cutoff value of 0.3 and 3. As for *lipA* variants only changes in transcript lower or larger the cutoff with a p-value < 0.05 were defined as significantly changed.

Tab. 2.8 Oligonucleotides used for quantitative real time PCR.

primer	sequence 5` to 3`
lipA	
*lipA*_fw	GCTTCCGGGAACAGATCCAA
*lipA*_rev	ACAGAAGGCCGATGTGTCCA
lipB	
*lipB*_fw	CGCCAATACGCTGTACTATA
*lipB*_rev	CTTTTGATTAGGGTCTGTGC
reference gene *sigA*	
*sigA*_fw	ATCGCCTGTCTGATCCACCA
*sigA*_rev	GGTATGTCGGACGCGGTATG

2.12. Construction of *B. subtilis lipA* and *lipB* expression vectors

Vectors generated in this study are listed in 2.2; Tab. 2.2. The plasmid backbone for all *B. subtilis* expression constructs was the pBSMul1 (Brockmeier, 2006) and based on it the previously constructed vector pBSMul1*lipAsslipA* (Skoczinski, 2012)**.** The *Eco*RI restriction site between the signal peptide coding sequence *sslipA* and the *lipA* gene on the pBSMul1*lipAsslipA* was deleted by QuikChange® PCR (2.10.2) using the primer

QC_Δ*Eco*RI_fw and QC_Δ*Eco*RI_rev (2.3; Tab. 2.3) resulting in the plasmid pBS*lipAsslipA* (2.2, Tab. 2.2). The pBSMul1*lipA*_SP for signal peptide-toolbox screening (Brockmeier, 2006) was constructed by deletion of the *Hin*dIII restriction site downstream of the *lipA* gene using the primer pair Δ*Hin*dIII_Cterm_fw and Δ*Hin*dIII_Cterm_rev (2.3; Tab. 2.3) on the pBSMul1*lipAsslipA* and reinsertion of *Hin*dIII upstream of the *sslipA* sequence with the primer pair *Hin*dIII_Nterm_fw and *Hin*dIII_Nterm_rev (2.3; Tab. 2.3). For pBSMul1*lipAssvpr* construction, the *vpr* gene was amplified from the *B. subtilis* 168 genome using the primer vpr_*Hin*dIII_fw and vpr_*Eco*RI_rev (2.3; Tab. 2.3) and cloned into the pBSMul1*lipA*_SP. The plasmid pBS*lipBsslipB* for *lipB* expression was constructed using Gibson Assembly (Gibson *et al.*, 2009). The *lipBsslipB* gene was amplified by Phusion® Standard PCR (2.10.1) from *B. subtilis* 168 genomic DNA using the primer GA_*lipBsslipB*_fw and GA_*lipBsslipB*_rev. The so generated *lipBsslipB* PCR product possessed primer mediated homologous regions complementary to the *Nde*I hydrolyzed pBSMul1. Using the Gibson Assembly reagent Master mix (2.8) the *lipBsslipB* PCR product and the linearized pBSMul1 were ligated resulting the *pBSlipBsslipB* (2.2, Tab. 2.2).

2.12.1.Generation of *lipA* site saturation mutagenesis library

(Fulton *et al.*, 2015; Nov, 2012)

QuikChange® PCR for SSM was done as explained in section 2.10.2 using the pBS*lipAsslipA* and the degenerated primer oligonucleotides containing an universal codon `NNS` designed in this study (see appendix). While N contains an equimolar mix of all dNTPs and S an equimolar mix of dCTP and dGTP, this results in 32 possible codons coding for all naturally occurring amino acids and the amber stop codon (TAG). *E. coli* DH5α was transformed with the *Dpn*I hydrolyzed, desalted and concentrated QuikChange® PCR product (2.10.2) by electroporation (2.9.2). In a second step, the mutagenesis vectors were isolated from 2,000-4,000 *E. coli* clones (2.6) and *B. subtilis* TEB1030 was transformed by protoplast formation (2.9.3). To achieve a library coverage of about 99.9 %, 184 *B. subtilis* TEB1030 transformants were picked for each mutated amino acid positions, which corresponds to a six times oversampling recommended by (Reetz *et al.*, 2008). Subsequent recalculation of the library size of 184 transformants was performed using TopLib (http://stat.haifa.ac.il/~yuval/toplib/) (Nov, 2012) assuming a mutagenesis yield of 90 %.

2.12.2.Site directed mutagenesis of *lipA* and *lipB*

Site directed mutagenesis of *lipA* and *lipB* was performed as described in section 2.12.1, using the expression vectors pBS*lipAsslipA* and pBS*lipBsslipB* and designed oligonucleotides with the desired codon (2.3; Tab. 2.3). Since a specific codon substitution was expected, resulting mutagenesis vectors were isolated from only few single clones and verified by sequencing (2.14).

2.13. Construction of *E. coli* lipase purification vectors

Vectors generated and used in this study are listed in 2.2; Tab. 2.2. The plasmid backbone for all *E. coli* BL21(DE3) expression constructs was the pET-22b (+) (Novagen, Darmstadt). The pET22*lipBΔss*-his was constructed by *Xba*I/*Xho*I cloning of the *lipB* gene into the pET-22b (+) (2.8) without a signal sequence. The *lipB* gene was amplified by Phusion® Standard PCR (2.10.1) from *B. subtilis* 168 genomic DNA using the primer *Xba*I_*lipB*_fw and *Xho*I_*lipB*_rev (2.3; Tab. 2.3).

2.14. DNA sequencing

DNA sequencing was performed by LGC genomics (Berlin) and MWG Eurofins (Ebersberg).

2.15. Heterologous *lipA* and *lipB* expression in *E. coli* BL21(DE3) and chromatographic purification of LipA and LipB

2.15.1.Heterologous *lipA* and *lipB* expression in *E. coli* BL21(DE3)

E. coli BL21(DE3) was transformed with pET22*lipAΔss*-his, pET22*lipAΔss* or pET22*lipBΔss*-his by electroporation (2.9.2). A single colony was cultivated in 25 ml LB_{Amp100} medium at 37 °C, 120-130 rpm for 16 h. *E. coli* BL21(DE3) expression culture was inoculated from this preculture to an $O.D._{580\ nm}$ of 0.05 in 500 ml LB_{Amp100} medium. Gene expression of *lipA* and *lipB* was induced by addition of 0.4 mM IPTG (Isopropyl β-D-1-thiogalactopyranoside; final concentration) dissolved in 70 % (v/v) EtOH at an $O.D._{580\ nm}$ 0.5-0.7. Expression was carried out at 37 °C, 120-130 rpm for 16 h. The cells were harvested by centrifugation at 4 °C, 6,000 *g* for 20 min and the supernatant was discarded. The subsequent procedure for purification is described in section 2.15.2 and 2.15.3.

2.15.2. Hydrophobic and Cation Exchange Chromatography of LipA for polyclonal antibody production

Modified according to (Eggert, 2001)

For LipA purification via Hydrophobic Interaction Chromatography (HIC) and Cation Exchange Chromatography (CEC) LipA coded on the *E. coli* expression vector pET22*lipAΔss*, without a His-tag was used. After *lipA* expression and LipA production (2.15.1) the pellet was resuspended in 15 ml HIC equilibration buffer (10 mM Kp_i pH 8) per gram of wet-weight cells. The resuspended cells were incubated at 4 °C, swinging for 16 h. The cells were disrupted using the FrenchPress Cell disrupter (Thermo Electron Corporation, Dreieich) as recommended by the manufacturer (3 passages, 500 psi). The suspension containing the disrupted cells was centrifuged at 4 °C, 6,000 *g* for 20 min to remove cell debris. All following steps were carried out at RT.

Hydrophobic Interaction Chromatography (HIC) The supernatant was applied on an equilibrated (HIC equilibration buffer) Phenyl Sepharose fast-flow high sub column (GE Healthcare Deutschland, Solingen) using the Äkta Explorer (Pharmacia Deutschland, Freiburg). The column was washed with HIC wash buffer (10 mM Kp_i pH 8, 30 % (v/v) ethylene glycol) until no further protein was detected with the 280 nm detector. LipA was eluted in 2 ml fractions from the column using the HIC elution buffer (10 mM Kp_i pH 8, 80 % (v/v) ethylene glycol). Fractions with LipA activity (2.17) were pooled and diluted 1:1 with CEC equilibration buffer (50 mM HEPES pH 7.5) for direct purification via Cation Exchange Chromatography.

Cation Exchange Chromatography (CEC) The Sulphopropyl sepharose fast-flow column (GE Healthcare Deutschland, Solingen) was equilibrated with CEC equilibration buffer (50 mM HEPES pH 7.5) to a pH 7.5. The diluted LipA elution from the HIC was applied on the CEC column using the Äkta Explorer (Pharmacia Deutschland, Freiburg). Unspecifically bound proteins were washed off using the CEC wash buffer (50 mM HEPES pH 7.5) until no further protein was detected with the 280 nm detector. Subsequent LipA elution was performed using CEC elution buffer with 200-300 mM NaCl (50 mM HEPES pH 7.5, 200 mM-300 mM NaCl). LipA was eluted in 2 ml fractions from the column using the CEC elution buffer. Fractions were tested for LipA activity (2.17) and active LipA containing fractions were pooled and buffered in storage buffer (10 mM glycine pH 11) using the Vivaspin 20 (MWC 10,000) (Sartorius AG, Göttingen).

2.4 mg total amount of purified LipA were used for polyclonal antibody production in rabbits using the 3-month procedure including 4 injections and bleedings (antibody number: DE13202) (Eurogentec Deutschland, Cologne). LipA antibody was tested for specificity and crossreaction using purified LipA (2.15.3) and whole cells of *B. subtilis* TEB1030 producing LipA.

2.15.3. Immobilized Metal Ion Affinity Chromatography (IMAC) of LipA and LipB for ELISA standards

For LipA and LipB purification via Immobilized Metal Ion Affinity Chromatography (IMAC), LipA and LipB coded on the *E. coli* expression vector pET22*lipAΔss*-his and pET22*lipBΔss*-his with an N- (*lipA*) or C- (*lipB*) terminal 6xHis-tag was used. After *lipA* and *lipB* expression and LipA and LipB production (2.15.1) the pellet was resuspended in 15 ml lysis buffer (50 mM NaH_2PO_4, 300 mM NaCl, 10 mM imidazole, pH 8) with 2 mg/ml lysozyme per gram of wet-weight cells. The resuspended cells were incubated at 4 °C, swinging for 30 min. The cells were disrupted using the FrenchPress Cell disrupter (Thermo Electron Corporation, Dreieich) as recommended by the manufacturer (3 passages, 500 psi). The suspension containing the disrupted cells was centrifuged at 4 °C, 6,000 *g* for 20 min to remove cell debris. The supernatant was used for IMAC. All following steps were carried out at RT. The Ni-NTA agarose (Qiagen, Hilden) was equilibrated with 3-fold of the column volume with lysis buffer and resuspended in 3 ml of lysis buffer. This Ni-NTA agarose-lysis buffer solution was added to the supernatant and incubated at 4 °C, swinging for 30 min. This solution was applied on a 10 ml PIERCE® Centrifuge Columns (Thermo Fisher Scientific Germany, Dreieich). The column was washed with washing buffer containing 20 mM imidazole (elution buffer diluted 12.5-fold with lysis buffer) 10 times with 3-fold column volume to remove unspecifically bound proteins. LipA or LipB, respectively, were eluted in 1 ml fractions with a total volume of 5 ml elution buffer (50 mM NaH_2PO_4, 300 mM NaCl, 250 mM imidazole, pH 8). Fractions with protein concentrations above 1 mg/ml (2.16) were pooled and buffered in storage buffer (10 mM glycine pH 11) using desalting PD-10 columns (GE Healthcare Deutschland, Solingen) as recommended by the manufacturer. The final protein concentration was determined as described in 2.16. Purified LipA and LipB were diluted to a final concentration of 0.6 mg/ml and split into 200 µl aliquots for usage as ELISA standard stock solutions (2.21).

2.16. Determination of protein concentration

Protein concentrations were determined with the Pierce™ Coomassie Plus (Bradford) Assay Kit (Thermo Fisher Scientific Germany, Dreieich) as recommended by the manufacturer.

2.17. Lipolytic activity assay

(Winkler & Stuckmann, 1979)

For detection of lipolytic activity of LipA, *p*-nitrophenyl-palmitate (*p*NPP) (Sigma Aldrich, Munich) was used as the substrate.

0.8 mM *p*-nitrophenyl-palmitate was dissolved in isopropanol and pre-warmed to 37 °C as well as 103.5 mg sodium desoxycholate and 50 mg gum arabic dissolved in 50 ml Sørensen phosphate buffer. Both prewarmed solutions were mixed and added to 10 µl sample. For Sørensen phosphate buffer pH 8, solution A (50 mM Na_2HPO_4) and solution B (50 mM KH_2PO_4) were diluted 17:1.

Lipase activity assays were performed in 96-well microtiter plates (Brand GmbH, Wertheim) with 190 µl of mixed substrate solution, absorbance at 410 nm was recorded in a time-dependent measurement at 37 °C for 15 min in a SpectraMax 250 (Molecular Devices, Biberach an der Riss) in intervals of 15 sec. The slope of all measurement points is determined by $O.D._{410\ nm}$/min. The lipolytic activity in U/ml is calculated as described below:

$$U/ml = \frac{dE/min * tV * F}{d * \varepsilon_{410\ nm} * sV}$$

dE/min: absorption alteration per minute = $O.D._{410\ nm}$/min

tV: total volume = 0.2 ml

F: dilution factor = 4 (screening 2.22); 2 (characterization 2.23)

$\varepsilon_{410\ nm}$: extinction coefficient of *p*-nitrophenolate= 15 ml/µmol*cm (Brockmeier, 2006)

d: optical path length = $V/r^2 * l/\pi$= 0.625 cm

sV: sample volume= 0.01 ml

2.18. TCA-NaDoc precipitation

Modified according to (Peterson, 1977)

100 µl cold 10 % (w/v) NaDoc (sodium desoxycholate) is added to 1 ml sample and incubated on ice for 10 min. After addition of 100 µl cold 40 % (v/v) TCA and incubation on ice for 20 min, the sample was centrifuged at 4 °C, 21,000 *g* for 30 min. The supernatant was discarded and the pellet containing the proteins was washed with 500 µl 80 % (v/v) acetone. After discarding the supernatant, the pellet was dried for 5 min. The pellet was resuspended in 50 mM Tris-HCl pH 8 and 2x SDS sample buffer (2.19) to an $O.D._{580\ nm}$ = 15 for SDS-PAGE with the BioRad System and $O.D._{580\ nm}$= 1.25 for SDS-PAGE with the Novex™-System (2.19).

2.19. SDS polyacrylamide gel electrophoresis (SDS-PAGE)

The separation of proteins according to their molecular weight was accomplished by SDS-PAGE. Denaturing conditions were achieved in the presence of SDS in a discontinuous (BioRad) and a continuous (Novex™) gel system. Samples were resuspended in 2x SDS-PAGE sample buffer (50 mM Tris-HCl pH 6.8, 4 % (w/v) SDS, 10 % (v/v) glycerol, 2 % (v/v) β-mercaptoethanol, 0.03 % (w/v) Bromphenol blue), boiled at 98 °C for 10 min and loaded onto the SDS gel. The molecular weight standard PageRuler™ Prestained Protein Marker (Thermo Fisher Scientific Germany, Dreieich) was used for size determination. The separated proteins were detected by qualitative immunodetection (2.20).

SDS-PAGE BioRad System (Laemmli, 1970)

Boiled samples were loaded onto a 5 % stacking gel (2.8 ml A. dest., 0.83 ml 37 % (v/v) acrylamide, 1.3 ml Tris-HCl pH 6.8 (0.5 M), 50 µl 10 % (w/v) SDS, 50 µl 10 % (w/v) APS, 5 µl TEMED) on top of a 16 % separation gel (2.1 ml A. dest., 5.3 ml 37 % (v/v) acrylamide, 2.5 ml Tris-HCl pH 8.8 (0.5 M), 100 µl 10 % (w/v) SDS, 100 µl 10 % (w/v) APS, 10 µl TEMED).

Discontinuous SDS-gel electrophoresis was carried out at 100 V for 15 min and at 200 V for 40 min using the gadget „Mini Protean II Dual Slap Cell“ (BioRad Laboratories GmbH, Munich) and 1 x SDS running buffer (0.025 M Tris, 0.2 M glycine, 0.003 M SDS ultra pure).

SDS-PAGE Novex™-System

Boiled samples were loaded onto a continuous NuPAGE® Novex® 4-12 % Bis-Tris Protein Gel (Thermo Fisher Scientific, Braunschweig). SDS-gel electrophoresis was carried out at 200 V for 60 min in the Xcell SureLock® (Thermo Fisher Scientific Germany, Dreieich) and 1 x MES running buffer (2.5 mM MES, 2.5 mM Tris, 0.005 % (w/v) SDS, 0.05 mM EDTA, pH 7.3).

2.20. Qualitative immunodetection of proteins *via* Western Blot

(Dunn, 1986)

Proteins from SDS gels were electrophoretically transferred at 150 mA for 15 min, and at 300 mA for 60 min onto a polyvinylidene difluoride (PVDF) membrane in a Mini-Protean 3 Cell (BioRad Laboratories GmbH, Munich) in 1 x Dunn carbonate buffer (0.003 M Na_2CO_3, 0.01 M $NaHCO_3$) with 20 % (v/v) methanol. The PVDF membranes were washed in methanol and A. dest. for one minute before protein transfer. The membrane was blocked with 3 % (w/v) bovine serum albumin dissolved in 0.2 % 1 x TBST (0.025 M Tris, 0.15 M NaCl, 0.0015 M KCl, 0.02 % (v/v) Tween 20) at 4°C for 16 h. The membranes were incubated with a specific polyclonal LipA antibody (Eurogentec Deutschland, Cologne) (2.15.2) or LipB antibody (Eggert, 2001) in dilution of 1:20,000 ($O.D._{580\ nm}$= 15) or in dilution of 1:5,000 ($O.D._{580\ nm}$= 1.25) and a second antibody goat-anti- rabbit HRP conjugate (BioRad Laboratories GmbH, Munich) in dilution 1: 5,000 in 0.2 % 1x TBST for 1h. After each antibody incubation step the membranes were washed in 0.2 % 1x TBST at RT for 30 min and 3 x 10 min. All incubation steps were accomplished on an orbital mixer. Signals were detected using freshly prepared ECL solution and the Stella X software (Raytest, Straubenhardt). The ECL solution is prepared by mixing 1 ml of 4°C cold solution A (0.025 % (w/v) luminol, 0.1 M Tris-HCl pH 8.6) with 100 µl solution B (0.1 % (w/v) light sensitive *p*-hydroxy coumarate in 100% DMSO) and 0.3 µl solution C (30 % H_2O_2).

2.21. Quantitative immunodetection of proteins *via* ELISA

For quantitative detection of LipA an Enzyme-Linked Immunosorbent Assay (ELISA) using a specific polyclonal LipA antibody (Eurogentec Deutschland, Cologne) (2.15.2) or LipB antibody (Eggert, 2001) was performed. The samples were diluted in 100 µl bicarbonate buffer (0.03 M Na_2CO_3, 0.07 M $NaHCO_3$ pH 9.6) (2.22, 2.23) and coated onto Polysorp®- 96-well microtiter plates (Thermo Fisher Scientific Germany, Dreieich) using the TECAN® robot system freedom evo (Tecan Group Ltd., Männedorf). After incubation at 4 °C, 100 rpm for 22 h and three times of washing with PBS (powder, pH 7.4; Sigma Aldrich, Taufkirchen), blocking with 1 % (w/v) bovine serum albumin diluted in PBS was performed at 22 °C, 150 rpm for 2.5 h followed by two additional washing steps with PBS. The polyclonal LipA or LipB antibody was diluted 1:5,000 in PBS and incubated at 22 °C, 150 rpm for 2 h, followed

by four times of washing with PBS. After another 3 h incubation with the goat-anti-rabbit HRP conjugate (BioRad Laboratories GmbH, Munich) diluted 1:5,000 in PBS, the microtiter plate was finally washed four times with PBS. Spectrophotometric indirect LipA quantification was carried out using the 1-step TMB ELISA substrate (3,3´,5,5´-tetramentylbenzidine; Thermo Fisher Scientific Germany, Dreieich) at 25 °C for 15 min in the SpectraMax 250 (Molecular Devices, Biberach an der Riss). Total amount of LipA or LipB in a given sample was calculated using an appropriate standard curve of purified LipA or LipB (2.15.3).

2.22. Screening for increased extracellular LipA activity and amount

The site saturation mutagenesis library using the *B. subtilis* expression vector pBS*lipAsslipA* (2.2, Tab. 2.2) was constructed as described in section 2.12.1. After that, a two-step screening procedure was applied.

Step I For screening of the *lipA* mutagenesis library, 184 transformants for each of the substituted amino acid position, as well as internal standards (Tab. 2.9), were freshly picked from *B. subtilis* protoplast regeneration plates (2.9.3) into 96-well microtiter plates (Greiner Bio-one, Frickenhausen) and cultivated as described in section 2.4.

Tab. 2.9 Overview of microtiter plate internal standards screening Step I.

plasmid	abbreviation	well number	function
pBSMul1	ev	E6, D7	lipase negative control
pBS*lipAsslipA*	*lipA*	A12,H1	lipase positive control

After *lipA* expression and LipA production at 25 °C, 900 rpm for 16 h the cultures were diluted 4-fold with LB medium in a 96-well v-cavity microtiter plate (Greiner Bio-one, Frickenhausen). After determination of $O.D._{580\ nm}$, the cells were harvested at 4 °C 2,000 *g* for 30 min. 10 µl of the culture supernatant was applied for a lipolytic activity assay (2.17).

Expression vectors of LipA clones with increased extracellular lipase activity were isolated from *B. subtilis* TEB1030 (2.6), sequenced (2.14) and *B. subtilis* TEB1030 was retransformed by protoplast formation (2.9.3).

Step II LipA clones were analyzed again for increased extracellular LipA activity as described above as three biological replicates. Again internal standards were also applied (Tab. 2.10), as well as empty cavities for application of purified LipA (2.15.3) as ELISA standard.

Tab. 2.10 Overview of MTP internal standards screening Step II.

plasmid	abbreviation	well number	function
pBSMul1	eV	A10-A12; B10-B12	lipase negative control
pBS*lipAsslipA*	*lipA*	C10-C12; D10-D12	lipase positive control
Empty cavities for ELISA standards	-	G1-G12; H1-H12	Purified LipA for extracellular LipA quantification

Additionally, the cultures were diluted 8-fold in 100 µl bicarbonate buffer (0.03 M Na_2CO_3, 0.07 M $NaHCO_3$ pH 9.6) in a 96-well v-cavity microtiter plate (Greiner Bio-one, Frickenhausen) and centrifuged at 4 °C, 2,000 *g* for 30 min. The culture supernatant was diluted 3.2-fold using the TECAN® robot system freedom evo (Tecan Group Ltd., Männedorf) and coated on Polysorp®- 96-well microtiter plates (Thermo Fisher Scientific Germany, Dreieich) as described in 2.21.

Purified LipA (2.15.3) was applied in a 2-fold dilution series, from 5 µg to 0.08 µg as a standard for quantification of LipA in the *B. subtilis* TEB1030 culture supernatant.

2.23. LipA and LipB variant characterization

B. subtilis TEB1030 was retransformed by protoplast formation (2.9.3) with expression vectors of LipA variants from screening (2.22) and with expression vectors from site directed mutagenesis of *lipA* and *lipB* (2.12.2).

Three biological replicates were freshly picked from *B. subtilis* protoplast regeneration plates into 48-well FlowerPlates® (FlowerPlate® (48 well MTP) without optodes, m2p-labs, Baesweiler) and cultivated as described in section 2.4.

Lipolytic activity assay After *lipA* or *lipB* expression and lipase production at 37 °C, 1,100 rpm for 6 h the cultures from 48-well FlowerPlates® were diluted 2-fold with LB medium in a 96-well v-cavity microtiter plate (Greiner Bio-one, Frickenhausen). This plate was used for determination of $O.D._{580\ nm}$ and afterwards the cells were harvested at 4 °C, 2,000 *g* for 30 min. 10 µl of the diluted culture supernatant was applied for a lipolytic activity assay (2.17).

ELISA For quantitative immunodetection *via* ELISA the cultures were also diluted 2-fold in 100 µl bicarbonate buffer (0.03 M Na_2CO_3, 0.07 M $NaHCO_3$ pH 9.6) in a second 96-well v-cavity microtiter plate (Greiner Bio-one, Frickenhausen). The cells were harvested by

centrifugation at 4 °C, 2,000 *g* for 30 min. The prediluted culture supernatant in bicarbonate buffer was diluted 3.2-fold using the TECAN® robot system freedom evo (Tecan Group Ltd., Männedorf) and coated on Polysorp®- 96-well microtiter plates (Thermo Fisher Scientific Germany, Dreieich) as described in 2.21.

Purified LipA (2.15.3) was applied diluted 2-fold, from 5 µg to 0.08 µg as a standard for quantification of LipA in the *B. subtilis* TEB1030 culture supernatant.

Western Blot 70 µl of each culture from 48-well FlowerPlates® were centrifuged at RT, 21,000 *g* for 10 min. The culture supernatant was applied for a TCA-NaDoc precipitation (2.18), the sample was adjusted to $O.D._{580\ nm}$ of 1.25 and analyzed using the SDS-PAGE Novex™-System (2.19) and qualitative immunodetection *via* Western Blot (2.20).

Real time PCR 500 µl of each culture from 48-well FlowerPlates® were centrifuged at RT, 21,000 *g* for 10 min. The supernatant was discarded and the pellet was treated for RNA isolation and subsequent quantitative real time PCR (2.11).

2.24. Computational methods

Analyses of DNA, amino acid sequences and construction of plasmid maps were performed using CloneManager9 (Scientific and Educational Software, USA).

Primer3 (Untergasser *et al.*, 2012) was used for oligonucleotide design for quantitative real time PCR.

Visualization of signals for protein immunodetection was performed with the Stella X software (Raytest, Straubenradt) and the AIDA Image Analyzer (Raytest, Straubenradt).

Gene expression analysis was performed using the REST 2009 software (Qiagen, Hilden).

Data calculation was performed using Microsoft Excel, for data visualization Prism5 and Microsoft PowerPoint was used.

For multiple sequence alignment ClustalW (Sievers *et al.*, 2011) and UniProt (Consortium, 2008) was used. Protein sequences for LipA multiple sequence alignment were obtained from the Pfam database (http://pfam.xfam.org) (Finn *et al.*, 2014).

3D protein structure modelling was carried out using SwissModel (Biasini *et al.*, 2014) for generation and YASARA View (Krieger *et al.*, 2004) for visualization.

3. Results and Discussion

3.1. Constitutively produced LipA is highly secreted by *B. subtilis* at the end of the exponential growth phase

Bacillus subtilis is commonly used as a microbial cell factory for high level protein production. Former approaches aimed at the optimization of the different protein production steps in *B. subtilis* which are considered as bottlenecks for efficient production (1.6), but these approaches did not pay attention to the target protein itself. This is known to influence its production and secretion in different ways (1.7) and therefore should also be considered for improvement of secretory protein production in *B. subtilis*. The *B. subtilis* lipase A (LipA) was chosen for this systematic analysis of single amino acid substitutions on homologous LipA production and secretion in *B. subtilis*. In order to produce detectable amounts of LipA by *B. subtilis*, the *lipA* gene was placed under control of the strong constitutive P_{HpaII} promoter on the *E. coli-B. subtilis* shuttle vector pBSMul1 (Brockmeier, 2006) (2.2; 2.12). This vector harbors the coding sequence of the LipA signal peptide (*sslipA*) for secretion of the adjacently coded inserted target protein. In frame fusion of the target protein gene sequence is mediated using the restriction enzyme *Eco*RI and resulted in a short spacer sequence of six base pairs respresenting the *Eco*RI restriction site between the *sslipA* gene and the target protein coding gene. Concerning the construction of the pBS*lipAsslipA* to generate the native, wild-type LipA (wtLipA), the *Eco*RI restriction site between the *sslipA* sequence and the *lipA* gene was subsequently deleted by QuikChange® PCR (2.10.2) to avoid the two additional amino acids at the LipA N-terminus coded by the recognition sequence of *Eco*RI (glutamic acid and phenylalanine) which could falsify single substitution analysis. The strain *B. subtilis* TEB1030 which lacks two lipolytic enzymes LipA and LipB was used as a production strain to avoid basal lipolytic activity (Tab. 2.1). It was transformed by protoplast formation (2.9.3) with the resulting pBS*lipAsslipA* for LipA production analysis and with the corresponding empty vector pBSMul1. *B. subtilis* TEB1030 was cultivated as three biological replicates in a microfermentation system using a 48-well FlowerPlate®for 24 h (2.4). In parallel, a growth curve of *B. subtilis* TEB1030 harboring the empty vector pBSMul1 and the *lipA* expression vector pBS*lipAsslipA* was monitored in a second 48-well FlowerPlate® in the BioLector® (2.4) to evaluate *B. subtilis* TEB1030 growth when constitutively expressing homologous *lipA*. Samples were taken 2, 4,

6, 8, 10 and 24 h after cultivation start to analyze LipA production within the cells (WC) and LipA secretion into the culture supernatant (S) using a lipolytic activity assay (2.17). Because *lipA* is expressed with a constitutive promoter (P_{HpaII}) LipA production does not need to be induced, but directly starts with growing of the cells. Fig. 3.1A shows the optical density of *B. subtilis* TEB1030 at 600 nm harboring the empty vector and producing LipA cultivated for 24 h in the BioLector® plotted on the left y-axis and the lipolytic volume activity at defined time points of cultivation normalized to the optical density at 600nm on the right y-axis. Comparing the growth of non-LipA producing *B. subtilis* TEB1030 (ev) with the LipA producing *B. subtilis* TEB1030 (LipA) a slight delay in growth could be observed when the cells produce LipA. While the non-LipA producing cells reach an $O.D._{600\ nm}$ of 2 after about 4 h of cultivation, LipA producing cells reach the same optical density 0.5 h later. This slight delay could be due to the cells metabolism switching to gene expression and protein production, which means that energy for biomass generation is bypassed for LipA production. This `metabolic burden` phenomenon known from heterologous protein production in *E. coli* describes the exhaustion of amino acids and nucleotides as prescursors for energy and biomass from the cellular metabolism for recombinant protein synthesis (Bhattacharya & Dubey, 1995; Carneiro *et al.*, 2013; Glick, 1995; Rahmen *et al.*, 2015b). Although LipA is a homologous protein, it is possible that the strong and constitutive production of LipA with the recombinant P_{HpaII} promoter needs higher energy resources as native production and so leading to the slightly growth delay in the exponential growth phase.

As shown by the lipolytic activity of LipA ((U/ml)/$O.D._{600\ nm}$) in whole cells, LipA is already detectable after 2 h of production (0.003 ± 0.006 (U/ml)/$O.D._{600\ nm}$). The extracellular lipase activity further increases from 10 h (0.050 ± 0.008 (U/ml)/$O.D._{600\ nm}$) to 24 h of LipA production (0.120 ± 0.016 (U/ml)/$O.D._{600\ nm}$) as well as the intracellular activity that reaches nearly the same value (0.100 ± 0.010 (U/ml)/$O.D._{600\ nm}$). This indicates that the still produced LipA accumulates in the cytoplasm or the membrane-cell wall interface and is no longer efficiently secreted. That could be explained by a reduced Sec secretion necessary in the stationary growth phase of *B. subtilis*. This hypothesis is supported by the finding that gene expression of Sec components like SecY, SecA and the signal recognition particle components Ffh and FtsY is drastically lowered in the stationary phase (Nicolas *et al.*, 2012).

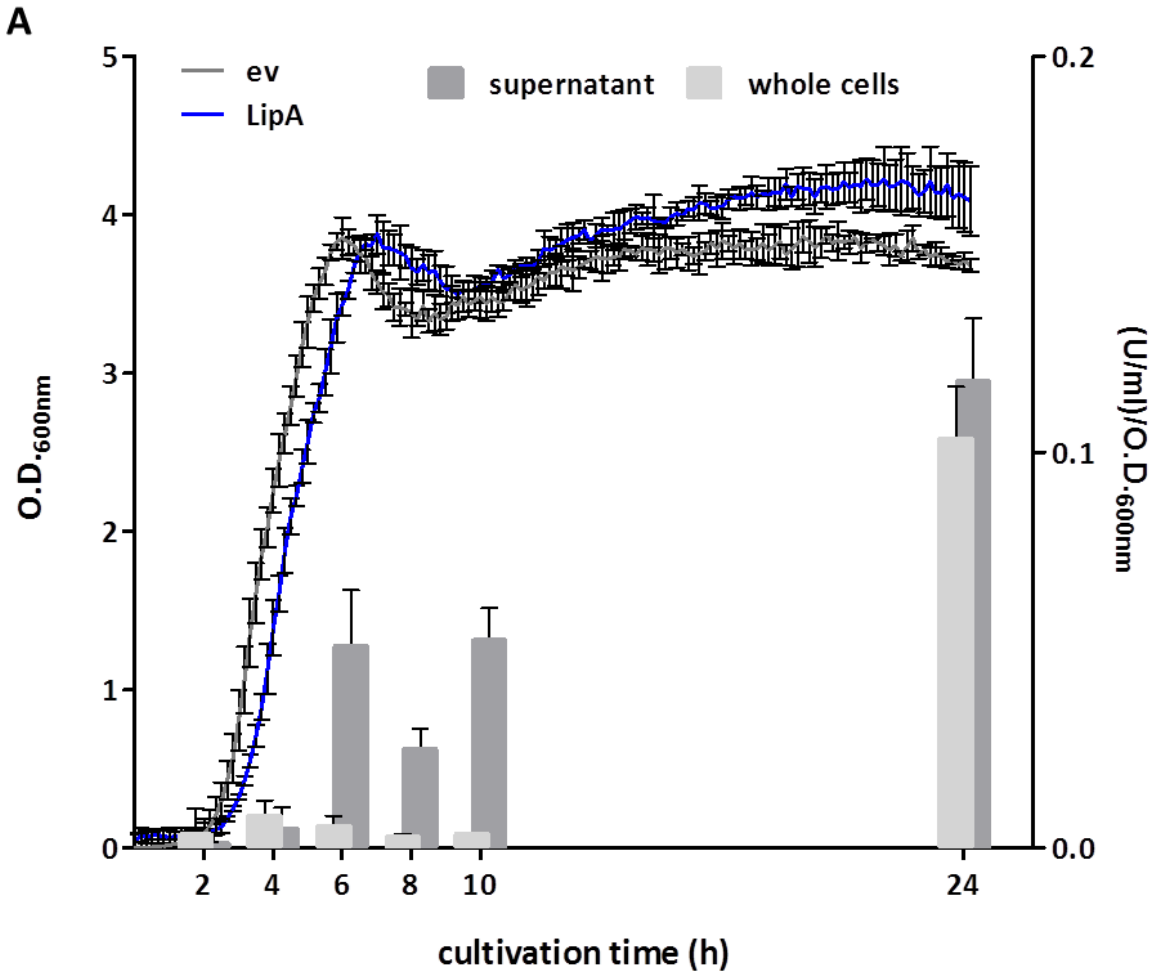

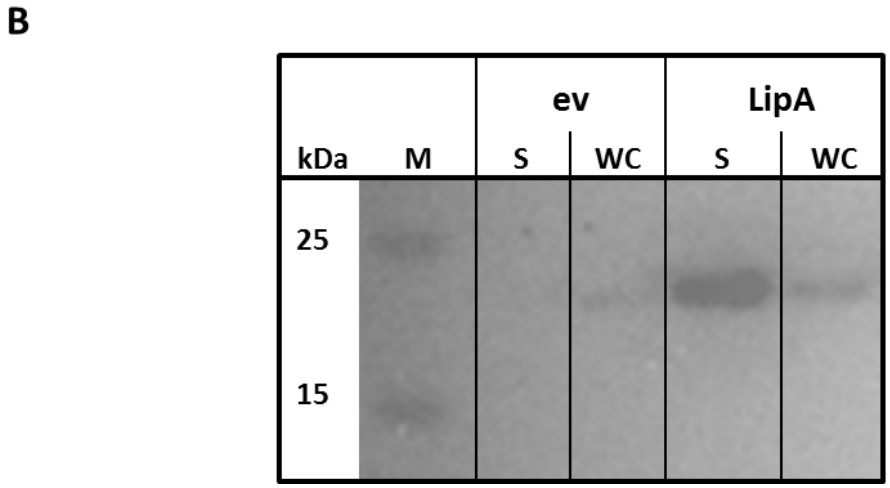

Fig. 3.1 Characterization of wild-type LipA production in *B. subtilis* TEB1030.
A Wild-type LipA production analysis in *B. subtilis* TEB1030. *B. subtilis* TEB1030 producing wtLipA was cultivated in a microfermentation system using a 48-well Flowerplate® for 24 h and online biomass measurement was performed in the BioLector®. The cultivation time (h) is plotted against the optical density at 600 nm on the left handed y-axis and against the lipolytic volume activity normalized to the optical density ((U/ml)/O.D.$_{600\ nm}$). The lines with error bars show *B. subtilis* TEB1030 growth when not producing LipA (ev; grey) and producing wtLipA (blue line) (O.D.$_{600\ nm}$). After 2, 4, 6, 8, 10 and 24 h of cultivation samples were taken to determine the lipase activity in the *B. subtilis* culture supernatant (bars in dark grey) and the *B. subtilis* whole cells (bars in light grey) that was normalized to the *B. subtilis* cell density at the corresponding

sampling time point. **B Western Blot analysis of *B. subtilis* whole cells and culture supernatant after 6 h of wtLipA production.** 10µl of the precipitated proteins from the culture supernatant and the whole cells ($O.D._{600\,nm}$ of 15) were applied on a 16 % discontinuous SDS gel. Immunodetection was performed using a specific polyclonal LipA antibody.

Native produced LipA is synthesized with a N-terminal signal peptide and is secreted cotranslationally into the *B. subtilis* culture supernatant (Zanen *et al.*, 2006), this secretion is confirmed for plasmid-based LipA production as it can be seen from the lipase activity of 0.050 ± 0.010 (U/ml)/$O.D._{600\,nm}$ in the culture supernatant after 6 h of production. Correlating with the decline in growth at the beginning of the stationary growth phase, the extracellular lipase activity drops after 8 h of LipA producing *B. subtilis* TEB1030 cultivation (0.020 ± 0.003 (U/ml)/$O.D._{600\,nm}$). Due to the fact that this decrease in *B. subtilis* TEB1030 growth could also be observed for the non-LipA producing *B. subtilis* TEB1030 it is a general *B. subtilis* growth behavior and not promoted by LipA production. *B. subtilis* is known for its so called multicellularity, which means that several subpopulations of different cell species can exist in one culture (Shank & Kolter, 2011). Probably during transition to the stationary growth phase *B. subtilis* differentiate into this subpopulations resulting in different cell morphologies and an altered absorption at 600 nm leading to this short decline in growth. After 10 h of cultivation the cell starts growing again and the extracellular lipase activity reaches its maximum (0.050 ± 0.008 (U/ml)/$O.D._{600\,nm}$) whereas the smallest amount of LipA is detected intracellularly (0.003 ± 0.001 (U/ml)/$O.D._{600\,nm}$). Here 98 % of the produced LipA is secreted and only 2 % remained in the cells.

This detailed analysis of wild-type LipA production was necessary to identify the optimal time point for the later presented production and secretion analysis of LipA variants that were generated (2.12.1) and screened (2.22) to identify beneficial different single amino acid and codon substitutions for production and secretion. Here, a time point is needed that first, allows the visualization of only slight differences between the different LipA variants and second, provides most efficient secretion. Additionally, an analysis within the stationary growth phase should be avoided due to the already mentioned *B. subtilis* multicellularity that also includes sporulation (Shank & Kolter, 2011) and could promote cell-to-cell differences in the analysis measurements. In contrast to the LipA production for 10 h where 98 % of the produced LipA is secreted and would therefore yield in higher extracellular detectable LipA amounts, after 6 h only 91 % (0.05 ± 0.01 (U/ml)/$O.D._{600\,nm}$) is secreted, but

here the cells are still in the exponential growth phase reducing the risk of *B. subtilis* subpopulations. The high secretion rate of LipA after 6 h of cultivation indicated by the extracellular lipase activity (Fig. 3.1A) was confirmed by immunodetection of high extracellular LipA amounts in the culture supernatant (S) and only slight amounts of LipA in the whole cells (WC) (Fig. 3.1B). Based on these results, the high LipA secretion rate after 6 h of LipA producing *B. subtilis* TEB1030 and the avoidance of sampling and analysis in the stationary growth phase, LipA variant analysis was performed after 6 h of strong constitutive LipA production by *B. subtilis* TEB1030 in a microfermentation system.

Plasmid-based *lipA* can be constitutively expressed in *B. subtilis* TEB1030. LipA production and secretion reaches its optimum after 6h of cultivation which provides a suitable time point for LipA variant characterization.

3.2. Development of a qualitative and quantitative LipA screening system

For the analysis of thousands generated *B. subtilis* TEB1030 LipA clones (2.12.1) regarding their extracellular lipase activity and extracellular lipase amount a suitable microtiterplate (MTP)-based screening system needs to be established. As already mentioned, LipA is produced from an expression vector in *B. subtilis* TEB1030 using a strong constitutive promoter (P_{HpaII}) (3.1). This avoids the need of *lipA* gene expression induction in the exponentially growth phase, but demand for identical MTP-culture inoculation and cultivation conditions to ensure comparable data sets for the screened LipA clones.

3.2.1. A suitable qualitative, activity-based screening system could be established

For optimal screening conditions several inoculation and cultivation conditions were tested for 96 *B. subtilis* TEB1030 wtLipA clones and evaluated according to the percentaged standard deviation of the measured optical density at $O.D._{580\ nm}$ and the measured volume activity (U/ml) in the 4-fold diluted *B. subtilis* TEB1030 culture supernatant (Fig. 3.2**;** Fig. 3.3). Due to the constitutive expression, LipA is directly synthesized when *B. subtilis* TEB1030 starts to grow and so each of the *B. subtilis* TEB1030 LipA clones for screening needs to be inoculated to the same optical density. Therefore, three different methods were tested to inoculate the wtLipA producing *B. subtilis* TEB1030 MTP expression culture to an $O.D._{580\ nm}$ of 0.05: a replicator, a multichannel pipette and the TECAN® robot system. The MTP-expression culture was inoculated from single LipA producing *B. subtilis* TEB1030 clones in selective LB medium. The microtiter plates were sealed with breathable foils (2.4) and cultivated at 37 °C, 900 rpm for 16 h. The smallest standard deviation of the averaged optical density (8.3 %) and a suitable deviation of extracellular lipase activity (22.6 %) resulted from 96 wtLipA clones inoculated with the TECAN® robot system (Fig. 3.2A).

Therefore, this inoculation method was chosen to identify the optimal inoculation culture, which means the preculture either inoculated from a cryo-conserved *B. subtilis* TEB1030 culture or from *B. subtilis* TEB1030 transformants from agar plates (2.9.3). Expression culture was inoculated and cultivated as described above. Only small differences (< 2 %) could be observed in the deviations determined for *B. subtilis* TEB1030 producing wtLipA inoculated from a cryo-conserved culture ($O.D._{580\ nm}$ 15.2 %; U/ml 29.2 %) and from transformants ($O.D._{580\ nm}$ 13.7 %; U/ml 28.8 %) (Fig. 3.2B).

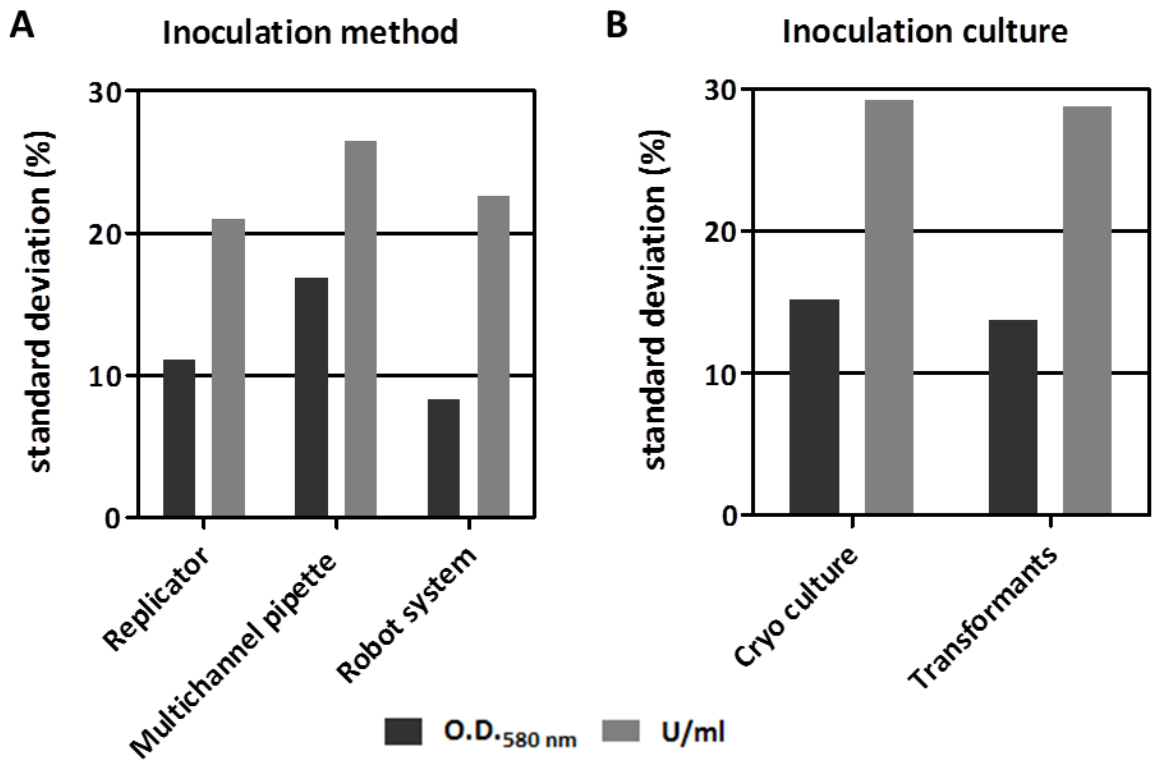

Fig. 3.2 Analyzed microtiterplate inoculation conditions.
A Inoculation method. Expression culture *B. subtilis* TEB1030 producing wtLipA was inoculated in selective LB medium to an $O.D._{580\ nm}$ of 0.05. After inoculation with a replicator, a multichannel, or the TECAN® robot system, *B. subtilis* TEB1030 producing wtLipA was cultivated at 37 °C for 16 h. The respective standard deviations (%) of the optical density ($O.D._{580\ nm}$) and of the lipolytic activity (U/ml) of 96 wtLipA clones are plotted. The TECAN® robot system was chosen and used to test the preculture inoculation shown in figure B. **B Inoculation culture.** Preculture of *B. subtilis* TEB1030 producing wtLipA was inoculated in selective LB medium from a cryo conserved culture and from *B. subtilis* TEB1030 transformants in a 96-well microtiterplate. Expression culture *B. subtilis* TEB1030 producing wtLipA was inoculated in selective LB medium to an $O.D._{580\ nm}$ of 0.05 with the TECAN® robot system and cultivated at 37 °C for 16 h. The respective standard deviations (%) of the optical density ($O.D._{580\ nm}$) and of the lipolytic activity (U/ml) of 96 wtLipA clones are plotted.

Nevertheless, preculture inoculation with *B. subtilis* TEB1030 transformants was chosen to exclude any possible long term storage effect on *B. subtilis* TEB1030 growth and production capacities due to inoculation from already freezed and partially thawed cells.

The results from wtLipA production analyses of *B. subtilis* TEB1030 cultivated in a microfermentation system (3.1) indicate that LipA secretion reaches its optimum in the exponential growth phase and provides therefore conditions to identify even slight differences in the LipA variants extracellular lipase activity and amount because metabolic active, exponentially growing cells focus their energy on a high protein synthesis rate thereby strengthening even small differences to detectable levels. In order to screen within this exponential growth phase, the growth and simultaneous LipA production of *B. subtilis*

TEB1030 *lipA* expression cultures should be kept at moderate levels during MTP cultivation. To identify moderate growth conditions, *B. subtilis* TEB1030 LipA producing MTP expression cultures were inoculated in selective LB medium with the TECAN® robot system to an $O.D._{580\ nm}$ of 0.05 from a *B. subtilis* TEB1030 transformants preculture and cultivated at 25 °C, 30 °C or 37 °C, 900 rpm for 16 h. Fig. 3.3A shows that the determined standard deviation for the optical density is the smallest for *B. subtilis* TEB1030 producing wtLipA when cultivation is performed either at 25 °C or 30 °C (both: 6.4 %) and the highest when cultivated at 37°C (13.3 %).

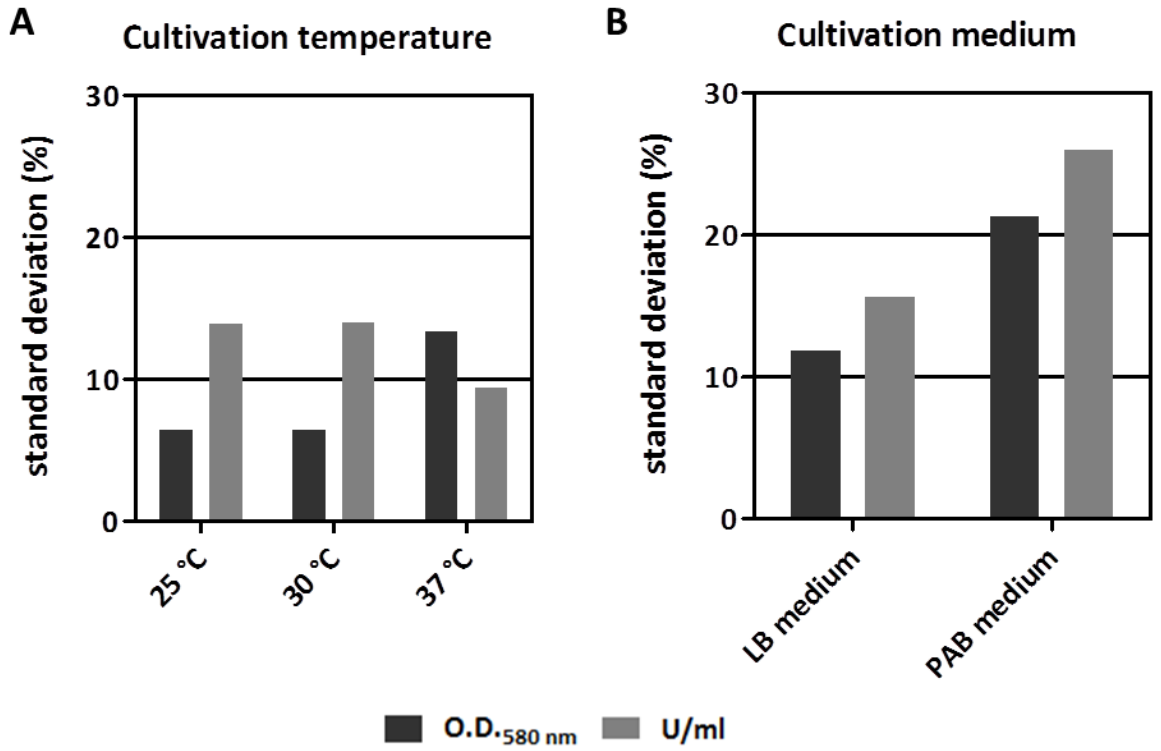

Fig. 3.3 Analyzed microtiterplate cultivation conditions.
A Cultivation temperature. Expression culture *B. subtilis* TEB1030 producing wtLipA was inoculated in selective LB medium in a 96-well microtiterplate to an $O.D._{580\ nm}$ of 0.05 with the TECAN® robot system and cultivated at 25 °C, 30 °C and 37 °C for 16 h. The respective standard deviations (%) of the optical density ($O.D._{580\ nm}$) and of the lipolytic activity (U/ml) of 96 wtLipA clones are plotted. 25 °C was chosen as the suitable cultivation temperature to identify the optimal cultivation medium in figure B. **B Cultivation medium.** Expression culture *B. subtilis* TEB1030 producing wtLipA was inoculated in selective LB as well as PAB medium in a 96-well microtiterplate to an $O.D._{580\ nm}$ of 0.05 with the TECAN® robot system and cultivated at 25 °C for 16 h. The respective standard deviation (%) of the optical density ($O.D._{580\ nm}$) and of the lipolytic activity (U/ml) of 96 wtLipA clones is plotted. LB medium was chosen as the suitable cultivation medium.

Contrary, the standard deviation of the extracellular lipase activity of wtLipA clones is reduced at 37 °C (9.4 %) compared to that of those clones synthesized at 25 and 30 °C

(13.9 %; 14 %). As explained above, the *B. subtilis* TEB1030 growth at moderate rates is the more important parameter for cultivation due to the metabolic active cells, these moderate growth is achieved by cultivation at 25°C and therefore screening of generated and produced LipA variants by *B. subtilis* TEB1030 will be carried out at 25 °C. In the last step for screening system establishment, two rich media were tested (Fig. 3.3B): the commonly used LB medium (2.4) and a so called Penassay broth medium (PAB medium), a *B. subtilis* specific rich medium usually used for *B. subtilis* cultivation when grown for protoplast formation (2.9.3). Compared to LB medium, PAB medium additionally includes beef extract, dextrose and mono- and dipotassium phosphate and could maybe promote a more reproducable and comparable *B. subtilis* growth due to enriched nutrition. However, cultivation of *B. subtilis* TEB1030 under the so far identified optimal LipA secretion and screening conditions in LB medium at 25 °C, 900 rpm for 16 h showed almost the half of the standard deviation for optical density (11.8 %) and extracellular lipase activity (15.6 %) compared to wtLipA clones cultivated in PAB medium (Fig. 3.3B) under the same conditions and is therefore used as the cultivation medium for screening of *B. subtilis* TEB1030 LipA clones.

In a final experiment, the best of each tested conditions (Fig. 3.2; Fig. 3.3), were combined to analyze 384 *B. subtilis* TEB1030 wtLipA clones (**Fig. 3.4**), in order to verify the developed screening system and to determine the *B. subtilis* TEB1030 wtLipA standard deviation for optical density and extracellular lipase activity, as a cutoff value to later identify LipA variants with increased extracellular lipase activity. Therefore, precultures for 384 *B. subtilis* TEB1030 wtLipA clones were inoculated from transformants, the MTP-expression culture was inoculated with the TECAN® robot system to an $O.D._{580\ nm}$ of 0.05 in selective LB medium and cultivated at 25 °C, 900 rpm for 16 h (2.4). As shown in **Fig. 3.4** from analysis of 384 *B. subtilis* TEB1030 wtLipA clones a standard deviation of 20.4 % for optical density and 18.7 % for extracellular lipase activity was determined, which are acceptable deviations for a microtiterplate-based screening system.

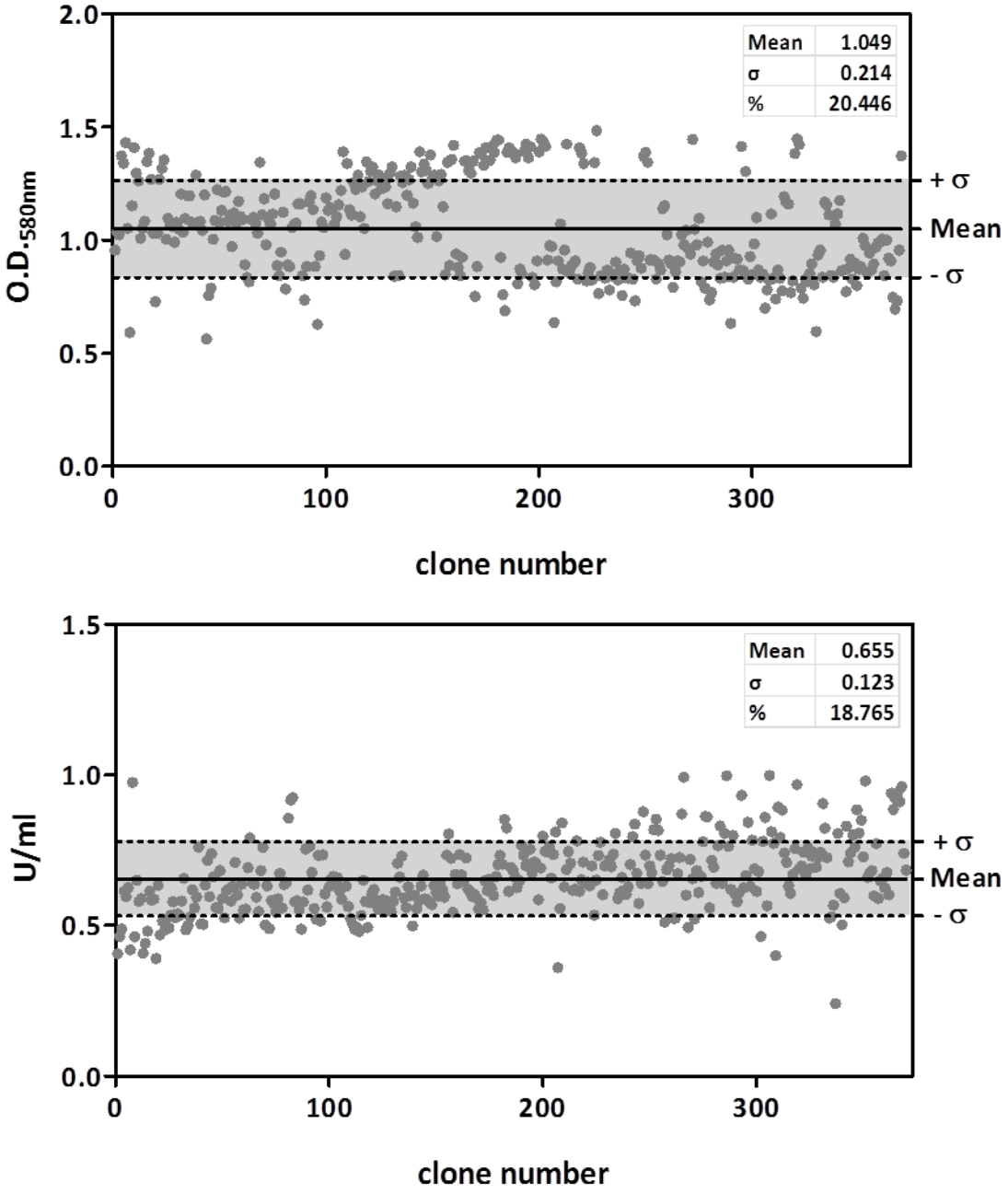

Fig. 3.4 Screening system verification by cultivation of 384 *B. subtilis* TEB1030 wtLipA clones.
Expression cultures of 384 *B. subtilis* TEB1030 wtLipA clones were cultivated using the here identified inoculation and cultivation conditions (robot system, transformants, 25°C, LB medium) at 900 rpm for 16 h. The optical density ($O.D._{580\ nm}$) as well as the extracellular lipase activity (U/ml) is plotted against the *B. subtilis* TEB1030 wtLipA clone number. The mean of the optical density (1.049 ± 0.214) and the lipase activity (0.655 ± 0.123 U/ml) is indicated with a black line. The corresponding standard deviation (σ) is marked with a black dotted line. The mean value, the standard deviation and the relative deviation (%) are listed in the insetted table.

With the here established conditions, *B. subtilis* TEB1030 can be comparably and reproducibly cultivated and analyzed in microtiterplates. Average standard deviations of 20 % for optical density and 18 % for the determination of extracellular lipase activity were determined.

3.2.2. Extracellular lipase amount can be quantified in *B. subtilis* culture supernatant by an application-adapted ELISA

Besides the qualitative screening for *B. subtilis* TEB1030 LipA clones showing increased extracellular lipase activity, a quantitative assay to determine the extracellular lipase amount is also needed to identify LipA variants with increased extracellular LipA amount. An enzyme-linked immunosorbent assay (ELISA) provides the possibility to quantify protein amounts using specific antibodies and suitable protein standards with defined concentrations. Therefore, the analyzed sample is coated on a polysterene MTP with specific binding properties for the respective protein and detected using specific antibodies. Due to the fact that LipA is a hydrophobic protein, so called Polysorp®-96-well microtiter plates were chosen (2.21) which bind hydrophobic proteins with high affinity. Because the screening is performed with the *B. subtilis* TEB1030 culture supernatants instead of purified LipA, coating conditions are needed which provide sufficient LipA detection and reduced background of other, unspecifically bound, proteins also present in the *B. subtilis* TEB1030 culture supernatant. Therefore, two coating conditions were tested using the single culture supernatant of 36 *B. subtilis* TEB1030 non-producing LipA (empty vector, ev) and producing LipA clones (Fig. 3.5A). The *B. subtilis* culture supernatants were diluted in 100 mM bicarbonate buffer pH 9.6 (2.21). 50 µl of each 2-fold diluted culture supernatant of non-LipA producing and LipA producing *B. subtilis* TEB1030 were coated at 4°C, 16 h as well as at 37 °C for 2 h, the extracellular lipase amount was detected as described in 2.21 and calculated using purified His-tagged LipA (2.15.3) as a reference. No background from unspecifically bound proteins in the culture supernatant from non-LipA producing *B. subtilis* TEB1030 (ev) could be observed when coated at 37 °C for 2 h (Fig. 3.5A), but the standard deviation of the detected extracellular lipase amount in the culture supernatant of LipA producing *B. subtilis* TEB1030 is too high for reliable data evaluations (1.72 ± 1.40 µg/ml). Otherwise, when coating at 4 °C, 16 h a small amount of unspecific bound proteins is detected (0.18 ± 0.15 µg/ml) but the measured amount of LipA in the culture supernatant of LipA producing *B. subtilis* TEB1030 can be differentiated (1.04 ± 0.50 µg/ml), therefore allowing a reliable measurement to quantify the extracellular lipase amount.

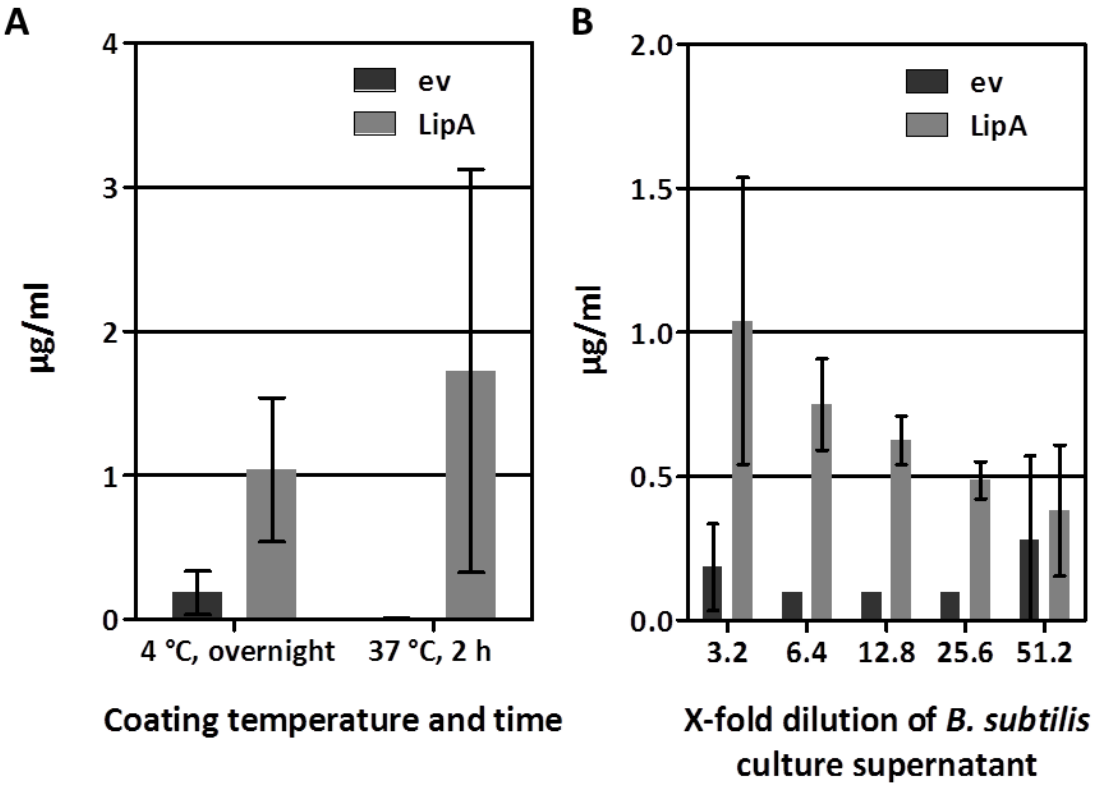

Fig. 3.5 ELISA conditions for the *B. subtilis* TEB1030 culture supernatant.
A Tested coating conditions. 2-fold diluted culture supernatant (in 100 mM bicarbonate buffer pH 9.6) of non-LipA producing (ev) and LipA producing *B. subtilis* TEB1030 was coated on Polysorp®- 96-well microtiter plates at 4 °C, overnight and at 37 °C, for 2 h. **B Tested dilution conditions.** The extracellular lipase amount (µg/ml), determined using purified LipA as a standard is plotted on the left hand side. The determined extracellular lipase amounts (µg/ml) in severalfold diluted culture supernatants of non-producing (ev) or LipA producing *B. subtilis* TEB1030 clones are plotted.

For the screening of different *B. subtilis* TEB1030 LipA clones it is necessary to find the optimal dilution for the *B. subtilis* TEB1030 culture supernatant to detect high and low amounts of LipA, because differences in the extracellular LipA amount are expected based on the mutagenesis.

Five different dilutions of LipA producing and non-producing *B. subtilis* TEB1030 culture supernatants (6 biological replicates) were coated at 4 °C, overnight and analyzed as described in 2.21. The culture supernatants were prediluted 1.6-fold and in a second step 2 -fold diluted and directly coated on the Polysorp®- 96-well microtiter plates using the TECAN® robot system. Due to the precisely pipetting of the robot system, it was not only used for the inoculation of the MTP-expression cultures for screening (3.2.1) but also for coating of the ELISA-MTP analysis plates and so reducing the deviation of this sensitive method.

The smallest (3.2-fold; 1.04 ± 0.50 µg/ml) and the highest (51.2-fold; 0.38 ± 0.23 µg/ml) dilution of the LipA producing *B. subtilis* TEB1030 culture supernatants show the highest deviation in extracellular lipase amount (Fig. 3.5B). This could be explained by a detection limit based on the chosen concentrations of the purified His-tagged LipA for calculation of LipA amount (µg/ml) in the culture supernatant. The signal detected in the smallest dilution (3.2-fold) ranged in the area of saturation of purified His-tagged LipA, therefore the interpolation via the purified His-tagged LipA standard curve is not uniformely. The *vice versa* effect is true for the highest dilution (51.2-fold), where the detected signal is smaller than the lowest concentration of purified His-tagged LipA making an adequate interpolation difficult. The dilutions 6.4-, 12.8- and 25.6-fold of the *B. subtilis* TEB1030 LipA producing culture supernatants show acceptable standard deviations in detected LipA amount, as well as dilution based differences in detected LipA amount (Fig. 3.5A).

The systematic mutational analysis of LipA is aimed at identifying beneficial amino acid substitutions for extracellular lipase activity and lipase amount. This means that it is necessary to establish the ELISA assay in order to detect rather higher extracellular LipA amounts than smaller ones. Therefore the 25.6-fold dilution (Fig. 3.5A) was chosen, which allows a wider detection range of increased LipA amount, and integrated into the quantitative screening assay.

In a final verification test, the culture supernatants of LipA producing *B. subtilis* TEB1030 clones (36 biological replicates) were prediluted 8-fold and subsequently diluted 3.2-fold with the TECAN® robot system in 50µl bicarbonate buffer and pipetted on a Polysorp®-96-well microtiter plate to achieve a final 25.6-fold dilution. The coating was performed at 4 °C, 16 h. In parallel a 2-fold dilution series of purified His-tagged LipA (2.15.3) was applied to identify the smallest possible, but necessary number of applied purified His-tagged LipA concentration for ELISA standards. A purified LipA concentration from 0.08 µg/ml to 5µg/ml (2.22) is suitable to detect a 2.5- to 5-fold increase in wtLipA in the *B. subtilis* TEB1030 culture supernatant within the linear absorption slope at 652 nm (Fig. 3.6).

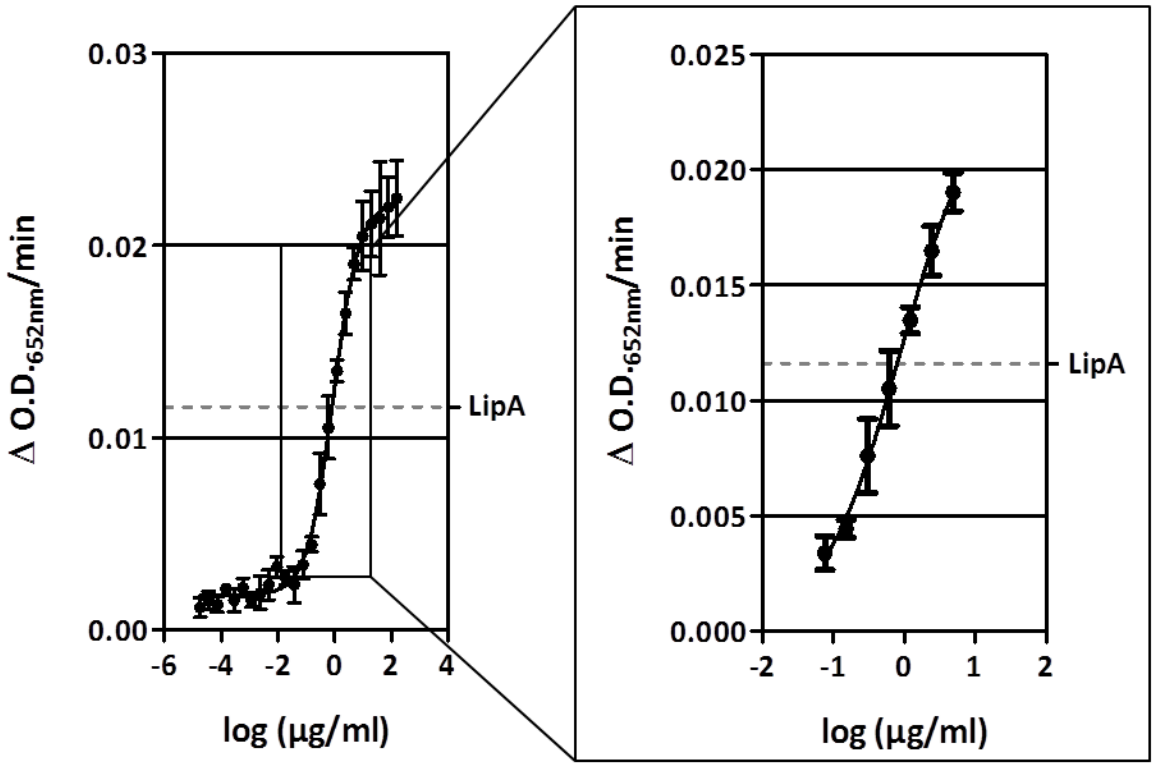

Fig. 3.6 Purified His-tagged LipA for ELISA standard curve.
Purified His-tagged LipA was diluted 2-fold in 100 mM bicarbonate buffer (pH 9.6), coated on a Polysorp®- 96-well microtiter plate at 4 °C, 16 h. The absorption slope per min at 652 nm is plotted against the LipA concentration (log µg/ml) for 24 dilutions on the left hand side. The dotted grey line indicates the absorption slope per min at 652nm for detected wtLipA (LipA) in a 25.6-fold diluted culture supernatant of *B. subtilis* TEB1030. This wtLipA concentration serves as a reference point in all further experiments and should therefore be in the standard curve range. The cutout on the right hand side shows the chosen purified His-tagged LipA concentrations for ELISA standards.

Taken together, a MTP-based screening system to analyze LipA producing *B. subtilis* TEB1030 clones could be established (2.22). This system includes comparable inoculation and cultivation conditions, a sufficient lipase activity assay and a suitable ELISA screening to quantify the extracellular lipase amount.

Extracellular LipA can be specifically quantified with an ELISA using a specific polyclonal LipA antibody in a suitable range from 2.5- to5-fold decrease or increase in LipA amount.

3.3. Generation of a *lipA* site saturation mutagenesis library

Highly conserved amino acids are generally known to be important for the protein`s function and stability (Lehmann & Pasamontes, 2000; Steipe *et al.*, 1994), therefore they were not considered for mutagenesis and screening of LipA to identify beneficial single amino acid susbtitutions. Conservation of each amino acid of LipA was calculated by a multiple sequence alignment (ClustalW) (Sievers *et al.*, 2011) of 64 protein sequences from 41 species within the *Firmicutes* phylum (2.24) (Finn *et al.*, 2014). Here, all sequences belonging to `lipase class two` were analyzed by counting each amino acid at each position and so calculating the conservation of the respective amino acid and position within LipA (see appendix Tab. 8.2). The most necessary amino acid residues for LipA are S77, D133 and H156 forming the catalytic triad (Van Pouderoyen *et al.*, 2001). The average conservation of these residues together with those of the conserved pentapeptide of α/β-hydrolases (A-H-S-M-G from position 75 to 79), where the catalytical S77 is embedded (Van Pouderoyen *et al.*, 2001), is 95 %. This was determined as the cutoff for conservation and subsequently 26 out of all 181 amino acids of LipA that showed a conservation ≥ 95 % were considered as highly conserved ones and were not applied for mutagenesis and screening (Fig. 3.7A; •). The codons coding for the remaining 155 amino acids (Fig. 3.7A; **x**) were mutated using oligonucleotides with a degenerated `NNS´ codon (Tab. 8.1) reducing the number of clones to screen 2-fold. Here, at the first and second position of the codon (N) every of the four bases adenine, guanine, thymine and cytosine (N) and at the third position only a guanine and a cytosine (S) can be introduced, resulting in 32 (instead of 64) possible codons, nonetheless coding for all 20 natural occurring amino acids (Sharp *et al.*, 1988). The constructed *B. subtilis lipA* expression vector pBS*lipAsslipA* (2.2; 2.12) was used for *lipA* mutagenesis exclusively with 155 different QuikChange PCRs® (2.10.2; 2.12.1) and library construction as shown in Fig. 3.7B. The *sslipA* sequence was not subjected for analysis due to the fact that the influence of single amino acid and codon substitutions only within the mature protein LipA on its production in *B. subtilis* should be analyzed.

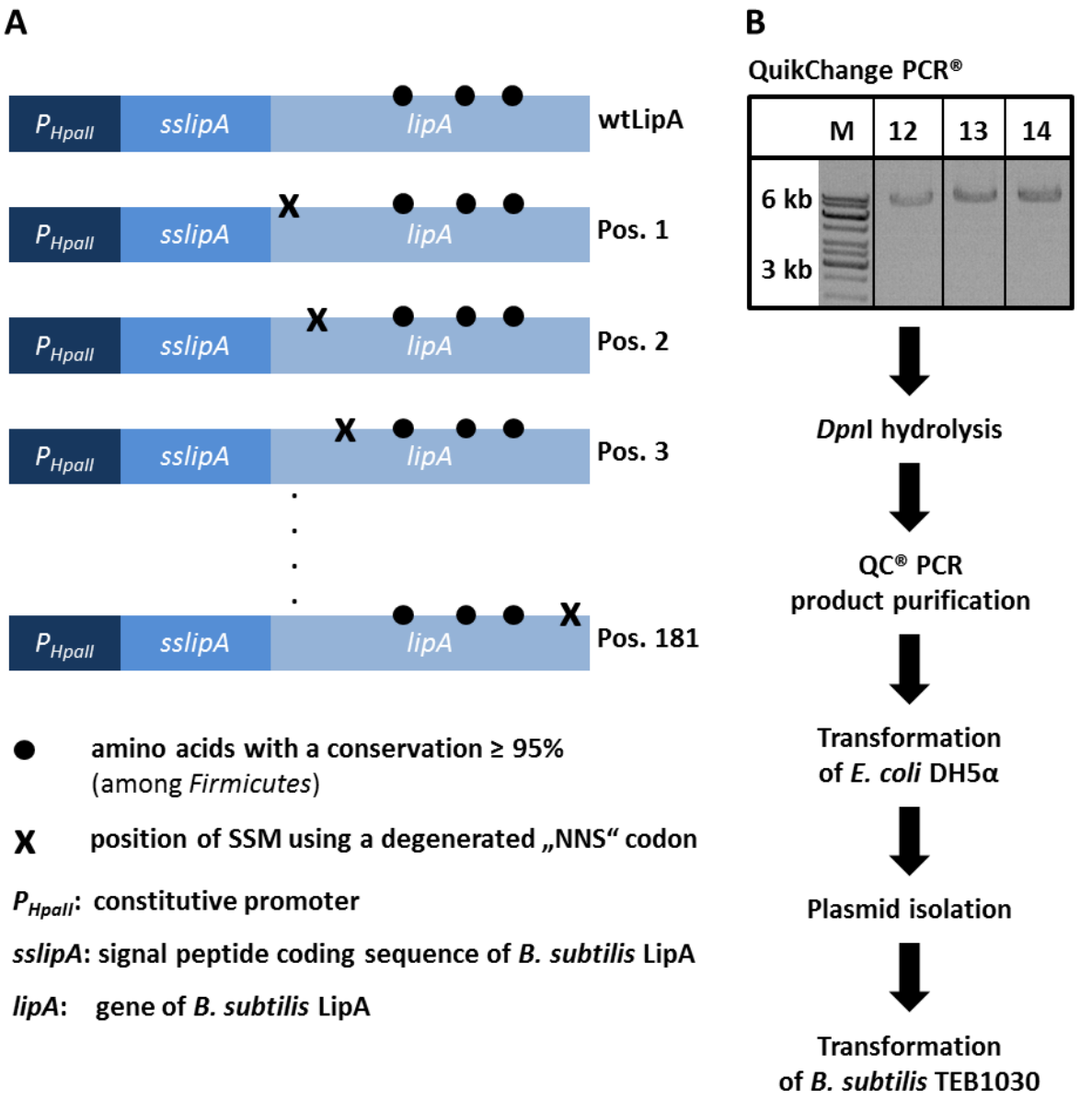

Fig. 3.7 Schematic overview of *lipA* site saturation mutagenesis library construction.
A *lipA* site saturation mutagenesis. The expression vector pBS*lipAsslipA*, where the native *lipA* gene is under control of the constitutive P_{HpaII} promoter, was used for *lipA* site saturation mutagenesis library. All codons coding for the 155 amino acid positions with a conservation < 95% (among the *Firmicutes*) (x) were mutated by QuikChange® PCR using a degenerated `NNS` codon. Codons coding for amino acid positions with a conservation ≥ 95% (•) were not considered for substitution and screening. **B Flowchart for library construction.** PCR products generated by QuikChange PCR® were applied for *Dpn*I hydrolysis to digest remaining template DNA. *E. coli* DH5α was transformed with the purified and concentrated PCR products. The plasmids were isolated and *B. subtilis* TEB1030 was transformed.

After QuikChange PCR® the remaining template vector DNA in each PCR sample was hydrolyzed using *Dpn*I (2.10.2; 2.12.1). In a first step, *E. coli* DH5α was transformed (2.9.1; 2.9.2) with the purified and concentrated PCR product (2.12.1) and the mutagenized vectors were isolated from 2,000-4,000 *E. coli* clones (2.6) to generate a sufficient number of LipA

clones thus ensuring the occurrence of all possible mutations. The still remaining amount of wild-type pBS*lipAsslipA* in the constructed library introduced into *B. subtilis* TEB1030 is controlled by a similar treated control sample without oligonucleotides. The amount of resulted clones in this control sample can only be caused by incomplete *Dpn*I hydrolysis and should be the same as in the actual sample therefore, allowing a determination of wild-type percentage in the library. Finally, *B. subtilis* TEB1030 was transformed with 20 ng of mutagenized vector DNA by protoplast formation (2.9.3).

In total, 184 *B. subtilis* TEB1030 LipA clones together with two controls, *B. subtilis* TEB1030 with the empty vector (pBSMul1; ev) and *B. subtilis* TEB1030 with the wild-type pBS*lipAsslipA* (*lipA*) were picked into 96-well microtiterplates for each mutated codon position (2.22). This clone number corresponds to a six times oversampling factor and is necessary to achieve a library coverage of about 99.9 % (Reetz *et al.*, 2008). Based on the chosen `NNS` codon, that allows the introduction of all 20 natural occurring amino acids, also the re-introduction of the wild-type codon is possible. These re-introduction events occur in one out of 32 cases (ca. 3 %) if the original codon sequence is coded by the `NNS` codon and is not possible if the original codon does not follow the `NNS` codon. Taking other possible factors based on the mutagenesis procedure into account that are difficult to determine experimentally, as the insertion of the used oligonucleotides into the mutagenized PCR products, the total percentage of the mutagenesis failure was assumed as 10 %. This way a mutagenesis yield of 90 % is supposed and the picked number of 184 LipA clones per mutated amino acid/codon lead to an actual full coverage probability of 93.87 % as it was calculated with TopLib (http://stat.haifa.ac.il/~yuval/toplib/) (Nov, 2012). This *B. subtilis* TEB1030 LipA variant library was subsequently analyzed in a two-step screening procedure for increased extracellular lipase activity and amount.

A *lipA* site saturation mutagenesis library with a full coverage probability of 93.87 % was generated using a degenerated `NNS` codon.

3.4. A two-step screening procedure led to the identification of 38 LipA variants with increased extracellular lipase amount

The generated LipA clones (3.3) were analyzed in a two-step screening procedure as described in section 2.22 and shown in Fig. 3.8. First the LipA clones were screened for increased levels of extracellular lipase activity compared to wtLipA. This is necessary and sufficient to reduce the LipA clone number and to remove non-active LipA clones. As described in section 3.2, 384 wild-type LipA clones (wtLipA) were analyzed for the mean and deviation of the measured optical density at 580 nm and the extracellular lipase activity (U/ml) (**Fig. 3.4**) when *B. subtilis* TEB1030 is cultivated and analyzed in microtiterplates. With this deviation value (σ) for lipase activity of 0.123 U/ml, a cutoff value was determined to identify LipA clones with increased extracellular lipase activities compared to wtLipA.

Thus, LipA clones with activities above wtLipA activity plus the respective standard deviation (wtLipA+σ U/ml) were declared as clones with increased extracellular lipase activities. From 29,624 generated LipA clones, 2 % did not grow resulting in 29,199 clones that were screened (Fig. 3.8; Tab. 3.1). From these, 19,350 LipA clones (66 %) show wtLipA like activities and 5,444 clones (19 %) (Tab. 3.1) were inactive with the majority located at the amino acid positions 26, 35, 41, 49, 101, 102, 104, 156, 160 and 181 and were therefore discarded (see appendix Tab. 8.3).

Tab. 3.1 Statistical overview of the first screening step.
In total 29,624 LipA clones were cultivated from which 29,199 clones were screened for increased extracellular lipase activity. 66 % showed wtLipA like activities, 19 % were inactive, 14 % showed a decrease in extracellular lipase activity. 1 % of the LipA clones with an increase in extracellular lipase activity were applied in the second screening step for increase extracellular lipase amount.

characteristics	%	total clone number
not grown	2	29,624
screened	98	
wt activities	66	29,199
inactive	19	
↓ activity	14	
↑ activity	1	

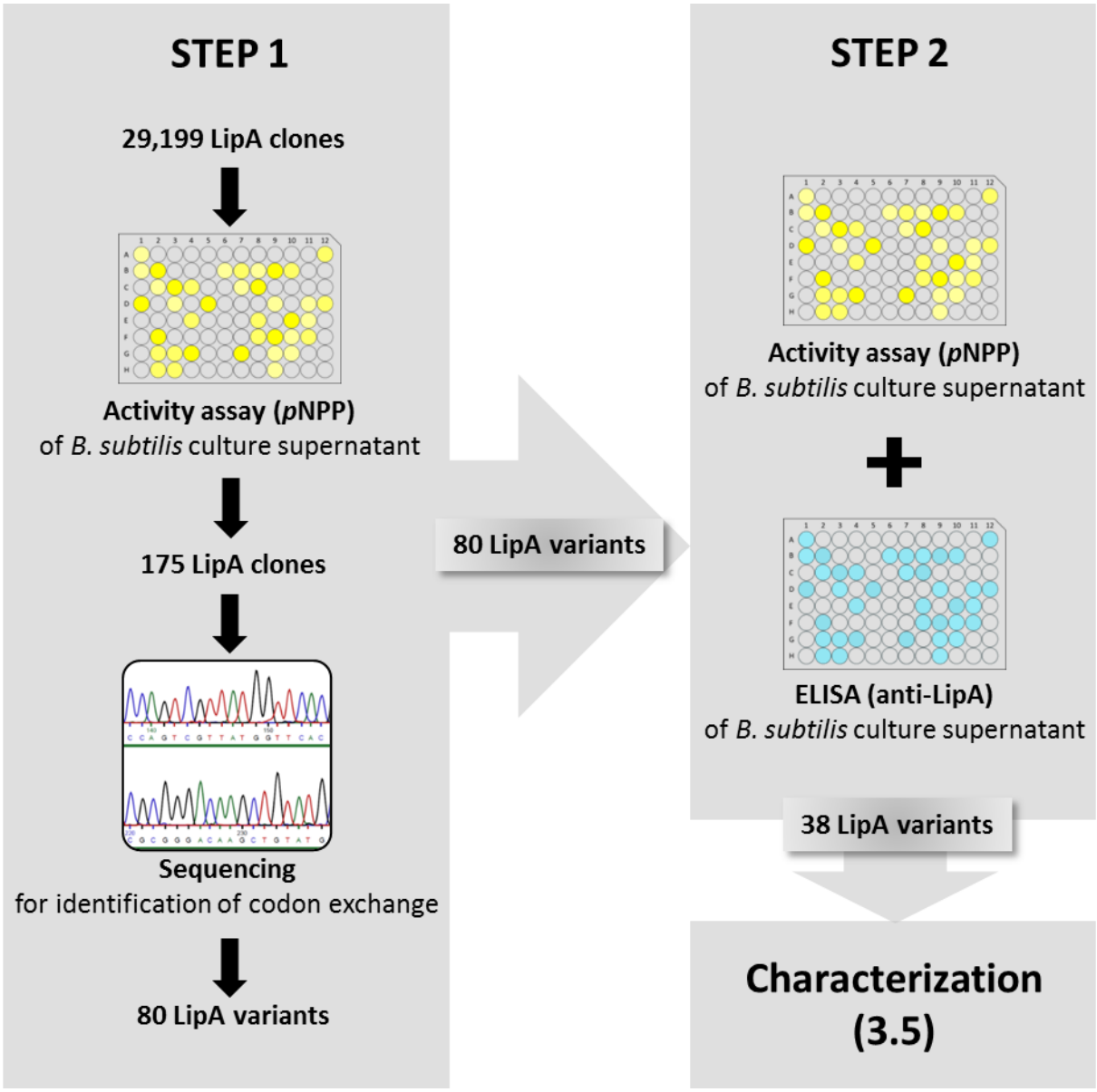

Fig. 3.8 Two-step screening procedure for *B. subtilis* TEB1030 LipA clones.
In a first step, 29,199 LipA clones were screened in microtiterplates for increased or similar levels of extracellular lipase activity compared to wild-type LipA (wtLipA), leading to the isolation of 175 LipA clones. These clones were sequenced and revealed 80 different LipA variants. These variants differ in the amino acid or codon substitution and were applied for a second microtiterplate screening step. Here again, the extracellular lipase activity was determined and also the extracellular lipase amount was quantified using an enzyme-linked immunosorbent assay (ELISA). Finally, 38 different LipA variants were identified with an increased extracellular lipase amount compared to wtLipA and increased extracellular lipase activity.

4,230 LipA clones (14 %) show a significant decrease in extracellular lipase activity compared to wtLipA. Based on the determined cutoff, only 175 LipA clones (1 %) show increased extracellular lipase activities (Tab. 3.1). Sequencing of these 175 LipA clones revealed 26 LipA clones as false-positive (wild-type sequence), 65 LipA clones as duplicates with the identical codon exchanges and four LipA clones with multiple amino acid substitutions. Taken together, 80 LipA variants were identified with different single amino acid and codon

substitutions. As shown in Fig. 3.9A, the substitutions are located at about 40 different amino acid positions over the entire LipA sequence leading to an increase in extracellular lipase activity from 1.2-fold to 3.4-fold in comparison to wtLipA. Accumulation spots of beneficial substitutions are between the N-terminal positions 11-18, in the LipA mid part between position 46-59 and in the C-terminal part between position 129-143 and 151-169. This distribution does not follow any kind of pattern concerning the structural location and orientation of the wtLipA amino acid residue at this position (see appendix Tab. 8.2). Additionally, this distribution is unaffected by the substituted wtLipA amino acid and their adjacent residues conservation (see appendix Tab. 8.2) .

In a second screening step (Fig. 3.8), *B. subtilis* TEB1030 producing each of the identified 80 different LipA variants was cultivated in microtiterplates as nine biological replicates to verify the increased extracellular lipase activity and to additionally quantify the extracellular lipase amount. For extracellular lipase amount quantification, the established enzyme-linked immunosorbent assay (ELISA) with a specific polyclonal LipA antibody was applied (2.22; 3.2.2). The increased extracellular lipase activity could be confirmed for 22 LipA variants with different amino acid substitutions. Eleven of these variants show increased extracellular lipase activities at similar levels of extracellular lipase amounts, which mean they exhibit an increased extracellular specific lipase activity when lipase activity is normalized to the measured protein amount. Due to the fact that the aim of this study is not primary focused on engineering LipA`s activity but on the different beneficial influences of single amino acid and codon substitutions on LipA`s production in *B. subtilis*, these variants were not further analyzed. The other eleven variants with increased extracellular lipase activity also show an up to 3-fold increase in extracellular lipase amount compared to wtLipA. 23 LipA variants showed similar extracellular lipase activities in comparison to wtLipA but an up to 4-fold increase in extracellular lipase amount. The increased extracellular LipA amount of these together 34 LipA variants is shown in Fig. 3.9B. These variants include four codon variants with two different codon exchanges for a single amino acid substitution twice at the amino acid position 12, and one each at positions 13, and 57. The 38 LipA amino acid and codon variants show increased protein amount ranging from a 1.3-fold increase with a substitution at the C-terminal amino acid position 154 to an enhancement of 4.4-fold at the N-terminal position 53 in comparison to wtLipA (3.7 ± 0.64 µg/ml) (Fig. 3.9B).

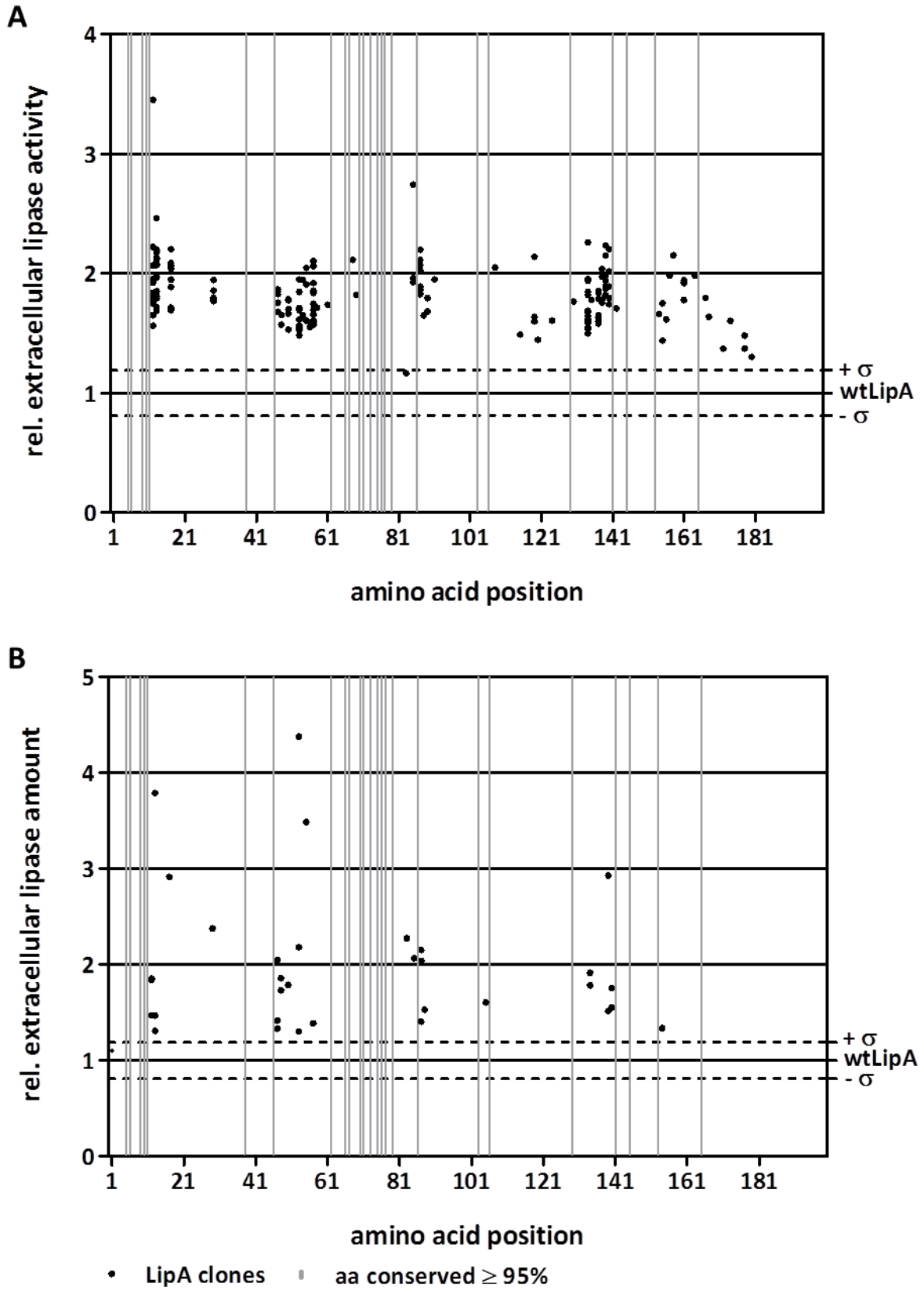

Fig. 3.9 Identified LipA clones and variants with increased extracellular lipase activity and amount.
A 80 different LipA variants with increased extracellular lipase activity. The relative extracellular lipase activities of *B. subtilis* TEB1030 producing each of the identified 80 LipA variants are plotted against the

respective substituted amino acid position. In a second screening step the extracellular lipase amount of *B. subtilis* TEB1030 producing each of the 80 LipA variants was quantified.**B 38 different LipA variants with increased extracellular lipase amount.** The relative extracellular lipase amounts of *B. subtilis* TEB1030 producing each of the identified 38 LipA variants are plotted against the respective substituted amino acid position. In figure A and B: the black dots represent the striking LipA variants, the grey bars mark the highly conserved amino acid position (≥ 95%). The black line represents the normalized wild-type LipA (wtLipA) extracellular lipase amount or activity and the grey dotted lines mark the wtLipA standard deviation (σ).

LipA is a very hydrophobic protein containing 59 % hydrophobic amino acids (UniProt: P37957). Therefore, the substitutions were considered concerning their chemical property to maybe reveal some kind of pattern linked to the amino acid hydrophobicity and the increased extracellular lipase amount (Tab. 3.2).

Tab. 3.2 Identified 34 LipA amino acid variants and their changes in hydrophobicity.
The LipA variants are listed with the wild-type (wt) amino acid and the variant hydrophobicity. The hydrophobicity values are based according to the hydrophobicity scale of (Kyte & Doolittle, 1982).

variant	wt amino acid	variant amino acid
I12F	4.5	2.8
I12L		3.8
I12V		4.2
G13N	-0.4	-3.5
G13S		-0.8
G13T		-0.7
F17E	2.8	-3.5
Q29H	-3.5	-3.2
T47H	-0.7	-3.2
T47P		-1.6
T47T		-0.7
N48G	-3.5	-0.4
N48Q		-3.5
N50D	-3.5	-3.5
P53D	-1.6	-3.5
P53E		-3.5
P53V		4.2
L55F	3.8	2.8
R57T	-4.5	-0.7
T83M	-0.7	1.9
Y85W	-1.3	-0.9
I87L	4.5	3.8
I87I		4.5
I87V		4.2
K88K	-3.9	-3.9
A105N	1.8	-3.5
M134K	1.9	-3.9
M134P		-1.6
M134Q		-3.5
Y139G	1.3	-0.4
Y139T		-0.7
L140A	3.8	1.8
L140Y		-1.3
V154E	4.2	-3.5

hydrophobicity scale	
R	-4.5
K	-3.9
N	-3.5
D	-3.5
Q	-3.5
E	-3.5
H	-3.2
P	-1.6
Y	-1.3
W	-0.9
S	-0.8
T	-0.7
G	-0.4
A	1.8
M	1.9
C	2.5
F	2.8
L	3.8
V	4.2
I	4.5

16 LipA variants do not change hydrophobicity, 13 LipA variants carry a substitution to a less hydrophobic amino acid while five LipA variants carry substitutions to more hydrophobic amino acids (Tab. 3.2). From this non-uniform distribution it can be concluded that also the change in hydrophobicity cannot be assigned to a specific pattern. A general conclusion of how every of the single amino acid and codon substitution within LipA contributes to its increased extracellular lipase amount and activity cannot be drawn solely based on the amino acid biochemical characteristics; therefore, the influence of the identified substitutions is analyzed and characterized regarding the different levels in *B. subtilis* LipA production (3.5).

The established two-step screening procedure led to the identification of 38 different LipA amino acid and codon variants.

3.5. 38 LipA variants show beneficial single amino acid/codon substitutions for LipA production

38 different amino acid and codon variants of LipA were identified showing an up to 4-fold increase in extracellular lipase amount and, in case of eleven variants, also show a 1.6-fold increase in extracellular lipase activity. These improvements could be due to the single amino acid and codon substitutions affecting three steps known as bottlenecks in *B. subtilis* protein production (1.6): 1) transcription, 2) translation and secretion that are a coupled process for LipA, or 3) improved maturation, folding, and activity. Based on the fact that these three steps are dependent on and influencing each other it is difficult to assign one effect to one specific production step and also complicate to differentiate between an amino acid or a codon-related effect. However, *B. subtilis* TEB1030 producing each of the variants was cultivated as three biological replicates in a microfermentation system (2.23) to analyze how every of the 38 different LipA variants contributes to its production and secretion. Online biomass measurement (2.23) was performed to analyze a possible influence of the substitutions on the growth behavior of *B. subtilis* TEB1030 producing LipA variants, because during heterologous production of LipA variants with silent substitutions in *E. coli* growth differences have been observed (Rahmen *et al.*, 2015b). As analyzed and determined by cultivation of *B. subtilis* TEB1030 producing wtLipA in section 3.1, LipA production and secretion reaches the optimum after 6 h of cultivation, therefore samples for *lipA* transcription analysis, LipA activity measurement and determination of extracellular LipA amount were taken after 6 h of LipA variant production. During 24 h of online biomass measurement no substantial growth effect of *B. subtilis* TEB1030 producing each of the 38 LipA variants could be observed compared to *B. subtilis* TEB1030 producing wtLipA (Fig. 3.10A). So an effect based on these single amino acid or codon substitutions on the growth and physiology of *B. subtilis* TEB1030 producing LipA can be excluded. This goes along with similar oxygen transfer rate (%) of *B. subtilis* TEB1030 cultures producing either wtLipA or LipA variants (Fig. 3.10B). The transfer rates decrease between 4 and 8 h of LipA production in all *B. subtilis* TEB1030 cultures indicating oxygen uptake by the cells which corresponds to the beginning of *B. subtilis* exponential growth (Fig. 3.10A). In contrast to the activity measurement of the *B. subtilis* TEB1030 culture supernatant during the two-step screening procedure (3.4), where the LipA volume activity was determined (U/ml), for characterization the extracellular specific lipase activity (U/mg) was now calculated by normalizing the

volume activity to the extracellular lipase amount (mg/ml) in the *B. subtilis* TEB1030 culture supernatant.

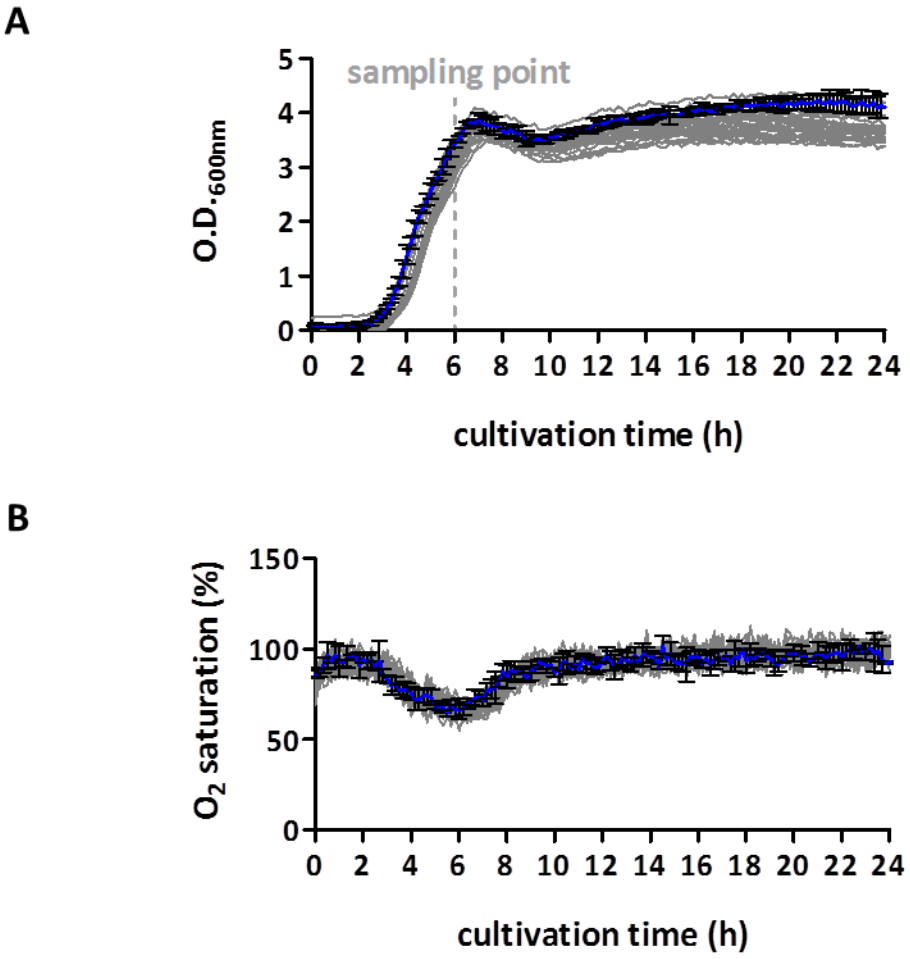

Fig. 3.10 Microfermentation of *B. subtilis* TEB1030 producing each of the 38 different LipA variants.
A 24 h online biomass measurement. *B. subtilis* TEB1030 producing each of the 38 different LipA variants was cultivated as three biological replicates in a microfermentation system using 48-well FlowerPlates®**.** Online biomass measurement was performed for 24 h in the BioLector®. The optical density at 600 nm (O.D. $_{600\ nm}$) is plotted against the cultivation time (h). The blue line indicates wtLipA optical density with corresponding error bars in black. The sampling point after 6 h of LipA production is marked. **B Oxygen saturation during microfermentation.** The percentaged oxygen saturation (%) of *B. subtilis* TEB1030 harboring the 38 different LipA variants is plotted against the cultivation time (h). The blue line indicates wtLipA oxygen saturation with corresponding error bars in black.

Additionally, the change in *lipA* transcript amount of the identified LipA variants was determined compared to wt*lipA.* This analysis is necessary because a codon substitution can influence the extracellular lipase amount on two different levels. First, the resulting changed amino acid lead to differences in LipA characteristics as stability or second, the *lipA* transcript amount is changed by the underlying nucleotide substitution that alters *lipA*

transcription rate or transcript stability (1.6). To analyze if the transcript amounts are affected, *real time* PCRs (2.11; 2.23) were performed to determine the fold change in *lipA* transcript amount based on a given codon substitution compared to wt*lipA*. Since *lipA* expression is under the control of the strong constitutive P_{HpaII} promoter (2.2), high *lipA* transcript amounts were expected to be compared by the very sensitive RT-qPCR method. Thus, emerging variations are not conclusively dependent on altered *lipA* gene expression but probably also on the sensitivity of the method. This sensitivity could influence the repeatability and reproducibility of determining the change in transcript amount (Bustin *et al.*, 2009). Therefore, the deviation of wt*lipA* transcript amount over 33 biological and two technical replicates was calculated resulting in a cutoff value of 0.4 to 2.2 (2.11). Although several LipA variants show mathematically significant changes in transcript amount ($p < 0.05$), the changes are within the range of this determined cutoff. Thus, it is not possible to make a certain reliable conclusion of those variants concerning their effect on *lipA* transcript amount and the subsequent protein amount. Therefore, only variants with increased changes in *lipA* transcript amount higher than the 2.2-fold cutoff and with $p < 0.05$ were declared as significantly affected on transcript level and are discussed in the following chapters (3.5.1; 3.5.2).

Based on the analyses of transcript, activity and amount of the LipA variants after 6 h of production (2.23), 12 LipA variants were identified as false-positive ones (Tab. 3.3), because they do not show a significant change in one of these three parameters.

In total, 26 out of the 38 characterized LipA variants were verified as harboring single amino acid or codon substitutions beneficial for *lipA* transcript amount, extracellular specific lipase activity and/or extracellular lipase amount (3.5.1; 3.5.2.).

All 38 single amino acid and codon substitution within LipA do not have a substantial effect on *B. subtilis* TEB1030 growth and 26 substitutions are beneficial for *lipA* transcription as well as extracellular specific activity and amount.

Tab. 3.3 False-positive LipA variants.
The table shows the structural location of the variant amino acid substitution (struc.), as well as the orientation (ori.) of the amino acid residues (s: surface; b: buried). The wild-type (wt) codon and the introduced variant codon are named together with the codon frequency per 1000 bp. The relative change in transcript level is shown together with the lower and upper deviation. Significant transcript changes compared to wt*lipA* above the cutoff of 2.2 and a p-value < 0.05 are marked with an asterisk. The relative extracellular specific lipase activity and the extracellular lipase amount are shown with the standard deviation and significant changes compared to wtLipA ($p < 0.05$) are marked with an asterisk.

variant	struc.	ori.	wt codon	frequency per 1000bp	variant codon	frequency per 1000bp	rel. change in transcript level	lower deviation	upper deviation	rel. specific activity	± std.	rel. lipase amount	± std.
false-positive LipA variants													
$I12L_{TTG}$	turn	s	ATT	36.2	TTG	15.8	1.275	0.417	0.646	0.805*	0.306	0.968	0.351
$I12V_{GTC}$	turn	s	ATT	36.2	GTC	17.3	1.372	0.423	0.646	0.780*	0.553	0.952	0.319
G13N	turn	s	GGA	21.8	AAC	17.8	1.064	0.376	0.555	0.718*	0.430	0.764*	0.314
Q29H	turn	s	CAG	18.5	CAC	7.5	0.831	0.169	0.236	0.932	0.379	1.096	0.274
T47H	coil	s	ACA	21.6	CAC	7.5	0.270	0.253	0.992	0.907	0.350	1.152	0.327
T47P	coil	s	ACA	21.6	CCA	7.4	1.456	0.373	0.446	0.961	0.347	1.030	0.272
T47T	coil	s	ACA	21.6	ACG	14.9	1.429	0.391	0.615	0.955	0.404	0.698*	0.282
N48G	αB	s	AAT	22.9	GGC	23.3	1.161	0.207	0.379	0.309*	0.300	1.418	0.257
L55F	αB	b	TTA	19.8	TTC	14.3	1.062	0.165	0.187	0.366*	0.392	1.172	0.328
T83M	αC	b	ACA	21.6	ATG	26.3	1.473	0.349	0.467	0.596*	0.391	0.927	0.442
Y85W	αC	s	TAC	12.6	TTG	15.8	1.408	0.396	0.766	0.733*	0.449	0.586*	0.321
I87L	αC	s	ATA	9.8	CTC	10.7	0.949	0.901	6.559	0.095	0.380	1.078	0.301

3.5.1. Six LipA variants show improved extracellular specific activity compared to wtLipA

Six LipA variants harbor single amino acid and codon substitutions leading to a significant increase in extracellular specific lipase activity in comparison to wtLipA (64 ± 13.1 U/mg) (Fig. 3.11; Tab. 3.4). Three of these LipA variants carry a substitution at I12, to the less hydrophobic amino acids phenylalanine, leucine or valine, resulting in a 2-fold increase in extracellular specific lipase activity (Fig. 3.11).

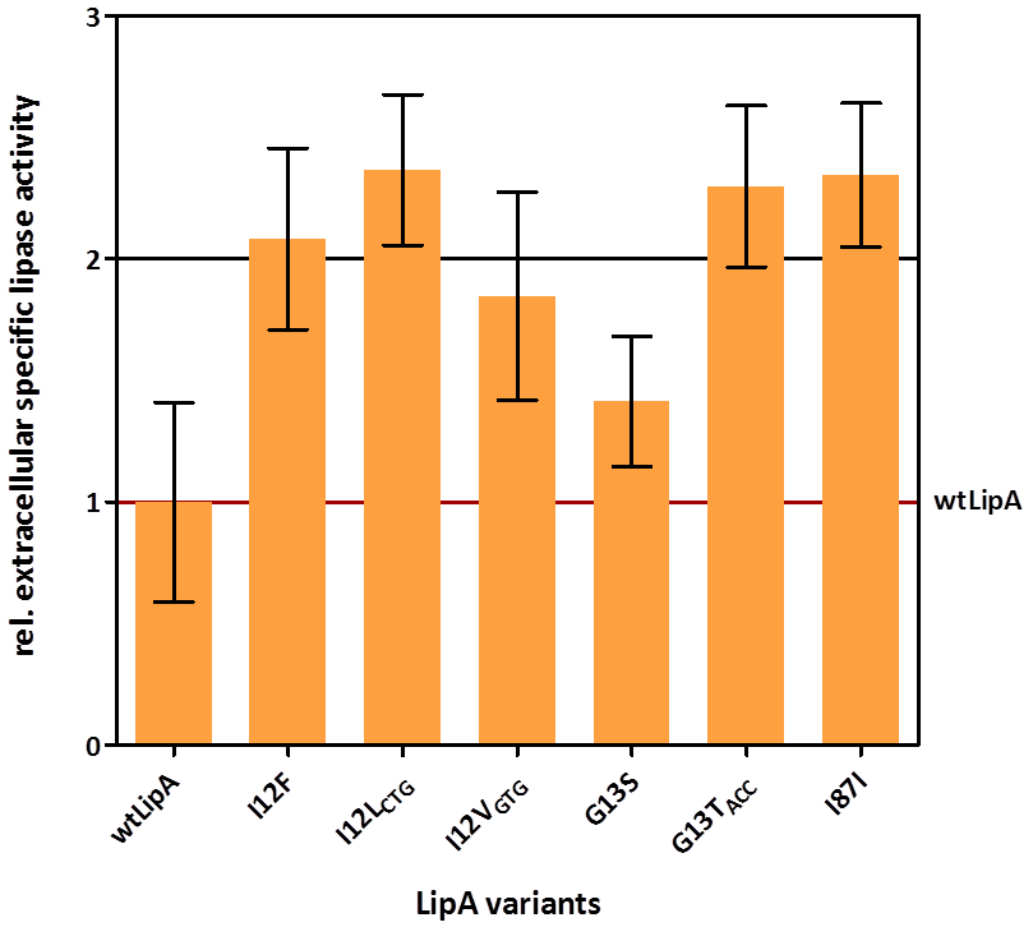

Fig. 3.11 Six LipA variants show increased extracellular lipase activity.
B. subtilis TEB1030 producing each of the six more active LipA variants was cultivated as three biological replicates in a 48-well Flowerplate® for 6 h and the extracellular specific lipase activity (U/mg) in the culture supernatant was calculated by normalizing the volume activity (U/ml) to the quantified extracellular lipase amount (mg/ml). The extracellular lipase activity was measured using *p*NPP as a substrate and the extracellular protein amount was determined by ELISA using a specific polyclonal LipA antibody. The relative extracellular specific lipase activities of LipA variants with significantly ($p < 0.05$) increased activity compared to wtLipA are plotted. The red line indicates the normalized wtLipA specific activity.

The I12 nitrogen atom forms the oxyanion hole together with the peptide backbone nitrogen atom of M78 and so stabilizes the tetrahedral transition state during substrate hydrolysis (Van Pouderoyen *et al.*, 2001). For the phenylalanine substitution in the I12F variant, not

only increased extracellular specific lipase activity but also a 1.6-fold increase in extracellular protein amount was observed (Fig. 3.12; Tab. 3.5) indicating an effect on both protein amount, that is discussed later (3.5.2), and specific activity at the same time. The introduction of the bigger, aromatic phenylalanine could induce a conformational change of LipA. This change could lead to a slight movement of the backbone nitrogen atoms improving the stabilization of the transition state, resulting in the significant 2-fold increase in extracellular specific lipase activity (Fig. 3.11; Tab. 3.4). Interestingly, a beneficial substitution at M78, the second amino acid forming the oxyanion hole and located adjacent to the catalytic active S77 (Van Pouderoyen *et al.*, 2001), for LipA activity has not been identified. I12 is located in a more flexible turn of LipA whereas M78 is located in the less flexible αC-helix (Van Pouderoyen *et al.*, 2001). Presumably conformational changes in the αC-helix are sterical hindered and substitutions here do not have any effect on specific lipase activity.

The substitution to the polar residues serine and threonine at G13 located next to I12 also lead to a significant higher extracellular specific lipase activity of 1.4-fold or 2-fold (Fig. 3.11). The replacement to serine with a bigger hydrophilic residue side chain could also lead to a structural change of LipA in the oxyanion hole region and so affecting indirectly the stabilization of the transition state in a positive way that results in the 1.4-fold increase in LipA activity of this variant (Fig. 3.11;Tab. 3.4). Especially for these mentioned variants with amino acid substitutions near the active centre of LipA, it is also possible that these substitutions increase the specific activity towards the used *p*-nitrophenyl palmitate substrate (2.17) by shifting the substrate affinity for the given substrate (Wilson & Agard, 1991) due to the already mentioned possible conformational change.

Besides these amino acid variants, also four codon variants with a 2-fold increase in extracellular specific lipase activity compared to wtLipA were identified. The LipA variants $I12L_{CTG}$, $I12V_{GTG}$,and $G13T_{ACC}$ show amino acid substitutions that were also identified, based on a different codon, with no effect neither on extracellular specific lipase activity nor on extracellular lipase amount ($I12L_{TTG}$, $I12V_{GTC}$) (Tab. 3.3) or affecting extracellular lipase amount positively ($G13T_{ACG}$) (Fig. 3.12; Tab. 3.5). The silent mutation at amino acid position I87 resulted in a significant 2-fold increase in extracellular specific lipase activity, but also in a 3.6-fold significant change in *lipA* transcript level (Tab. 3.4). These results indicate, in all four cases, a codon and not an amino acid related effect on LipA extracellular specific activity, that is based on a translation correlated folding efficiency.

The translation velocity is known to be crucial for the protein`s activity, because it determines the time for the protein to fold into its native conformation (Komar *et al.*, 1999). Substitutions to frequent codons can negatively affect a protein`s activity by fasten its translation thereby limiting the time for the synthesized protein to fold correctly resulting in protein misfolding and a decrease in the enzyme activity (Spencer *et al.*, 2012). The *vice versa* effect, which means increased activity based on a more efficient folding promoted by slower translation, could explain the significant 2-fold increase in extracellular specific activity of the LipA variants $I12L_{CTG}$, $I12V_{GTG}$, $G13T_{ACC}$ and I87I (Fig. 3.11;Tab. 3.4). A deceleration in translation can either be due to the introduction of a rare codon (Smensen *et al.*, 1989; Spencer *et al.*, 2012) or due to a limitation in tRNA availability for frequent codons (Spencer *et al.*, 2012). Two different G13T variants were identified and characterized: The LipA variant $G13T_{ACG}$ shows a significant change in *lipA* transcript amount of 2.7-fold (see 3.5.2), resulting in a significant 1.7-fold increase in extracellular lipase amount and in a significant specific activity reduction to 0.7 (Fig. 3.12; Tab. 3.5). Here, the most frequent glycine codon (21.8 per 1000 bp) is substituted to the second less frequent codon coding for threonine ACG with a frequency of 14.9 per 1000bp (Tab. 3.5). In contrast, the rare ACC codon (9 per 1000 bp) in the $G13T_{ACC}$ variant (Fig. 3.11; Tab. 3.4) shows no effect on *lipA* transcript amount (Tab. 3.4) but significantly increases its extracellular specific activity 2.3-fold (Fig. 3.11; Tab. 3.4). Therefore, this increase is not based on the introduced threonine but on the introduced rare ACC codon, that probably slows down translation. This way, the $G13T_{ACC}$ variant has got more time to fold correctly into its native conformation and results in the significant higher extracellular specific lipase activity. The fact that the identical amino acid substitutions at position 12 based on different codons were identified, with no significant change in extracellular specific lipase activity or amount compared to wtLipA ($I12L_{TTG}$ and $I12V_{GTC}$; Tab. 3.3), also indicates a codon-specific effect here. For the I12 variants, the most frequently used isoleucine codon ATT (36.2 per 1000 bp) is either substituted to the most frequent leucine codon CTG (23 per 1000 bp) or to the second frequent valine codon GTG (17.3 per 1000 bp).

Furthermore, the isoleucine at position 87, natively coded by the rare ATA codon (9.8 per 1000 bp) is also substituted by the second less frequent ATC codon (27.2 per 1000 bp) (Tab. 3.4).This increased extracellular specific lipase activity of the variants $I12L_{CTG}$, $I12V_{GTG}$ and I87I (Fig. 3.11; Tab. 3.4) cannot be explained by changes in the codon frequency promoting a slower translation and this way a more efficient folding but with a slower translation determined by tRNA limitation. Several most frequently used codons are encoded by wobble-base pairing, because they do not have a related tRNA gene (Spencer *et al.*, 2012). Protein synthesis based on wobble-base pairing can be decelerated by higher dissociation rates between the tRNA and the mRNA, this way slowdown translation (Spencer *et al.*, 2012). This results in an increased extracellular specific lipase activity as determined for the LipA variants $I12L_{CTG}$, $I12V_{GTG}$ and I87I (Fig. 3.11; Tab. 3.4), again due to a more efficient folding based on the increased time of the protein to properly fold into its native conformation.

The ATC codon introduced in the I87I variant also leads to a significant 3.6-fold change in *lipA* transcript amount (Tab. 3.4), suggesting an effect on both, *lipA* transcript amount and extracellular lipase activity. Surprisingly, the increased change in *lipA* transcript amount does not result in a corresponding increase in extracellular lipase amount as for the mentioned $G13T_{ACG}$ variant (3.5.2), in contrast it is decreased to 0.7 (Tab. 3.4). A possible explanation for this contradiction could be that the I87I variant is indeed slower translated but also more prone to degradation, because the changed translation velocity and the resulting folding behavior could induce a proteolytic hydrolysis of this variant by the remaining proteases of the *B. subtilis* strain TEB1030 (Kawamura & Doi, 1984).

Specific lipase activity can be increased by single amino acid substitutions and also by synonymous codon substitutions improving translation presumably promoting a more efficient folding of LipA.

Tab. 3.4 Six LipA variants show increased extracellular specific lipase activity.
The table shows the structural location of the variant amino acid substitution (struc.), as well as the orientation (ori.) of the amino acid residues (s: surface; b: buried). The wild-type (wt) codon and the introduced variant codon are named together with the codon frequency per 1000 bp. The relative change in transcript level is shown together with the lower and upper deviation. Significant transcript changes compared to wt*lipA* above the cutoff of 2.2 and a p-value < 0.05 are marked with an asterisk. The relative extracellular specific lipase activity and the extracellular lipase amount are shown with the standard deviation and significant changes compared to wtLipA ($p < 0.05$) are marked with an asterisk.

variant	struc.	ori.	wt codon	frequency per 1000bp	variant codon	frequency per 1000bp	rel. change in transcript level	lower deviation	upper deviation	rel. specific activity	± std.	rel. lipase amount	± std.
LipA variants with increased extracellular specific lipase activity													
I12F	turn	s	ATT	36.2	TTC	14.3	1.688	0.360	0.540	2.082*	0.373	1.599*	0.216
$I12L_{CTG}$	turn	s	ATT	36.2	CTG	23.0	1.032	0.358	0.683	2.365*	0.309	0.931	0.320
$I12V_{GTG}$	turn	s	ATT	36.2	GTG	17.3	1.336	0.302	0.560	1.846*	0.427	0.968	0.315
G13S	turn	s	GGA	21.8	TCG	6.5	1.412	0.488	0.544	1.414*	0.269	0.598*	0.355
$G13T_{ACC}$	turn	s	GGA	21.8	ACC	9.0	1.237	0.423	0.504	2.297*	0.332	0.465*	0.193
I87I	αC	s	ATA	9.8	ATC	27.2	3.581*	0.645	0.862	2.345*	0.296	0.718*	0.370

3.5.2. 21 LipA variants show increased extracellular lipase amount compared to wtLipA

Despite the six identified LipA variants with single amino acid and codon substitutions that were identified as beneficial for extracellular specific lipase activity for several reasons (3.5.1), 21 LipA variants were identified with significant 1.3- to 2.3-fold increase in extracellular lipase amount at prevalently similar or decreased levels of extracellular specific lipase activity compared to wtLipA (Tab. 3.5), with variant I12F being the exception also showing a significant 2-fold increase in extracellular specific lipase activity (Fig. 3.11; Tab. 3.4).

The LipA variant $G13T_{ACG}$ is the only one exhibiting a significant change in *lipA* transcript level of 2.7-fold compared to wtlipA. This could explain the 1.6-fold increase in extracellular lipase amount (Fig. 3.12; Tab. 3.5). The transcript amount of all other 20 LipA variants is not significantly changed compared to wt*lipA* transcript (Tab. 3.5, 2.11).

Two R57T variants based on two different threonine codons ACC and ACG (Tab. 3.5) were identified. Both variants show a similar significant increase in extracellular lipase amount of 1.4-fold and a similar significant decrease in extracellular specific lipase activity to 0.7 compared to wtLipA. This rather suggests an amino acid effect than a codon effect on these substitutions. These R57T variants and five other LipA variants (N50D, P53D, P53E, P53V and M134Q) with significant increased extracellular lipase amount show amino acid substitutions located either in the αB-helix of LipA or show a substitution to glutamine at position 134 located in a loop structure (M134Q) (Fig. 3.12). Amino acid positions in the αB-helix are known to contribute to detergent tolerance when substituted to amino acids with opposite charges concerning the tested detergent (Fulton *et al.*, 2015) and to ionic liquid resistance when charged and/or polar residues are introduced (Frauenkron-Machedjou *et al.*, 2015). Therefore, it is possible that the higher extracellular LipA amount of these variants is due to a stability effect in the culture supernatant of *B. subtilis*. This stability issue could also explain the 2-fold higher extracellular LipA amount of the variant M134Q (Fig. 3.12; Tab. 3.5).

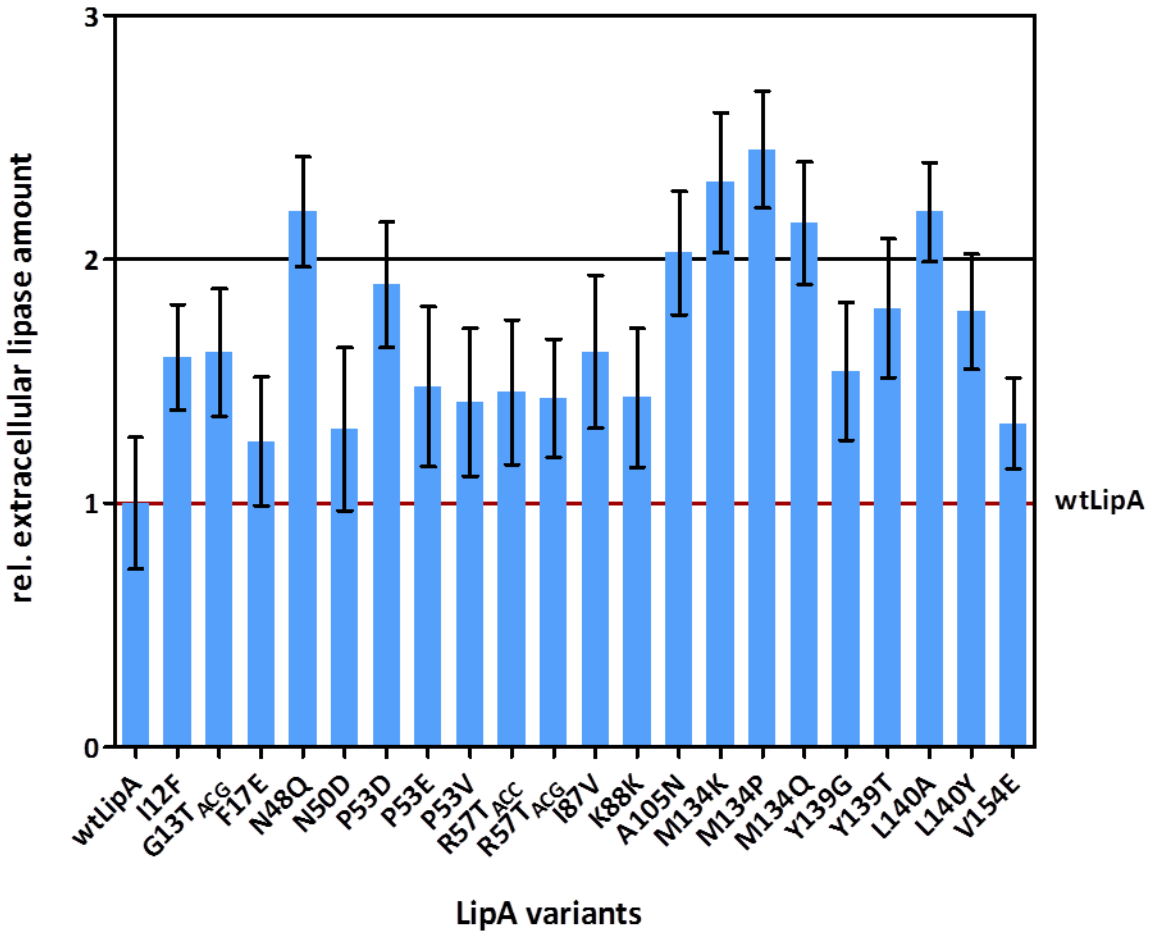

Fig. 3.12 21 LipA variants with higher extracellular lipase amount.
B. subtilis TEB1030 producing each of the 21 LipA variants with increased extracellular lipase amount was cultivated as three biological replicates in a 48-well Flowerplate® for 6 h and the extracellular lipase amount (mg/ml) was quantified by ELISA using a specific polyclonal LipA antibody. The relative extracellular lipase amount of LipA variants with significant ($p < 0.05$) beneficial changes compared to wtLipA are plotted. The red line indicates the normalized extracellular wtLipA amount.

It is known that more polar residues like the introduced glutamine in this variant are generally preferred on the protein surface to obtain enhanced stability (Kamal *et al.*, 2011). Therefore, the M134Q LipA variant which has a less polar methionine substituted by a polar glutamine is probably not more efficiently secreted but gained higher stability in the *B. subtilis* culture supernatant.

For the 13 other LipA variants with similar transcript levels compared to wtlipA (I12F, F17E, N48Q, I87V, K88K, A105N, M134K, M134P, Y139G, Y139T, L140A, L140Y, and V154E; Fig. 3.12;Tab. 3.5) there are no stability effects of these amino acid positions or substitutions described in literature so far excepting the amino acid positions N48 and A105. These two have been previously identified during thermal unfolding simulations as so called `weak spot

residues`, whose mutation could maybe enhance LipA`s thermostability (Rathi *et al.*, 2016), but was not proven experimentally so far. Thus, it is possible that new positions and substitutions that contribute to LipA stability were identified or that these variants are more efficiently secreted. No preference could be observed concerning the chemical property of the introduced amino acid compared to the wild-type amino acid and the corresponding position. Eleven variants show substitutions to less hydrophobic amino acids, I12F, F17E, P53D, P53E, A105N, M134K, M134P, M134Q, L140A, L140Y and V154E. These substitutions are found in all parts of the LipA primary sequence, the N-terminal part (position 12 and 17), the mid (positions 53 and 105) and the C-terminal part (position 134, 140 and 154). Five variants exhibits substitutions to more hydrophobic amino acids, P53V and $R57T_{ACC}$, $R57T_{ACG}$, Y139G, and Y139T in the mid part of the LipA primary sequence, while the substitutions to glutamine, aspartate and valine within the variants N48Q, N50D and I87V do not change the hydrophobicity of these residues. A negative effect on homologous secretion was formerly described for randomly distributed amino acid substitutions within lipase A of *Pseudomonas aeruginosa* (Hausmann *et al.*, 2008). This finding in turn underlines the suggestion that the mentioned single amino acid substitutions could also increase the extracellular lipase amount of LipA based on an improved secretion.

Despite of this, it is known for the homologous production of the *E. coli* LamB protein, that also the amino acids at the matured N-terminus of the translocated protein are necessary for efficient transport (Rasmussen & Silhavy, 1987). This could also explain the effect of the identified substitutions F17E in the N-terminal part of LipA. Here, the introduction of the negatively charged glutamate in the F17E variant decreases the net charge of LipA to -1. This influence of the N-terminal net charge on efficient protein secretion was former described with a statistical analysis for Gram-negative bacteria but was actually excluded for Gram-positive organisms in this study (Kajava *et al.*, 2000), however the results shown here in turn may indicate a beneficial influence of the amino acid net charge on LipA secretion as shown by the increased extracellular protein amount of this particular F17E variant in *B. subtilis*. Concerning the two N-terminal substitutions I12F and N48Q, the two substitutions within the mid part (I87V, A105N) and the substitutions within the C-terminal part of LipA (M134K, M134P, M134Q, Y139G, Y139T, L140A, L140Y, and V154E) it is possible that these introduced amino acids have a higher affinity to or show a better interaction with translocation machinery components.

Tab. 3.5 21 LipA variants with higher extracellular lipase amount.

The table shows the structural location of the variant amino acid substitution (struc.), as well as the orientation (ori.) of the amino acid residues (s: surface; b: buried). The wild-type (wt) codon and the introduced variant codon are named together with the codon frequency per 1000 bp. The relative change in transcript level is shown together with the lower and upper deviation. Significant transcript changes compared to wt*lipA* above the cutoff of 2.2 and a p-value < 0.05 are marked with an asterisk. The relative extracellular specific lipase activity and the extracellular lipase amount are shown with the standard deviation and significant changes compared to wtLipA ($p < 0.05$) are marked with an asterisk.

variant	struc.	ori.	wt codon	frequency per 1000bp	variant codon	frequency per 1000bp	rel. change in transcript level	lower deviation	upper deviation	rel. specific activity	± std.	rel. lipase amount	± std.
LipA variants with higher extracellular LipA amount													
I12F	turn	s	ATT	36.2	TTC	14.3	1.688	0.360	0.540	2.082*	0.373	1.599*	0.216
$G13T_{ACG}$	turn	s	GGA	21.8	ACG	14.9	2.720*	0.862	1.180	0.761*	0.384	1.618*	0.261
F17E	αA	s	TTC	14.3	GAG	22.6	2.074	0.566	0.972	0.540*	0.364	1.254*	0.263
N48Q	αB	s	AAT	22.9	CAG	18.5	2.155	0.640	1.199	0.565*	0.267	2.194*	0.226
N50D	αB	s	AAC	17.8	GAC	19.0	0.849	0.329	0.426	0.777*	0.453	1.303*	0.334
P53D	αB	s	CCG	16.3	GAC	19.0	1.044	0.203	0.34	0.686*	0.423	1.895*	0.257
P53E	αB	s	CCG	16.3	GAG	22.6	0.980	0.140	0.179	0.850*	0.368	1.477*	0.328
P53V	αB	s	CCG	16.3	GTG	17.3	1.252	0.329	0.458	0.737*	0.291	1.414*	0.302
$R57T_{ACC}$	αB	s	CGA	4.3	ACC	9.0	0.768	0.295	0.687	0.753*	0.395	1.454*	0.297
$R57T_{ACG}$	αB	s	CGA	4.3	ACG	14.9	0.853	0.217	0.327	0.702*	0.379	1.431*	0.242
I87V	αC	s	ATA	9.8	GTG	17.3	1.250	1.224	8.626	1.060	0.311	1.621*	0.314
K88K	αC	s	AAA	48.4	AAG	20.8	1.579	0.352	0.467	0.360*	0.274	1.433*	0.285
A105N	coil	s	GCG	19.8	AAC	17.8	1.236	0.302	0.334	0.535*	0.324	2.026*	0.253
M134K	coil	s	ATG	26.3	AAG	20.8	1.098	0.336	0.509	0.852	0.385	2.314*	0.286
M134P	coil	s	ATG	26.3	CCG	16.3	0.63	0.138	0.127	0.231*	0.295	2.45*	0.239
M134Q	coil	s	ATG	26.3	CAG	18.5	0.801	0.209	0.246	0.413*	0.325	2.147*	0.250
Y139G	αE	s	TAC	12.6	GGG	11.2	1.749	0.682	0.829	0.630*	0.350	1.540*	0.282
Y139T	αE	s	TAC	12.6	ACG	14.9	2.074	0.463	0.548	0.508*	0.423	1.799*	0.285
L140A	αE	s	TTA	19.8	GCG	19.8	1.620	0.371	0.486	0.394*	0.270	2.194*	0.203
L140Y	αE	s	TTA	19.8	TAC	12.6	1.603	0.514	1.324	0.558*	0.371	1.786*	0.236
V154E	coil	s	GTT	18.6	GAG	22.6	0.925	0.279	0.38	0.584*	0.273	1.326*	0.186

This was observed for the LamB protein of *E. coli* where single mutations in the C-terminal part could complement secretion deficiencies of a mutated signal peptide by a higher affinity to the cytosolic SecB chaperone (Altman *et al.*, 1990). Although LipA is secreted cotranslational in *B. subtilis*, thus retaining in an unfolded conformation while secretion takes place simultaneously to translation, (Fekkes & Driessen, 1999; Tjalsma *et al.*, 2004; Ton-That *et al.*, 2004; Zanen *et al.*, 2006), it is still possible that during the secretion process LipA and, in a more efficient way, its variants in some kind interact with components of the secretion pathway like SRP, SecATPase or SecYEG translocon (Fekkes & Driessen, 1999; Tjalsma *et al.*, 2004; Ton-That *et al.*, 2004; Zanen *et al.*, 2006). The K88K variant with the synonymous codon substitution showed a 1.4-fold increase in extracellular lipase amount at similar levels of *lipA* transcript compared to wtLipA (Fig. 3.12; Tab. 3.5), this means that the increase in extracellular lipase amount could not be explained by an underlying correlated increase in *lipA* transcript level, which in turn would be possible based on the introduced codon exchange (Tab. 3.5). Because K88K is a silent substituted variant, also a changed interaction with components of the translocation machinery can be excluded, as they were discussed for the variants M134K, M134P, M134Q, Y139G, Y139T, L140A, L140Y, and V154E. Therefore, an influence of this silent substitution is probably due to a higher stability of this K88K variant. As described for the variant $G13T_{ACG}$ in section 3.5.1, the codon frequency can determine the translation efficiency and so promoting a more efficient folding of the protein. In the case of this silent K88K variant, a less frequent AAG codon (frequency 20.8 per 1000 bp) is introduced that decrease the translation and increase the folding efficiency in this way not resulting in an increased extracellular specific lipase activity but in a more stable LipA variant represented by the increased extracellular lipase amount (Fig. 3.12; Tab. 3.5).

Higher extracellular lipase amount of LipA variants could be explained with increased *lipA* transcript level, enhanced LipA stability in the culture supernatant or improved secretion of LipA.

3.5.3. Recovery of signal peptide-mediated secretion deficiency by single amino acid substitutions within LipA

Several previous studies assay the Sec-specific signal peptide to optimize protein secretion in *B. subtilis,* especially for heterologous proteins (Brockmeier *et al.*, 2006; Caspers *et al.*, 2010; Degering *et al.*, 2010). They started with a screening of all homologous signal peptides from *B. subtilis* (Brockmeier *et al.*, 2006), followed by a screening of also heterologous signal peptides from *B. licheniformis* (Degering *et al.*, 2010) and finally applied a saturation mutagenesis for the N-domain of a homologous signal peptide (Caspers *et al.*, 2010). The results from these studies revealed that target protein secretion, in some cases, can be improved by an altered or even a different signal peptide, but also indicated that the signal peptide must be specifically adjusted to the target protein. This means that an optimal signal peptide from one target protein cannot be transferred to any other optional protein without prior adaptation and suggested some kind of influence of the target protein on its secretion.

Summarized so far it is known that first, efficient and inefficient signal peptides exist depending on the translocated protein and second that the target protein, LipA in this case, could possibly influence its secretion by for example possible interactions of amino acids with components of the translocation machinery (3.5.2). These findings should be combined here to prove the dependency of the efficient target protein secretion on the chosen signal peptide and to confirm the positive influence of single amino acid substitutions on LipA secretion by *B. subtilis*. The fusion of an inefficient homologous signal peptide to LipA should reduce LipA secretion first to analyze the effect of subsequently introduced single amino acids within LipA that were identified as increasing extracellular LipA amount. This way it is possible to analyze if decreased secretion mediated by an inefficient signal peptide can be recovered by altering LipA, thus confirming the impact of the translocated target protein on its secretion.

To identify an inefficient homologous *B. subtilis* signal peptide, the former generated signal peptide-toolbox with all 173 Sec-specific signal peptides from *B. subtilis* (Brockmeier, 2006) was used. This library was introduced into the pBSMul1*lipA*_SP (Tab. 2.2; 2.12), *E. coli* DH5α was transformed (2.9.1) the plasmids were isolated (2.6) and *B. subtilis* TEB1030 was transformed by protoplast formation (2.9.3). The so generated signal peptide library was analyzed as already described for the first step of the site saturation mutagenesis library screening with the remarkable difference, that clones with decreased extracellular lipolytic

activity and amount should be identified here (2.22). Therefore, 558 *B. subtilis* TEB1030 clones were picked to achieve a three times oversampling, regarding the number of possibly introduced signal peptides, and therefore a library coverage of about 95 % (Reetz *et al.*, 2008). Using the here established ELISA (3.2.2) to quantify the extracellular lipase amount, the signal peptide of the minor extracellular serine protease Vpr (Accession number: P29141) was identified to significantly reduce extracellular lipase amount of wtLipA to 40 % (Fig. 3.13A).

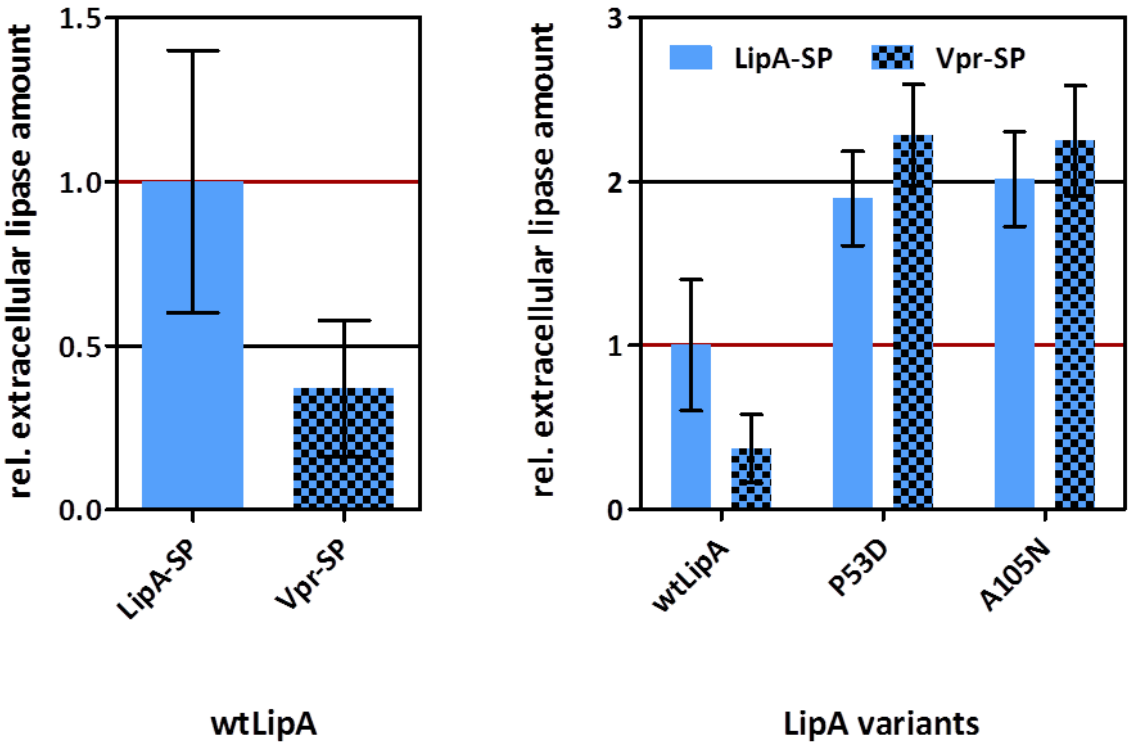

Fig. 3.13 Interactive effects of LipA with the homologous inefficient Vpr signal peptide.
A Extracellular lipase amount of LipA secreted with its native LipA signal peptide and the homologous Vpr signal peptide. The significantly ($p < 0.05$) reduced relative extracellular lipase amount (mg/ml) of wtLipA secreted with the homologous Vpr signal peptide (Vpr-SP) compared to the wtLipA situation is plotted. ELISA was used for extracellular lipase amount quantification. The red line indicates the normalized extracellular lipase amount of wtLipA secreted with its native LipA signal peptide (LipA-SP)**. B LipA variants with increased extracellular lipase amount secreted with the native LipA signal peptide and the homologous Vpr signal peptide**. The significantly ($p < 0.05$) increased relative extracellular lipase amount of LipA variants either secreted with the LipA-SP or with the Vpr-SP compared to the corresponding wtLipA situation is plotted. The red line indicates the normalized extracellular lipase amount of wtLipA secreted with the native LipA-SP.

The second step was then the introduction of here identified beneficial single amino acid substitutions for extracellular lipase amount (3.5.2) using site directed mutagenesis (2.12.2) in order to analyze the possible recovery of the signal peptide mediated secretion deficiency. Therefore, LipA with one of the two chosen identified beneficial single amino acid

substitutions for extracellular lipase amount, P53D and A105N (3.5.2; Fig. 3.12; Tab. 3.5) was analyzed with both, the native LipA signal peptide (LipA-SP) and the homologous Vpr signal peptide (Vpr-SP) compared to the respective wild-type situation, which means wtLipA secreted with its native LipA-SP and secreted with the homologous Vpr-SP (Fig. 3.13B).

The single amino acid substitutions P53D and A105N lead to a significantly 2.3-fold increase in extracellular lipase amount of LipA secreted with its native LipA-SP, compared to the respective wtLipA situation (Fig. 3.13B). The similar beneficial effect of the single amino acid substitutions could be observed for LipA secreted with the homologous Vpr-SP (Fig. 3.13B). Here, the substitutions actually increase the extracellular lipase amount significantly 6-fold compared to the corresponding wtLipA situation this way achieving similar amounts of extracellular altered LipA secreted with the inefficient Vpr-SP as determined for altered LipA secreted with the LipA-SP. Concerning the intended recovery of the Vpr signal peptide mediated inefficient LipA secretion (Fig. 3.13A) it is not only possible to achieve similar levels of extracellular lipase amount compared to wtLipA secreted with the LipA-SP but also to further increase extracellular lipase amount of poorly secreted LipA with the inefficient Vpr-SP significantly 2.3-fold based on introduced amino acids aspartic acid (P53D) and asparagine (A105N) (Fig. 3.13B). The secretion of proteins is dependent on the presence of the secretion mediating signal peptide. The signal peptide function as a targeting signal for secretory proteins, which is composed of three conserved domains: a positively charged N-domain, a hydrophobic core region and a polar C-region (Tjalsma *et al.*, 2000). Concerning the Sec-mediated secretion of proteins and the role of the signal peptide, a so called `positive-inside role` was proposed (Van Roosmalen *et al.*, 2004). This means that in the first step in translocation, the positively charged N-domain of the signal peptide is attracted by the negatively charged cytoplasmic membrane. In a second step, the signal peptide forms a loop structure and is pulled through the Sec translocon. This way, the whole protein passes the signal peptide within the translocation pore during its translocation (Fig. 3.14). This could be the situation that facilitates some kind of interaction of the introduced aspartic acid (P53D) and the introduced asparagine (A105N) with the homologous Vpr-signal peptide and so improving LipA secretion which results in the 6-fold increase in extracellular lipase amount and completely recovers Vpr-SP mediated secretion deficiency of LipA.

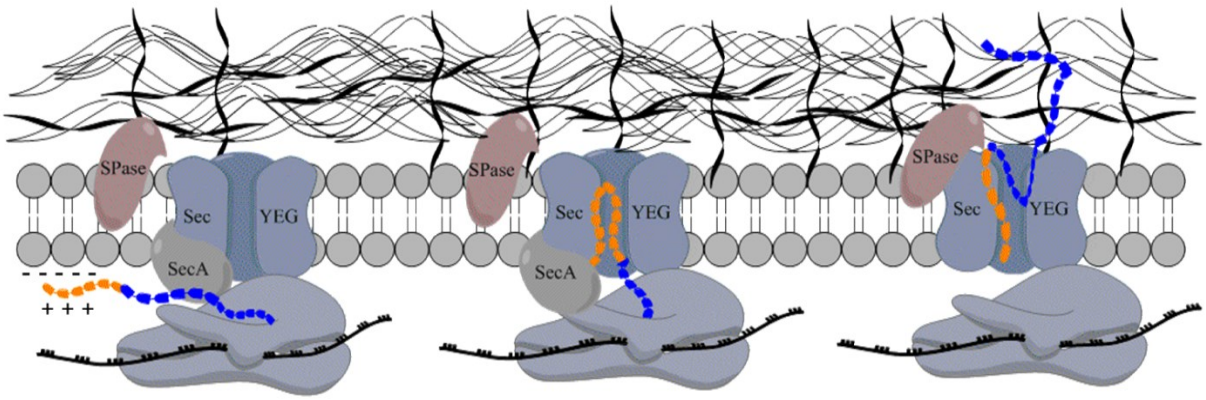

Fig. 3.14 The `positive-inside rule`.
Modified according to (Van Roosmalen *et al.*, 2004). First, the positively charged N-terminal domain of the signal peptide (yellow) is attracted by the negatively charged cytoplasmic membrane. In a second step, the signal peptide is pulled through the Sec translocon, while forming a loop structure. This way the whole protein (blue) passes the signal peptide in the third step during translocation. SecA: SecATPase; SecYEG: Sec translocon; SPase: Signal peptide peptidase.

A detailed hypothesis, based on a sequence comparison of both signal peptides, of how the introduced hydrophilic amino acids interact with the Vpr signal peptide is difficult, because although signal peptides share a common domain organization (positively charged N-domain, hydrophobic core region and a polar C-region) the detailed amino acid composition within this domains is highly variable (Tjalsma *et al.*, 2000). However, based on the fact that in both cases (P53D and A105N) a hydrophobic amino acid is substituted with a hydrophilic one maybe allow the suggestion of an improved interaction of these with the central hydrophobic region of the signal peptide. A general interaction is shown by comparable extracellular LipA amounts after secretion of altered LipA with both signal peptides (Fig. 3.13B) and a specific more efficient interaction with hydrophobic amino acids is shown with the Vpr-SP due to a different detailed amino acid composition of the LipA-SP and the Vpr-SP. As previously discussed in 3.5.2, both positions P53 and A105 are known in relation to LipA stability, probably providing an additional explanation for the increase in extracellular lipase amount. The proline at position 53 is located in the αB-helix of LipA that was described to contribute to LipA stability towards detergents and ionic liquids (Frauenkron-Machedjou *et al.*, 2015; Fulton *et al.*, 2015) and the alanine at position 105 was identified as a possible `weak spot` during thermal unfolding simulations (Rathi *et al.*, 2016). This means that mutations here maybe improve LipA`s thermostability. Taken together, probably two effects lead to the increased extracellular lipase amount here that confirms the recovery of the Vpr signal peptide mediated secretion deficiency of LipA by introduction of single amino acid

substitutions: on the one hand the increased secretion of LipA by an improved interaction with the Vpr signal peptide and on the other hand the production of a more stable LipA in the *B. subtilis* culture supernatant.

Beneficial single amino acid substitutions within LipA can complement a signal peptide mediated secretion deficiency.

3.6. Universal rational combination of beneficial single amino acid substitutions is not possible

Several single amino acid substitutions within LipA were identified that are beneficial for *lipA* transcription (3.5.1; 3.5.2), LipA extracellular specific lipase activity (3.5.1) and extracellular lipase amount (3.5.2). For two amino acid substitutions that increase the extracellular lipase amount up to 2-fold (3.5.2) it was also possible to show that these substitutions within LipA are able to complement signal peptide mediated secretion deficiencies (P53D and A105N) (3.5.3). These results obtained with LipA, a favored model protein for industrial relevant protein engineering (1.5) give new global insights for engineering on the protein production level on the one hand but also reveal new substitutions within LipA that are beneficial for its activity (3.5.1) and stability (3.5.2) in the culture supernatant. Concerning the role of LipA as a model protein for the improvement of industrial relevant lipases towards a specific function, two questions go along with the gained results. First, whether these identified beneficial single amino acid substitutions can be combined in the manner of a direct rational protein engineering approach (3.6.1; 3.6.2) and second, whether these substitutions can be transferred to another protein with the similar outcome (3.7). To answer the first question, combinatorial effects as well as additive effects were analyzed. Combinatorial effects mean the generation of a LipA variant that show an increase in extracellular specific lipase activity combined with a higher extracellular lipase amount, and additive effects to further increase only the extracellular lipase amount by joining to respective mutations. Therefore, single substitutions were chosen, that only show one specific effect on LipA production and secretion, either increased activity or amount. This specific effect in turn should rely on the introduced amino acid and not on the introduced codon or nucleotide. These selection criteria are necessary to minimize multiple effects that were already observed for single substitutions (3.5.1; 3.5.2) and could complicate the evaluation of the double mutants. The single amino acid substitution G13S (3.5.1) was chosen for increasing the extracellular specific lipase activity and four single amino acid substitutions were chosen that led to higher extracellular lipase amount N48Q, P53D, A105N and Y139T (3.5.2), maybe due to enhance LipA stability in the culture supernatant (N48Q, P53D, A105N) or by improving LipA secretion into the *B. subtilis* culture supernatant (Y139T) (3.5.2).

The substitutions were introduced by site directed mutagenesis (2.12.2) and *B. subtilis* TEB1030 transformed with the generated expression vectors was cultivated as described for the analysis of the identified 38 LipA variants with beneficial single substitutions (2.23). Different effects based on the analyzed amino acid combination could be observed and are described and discussed in the following.

3.6.1. A combination of activity and protein amount related amino acid substitutions is not beneficial

No combinatorial effect could be observed when combining a single amino acid substitution beneficial for lipase activity (G13S) and an amino acid substitution A105N and Y139T increasing extracellular lipase amount (Fig. 3.15A and B). Concerning the *lipA* transcript level of variants with combined amino acid substitution no significant changes could be observed (Tab. 3.6) based on the determined cutoff of 2.2 and 0.4 (2.11; 3.5). The single amino acid substitution beneficial for extracellular specific lipase activity G13S is combined with protein amount increasing A105N, the extracellular specific lipase activity of the double mutant G13S/A105N is indeed significantly increased 2.8-fold compared to wtLipA (42.7 ± 9.1 U/mg) and reaches similar levels compared to the G13S single LipA variant (Fig. 3.15A; Tab. 3.6). In contrast to the increased extracellular specific lipase activity of the G13S/A105N variant the extracellular lipase amount is only slightly increased compared to wtLipA but reduced compared to the single A105N variant (Fig. 3.15A; Tab. 3.6). This indicates the implementation of the G13S substitution increasing the extracellular specific lipase activity of the double mutant and replacing the influence of the A105N substitution. Interestingly, the second combinatorial double mutant G13S/Y139T shows a different effect when both single amino acid substitutions are combined. Here, the extracellular specific lipase activity is unaffected compared to wtLipA and 2.5-fold reduced when compared to the G13S single variant (Fig. 3.15B; Tab. 3.6). Whereas the extracellular lipase amount is significantly increased 1.4-fold compared to wtLipA, but reduced compared to the single A105N variant (Fig. 3.15B).

Tab. 3.6 Combinatorial and additive effects of single amino acid substitutions.
The table shows the single and combined amino acid substitutions and the structural location of the variant amino acid substitution (struc.), as well as the orientation (ori.) of the amino acid residues (s: surface; b: buried). The wild-type (wt) codon and the introduced variant codon are named together with the codon frequency per 1000 bp. The relative change in transcript level is shown together with the lower and upper deviation. Significant transcript changes compared to wt*lipA* above the cutoff of 2.2 and a p-value < 0.05 are marked with an asterisk. The relative extracellular specific lipase activity and the extracellular lipase amount are shown with the standard deviation and significant changes compared to wtLipA ($p < 0.05$) are marked with an asterisk.

variant	struc.	ori.	wt codon	frequency per 1000bp	variant codon	frequency per 1000bp	rel. change in transcript level	lower deviation	upper deviation	rel. specific activity	± std.	rel. lipase amount	± std.
single amino acid substitutions													
G13S	turn	s	GGA	21.8	TCG	6.5	1.778	0.573	1.177	2.515*	0.453	0.962	0.519
N48Q	αB	s	AAT	22.9	CAG	18.5	1.319	0.511	0.747	0.126*	0.571	2.772*	0.318
P53D	αB	s	CCG	16.3	GAC	19.0	1.846	0.438	1.232	0.766	0.475	1.893*	0.455
A105N	coil	s	GCG	19.8	AAC	17.8	2.122	0.558	1.339	0.788	0.304	2.404*	0.387
Y139T	αE	s	TAC	12.6	ACG	14.9	0.854	0.166	0.199	1.137	0.375	2.241*	0.305
combinatorial effects in activity and protein amount (3.6.1)													
G13S/N48Q							1.179	0.193	0.228	0.584*	0.464	2.492*	0.376
G13S/P53D							1.783	0.736	1.334	1.617*	0.401	1.372*	0.429
G13S/A105N							2.077	0.604	1.234	2.876*	0.431	1.412*	0.499
G13S/Y139T							1.172	0.150	0.202	0.845	0.477	1.390*	0.406
additive effects in protein amount (3.6.2 and 3.6.3)													
N48Q/P53D							1.537	0.302	0.535	0.401*	0.380	1.300	0.499
N48Q/ A105N							1.284	0.27	0.325	2.179*	0.332	0.784	0.661
N48Q/Y139T							1.231	0.269	0.4	1.935*	0.272	0.962	0.580
P53D/A105N							1.638	0.721	1.591	0.813	0.423	2.622*	0.474
P53D/Y139T							1.457	0.229	0.289	0.557*	0.454	2.692*	0.417
A105N/Y139T							1.403	0.246	0.330	0.371*	0.441	3.592**	0.416

Here, both beneficial single amino acid substitutions compensate each other when combined, preventing a combination of the two beneficial effects. For both described situations G13S/A105N and G13S/Y139T, some kind of interactive effects between the single substitutions could be a possible explanation.

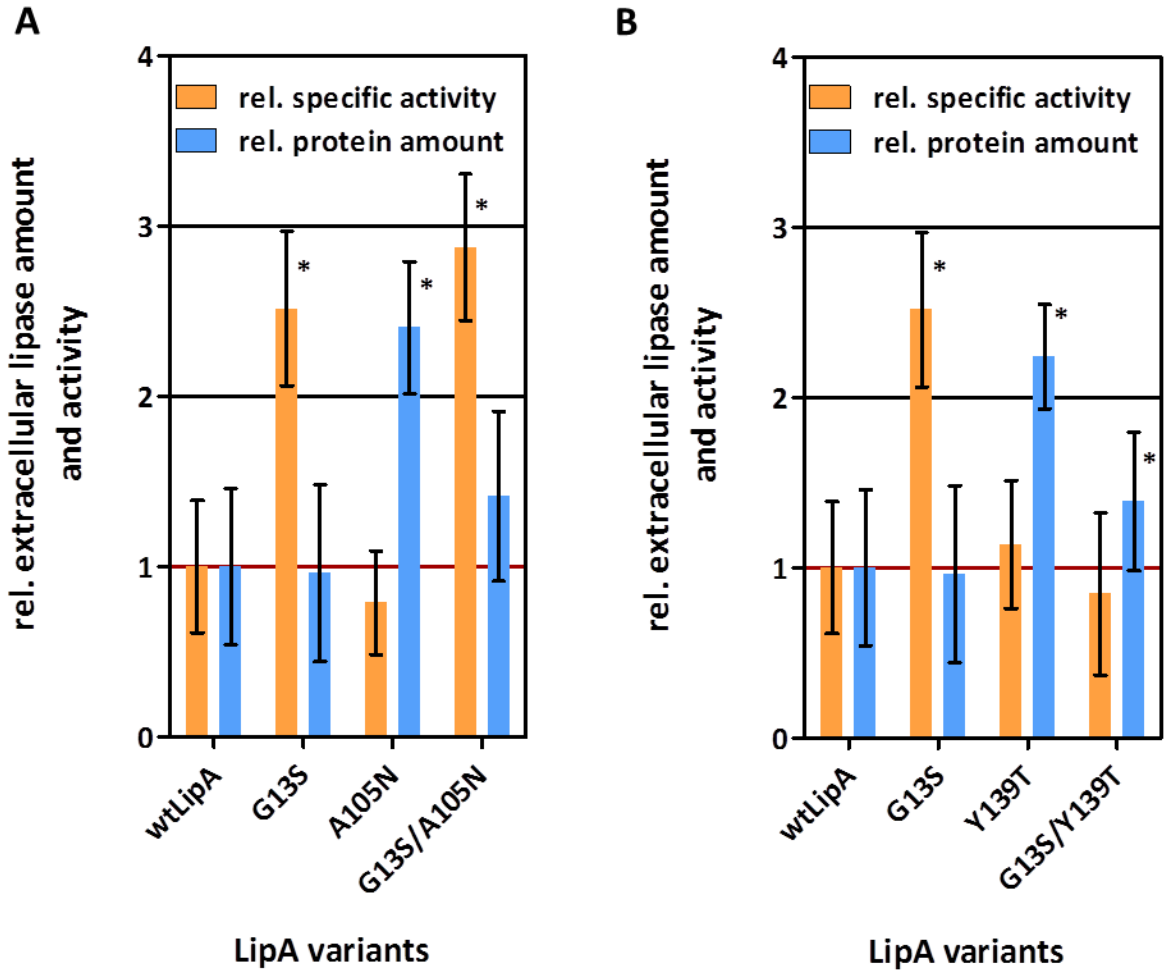

Fig. 3.15 Combinatorial effects of increased activity and amount are not possible.
A and B *B. subtilis* TEB1030 producing each of the single and combined LipA variants was cultivated for 6 h in a 48-well Flowerplate® and the relative extracellular specific lipase activity in the culture supernatant was calculated by normalizing the volume activity (U/ml) to the determined protein amount (mg/ml). The extracellular lipase activity was measured using *p*NPP as a substrate and the extracellular protein amount was determined by ELISA using a specific polyclonal LipA antibody. The relative extracellular specific lipase activity (orange) and the relative extracellular lipase amount (blue) of each single and combined LipA variant is plotted. The red line indicates the normalized extracellular specific lipase activity (orange) and the extracellular lipase amount (blue) of wtLipA. Significant changes, with a p-value < 0.05, compared to wtLipA, are marked with an asterisk.

The substituted positions 13, 105 and 139 are located in structural flexible regions (Van Pouderoyen *et al.*, 2001). As shown in the structural wild-type situation for the G13/A105 variant (Fig. 3.16A) and the G13/Y139 variant (Fig. 3.16B), position 13 is located in a loop-

structure, position 105 is found in a coil and position 139 is located in the αE-helix that only consists of four amino acids (Tab. 3.6). The effect of the single substitution G13S located next to the I12 that is part of the oxyanion hole (Van Pouderoyen *et al.*, 2001) was already discussed in section 3.5.1.

Here, it is possible that the introduction of the polar serine leads to a bending of the loop structure, which in turn causes a conformational change and so indirectly stabilizing the transition state during substrate hydrolysis. The additional introduction of the asparagine at position 105 does not seem to counteract this conformational change, so the effect of the G13S substitution resulting in increased extracellular specific lipase activity is predominant. In contrast, the substitution to the polar asparagine at A105 increases extracellular lipase amount 2-fold (Fig. 3.15A) and was discussed as a possible spot which substitution could enhance LipA stability in the culture supernatant (3.5.2) (Rathi *et al.*, 2016).

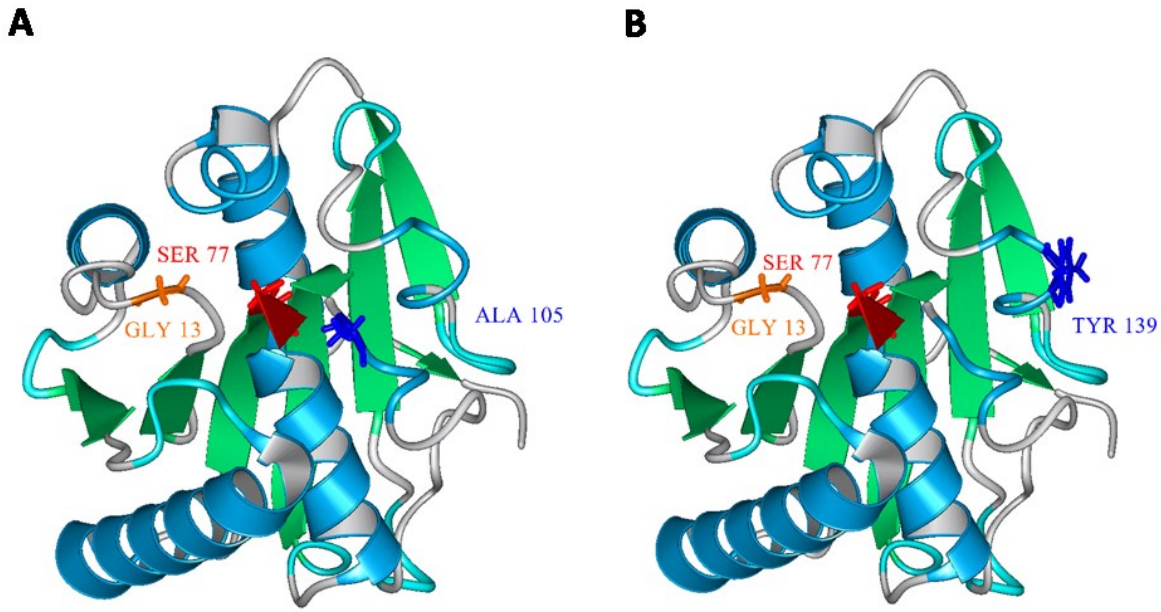

Fig. 3.16 Structural representation of the combined single amino acid positions.
Structure of LipA (PDB: 1I6W) with highlighted wild-type residues exchanged in variant G13S/A105N (**A**) and variant G13S/Y139T (**B**). The wild-type amino acid residues are presented as stick models for those residues with substitutions increasing the relative extracellular specific lipase activity in orange and with substitutions increasing relative extracellular lipase amount in blue. The catalytic serine (Ser 77) is plotted in red.

Based on the result of the double mutant G13S/A105N (Fig. 3.15A), it seems that the A105N effect is not as `strong` as the one shown by G13S, resulting in a double mutant variant which behaves like G13S (Fig. 3.15A). In contrast, the amino acid substitutions G13S and Y139T compensate each other to wtLipA levels for extracellular lipase activity and amount (Fig. 3.15B). Here, it is possible that the substitution of the big, aromatic tyrosine (Fig. 3.16B)

with the smaller uncharged threonine at position 139 resulted in a structural, conformational change that also negatively influences the serine substitution at position 13. So the beneficial effect of the G13S substitution is abolished (Fig. 3.15B). The increase in extracellular lipase amount due to the Y139T of 2-fold in the single variant is reduced to 1.3-fold in the combined variant G13S/Y139T (Fig. 3.15B). For the substitution Y139T or the position 139 in LipA, nothing is known so far concerning any kind of structural stability effect. Nevertheless, based on the gained results (Fig. 3.15B) structural interactive effects of the Y139T with the G13S could not be excluded and could maybe explain the indeed increased extracellular lipase amount in the double variant G13S/Y139T (Fig. 3.15B). Based on the analyzed combined variants it is not possible to generate a LipA variant that shows increased extracellular specific lipase activity as well as increased extracellular lipase amount. The results show that only one effect is implemented (Fig. 3.15A) or both effects compensate each other (Fig. 3.15B).

The generation of LipA variants with combinatorial beneficial single amino acid substitutions for LipA extracellular specific activity and amount was not successful with the chosen substitutions.

3.6.2. The LipA variant A105N/Y139T shows an additive effect in extracellular lipase amount

A possible combinatorial effect of the chosen amino acid substitutions could not be confirmed (3.6.1) indicating that no general predictions for combinatorial effects observed for single amino acid substitutions can be drawn. This assumption is underlined with the results from the analysis of additive effects, because no addition of effects could be observed on the level of extracellular lipase amount when the beneficial single amino acid substitutions N48Q and P53D were combined with the substitutions Y139T and A105N (Fig. 3.17A and B; Tab. 3.6).

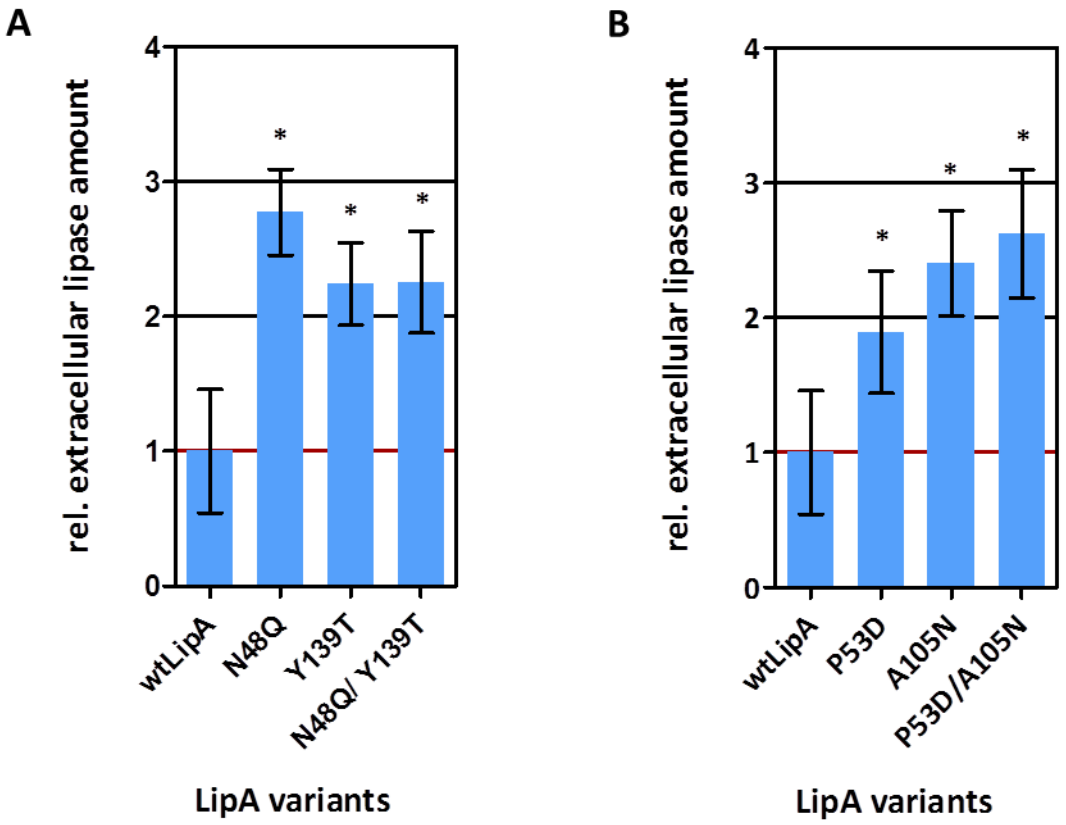

Fig. 3.17 The LipA variants N48Q/Y139T (A) and P53D/A105N (B) show no additive effect in extracellular lipase amount.
B. subtilis TEB1030 producing each of the single and combined LipA variants was cultivated for 6 h in a 48-well Flowerplate® and the relative extracellular lipase amount (mg/ml) was determined by ELISA using a specific polyclonal LipA antibody. The relative extracellular lipase amount (blue) of each single and combined LipA variant is plotted. The red line indicates the normalized extracellular lipase amount (blue) of wtLipA. Significant changes, with a p-value < 0.05, compared to wtLipA, are marked with an asterisk.

No significant changes in *lipA* transcript level of variants with combined amino acid substitution could be observed (Tab. 3.6) based on the determined cutoff of 2.2 and 0.4 (3.5). The variant with the combined substitutions N48Q/Y139T showed a significant 2.3-fold increase in extracellular lipase amount compared to wtLipA (Fig. 3.17A; Tab. 3.6). This result correlates with the quantified extracellular lipase amount for the both variants with the single substitutions N48Q and Y139T that also show a 2.3- to 2.8-fold significant increase of extracellular lipase amount compared to wtLipA (Fig. 3.17A; Tab. 3.6). So in this case a further increase in extracellular lipase amount is not possible. The similar effect was observed for the combination of the substitutions P53D and A105N. The double mutant showed a significant 2.6-fold higher extracellular lipase amount compared to wtLipA (Fig. 3.17B; Tab. 3.6), but this increase is not additive compared to each of the single substitutions, that show a significant 1.8-fold (P53D) and a significant 2.4-fold increase in extracellular lipase amount. As mentioned before, a clear reason or conclusion why the identified single amino acid substitutions lead to an up to 2.3-fold increase in extracellular lipase amount (3.5.2) could not be given, but a few substitutions are localized at positions that are linked to LipA stability, as for example the positions N48 and P53 within the αB-helix of LipA (3.5.2) (Frauenkron-Machedjou *et al.*, 2015; Fulton *et al.*, 2015). Also the alanine at position 105 was previously noticed concerning LipA thermostability (Rathi *et al.*, 2016). Therefore, it is possible that for the double mutants a structural interactive effect occurs that prevent a further stabilization of the lipase resulting in similar extracellular lipase amount compared to the variants with single amino acid substitutions (Fig. 3.17; Tab. 3.6; Fig. 3.18).

Despite the structure concerning stability issue, the limitation for extracellular lipase amount increase could also be a physiological effect of the *B. subtilis* cell. A similar effect was already mentioned during *B. subtilis* TEB1030 producing wtLipA cultivation (3.1). Here it was observed, that after 24 h cultivation of *B. subtilis* TEB1030 producing wtLipA the extracellular lipase activity reaches its optimum, as indicated from the intracellular accumulating lipase activity (3.1; Fig. 3.1A).

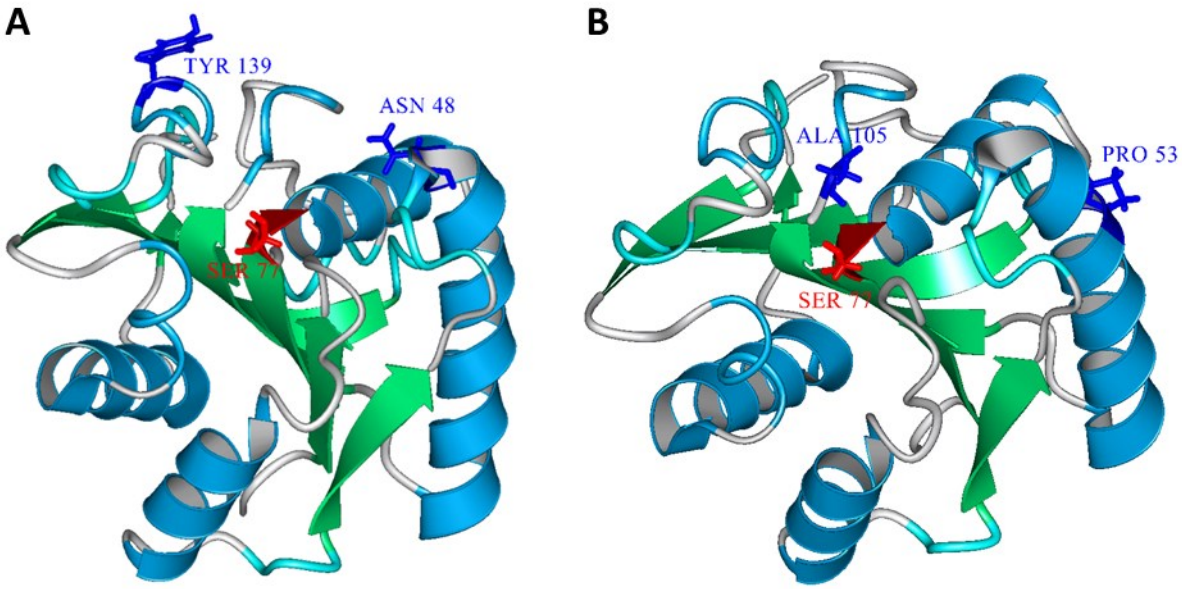

Fig. 3.18 Structural representation of the analyzed additive effects of single amino acid positions.
Structure of LipA (PDB: 1I6W) with highlighted wild-type residues exchanged in variant N48Q/Y139T (**A**) and variant P53D/A105N (slightly moved to the front and to the left) (**B**). The wild-type amino acid residues are presented as stick models for those residues with substitutions increasing relative extracellular lipase amount in blue. The catalytic serine (Ser 77) is plotted in red.

Due to the fact that the identified single amino acid substitutions N48Q, P53D, A105N and Y139T significantly increase the extracellular lipase amount up to 2.4-fold after 6 h of LipA production by *B. subtilis* TEB1030 (Fig. 3.17), it is possible that the observed limitation effect in extracellular accumulation already occurs after a shorter production time. This effect could be explained by a kind of feedback loop, based on extracellular lipase detection and intracellular signal transduction that prevents the *B. subtilis* cell from further secreting the LipA variants. In contrast to these combined amino acid substitutions that show no additive effects in extracellular lipase amount (Fig. 3.17; Tab. 3.6), a further increase in extracellular lipase amount was observed when the single amino acid substitutions A105N and Y139T were combined (Fig. 3.19A; Tab. 3.6; Fig. 3.19B). The single LipA variants A105N and Y139T show a significant increase in extracellular LipA amount of up to 2.4-fold compared to wtLipA (3.5 ± 0.8 µg/ml) (Fig. 3.19A; Tab. 3.6). The LipA double mutant A105N/Y139T shows a significant 3.6-fold increase in extracellular LipA amount (Fig. 3.19A; Tab. 3.6) compared to wtLipA as well as a significant increase of 1.2-fold when compared to the LipA single variants (Fig. 3.19A; Tab. 3.6).

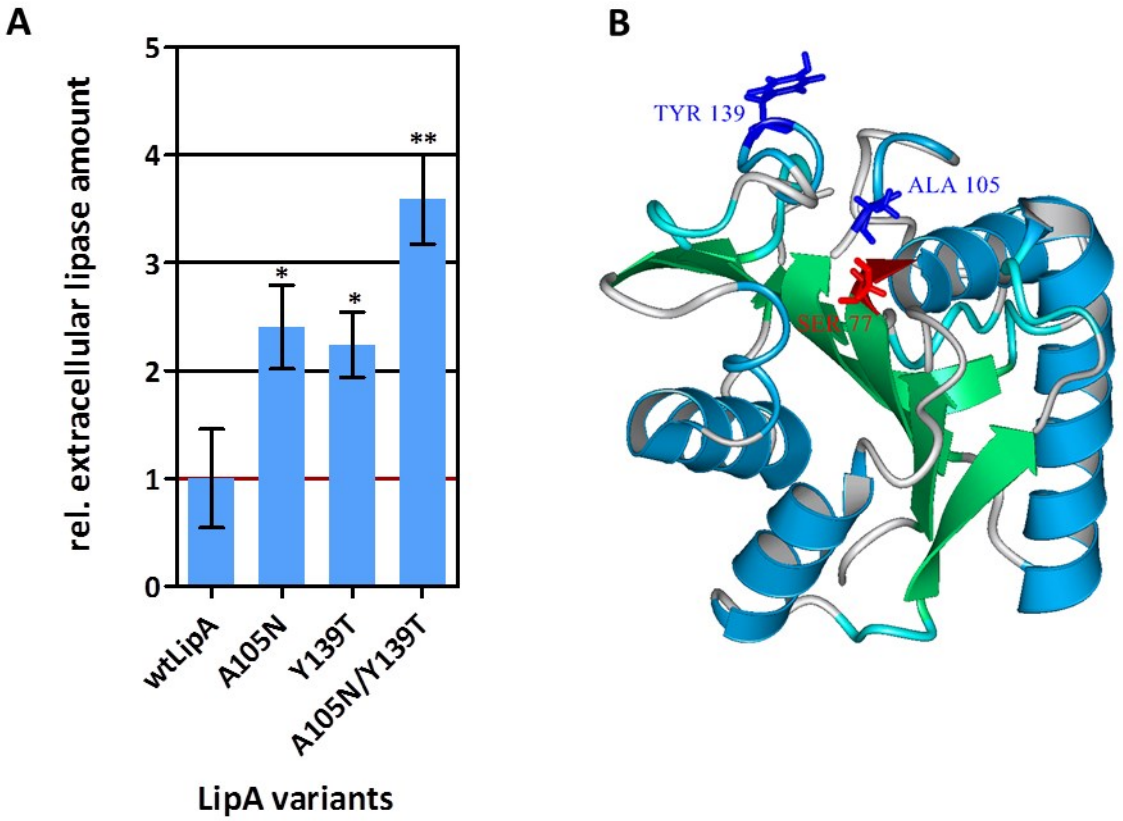

Fig. 3.19 The LipA variant A105N/Y139T shows an additive effect in extracellular lipase amount.
A Additive effect in extracellular lipase amount in LipA variant A105N/Y139T. *B. subtilis* TEB1030 producing each of the single and combined LipA variants was cultivated for 6 h in a 48-well Flowerplate® and the relative extracellular lipase amount (mg/ml) was determined by ELISA using a specific polyclonal LipA antibody. The relative extracellular lipase amount of each single and combined LipA variant is plotted. The red line indicates the normalized extracellular lipase amount of wtLipA. Significant changes, with a p-value < 0.05, compared to wtLipA, are marked with an asterisk, significant changes, with a p-value < 0.05, compared to wtLipA and to the single LipA variants are marked with two asterisks. **B Structural wild-type situation for A105N/Y139T variant**. Structure of LipA (PDB: 1I6W) with highlighted wild-type residues exchanged in variant A105N/Y139T. The wild-type amino acid residues are presented as stick models for those residues with substitutions increasing the relative extracellular lipase amount in blue. The catalytic serine (Ser 77) is plotted in red.

For these two selected single amino acid substitutions, it was possible to further increase the extracellular lipase amount. This increase is possibly based on an increased stability of LipA in the culture supernatant, which in turn is due to some kind of structural interaction of both amino acid substitutions (Fig. 3.19B). Such additive effects were also observed by combining thermostability-related amino acid substitutions, in this case twelve beneficial amino acid substitutions were introduced by several rounds of *in vitro* evolution improving LipA temperature optimum about 30 °C (Kamal *et al.*, 2011).

The fact that already the beneficial impact of single amino acid substitutions on the extracellular lipase amount can be due to either an effect on stability or secretion, or both,

makes it difficult to explain the non-uniform results of the double variants. From six double mutants with rationally predicted additive effects on extracellular lipase amount (Tab. 3.6), only the double mutant A105N/Y139T showed an additive effect (Fig. 3.19), while the others seem to be in some kind limited in extracellular lipase amount. These results indicate that a rational LipA design based on single amino acid substitutions is very difficult, because additive effects seem to be random especially for the chosen substitutions. A more effective approach would be the previously described one for improving LipA thermostability and LipA temperature optimum by applying several iterative mutagenesis rounds and so further improving based on the already beneficial substitutions (Kamal *et al.*, 2011).

A general addition of effects from single amino acid substitutions is not possible. Only one LipA variant A105N/Y139T shows an additive effect on extracellular lipase amount.

3.7. Transfer of beneficial amino acid substitutions for lipase production by *B. subtilis*

The systematic mutational analysis of LipA revealed a huge impact of single codon and amino acid substitutions on its production by *B. subtilis*. Regarding *B. subtilis* role as a `microbial cell factory` for secretory protein production (Westers *et al.*, 2004b) and its continuous optimization as a production host, it is necessary to know if these observed target protein effects are specific for LipA or more general. Therefore, the *B. subtilis* lipase B (LipB) (UniProt: Q79F14) (Eggert *et al.*, 2003) was chosen as a model protein to analyze the transferability of the results gained for LipA. LipB is described as a paralogous protein of LipA (Eggert *et al.*, 2003) with an amino acid sequence identity (without signal peptide) of 73.63 % as determined by sequence alignment using ClustalW (Sievers *et al.*, 2011) (2.24) and UniProt (Consortium, 2008) (2.24). For this transfer purpose a homologous protein is chosen to exclude side effects that could influence the protein production by *B. subtilis* as for example the different codon usage within heterologous genes. The high sequence identity is an advantage for adequate sequence alignment and allows a suitable transfer of selected amino acid substitutions.

3.7.1. Plasmid-based constitutive LipB production

The *B. subtilis* lipase B (LipB) was chosen as the model protein to analyze the transferability of selected single beneficial amino acid substitutions from LipA. Therefore, the similar expression vector was constructed for *lipB* as already for *lipA* (3.1; 2.12). The *lipB* gene, amplified from the genome of *B. subtilis* 168 (2.12) together with its native signal sequence *sslipB* was placed under control of the strong constitutive P_{HpaII} promoter on the pBSMul1 (Brockmeier, 2006) by Gibson-Assembling (Gibson *et al.*, 2009) (2.12). *B. subtilis* TEB1030 was transformed by protoplast formation (2.9.3) with the resulting pBS*lipBsslipB* (2.2) and the corresponding empty vector pBSMul1 (ev) for wild-type LipB (wtLipB) production analysis. As already described for LipA production analysis (3.1) *B. subtilis* TEB1030 with the respective vectors was cultivated for 24 h as three biological replicates in a microfermentation system using a 48-well FlowerPlate® (2.4). In parallel, a growth curve of *B. subtilis* TEB1030 harboring the empty vector pBSMul1 and the *lipB* expression vector pBS*lipBsslipB* was monitored in a second 48-well FlowerPlate® in the BioLector® (2.4), to evaluate *B. subtilis* TEB1030 growth when expressing homologous *lipB.* Samples were taken

2, 4, 6, 8, 10 and 24 h after cultivation start to analyze LipB production within the cells (WC) and LipB secretion into the culture supernatant (S) using a lipolytic activity assay (2.17). As observed for *B. subtilis* TEB1030 growth when producing LipA (3.1; Fig. 3.1), also *B. subtilis* TEB1030 producing LipB shows a slight growth delay in contrast to the cells harboring the empty vector pBSMul1 (ev) (Fig. 3.20A). *B. subtilis* TEB1030 non-producing LipB reaches an $O.D._{600\ nm}$ of 2 after 5 h of cultivation and the LipB producing cells after 6 h of cultivation (Fig. 3.20A). The reason for this delay could be, as well as for *B. subtilis* TEB1030 growth when producing LipA, the `metabolic burden` phenomenon, that describes the energy rerouting of the growing cells from metabolism to target gene expression and target protein synthesis (Bhattacharya & Dubey, 1995; Carneiro *et al.*, 2013; Glick, 1995; Rahmen *et al.*, 2015b). This situation is described for recombinant protein production, but is also possible for homologous LipB production based on the strong constitutive P_{HpaII} promoter. In contrast to LipA production by *B. subtilis* TEB1030 where a continuous increase in extracellular lipase activity normalized to the optical density ((U/ml)/$O.D._{600\ nm}$) could be observed (3.1; Fig. 3.1), the extracellular LipB activity decreases from 4 h of production (0.03 ± 0.003 (U/ml)/$O.D._{600\ nm}$) to 10 h of LipB production (0.018 ± 0.002 (U/ml)/$O.D._{600\ nm}$). Whereas LipA seems to accumulate extracellularly after 24 h of production (3.1; Fig. 3.1), LipB was no longer detectable after 24 h of *B. subtilis* TEB1030 cultivation (Fig. 3.20A). Due to the fact that LipB is a paralogous protein of LipA with similar substrate specificities but different expression and regulation conditions (Eggert *et al.*, 2003), it is probably produced under physiological conditions to compensate missing LipA function if necessary. Because of this alternative function it is possible that LipB is not as stable as the major lipid degrading LipA in the culture supernatant and maybe more prone to degradation by the remaining five extracellular proteases of *B. subtilis* TEB1030 (Eggert, 2001). This decrease in extracellular LipB activity correlates with a decline in *B. subtilis* TEB1030 growth (Fig. 3.20A). Similar to *B. subtilis* TEB1030 growth when producing LipA (Fig. 3.1A), the LipB producing cells reached their growth optimum after 6 h of cultivation at the transition from the exponential to the stationary growth phase (Fig. 3.20A). The *B. subtilis* TEB1030 growth correlates with the measured extracellular lipase activity as already observed for LipA producing cells.

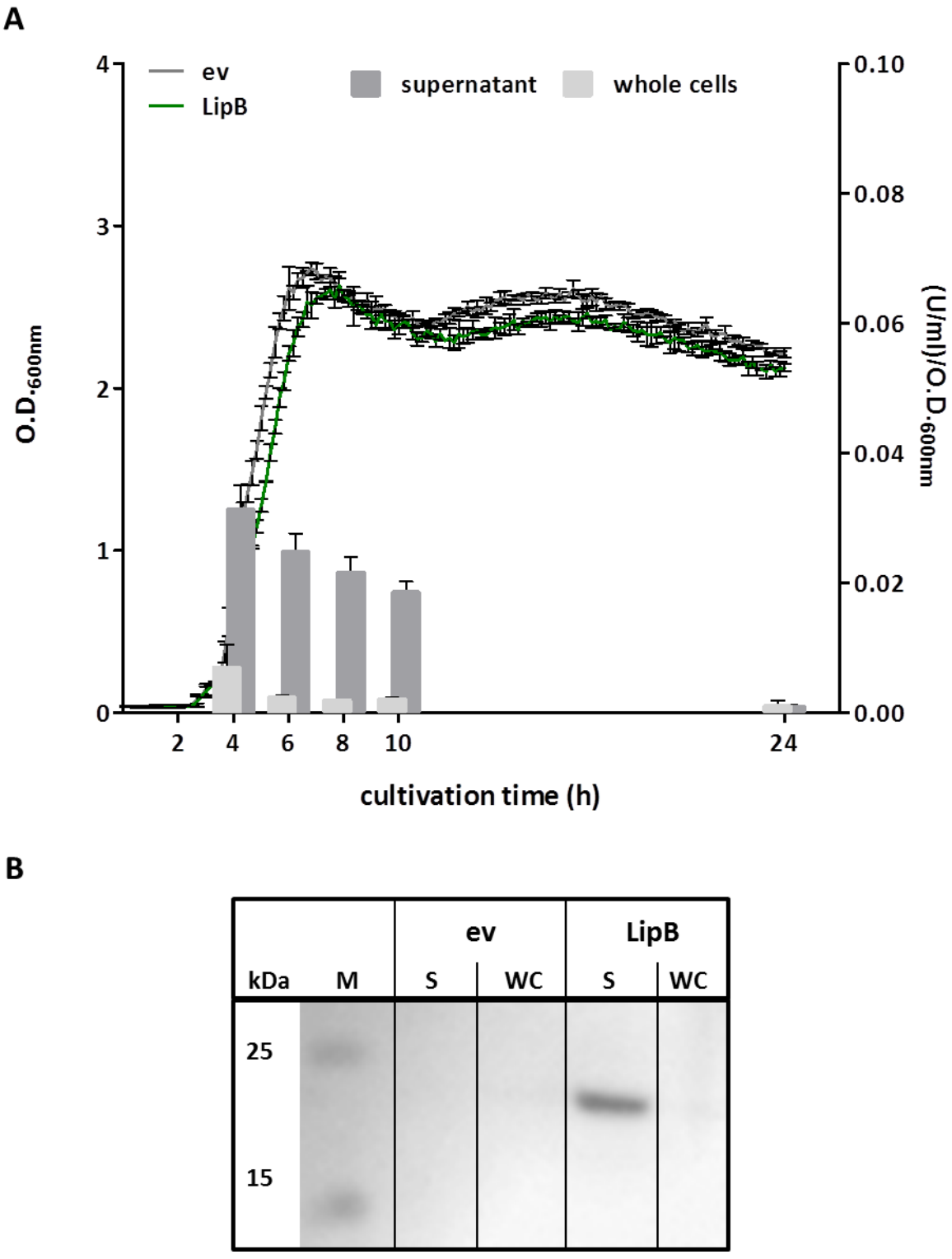

Fig. 3.20 Characterization of wild-type LipB production in *B. subtilis* TEB1030.

A Wild-type LipB production analysis in *B. subtilis* TEB1030. *B. subtilis* TEB1030 producing wtLipB was cultivated in a microfermentation system using a 48-well Flowerplate® for 24 h and online biomass measurement was performed in the BioLector®. The cultivation time (h) is plotted against the optical density at 600 nm on the left handed y-axis and against the lipolytic volume activity normalized to the optical density ((U/ml)/O.D.$_{600\ nm}$). The lines with error bars show *B. subtilis* TEB1030 growth when not producing LipB (ev; grey) and producing wtLipB (green line) (O.D.$_{600\ nm}$). After 2, 4, 6, 8, 10 and 24 h of cultivation samples were taken to determine the lipase activity in the *B. subtilis* culture supernatant (bars in dark grey) and the *B. subtilis* whole cells (bars in light grey) that was normalized to the *B. subtilis* growth at the corresponding sampling time

point. **B Western Blot analysis of *B. subtilis* whole cells and culture supernatant after 6 h of wtLipB production.** 10µl of the precipitated proteins in the culture supernatant and the whole cells ($O.D._{580\ nm}$ of 15) were applied on a 16 % discontinuous SDS-Gel. Immunodetection was performed using a specific polyclonal LipB antibody.

The optical density of LipB producing cells decreases from 8 h to 10 h of cultivation (Fig. 3.20A), which is probably due to *B. subtilis* multicellularity leading to several morphological different cell subpopulations varying in absorption during O.D. measurement (Shank & Kolter, 2011). For *B. subtilis* TEB1030 producing LipA a cultivation for 6 h was identified as the most suitable one for LipA production analysis (3.1; Fig. 3.1), this could also be confirmed for LipB production: As well as LipA, LipB is secreted into the culture supernatant by *B. subtilis* (Eggert, 2001) and harbors a Sec-specific signal peptide (Tjalsma *et al.*, 2000), therefore comparable cultivation and analysis conditions should be established. After 6 h of cultivation LipB production and secretion reached its optimum, with 92 % LipB activity detected in the culture supernatant compared to the whole cells (Fig. 3.20A). This activity-based result showing high amounts of LipB in the culture supernatant after 6 h of cultivation compared to very low amounts of intracellularly detectable LipB was confirmed by immunodetection of LipB in the whole cells and in the culture supernatant using a LipB specific polyclonal antibody (Fig. 3.20B). This way, similar microfermentation and analysis conditions were established for LipB, which simplifies the comparison of transferred single amino acid substitutions.

Plasmid-based *lipB* can be constitutively expressed in *B. subtilis* TEB1030. LipB production and secretion can be analyzed under similar conditions as LipA production thus simplifying the comparative analysis of single amino acid substitutions.

3.7.2. Site directed mutagenesis of *lipB* based on a rational design

Selection of beneficial single amino acid substitutions within LipA for transfer and analysis within LipB was performed according to the same parameters as set for combinatorial and additive effects (3.6). Amino acid substitutions were chosen, that only show one specific effect on LipA production based on the introduced amino acid. This results in the identification of the single amino acid substitutions G13S, N48Q, P53D, A105N and Y139T, which also have been analyzed for combinatorial and additive effects in LipA (3.6). The lipase B (UniProt: Q79F14) consists of 182 amino acids, whereas LipA (UniProt: P37957) contains 181 amino acids, this leads to a shift of one amino acid, when both sequences are aligned (Fig. 3.21). In three out of the chosen five cases the wild-type amino acid in LipB corresponds to the wild-type one in LipA, but shifted by one amino acid position (N48→N49; P53→P54; A105→A106) (Fig. 3.21). For two positions another amino acid is coded in LipB, the G13 in LipA corresponds to S14 in LipB and at position 140 a serine is found in LipB instead of a threonine in LipA. Based on the results that were gained from the systematic mutational analysis of LipA (3.5) it is known that codon substitutions play a crucial role in efficient LipA production. This happens either by nucleotide substitutions enhancing *lipA* transcript amount (3.5.2) or by the codon frequencies that alter translation efficiency and so influencing LipA specific activity (3.5.1). Therefore, selection of the triplet coding for the respective amino acid chosen to be introduced was performed using the codon harmonization principle as a basis (Angov *et al.*, 2008). This principle describes the codon adaptation for heterologous genes to the codon usage of the expression host. Therefore, the codons of the target gene are adapted to the expression host genome by comparing the codon frequencies of the originating host and the expression host. Here, this approach was adapted for mutational transfer between two proteins, which means the codon frequencies were compared between LipA and LipB, figuratively representing the `originating host` (LipA) and the `expression host` (LipB). Due to the fact, that LipA and LipB are originally coded by the same host the harmonization results in most cases, except for the $P54D_{GAT}$ variant, in the introduction of the identical codon within *lipB* as well as for *lipA* (Tab. 3.7).

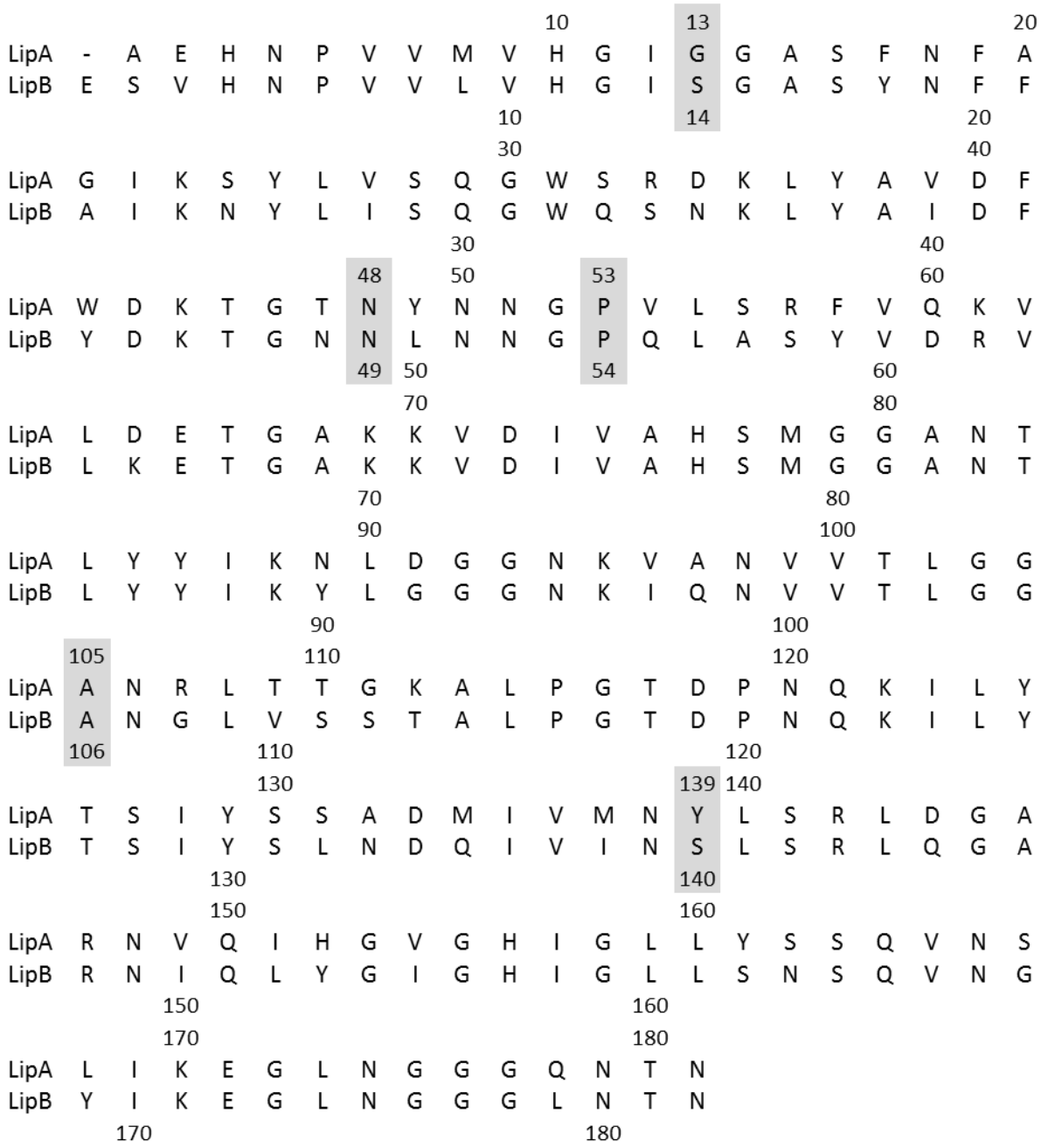

Fig. 3.21 Amino acid sequence alignment of LipA and LipB.
The amino acid sequences of LipA (UniProt: P37957) and LipB (UniProt: Q79F14) without the signal peptide sequences were aligned using ClustalW. Selected amino acid positions which substitutions are transferred to LipB are marked in light grey.

In LipA the glycine at position 13 is substituted to serine (G13S) resulting in a 1.4-fold increase in extracellular specific lipase activity (3.5.1; Fig. 3.11; Tab. 3.4). This G13 corresponds to the serine at position 14 in LipB (Fig. 3.21), maybe the introduction of a glycine here (S14G) possibly results in the *vice versa* effect observed for LipA-G13S, which

means a decrease in extracellular specific lipase activity. Therefore, it was decided to introduce a glycine with the similar codon that is found in the wildtype sequence of LipA.

Tab. 3.7 Selected and transferred single amino acid substitutions.
The table shows the amino acid position within the respective protein. The wild-type (wt) amino acid, codon and the introduced variant amino acid and codon are named together with the codon frequency per 1000 bp. The codon frequencies are colored accordingly from rare (orange) to frequent (green).

protein	position	wt amino acid	wt codon	wt frequency per 1000 bp	variant amino acid	variant codon	variant frequency per 1000 bp
LipA	13	glycine	GGA	21.8	serine	TCG	6.5
LipB	14	serine	AGT	6.8	glycine	GGA	21.8
LipA	48	asparagine	AAT	22.9	glutamine	CAG	18.5
LipB	49	asparagine	AAC	17.8	glutamine	CAG	18.5
LipA	53	proline	CCG	16.3	aspartic acid	GAC	19
LipB	54	proline	CCG	16.3	aspartic acid	GAC	19
LipB	54	proline	CCG	16.3	aspartic acid	GAT	33.2
LipA	105	alanine	GCG	19.8	asparagine	AAC	17.8
LipB	106	alanine	GCT	18.6	asparagine	AAC	17.8
LipA	139	tyrosine	TAC	12.6	threonine	ACG	14.9
LipB	140	serine	AGC	14.4	threonine	ACG	14.9

frequent	less frequent	less rare	rare

The N48 in LipA is substituted to glutamine coded by the rarest possible codon (Tab. 3.7). In order to achieve the similar beneficial effect on extracellular lipase amount (3.5.2; Fig. 3.12; Tab. 3.5), the asparagine at position 49 in LipB was also substituted to glutamine coded by the rare CAG codon (Tab. 3.7).The LipA P53D codon is substituted to the rare aspartic acid codon GAC, the identical substitution was chosen for the P54D in LipB (Tab. 3.7). Additionally, also the frequent used aspartic acid codon GAT was introduced in a second P54D LipB variant to exemplary analyze a possible effect on LipB production based on the codon frequency. This dependency of codon frequency, translation efficiency, enzyme folding and activity was indicated from the increased specific activity results gained for LipA (3.5.1), because for three single amino acid substitutions in LipA, I12L, I12V and G13T (3.5), two codon substitutions with different ($G13T_{ACC}$: 3.5.1; Fig. 3.11; Tab. 3.4; $G13T_{ACG}$: 3.5.2; Fig. 3.12; Tab. 3.5) or no effects ($I12L_{TTG}$; $I12V_{GTC}$: 3.5; Tab. 3.3; $I12L_{CTG}$; $I12V_{GTG}$: 3.5.1; Fig. 3.11; Tab. 3.4) were identified. As well as for A105 in LipA leading to a 2-fold increase in

extracellular lipase amount (3.5.2; Fig. 3.12; Tab. 3.5), the A106 in LipB was substituted with asparagine using the rare AAC codon (Tab. 3.7). The aromatic, hydrophobic tyrosine at position 139 in LipA was substituted with the uncharged, hydrophilic threonine. At the equivalent position 140 in wild-type LipB an uncharged serine is localized (Fig. 3.21) and was also substituted with an uncharged, hydrophilic threonine. This way, based on a different wild-type initial position, it would be interesting to elucidate whether the similar variant amino acid is able to achieve the similar beneficial effect in a different protein. The this way rationally designed oligonucleotides for *lipB* site directed mutagenesis are listed in Tab. 2.3 and mutagenesis was performed as described in 2.12.2. *B. subtilis* TEB1030 was transformed by protoplast formation (2.9.3) with the generated *lipB* mutagenesis vectors and analyzed under similar conditions as described for LipA production (2.23).

Rational design-based site directed *lipB* mutagenesis for transfer of single beneficial amino acid substitutions was performed using codon harmonization.

3.7.3. Rational design of an improved LipB variant is not generally possible

B. subtilis TEB1030 producing wtLipB and the six LipB variants harboring four different single amino acid substitution S14G, N49Q, A106N and S140T (Fig. 3.21; Tab. 3.7) and two codon substitution coding for one amino acid $P54D_{GAC}$ and $P54D_{GAT}$ (Fig. 3.21; Tab. 3.7) were cultivated and analyzed as previously performed for the identified LipA variants (2.23). *B. subtilis* TEB1030 growth is not substantially influenced compared to wtLipB when producing the different LipB variants over 24 h in a microfermentation system (Fig. 3.22A).

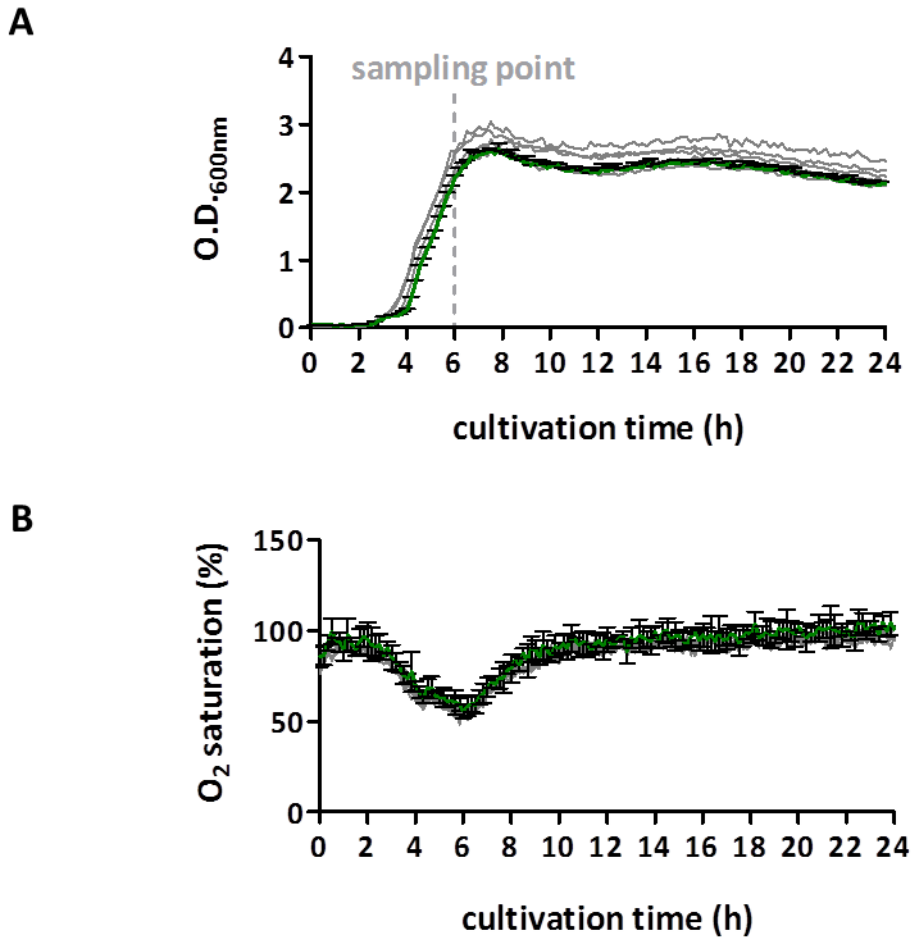

Fig. 3.22 Microfermentation of *B. subtilis* TEB1030 producing each of the six LipB variants.
A 24 h online biomass measurement. *B. subtilis* TEB1030 producing each of the six LipB variants was cultivated as three biological replicates in a microfermentation system using 48-well FlowerPlates®. Online biomass measurement was performed for 24 h in the BioLector®. The cultivation time (h) is plotted against the optical density at 600 nm (O.D. $_{600\ nm}$). The green line indicates wtLipB optical density with corresponding error bars in black. The sampling point after 6 h of LipA production is marked. **B Oxygen saturation during microfermentation.** The percentaged oxygen saturation (%) of *B. subtilis* TEB1030 harboring the 38 different LipA variants is plotted against the cultivation time (h). The green line indicates wtLipB oxygen saturation with corresponding error bars in black.

As already observed when producing wtLipA and its 38 different variants (3.5; Fig. 3.10), *B. subtilis* TEB1030 producing wtLipB and its variants is exponentially growing after 4 h of cultivation (Fig. 3.22A) getting along with a decrease in oxygen saturation in the cultivation system (Fig. 3.22B). This decrease reaches its maximum at 50 % of measured soluble oxygen (Fig. 3.22B), which is based on the oxygen consumption of *B. subtilis* TEB1030 cells for their growth. For the analyzed six single amino acid substitutions no significant changes in *lipB* transcript amount could be observed compared to wt*lipB* transcript (Tab. 3.8), dependent on the determined cutoff values of 0.3 and 3 (2.11). The single amino acid substitution G13S identified in LipA as increasing the extracellular specific lipase activity significantly up to 2.5-fold compared to wtLipA (Fig. 3.23) was transferred to LipB as a S14G substitution expecting a decrease in extracellular specific lipase activity based on the switched properties of the respective wt and variant. In contrast to G13S-LipA, S14G-LipB show similar extracellular specific lipase activity compared to wtLipB (Fig. 3.23; Tab. 3.8). The substituted serine at position 14 is one of the closest residues to the catalytic serine at position 78, as it is proposed from the published 3D model (Eggert *et al.*, 2001). Nevertheless, the huge substitution from the hydrophilic, polar serine to the hydrophobic, smallest amino acid glycine at this position does not affect the extracellular specific lipase activity of LipB. It is possible that a conformational change based on the glycine introduction at position 14 in LipB is too small to be detected with the *p*-nitrophenyl ester substrate that was used for analysis (2.17) and would maybe be detectable with another substrate implying a substrate specificity change. Interestingly, the three other amino acid substitutions N49Q, A106N and S140T that were expected to increase LipB extracellular lipase amount (Fig. 3.25; Tab. 3.8), as it was proven for LipA (Fig. 3.23), show huge effects on extracellular specific lipase activity (Fig. 3.23; Tab. 3.8). These effects ranged from almost no activity for the A106N-LipB variant to a significant increase in extracellular lipase activity of 1.5-fold compared to wtLipB for the N49Q variant (Fig. 3.23; Tab. 3.8).

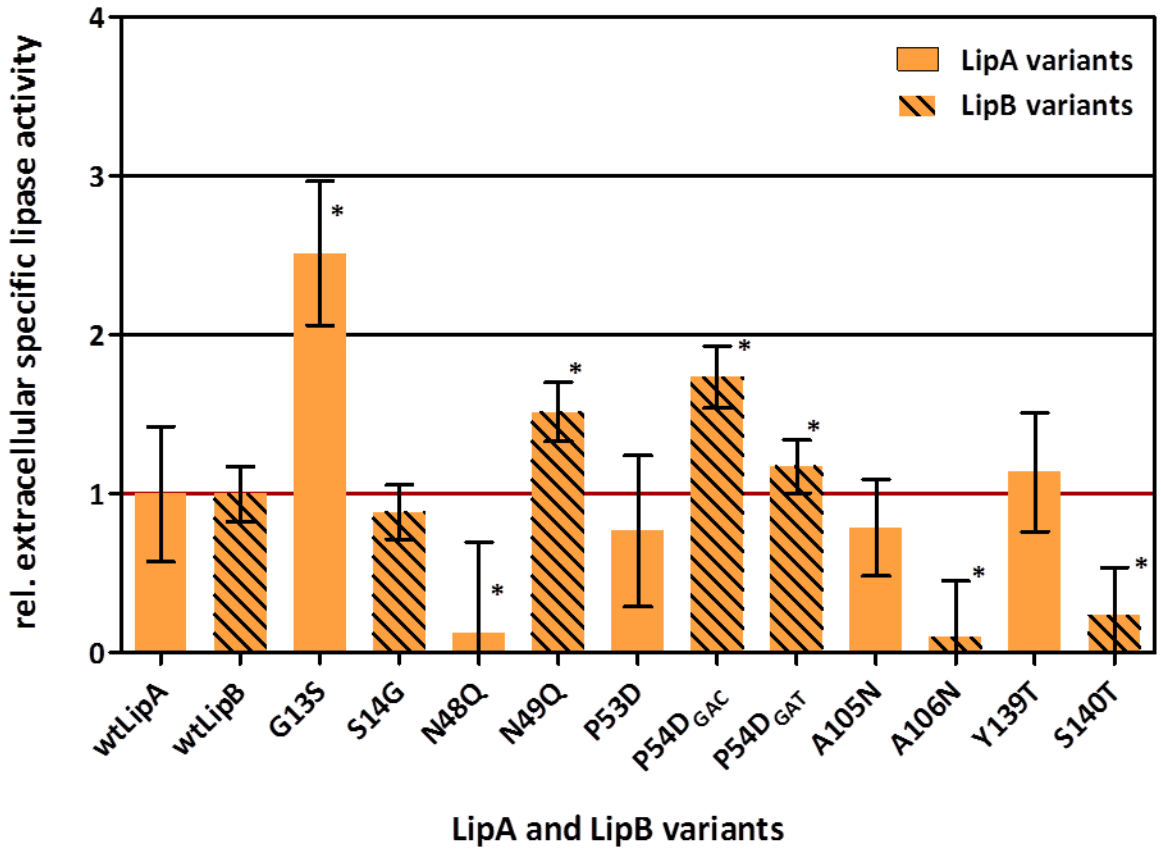

Fig. 3.23 Extracellular specific activity of LipA and LipB variants with corresponding single amino acid substitutions.
B. subtilis TEB1030 producing each of the six LipB variants was cultivated as three biological replicates a 48-well Flowerplate® for 6 h and the relative extracellular specific lipase activity in the culture supernatant was calculated by normalizing the volume activity (U/ml) to the quantified protein amount (mg/ml). The extracellular lipase activity was measured using *p*NPP as a substrate and the extracellular protein amount was determined by ELISA using a specific polyclonal LipB antibody. The relative extracellular specific lipase activities of LipB variants and the corresponding LipA variants are plotted. The red line indicates the normalized wtLipA and wtLipB specific activity. Significant changes ($p < 0.05$) are marked with an asterisk.

To structurally explain this amino acid effect on extracellular specific lipase activity for LipB, a 3D homology model was created (Fig. 3.24B) using the LipA X-ray structure (PDB: 1I6W) as a reference (2.24) (Biasini *et al.*, 2014). The comparison of the structural localization of the positions N49, A106 and S140 within LipB (Fig. 3.24B) with the corresponding positions N48, A105 and Y139 within LipA (Fig. 3.24A) showed no great differences concerning the orientation of the wild-type amino acids. The two residues N48 and A105N are orientated to the catalytic serine at position 77-LipA and 78-LipB (Fig. 3.24A and B), as well as the already discussed S14 and its substitution to glycine. The Y139-LipA and the S140-LipB are both located in a flexible loop structure partially covering the catalytic triad.

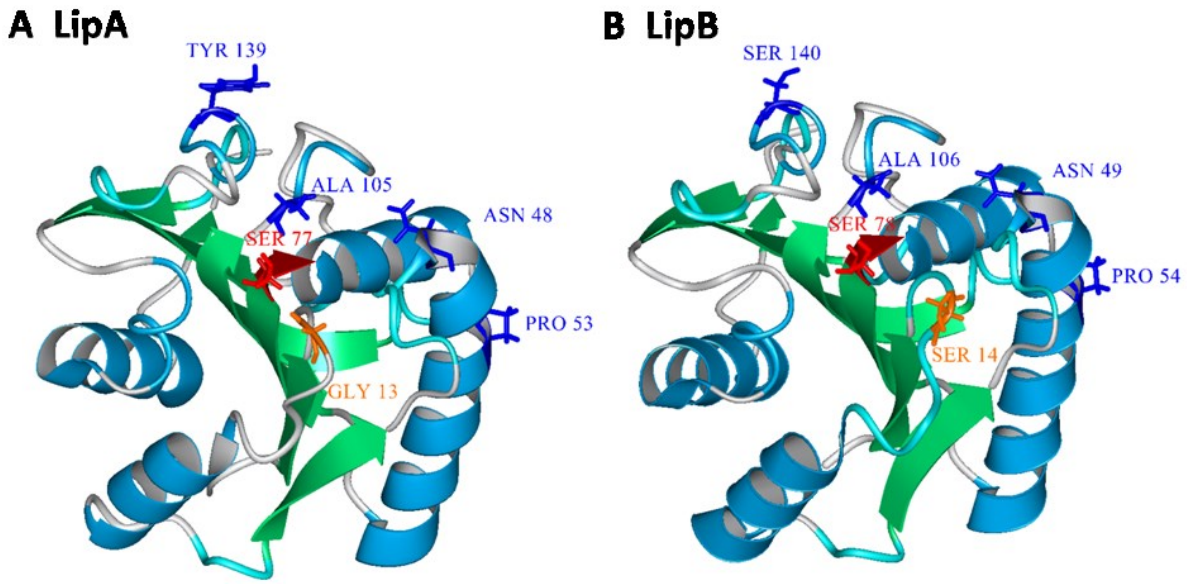

Fig. 3.24 Structural representation of wtLipA and wtLipB with the identified and transferred single amino acid positions.
Structure of LipA (PDB: 1I6W) with highlighted wild-type residues transferred to LipB (**A**) and 3D homology model of LipB (based on LipA) with highlighted wild-type residues (**B**). The wild-type amino acid residues are presented as stick models for those residues with substitutions increasing the relative extracellular specific lipase activity in orange and with substitutions increasing relative extracellular lipase amount in blue. The catalytic serine (Ser 77) is plotted in red.

Based on the different substrate preferences of LipA and LipB (Eggert *et al.*, 2001), it is possible that the conformational changes that occur are not detectable with the used long chain *p*-nitrophenyl palmitate substrate similarly in both lipases. While the N48Q-LipA substitutions lead to an almost inactive lipase in the culture supernatant the corresponding substitution in LipB, N49Q increases extracellular specific lipase activity significantly 1.5-fold (Fig. 3.23) and the *vice versa* effect was observed for A105N-LipA/A106N-LipB. While the extracellular specific lipase activity of the LipA is unaffected by the A105N substitution compared to wtLipA, the introduction of asparagine at position 106 in LipB significantly reduces extracellular specific lipase activity compared to wtLipB (Fig. 3.23). Position 139 in LipA corresponds to position 140 in LipB (Fig. 3.21), in the wild-type situation, these positions code for different amino acids, Y139-LipA and S140-LipA, but the same amino acid was introduced (Tab. 3.7), resulting in different extracellular specific lipase activities (Fig. 3.23). Y139T-LipA relative specific activity is unaffected compared to wtLipA while the extracellular specific activity of S140T-LipB is significantly reduced to 0.2 compared to wtLipB (Fig. 3.23; Tab. 3.8). These differences in both variant lipases could again be explained by different substrate specificities that probably impede the detection of slight conformational

changes or the influence of the introduced threonine is caused by the different initial wild-type amino acids tyrosine and serine. The single amino acid substitution P53D was identified in LipA to increase extracellular lipase amount significantly 1.9-fold compared to wtLipA (Fig. 3.25). Both glutamic acid codons, the rare GAC codon and the frequent GAT codon, were introduced (Tab. 3.6) to analyze possible codon specific effects as previously for other amino acid substitutions for LipA (3.5; I12L, I12V and G13T). The effect to increase the extracellular lipase amount could not be transferred to LipB, the extracellular lipase amount is either slightly reduced ($P54D_{GAC}$) or unaffected ($P54D_{GAT}$) compared to wtLipB (Fig. 3.25; Tab. 3.8). Instead the extracellular specific lipase activity of both variants is increased significantly up to 1.7-fold (Fig. 3.23; Tab. 3.8) compared to wtLipB. This increase was observed for both codon substitutions and indicates that no codon-specific effect is introduced here, but that the substitution of the proline to the aspartic acid is maybe the reason for LipB increase in specific activity.

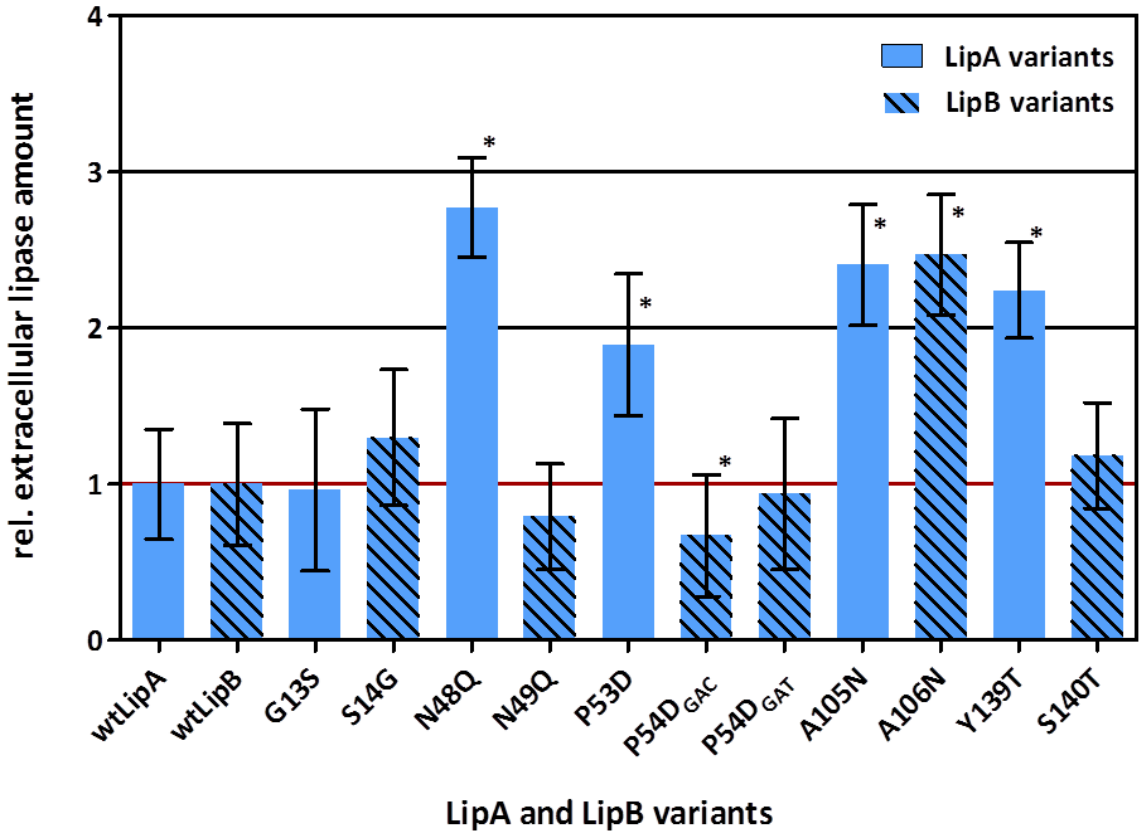

Fig. 3.25 Extracellular lipase amount of LipA and LipB variants with corresponding single amino acid substitutions.
B. subtilis TEB1030 producing each of the six LipB variants was cultivated as three biological replicates in a 48-well Flowerplate® for 6 h. The extracellular lipase amount was determined by ELISA using a specific polyclonal LipB antibody. The relative extracellular lipase amount of LipB variants and the corresponding LipA variants are plotted. The red line indicates the normalized wtLipA and wtLipB lipase amount. Significant changes ($p < 0.05$) are marked with an asterisk.

Tab. 3.8 LipB variants with transferred single amino acid substitutions.
The table shows the structural location of the variant amino acid substitution (struc*.), as well as the orientation (ori*.) of the amino acid residues (s: surface; b: buried). The astersisks (struc.* and ori.*) represent that these data are based on a LipB homology model generated with LipA. The wild-type (wt) codon and the introduced variant codon are named together with the codon frequency per 1000 bp. The relative change in transcript level is shown together with the lower and upper deviation. Significant transcript changes compared to wt*lipA* above the cutoff of 3 and a p-value < 0.05 are marked with an asterisk. The relative extracellular specific lipase activity and the extracellular lipase amount are shown with the standard deviation and significant changes compared to wtLipA ($p<0.05$) are marked with an asterisk.

variant	struc.*	ori.*	wt codon	frequency per 1000bp	variant codon	frequency per 1000bp	rel. change in transcript level	lower deviation	upper deviation	rel. specific activity	± std.	rel. lipase amount	± std.
S14G	turn	s	AGT	6.8	GGA	21.8	2.747	1.489	2.969	0.885	0.171	1.298	0.435
N49Q	αB	s	AAC	17.8	CAG	18.5	0.759	0.424	0.576	1.516*	0.186	0.792	0.340
$P54D_{GAC}$	αB	s	CCG	16.3	GAC	19	2.219	1.357	3.403	1.735*	0.195	0.671*	0.390
$P54D_{GAT}$	αB	s	CCG	16.3	GAT	33.2	0.981	0.539	0.764	1.174*	0.167	0.937	0.484
A106N	coil	s	GCT	18.6	AAC	17.8	1.15	0.571	1.458	0.097*	0.355	2.468*	0.387
S140T	αE	s	AGC	14.4	ACG	14.9	1.253	0.709	2.646	0.236*	0.302	1.183	0.339

This could also be explained with the different substrate specificities of LipA and LipB (Eggert *et al.*, 2001) as already mentioned for the other single amino acid substitutions that unexpectedly affect or does not affect the extracellular specific lipase activity (S14G, N49Q, A106N and Y139T). Five out of the six generated LipB variants harbor single amino acid substitutions that were identified in LipA as those beneficial for extracellular lipase amount at similar levels of *lipA* transcript level, either caused by an amino acid position stability effect (N48Q, P53D and A105N) or probably based on improved secretion of LipA (Y139T) (3.5.2; Fig. 3.12; Tab. 3.5). The transfer of these substitutions to LipB (Fig. 3.21; Tab. 3.7) resulted also in an increase in extracellular lipase amount for the substitution A106N. This LipB variant shows a significant 2.5-fold increase in extracellular lipase amount compared to wtLipB at similar levels of *lipB* transcript (Fig. 3.25; Tab. 3.8), so reflecting the similar effect observed for the A105-LipA variant, also exhibiting a significant 2.5-fold higher extracellular lipase amount compared to wtLipA with unaffected *lipA* transcript levels (Fig. 3.25; Tab. 3.5). Taken together, a rational transfer of single amino acid substitutions identified as beneficial for LipA production by *B. subtilis* do not resulted in the same outcome when applied for production of paralogous LipB. Five amino acid substitutions S14G, N49Q, P54D, A106N and S140T were introduced in LipB (Tab. 3.7), with the glutamic acid in the P54D-LipB variant is either coded by the rare GAC codon or the frequent GAT codon (Tab. 3.7). Only the positive effect of A105N-LipA substitution on LipA extracellular lipase amount could be transferred successfully to LipB (Fig. 3.25; Tab. 3.8). The LipB variants N49Q, P54D and S140T were, different from prediction, not or only slightly affected on the level of extracellular lipase amount (Fig. 3.25; Tab. 3.8) but significantly influence extracellular specific lipase activity of LipB (Fig. 3.23; Tab. 3.8). Also the S14G-LipB variant showed an unexpected result: despite the localization of the S14 near the catalytic S78 of LipB (Eggert *et al.*, 2001), the introduction of the small hydrophobic glycine does not impact the extracellular specific lipase activity.

The generation of a rationally predicted improved LipB variant based on the transfer of beneficial single amino acid substitutions identified for the paralogous LipA is possible for only one out of six tested specific amino acid substitutions (A105/106N).

4. Conclusion

The industrial demand for microbial enzymes with specific properties for certain enzymatic reactions and conversion is steadily increasing (1.1). To comply this demand that combines on the one hand the necessity of high amounts of the respective enzymes and on the other hand optimized enzyme properties, a large number of optimization strategies concerning protein production and protein engineering have been accomplished in the recent years. An industry relevant microbial cell factory and subject of still ongoing optimization approaches for high level protein production is *Bacillus subtilis* (1.6), additionally harboring one of the smallest known `true lipases`, LipA which is prominently used as a model for enzyme engineering (1.5). Despite detailed optimization of every step in the *B. subtilis* protein production pipeline (transcription, translation and targeting, translocation, maturation and folding as well as possible extracellular protease degradation) considered as possible bottlenecks (1.6), problems still occur especially in heterologous target protein production. This fact together with the incidentally gained results from different non-optimization approaches that reveal significant and diverse effects on protein production mediated by the target protein itself (1.7) open up a new fundamental point of view regarding efficient protein production and engineering. This point of view questions the importance of the target protein with all its functions and properties as a determining parameter for its efficient production. The here presented systematic mutational analysis of the model protein LipA from *B. subtilis* provides, for the first time, a global view on how single amino acid and codon substitutions within the target protein influence the complete production pipeline starting from *lipA* transcription and ending with its native conformation in the *B. subtilis* culture supernatant. The complex influences of the target protein LipA should be considered from two perspectives and are summarized in Fig. 4.1: beneficial effects on the protein production efficiency within *B. subtilis* as a microbial cell factory and beneficial effects on LipA`s enzymatic activity in the *B. subtilis* culture supernatant. The presented study is indeed able to narrow down possible explanations for the effect of a single amino acid or codon substitution by quantifying different steps in LipA production. But it is still challenging to give conclusive statements about a certain effect because protein production is a complex and interlaced process. Even the transcribed mRNA, product of the first step in protein biosynthesis, can influence protein production on different levels: Firstly, increased

transcript stability due to exchanged nucleotides may increase also the protein amount, like discussed for variant G13T$_{ACG}$ (3.5.2; Tab. 3.5). Secondly, even so called silent mutations not altering the amino acid encoding nucleotide sequence therefore possibly affecting mRNA transcript stability and amount (see I87I; 3.5.1; Tab. 3.4). These findings get of special interest concerning codon optimization approaches. For efficient heterologous gene expression and protein production in *B. subtilis* and other common expression systems such as *E. coli*, codon optimization of the target gene to the codon usage of the expression host is a popular approach intending high level protein production.

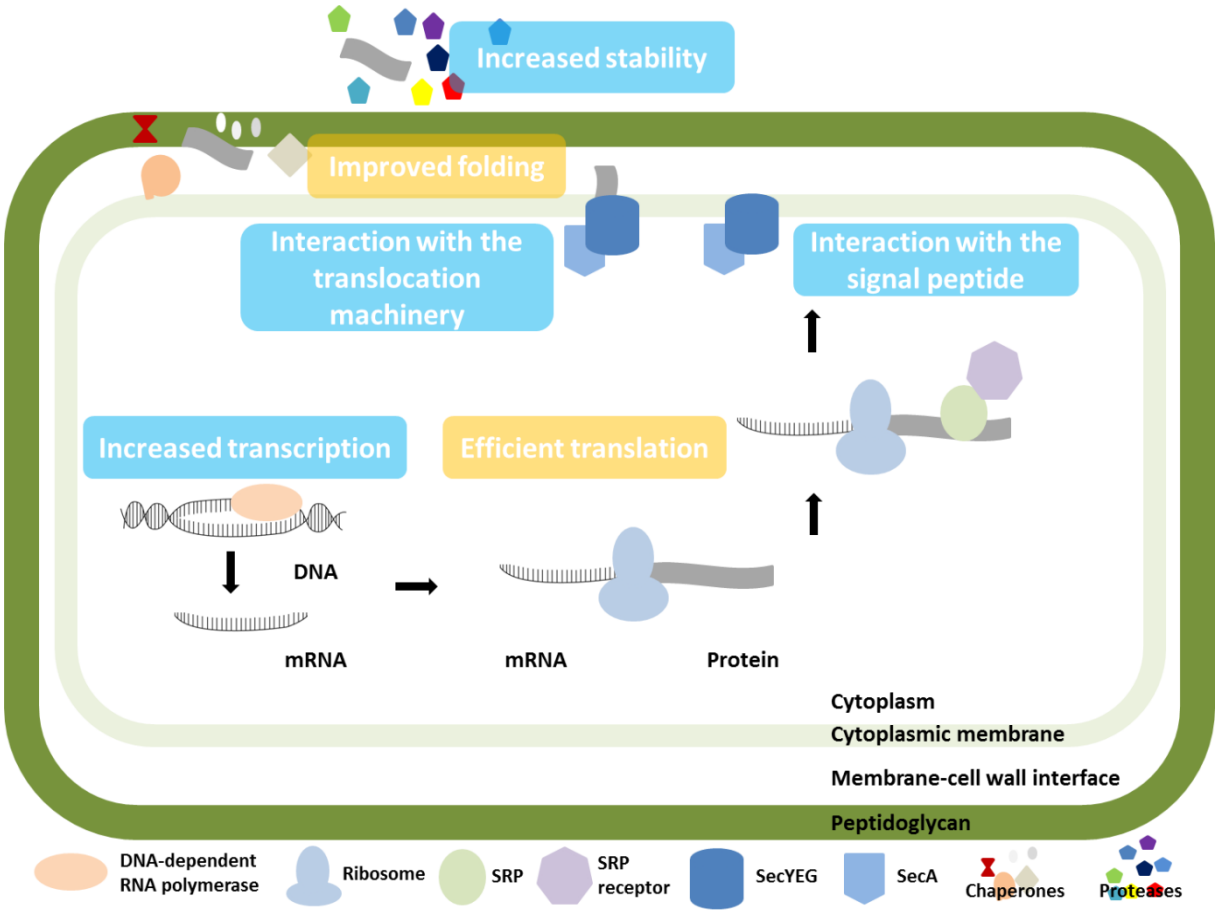

Fig. 4.1 Effects of single amino acid and codon substitutions on LipA production in *B. subtilis*.
Modified according to (Nijland & Kuipers, 2008). Summary of identified effects on LipA production in *B. subtilis* based on single amino acid and codon substitutions within LipA. Blue: amino acid mediated effects; Yellow: Codon-specific effects.

Of course, with only two identified LipA variants (I87I; 3.5.1; Tab. 3.4 and G13T$_{ACG}$ 3.5.2; Tab. 3.5) no general rule can be inferred concerning the frequency of the introduced codon, but it can be concluded that the prediction of transcription efficiencies based on the codon usage of the expression host is difficult. In many cases, based or independent from the applied codon optimization the target protein is synthesized but not functional. This failure is based

on codon-mediated translation velocity control (Chartier *et al.*, 2012), demonstrating a second important point for codon specific effects on the level of protein translation. This codon-mediated control of translation velocity is based on codon frequency as well as tRNA abundance influencing translation velocity which in turn impacts correct folding of proteins. Slow translation levels are necessary for correct enzyme folding and this way represents the basis for the enzyme`s catalytic active conformation. This is also true for Sec-dependent secreted proteins in *B. subtilis* even if they firstly fold after secretion and could be proven for LipA variants with the codon substitutions $I12L_{CTG}$, $I12V_{GTG}$ and $G13T_{ACC}$ (3.5.1; Fig. 3.11; Tab. 3.4) and for the silent mutation I87I (3.5.1; Fig. 3.11; Tab. 3.4) within the homologously produced LipA, which increases the extracellular specific lipase activity up to 2.4-fold. Whereas increased extracellular specific lipase activity of the variants $I12L_{CTG}$, $I12V_{GTG}$ could be explained by improved LipA folding due to limited tRNA abundance which results in wobble base pairing known for higher dissociation rates between the mRNA and tRNA and so in turn slowing down the translation process (3.5.1), the more efficient folding of the $G13T_{ACC}$ variant is based on the introduction of a rare codon decreasing translation velocity (3.5.1). The variant I87I exhibits an increased transcript amount (affected by exchanged nucleotide) that does not results in an higher protein amount probably caused by proteolytic degradation by the *B. subtilis* secretion quality control mechanisms, but this variant showed an increased extracellular specific lipase activity by a rare codon mediated decreased translation velocity followed by an efficient protein folding (3.5.1).

This means, that the use of codon optimization for the production of enzymes in *B. subtilis* should be considered carefully and probably results in severe effects when a heterologous enzyme is produced that is not adapted physiologically to *B. subtilis* as the analyzed homologous LipA protein. Interestingly, it seems that, different than generally assumed (Song *et al.*, 2015), *B. subtilis* exhibits some kind of codon bias that results in an improved translation and subsequent folding detected in the higher extracellular specific activity of the already mentioned LipA variants $I12L_{CTG}$, $I12V_{GTG}$ and $G13T_{ACC}$ and the `silent` mutation I87I (3.5.1).

The identification of the activity improved (but amount reduced) LipA variant I87I underlines the often discussed idea that synonymous codons are indeed not `silent` but that the usage of certain codons has a function and a necessity for mediating translation velocity profiles and this way influences the activity of the enzyme.

The fact that LipA production can be influenced on more than one production step should also be kept in mind when optimization is focused on the secretion step, because the main secretory proteins in *B. subtilis*, including LipA, are secreted cotranslationally (Fu *et al.*, 2007; Tjalsma *et al.*, 2004) which means that also here, different steps (like translation, targeting and translocation and simultaneous folding) must be considered as interdependent due to the nested process. *B. subtilis* has the ability to secrete large amounts of proteins directly into the culture supernatant (1.6) dependent on the presence of a signal peptide. These signal peptides, especially Sec-SRP secretion mediating signal peptides (1.6) are mandatory for cotranslational protein recognition and secretion and have been intensively studied and optimized to improve the protein secretion process in *B. subtilis*, but without the identification of a general signal peptide composition for efficient secretion. This missing general conclusion is based on the specific adjustment of the signal peptide to the target protein destined to be secreted. This was formerly assumed (Brockmeier *et al.*, 2006; Degering *et al.*, 2010) and is confirmed by the results gained for the recovery of signal peptide-mediated secretion deficiency of LipA (3.5.3). Here, the homologous Vpr signal peptide from *B. subtilis* decreases LipA secretion by about 60 %, although the used secretion pathway is identical for the LipA-SP and Vpr-SP and subsequently LipA secretion is re-established with the single amino acid substitutions P53D and A105N within LipA (3.5.3). This result proves on the one hand the dependency of the target protein secretion from the chosen signal peptide and, what is more fundamental, on the other hand shows the even more crucial impact on successful secretion of the target protein itself. As discussed in section 3.5.3 and pictured there in Fig. 3.14, the whole protein sequence can interact with its signal peptide during Sec-mediated translocation (`positive-inside rule`) and may thereby affecting its own secretion. This is supported by the finding that even mutations in the mid part of LipA (P53D and A105N) can re-constitute secretion defects by Vpr-SP.

Additionally to the concluded signal peptide-target protein interaction, efficient secretion of LipA seems also to be influenced by the target protein interaction with components of the

translocation machinery as formerly described for LamB in *E. coli* (Altman *et al.*, 1990) and concluded from the increased extracellular lipase amount of twelve LipA variants with different amino acid substitutions (I12F, N48Q, I87V, A105N,M134K, M134P, M134Q, Y139G, Y139T, L140A, L140Y, and V154E) discussed in section 3.5.2. In the context of the use of microbial cell factories in general and especially in the use of *B. subtilis* as such, it can be concluded that current optimization strategies and approaches are sufficient to produce the majority of recombinant proteins (1.6), but that also the target protein itself can at least strongly affect its production as it was shown for the homologous LipA in this study.

B. subtilis LipA is a popular model for engineering industrial relevant lipases (1.5) using directed evolution approaches that include random mutagenesis and also rational design strategies to generate enzymes with certain properties (Porter *et al.*, 2016). Random mutagenesis is often labor intensive, because a huge number of clones needs to be screened for the respective wanted property, but can result, as shown here, in the identification of a relatively high number of 27 promising improved variants (3.5.1; 3.5.2) either in activity towards the given substrate (3.5.1) or increased in stability in the *B. subtilis* culture supernatant (3.5.2). Results from those screenings based on random mutagenesis as well as structural and homology information of a certain protein or enzyme family are often collected in data bases as the `3DM` data base that are used for rational design approaches (Kuipers *et al.*, 2010). Rational protein design that combines experimentally gained results with protein sequence and structure homology information is a useful tool for the generation of for example a highly thermostable LipA variant of *B. subtilis* that combines several rationally chosen single mutations (Kamal *et al.*, 2011). However, the addition of known beneficial effects cannot be deemed as a general solution for every demand, but as an individual case dependent on the analyzed enzyme property and amino acid substitution. This was shown in this work for a LipA variant with predicted increased extracellular specific lipase activity and amount that indeed exhibit not the expected properties but a counteracting effect of the combined amino acids (3.6.1). In contrast, additive effects in extracellular LipA amount could be successfully generated for combining the single amino acid substitutions A105N and Y139T (3.6.2) resulting in a nearly 4-fold higher extracellular lipase amount compared to wild-type LipA. Here, it was demonstrated that a rational design based on experimental data will not always result in further production optimization. But

due to the fact that full landscape analyses like performed in this work are time- and cost-intensive, the here generated data are an invaluable basis for rational design approaches and a good starting point for further optimizations. The already mentioned `3DM` data base cannot only be used to combine known beneficial substitutions in the same protein but also to rationally transfer amino acid substitutions from one engineered protein or enzyme to another one (Kuipers *et al.*, 2010). Also this transfer as well as the combination and addition of beneficial amino acid substitutions is a process that cannot be put in a general manner for the entity of proteins and enzymes within a specific family. In fact, beneficial substitutions in mammalian proteins that share sequence similarity and common tertiary structures were successfully transferred mediating enhanced endoplasmatic reticulum retention (De Jaco *et al.*, 2006). Similarly, the transfer of a beneficial single amino acid substitution for LipA production in *B. subtilis* to the paralogous LipB (3.7.3) was also successful. But the fact that this transfer failed for the other five designed variants (S14G, N49Q, P54D and S140T; 3.7.3) confirms the limits of this approach and demands for maintaining screening approaches and their combination with rational approaches.

This work combines the optimization of protein production in the *B. subtilis* cell factory and protein engineering using a homologous model protein LipA, thus providing a detailed global view on how single amino acid and codon substitutions influencing every step in *B. subtilis* protein production from transcription, over cotranslational secretion to a finally active and stable LipA in the *B. subtilis* culture supernatant. The gained results should be regarded in future developments in protein engineering as well as in new optimization approaches for microbial cell factories not only as a fundamental and all production steps embracing basis for rational approaches but also to demonstrate the limits of those approaches.

5. Abstract

Optimization of *Bacillus subtilis* as a `microbial cell factory` for high level secretory protein production in industrial applications is still an ongoing process with permanently upcoming new strategies. These strategies address to improve every step in the *B. subtilis* protein production pipeline: transcription, translation, secretion, maturation and folding and proteolysis in the culture supernatant. Although optimization of these bottlenecks increases *B. subtilis* secretory protein production to 20 g/l for homologous proteins, the successful production of recombinant proteins is still a major drawback. Obviously, also the target protein itself and even its codon composition can influence its production and secretion.

This study combines the first systematic mutational analysis for single amino acid and codon substitutions beneficial for protein production with a subsequent detailed characterization of substitution dependent effects on transcription, activity and protein amount. This allows the application of an experimentally generated rational protein design for the combination and transfer of selected beneficial single amino acid substitutions and their effects. For this purpose the well-known homologous lipase A (LipA) from *B. subtilis* popular used as a model protein for engineering of industrial relevant enzymes was subjected to site saturation mutagenesis. The generated 30,000 LipA clones were investigated with a TECAN® robot screening system, specifically developed for this application for both qualitative and quantitative determination of extracellular LipA production in *B. subtilis*. Subsequent characterization revealed 38 LipA variants with at least 2-fold increase in extracellular amount or activity and allowed a detailed insight in how different single amino acid or codon substitution can positively affect protein production on the level of 1) *lipA* gene expression, 2) extracellular LipA specific activity, or 3) amount of extracellular LipA protein. Furthermore, rational combinations of six beneficial amino acid substitutions within LipA and their transfer to the paralogous LipB protein of *B. subtilis* revealed that increasing extracellular LipA amount 4-fold and also a transfer to LipB with a similar effect is possible in some, but not all cases.

In conclusion, the results from this systematic analysis and characterization provide a global, deep view on the dependency of a successful `microbial cell factory` on the target protein, this way providing new starting points for rational protein engineering and efficient protein production in *B. subtilis* and simultaneously showing the limits of those approaches.

6. Zusammenfassung

Bacillus subtilis als “microbial cell factory” für die Produktion und Sekretion großer Proteinmengen ist auch weiterhin Gegenstand andauernder und neuartiger Optimierungsprozesse und -strategien für die industrielle Anwendung. Solche Strategien zielten bisher auf die Optimierung jedes einzelnen Schrittes der Proteinbiosynthese in *B. subtilis* ab; also Transkription, Translation, Sekretion, Reifung und Faltung sowie Proteolyse des Proteins im Kulturüberstand. Die Optimierung dieser limitierenden Prozesse erhöhte zwar die Proteinausbeute für sekretierte, homologe Proteine auf bis zu 20 g/l, allerdings stellt die Produktion rekombinanter Proteine in *B. subtilis* weiterhin ein großes Problem dar, da auch die Gen- und Proteinsequenz des Zielproteins selbst offensichtlich dessen Produktion und Sekretion beeinflusst.

Die vorliegende Arbeit kombiniert die erste systematische, Mutagenese-basierte Analyse einzelner Aminosäure- und Codonsubstitutionen mit einer anschließenden, detaillierten Charakterisierung ihrer Effekte auf die Transkription, Aktivität und Proteinmenge. Aufbauend auf diesen experimentellen Daten konnten weitere Varianten mit Hilfe des „rationalen Designs“ generiert werden, bei denen Effekte vorteilhafter Substitutionen kombiniert und übertragen werden. Ziel der durchgeführten Sättigungsmutagenese war die bereits gut charakterisierte Lipase LipA aus *B. subtilis*, die bereits in vielen anderen Studien als Modelprotein für das “protein engineering“ industriell relevanter Enzyme eingesetzt wurde. Die dafür erzeugte LipA-Bibliothek mit etwa 30.000 Klonen wurde im Hinblick auf die qualitative und quantitative Bestimmung der Lipaseproduktion und -sekretion durch *B. subtilis* mit einer TECAN® Robotersystem-unterstützten Methode durchmustert, die im Rahmen dieser Arbeit etabliert wurde. Die anschließende Charakterisierung zeigte für 38 LipA-Varianten eine mindestens zweifach erhöhte extrazelluläre Proteinmenge oder enzymatische Aktivität und ermöglicht damit Erklärungsansätze, wie einzelne Aminosäure- oder Codonsubstitutionen die Proteinproduktion auf verschiedenen Ebenen positiv beeinflussen können; diese sind 1) die *lipA*-Genexpression, 2) die extrazelluläre spezifische Enzymaktivität sowie 3) die extrazelluläre Proteinmenge der Lipase LipA.

Weiterhin wurden mit Hilfe des „rationalen Designs“ sechs vorteilhafte Aminosäuresubstitutionen ausgesucht, welche für die Lipase LipA kombiniert, aber auch auf die paraloge Lipase LipB übertragen wurden. Auf diese Weise konnte die extrazelluläre

Proteinmenge einer LipA-Variante weiter, insgesamt vierfach, erhöht werden und auch eine Übertragung auf LipB zeigte in einigen, aber nicht in allen Fällen den erwarteten Effekt.

Damit liefern die Ergebnisse der hier durchgeführten systematischen Analyse und Charakterisierung einen umfassenden, detaillierten Einblick in die Zielprotein-Abhängigkeit für die erfolgreiche Proteinproduktion sogar in etablierten Wirtsorganismen. Somit bietet die vorliegende Arbeit zum einen neue Ansatzpunkte für das rationale “protein engineering“ und eine Optimierung der Proteinproduktion in *B. subtilis*, zum anderen zeigt sie aber auch die Grenzen solcher Methoden auf.

7. References

Adrio, J. L. & Demain, A. L. (2014). Microbial enzymes: tools for biotechnological processes. *Biomolecules* **4**, 117–39.

Ahmad, S., Kamal, M. Z., Sankaranarayanan, R. & Rao, N. M. (2008). Thermostable *Bacillus subtilis* lipases: *in vitro* evolution and structural insight. *Journal of Molecular Biology* **381**, 324–40.

Ali, Y. Ben, Verger, R. & Abousalham, A. (2012). Lipases or Esterases: Does it really matter? Toward a new Bio-physico-chemical classification. In *Lipases and Phospholipases: Methods and Protocols*, pp. 31–51. Edited by G. Sandoval. Totowa, NJ: Humana Press.

Altman, E., Emr, S. D. & Kumamoto, C. A. (1990). The presence of both the signal sequence and a region of mature LamB protein is required for the interaction of LamB with the export factor SecB. *The Journal of Biological Chemistry* **265**, 18154–60.

Alvarez-Macarie, E., Augier-Magro, V. & Baratti, J. (1999). Characterization of a thermostable esterase activity from the moderate thermophile *Bacillus licheniformis*. *Bioscience, Biotechnology, and Biochemistry* **63**, 1865–70.

Andersson, H. & Von Heijne, G. (1991). A 30-residue-long "export initiation domain" adjacent to the signal sequence is critical for protein translocation across the inner membrane of *Escherichia coli*. *Proceedings of the National Academy of Sciences of the United States of America* **88**, 9751–4.

Angov, E., Hillier, C. J., Kincaid, R. L. & Lyon, J. A. (2008). Heterologous protein expression is enhanced by harmonizing the codon usage frequencies of the target gene with those of the expression host. *PloS One* **3**, e2189.

Antelmann, H., Tjalsma, H., Voigt, B., Ohlmeier, S., Bron, S., Van Dijl, J. M. & Hecker, M. (2001). A proteomic view on genome-based signal peptide predictions. *Genome research* **11**, 1484–502.

Arpigny, J. L. & Jaeger, K. E. (1999). Bacterial lipolytic enzymes: classification and properties. *The Biochemical Journal* **343 Pt 1**, 177–83.

Asoodeh, A., Emtenani, S. & Emtenani, S. (2014). Expression and biochemical characterization of a thermophilic organic solvent-tolerant lipase from *Bacillus sp.* DR90. *The Protein Journal* **33**, 410–21.

Bensing, B. A. & Sullam, P. M. (2002). An accessory sec locus of *Streptococcus gordonii* is required for export of the surface protein GspB and for normal levels of binding to human platelets. *Molecular Microbiology* **44**, 1081–94.

Bensing, B. A. & Sullam, P. M. (2010). Transport of preproteins by the accessory Sec system requires a specific domain adjacent to the signal peptide. *Journal of Bacteriology* **192**, 4223–32.

Bensing, B. A., Yen, Y. T., Seepersaud, R. & Sullam, P. M. (2012). A Specific interaction between SecA2 and a region of the preprotein adjacent to the signal peptide occurs during transport via the accessory Sec system. *The Journal of Biological Chemistry* **287**, 24438–47.

Bhattacharya, S. K. & Dubey, A. K. (1995). Metabolic burden as reflected by maintenance coefficient of recombinant *Escherichia coli* overexpressing target gene. *Biotchnology Letters* **17**, 1155–1160.

Biasini, M., Bienert, S., Waterhouse, A., Arnold, K., Studer, G., Schmidt, T., Kiefer, F., Cassarino, T. G., Bertoni, M. & other authors. (2014). SWISS-MODEL:

modelling protein tertiary and quaternary structure using evolutionary information. *Nucleic Acids Research* **42**, W252–8.

Bolhuis, A., Tjalsma, H., Smith, H. E., De Jong, A., Meima, R., Venema, G., Bron, S. & Van Dijl, J. M. (1999). Evaluation of bottlenecks in the late stages of protein secretion in *Bacillus subtilis*. *Applied and Environmental Microbiology* **65**, 2934–41.

Bornscheuer, U. T., Bessler, C., Srinivas, R. & Krishna, S. H. (2002). Optimizing lipases and related enzymes for efficient application. *Trends in Biotechnology* **20**, 433–437.

Brady, L., Brzozowski, A. & Derewenda, Z. (1990). A serine protease triad forms the catalytic centre of a triacylglycerol lipase. *Nature* **343**, 767–770.

Brockmeier, U. (2006). New strategies to optimize the secretion capacity for heterologous proteins in *Bacillus subtilis*. Disseration, Heinrich-Heine-Universität Düsseldorf.

Brockmeier, U., Caspers, M., Freudl, R., Jockwer, A., Noll, T. & Eggert, T. (2006). Systematic screening of all signal peptides from *Bacillus subtilis*: a powerful strategy in optimizing heterologous protein secretion in Gram-positive bacteria. *Journal of Molecular Biology* **362**, 393–402.

Brzozowski, A., Derewenda, U., Derewenda, Z. S., Dodson, G. G., Lawson, D. M., Turkenburg, J. P., Bjorkling, F., Huge-Jensen, B., Patkar, S. a & Thim, L. (1991). A model for interfacial activation in lipases from the structure of a fungal lipase-inhibitor complex. *Nature* **351**, 491–4.

Bräutigam, S., Bringer-Meyer, S. & Weuster-Botz, D. (2007). Asymmetric whole cell biotransformations in biphasic ionic liquid/water-systems by use of recombinant *Escherichia coli* with intracellular cofactor regeneration. *Tetrahedron: Asymmetry* **18**, 1883–1887.

Bulmer, M. (1988). Codon usage and intragenic position. *Journal of Theoretical Biology* **133**, 67–71.

Burkholder, P. R. & Giles, N. H. (1947). Induced biochemical mutations in *Bacillus subtilis*. *American Journal of Botany* **34**, 345–348.

Bustin, S. A., Benes, V., Garson, J. A., Hellemans, J., Huggett, J., Kubista, M., Mueller, R., Nolan, T., Pfaffl, M. W. & other authors. (2009). The MIQE guidelines: minimum information for publication of quantitative real-time PCR experiments. *Clinical Chemistry* **55**, 611–22.

Cambillau, C. & Tilbeurgh, H. Van. (1993). Structure of hydrolases: lipases and cellulases. *Current Opinion in Structural Biology* **3**, 885–895.

Carneiro, S., Ferreira, E. C. & Rocha, I. (2013). Metabolic responses to recombinant bioprocesses in *Escherichia coli*. *Journal of Biotechnology* **164**, 396–408. Elsevier B.V.

Caspers, M., Brockmeier, U., Degering, C., Eggert, T. & Freudl, R. (2010). Improvement of Sec-dependent secretion of a heterologous model protein in *Bacillus subtilis* by saturation mutagenesis of the N-domain of the AmyE signal peptide. *Applied Microbiology and Biotechnology* **86**, 1877–85.

Chaney, J. L. & Clark, P. L. (2015). Roles for synonymous codon usage in protein biogenesis. *Annual Review of Biophysics* **44**, 143–66.

Chang, S. & Cohen, S. (1979). High frequency transformation of *Bacillus subtilis*

protoplasts by plasmid DNA. *Molecular and General Genetics* **115**, 111–115.

Chartier, M., Gaudreault, F. & Najmanovich, R. (2012). Large-scale analysis of conserved rare codon clusters suggests an involvement in co-translational molecular recognition events. *Bioinformatics* **28**, 1438–45.

Chen, P. T., Shaw, J.-F., Chao, Y.-P., David Ho, T.-H. & Yu, S.-M. (2010). Construction of chromosomally located T7 expression system for production of heterologous secreted proteins in *Bacillus subtilis*. *Journal of Agricultural and Food Chemistry* **58**, 5392–9.

Cheng, F. & Schwaneberg, U. (2015). Directed evolution 2.0: improving and deciphering enzyme properties. *Chemical Communications* **51**, 9760–9772. Royal Society of Chemistry.

Consortium, T. U. (2008). The universal protein resource (UniProt). *Nucleic Acids Research* **36**, D190–5.

Craven, M. G., Henner, D. J., Alessi, D., Schauer, A. T., Ost, K. A., Deutscher, M. P. & Friedman, D. I. (1992). Identification of the rph (RNase PH) Gene of *Bacillus subtilis*: Evidence for Suppression of Cold-Sensitive Mutations in *Escherichia coli*. *Journal of Bacteriology* **174**, 4727–4735.

Curran, J. F. (1989). Rates of aminoacyl-tRNA selection at 29 sense codons *in vivo*. *Journal of Molecular Biology* **209**, 65–77.

Dartois, V., Baulard, A., Schanck, K. & Colson, C. (1992). Cloning, nucleotide sequence and expression in *Escherichia coli* of a lipase gene from *Bacillus subtilis* 168. *Biochimica et Biophysica Acta* **1131**, 253–60.

Degering, C., Eggert, T., Puls, M., Bongaerts, J., Evers, S., Maurer, K.-H. & Jaeger, K.-E. (2010). Optimization of protease secretion in *Bacillus subtilis* and *Bacillus licheniformis* by screening of homologous and heterologous signal peptides. *Applied and Environmental Microbiology* **76**, 6370–6.

De Jaco, A., Comoletti, D., Kovarik, Z., Gaietta, G., Radic, Z., Lockridge, O., Ellisman, M. H. & Taylor, P. (2006). A mutation linked with autism reveals a common mechanism of endoplasmic reticulum retention for the α, β-hydrolase fold protein family. *The Journal of Biological Chemistry* **281**, 9667–76.

De Smit, M. H. & Van Duin, J. (1994). Translational initiation on structured messengers. *Journal of Molecular Biology* **235**, 173–184.

Deutscher, M. P. & Reuven, N. B. (1991). Enzymatic basis for hydrolytic versus phosphorolytic mRNA degradation in *Escherichia coli* and *Bacillus subtilis* . *Proceedings of the National Academy of Sciences* **88**, 3277–3280.

Dugaiczyk, A., Boyer, H. W. & Goodman, H. M. (1975). Ligation of Eco RI endonuclease-generated DNA fragments into linear and circular structures. *Journal of Molecular Biology* **96**, 171–84.

Dunn, S. D. (1986). Effects of the modification of transfer buffer composition and the renaturation of proteins in gels on the recognition of proteins on Western blots by monoclonal antibodies. *Analytical Biochemistry* **157**, 144–53.

Duplay, P. & Hofnung, M. (1988). Two regions of mature periplasmic maltose-binding protein of *Escherichia coli* involved in secretion. *Journal of Bacteriology* **170**, 4445–50.

Edelheit, O., Hanukoglu, A. & Hanukoglu, I. (2009). Simple and efficient site-directed mutagenesis using two single-primer reactions in parallel to generate mutants

for protein structure-function studies. *BMC Biotechnology* **9**, 61.

Eggert, T., Pencreac'h, G., Douchet, I., Verger, R. & Jaeger, K. E. (2000). A novel extracellular esterase from *Bacillus subtilis* and its conversion to a monoacylglycerol hydrolase. *European Journal of Biochemistry* **267**, 6459–69.

Eggert, T., Van Pouderoyen, G., Dijkstra, B. W. & Jaeger, K. E. (2001). Lipolytic enzymes LipA and LipB from *Bacillus subtilis* differ in regulation of gene expression, biochemical properties, and three-dimensional structure. *FEBS letters* **502**, 89–92.

Eggert, T. (2001). Die lipolytischen Enzyme LipA und LipB von *Bacillus subtilis*: Charakterisierung und Optimierung mit gerichteter Evolution. Dissertation, Ruhr-Universität Bochum.

Eggert, T., Brockmeier, U., Dröge, M. J., Quax, W. J. & Jaeger, K.-E. (2003). Extracellular lipases from *Bacillus subtilis*: regulation of gene expression and enzyme activity by amino acid supply and external pH. *FEMS Microbiology Letters* **225**, 319–324.

Even, S., Pellegrini, O., Zig, L., Labas, V., Vinh, J., Bréchemmier-Baey, D. & Putzer, H. (2005). Ribonucleases J1 and J2: two novel endoribonucleases in *B. subtilis* with functional homology to *E. coli* RNase E. *Nucleic Acids Research* **33**, 2141–52.

Fekkes, P. & Driessen, A. J. (1999). Protein targeting to the bacterial cytoplasmic membrane. *Microbiology and Molecular Biology Reviews* **63**, 161–73.

Fekkes, P., Van der Does, C. & Driessen, A. J. (1997). The molecular chaperone SecB is released from the carboxy-terminus of SecA during initiation of precursor protein translocation. *The EMBO Journal* **16**, 6105–13.

Feltcher, M. E., Gibbons, H. S., Ligon, L. S. & Braunstein, M. (2013). Protein export by the mycobacterial SecA2 system is determined by the preprotein mature domain. *Journal of Bacteriology* **195**, 672–81.

Finn, R. D., Bateman, A., Clements, J., Coggill, P., Eberhardt, R. Y., Eddy, S. R., Heger, A., Hetherington, K., Holm, L. & other authors. (2014). Pfam: the protein families database. *Nucleic Acids Research* **42**, D222–30.

Frauenkron-Machedjou, V. J., Fulton, A., Zhu, L., Anker, C., Bocola, M., Jaeger, K.-E. & Schwaneberg, U. (2015). Towards understanding directed evolution: more than half of all amino acid positions contribute to ionic liquid resistance of *Bacillus subtilis* lipase A. *Chembiochem : a European Journal of Chemical Biology* **16**, 937–45.

Fu, L. L., Xu, Z. R., Li, W. F., Shuai, J. B., Lu, P. & Hu, C. X. (2007). Protein secretion pathways in *Bacillus subtilis*: implication for optimization of heterologous protein secretion. *Biotechnology Advances* **25**, 1–12.

Fulton, A. (2014). Exploring the full sequence landscape of *Bacillus subtilis* lipase A towards thermostability and detergent resistance. Dissertation, Heinrich-Heine-Universität Düsseldorf.

Fulton, A., Frauenkron-Machedjou, V. J., Skoczinski, P., Wilhelm, S., Zhu, L., Schwaneberg, U. & Jaeger, K.-E. (2015). Exploring the protein stability landscape: *Bacillus subtilis* lipase A as a model for detergent tolerance. *Chembiochem: a European Journal of Chemical Biology* **16**, 930–6.

Funke, S. (2005). Optimierung einer Lipase aus *Bacillus subtilis* mit neuen Methoden der gerichteten Evolution. Dissertation, Heinrich-Heine-Universität, Düsseldorf.

Funke, S. A., Eipper, A., Reetz, M. T., Otte, N., Thiel, W., Van Pouderoyen, G., Dijkstra, B. W., Jaeger, K.-E. & Eggert, T. (2009). Directed Evolution of an enantioselective *Bacillus subtilis* lipase. *Biocatalysis and Biotransformation* **21**, 67–73.

Gibson, D. G., Young, L., Chuang, R.-Y., Venter, J. C., Hutchison, C. A. & Smith, H. O. (2009). Enzymatic assembly of DNA molecules up to several hundred kilobases. *Nature Methods* **6**, 343–345.

Glick, B. R. (1995). Metabolic load and heterologous gene expression. *Biotechnology Advances* **13**, 247–261.

Gong, J.-S., Lu, Z.-M., Li, H., Shi, J.-S., Zhou, Z.-M. & Xu, Z.-H. (2012). Nitrilases in nitrile biocatalysis: Recent progress and forthcoming research. *Microbial Cell Factories* **11**, 142.

Hanahan, D. & Harbor, C. S. (1983). Studies on transformation of *Escherichia coli* with plasmids. *Journal of Molecular Biology* **166**, 557–580.

Hausmann, S., Wilhelm, S., Jaeger, K.-E. & Rosenau, F. (2008). Mutations towards enantioselectivity adversely affect secretion of *Pseudomonas aeruginosa* lipase. *FEMS Microbiology Letters* **282**, 65–72.

Hemilä, H. & Sibakov, M. (1991). Production of heterologous proteins in *Bacillus subtilis*: the effect of the joint between signal sequence and mature protein on yield. *Applied Microbiology and Biotechnology* **36**, 61–4.

Henner, D. J., Ferrari, E., Perego, M. & Hoch, J. A. (1988). Location of the targets of the hpr-97, sacU32(Hy), and sacQ36(Hy) mutations in upstream regions of the substilisin promoter. *Journal of Bacteriology* **170**, 296–300.

Heo, K. H., Cho, K. M., Lee, C. K., Kim, G. M., Shin, J. H., Kim, J. S. & Kim, H. J. (2013). Characterization of a fibrinolytic enzyme secreted by *Bacillus amyloliquefaciens* CB1 and its gene cloning. *Journal of Microbiology and Biotechnology* **23**, 974–983.

Heravi, K. M., Wenzel, M. & Altenbuchner, J. (2011). Regulation of mtl operon promoter of Bacillus subtilis: requirements of its use in expression vectors. *Microbial cell factories* **10**, 83. BioMed Central Ltd.

Hodak, H., Clantin, B., Willery, E., Villeret, V., Locht, C. & Jacob-Dubuisson, F. (2006). Secretion signal of the filamentous haemagglutinin, a model two-partner secretion substrate. *Molecular Microbiology* **61**, 368–82.

Huang, X. & Helmann, D. (1998). Identification of target promoters for the *Bacillus subtilis* σx factor using a consensus-directed search. *Journal of Bacteriology* **279**, 165–173.

Jaeger, K. E. & Reetz, M. T. (1998). Microbial lipases form versatile tools for biotechnology. *Trends in Biotechnology* **16**, 396–403.

Jaeger, K.-E., Ransac, S., Koch, H. B., Ferrato, F. & Dijkstra, B. W. (1993). Topological characterization and modeling of the 3D structure of lipase from *Pseudomonas aeruginosa*. *FEBS Letters* **332**, 143–9.

Jandová, Z. & Tichý, P. (1987). Selective regeneration of *Bacillus subtilis* protoplasts transformed to kanamycin resistance. *Folia Microbiologica* **32**, 82–4.

Jongbloed, J. D., Martin, U., Antelmann, H., Hecker, M., Tjalsma, H., Venema, G., Bron, S., Van Dijl, J. M. & Müller, J. (2000). TatC is a specificity determinant for protein secretion via the twin-arginine translocation pathway. *The Journal of Biological Chemistry* **275**, 41350–7.

Jongbloed, J. D. H., Antelmann, H., Hecker, M., Nijland, R., Bron, S., Airaksinen, U., Pries, F., Quax, W. J., Van Dijl, J. M. & Braun, P. G. (2002). Selective contribution of the twin-arginine translocation pathway to protein secretion in *Bacillus subtilis*. *The Journal of Biological Chemistry* **277**, 44068–78.

Kajava, A. V, Zolov, S. N., Kalinin, A. & Nesmeyanova, M. A. (2000). The net charge of the first 18 residues of the mature sequence affects protein translocation across the cytoplasmic membrane of gram-negative bacteria. *Journal of Bacteriology* **182**, 2163–9.

Kakeshita, H., Kageyama, Y., Ara, K., Ozaki, K. & Nakamura, K. (2010). Enhanced extracellular production of heterologous proteins in *Bacillus subtilis* by deleting the C-terminal region of the SecA secretory machinery. *Molecular Biotechnology* **46**, 250–7.

Kamal, M. Z., Ahmad, S., Molugu, T. R., Vijayalakshmi, A., Deshmukh, M. V, Sankaranarayanan, R. & Rao, N. M. (2011). *In vitro* evolved non-aggregating and thermostable lipase: structural and thermodynamic investigation. *Journal of Molecular Biology* **413**, 726–41. Elsevier Ltd.

Kamal, M. Z., Mohammad, T. A. S., Krishnamoorthy, G. & Rao, N. M. (2012). Role of active site rigidity in activity: MD simulation and fluorescence study on a lipase mutant. *PloS One* **7**, e35188.

Kang, Z., Yang, S., Du, G. & Chen, J. (2014). Molecular engineering of secretory machinery components for high-level secretion of proteins in *Bacillus* species. *Journal of Industrial Microbiology & Biotechnology* **41**, 1599–607.

Kawamura, F. & Doi, R. H. (1984). Construction of a *Bacillus subtilis* Double Mutant Deficient in Extracellular Alkaline and Neutral Proteases. *Journal of Bacteriology* **160**, 442–444.

Kazlauskas, R. J. (1994). Elucidating structure-mechanism relationships in lipases: prospects for predicting and engineering catalytic properties. *Trends in Biotechnology* **12**, 464–72.

Kazuo, K. & Ogasawara, N. (2002). Genome biology of a model bacterium, *Bacillus subtilis* . *International Congress Series* **1246**, 15–25.

Khokhlova, O. V & Nesmeyanova, M. A. (2003). Interaction of SecB and SecA with the N-terminal region of mature alkaline phosphatase on its secretion in *Escherichia coli*. *Molekuliarnaia Biologiia* **37**, 712–8.

Kim, M. H., Kim, H. K., Lee, J. K., Park, S. Y. & Oh, T. K. (2000). Thermostable lipase of *Bacillus stearothermophilus*: high-level production, purification, and calcium-dependent thermostability. *Bioscience, Biotechnology, and Biochemistry* **64**, 280–6.

Kohara, A., Yamamoto, Y. & Kikuchi, M. (1991). Alteration of N-terminal residues of mature human lysozyme affects its secretion in yeast and translocation into canine microsomal vesicles. *The Journal of Biological Chemistry* **266**, 20363–8.

Komar, A., Lesnik, T. & Reiss, C. (1999). Synonymous codon substitutions affect ribosome traffic and protein folding during *in vitro* translation. *FEBS letters* **462**, 387–391.

Kontinen, V. P. & Sarvas, M. (1993). The PrsA lipoprotein is essential for protein secretion in *Bacillus subtilis* and sets a limit for high-level secretion. *Molecular Microbiology* **8**, 727–37.

Kouwen, T. R. H. M., Antelmann, H., Van der Ploeg, R., Denham, E. L., Hecker, M. & Van Dijl, J. M. (2009a). MscL of *Bacillus*

subtilis prevents selective release of cytoplasmic proteins in a hypotonic environment. *Proteomics* **9**, 1033–43.

Kouwen, T. R. H. M., Van der Ploeg, R., Antelmann, H., Hecker, M., Homuth, G., Mäder, U. & Van Dijl, J. M. (2009b). Overflow of a hyper-produced secretory protein from the *Bacillus* Sec pathway into the Tat pathway for protein secretion as revealed by proteogenomics. *Proteomics* **9**, 1018–32.

Krieger, E., Darden, T., Nabuurs, S. B., Finkelstein, A. & Vriend, G. (2004). Making optimal use of empirical energy functions: Force-field parameterization in crystal space. *Proteins: Structure, Function, and Bioinformatics* **57**, 678–683.

Krishnappa, L., Monteferrante, C. G., Neef, J., Dreisbach, A. & Van Dijl, J. M. (2014). Degradation of extracytoplasmic catalysts for protein folding in *Bacillus subtilis*. *Applied and Environmental Microbiology* **80**, 1463–8.

Kuipers, R. K., Joosten, H.-J., Van Berkel, W. J. H., Leferink, N. G. H., Rooijen, E., Ittmann, E., Van Zimmeren, F., Jochens, H., Bornscheuer, U. & other authors. **(2010).** 3DM: systematic analysis of heterogeneous superfamily data to discover protein functionalities. *Proteins* **78**, 2101–13.

Kumamoto, C. a & Francetić, O. (1993). Highly selective binding of nascent polypeptides by an *Escherichia coli* chaperone protein in vivo. *Journal of Bacteriology* **175**, 2184–8.

Kunst, F., Ogasawara, N., Moszer, I., Albertini, A. M., Alloni, G., Azevedo, V., Bertero, M. G., Bessières, P., Bolotin, A. & other authors. **(1997).** The complete genome sequence of the gram-positive bacterium *Bacillus subtilis*. *Nature* **390**, 249–56.

Kyte, J. & Doolittle, R. F. (1982). A simple method for displaying the hydropathic character of a protein. *Journal of Molecular Biology* **157**, 105–32.

Laemmli, U. K. (1970). Cleavage of Structural Proteins during the Assembly of the Head of Bacteriophage T4. *Nature* **227**, 680–685.

Lang, D. A., Mannesse, M. L., De Haas, G. H., Verheij, H. M. & Dijkstra, B. W. (1998). Structural basis of the chiral selectivity of *Pseudomonas cepacia* lipase. *European Journal of Biochemistry / FEBS* **254**, 333–40.

Lee, B. H., Kim, B. K., Lee, Y. J., Chung, C. H. & Lee, J. W. (2010). Industrial scale of optimization for the production of carboxymethylcellulase from rice bran by a marine bacterium, *Bacillus subtilis* subsp. *subtilis* A-53. *Enzyme and Microbial Technology* **46**, 38–42.

Lee, D., Koh, Y., Kim, K., Kim, B., Choi, H., Kim, D., Suhartono, M. T. & Pyun, Y. (1999). Isolation and characterization of a thermophilic lipase from *Bacillus thermoleovorans* ID-1. *FEMS Microbiology Letters* **179**, 393–400.

Lehmann, M. & Pasamontes, L. (2000). The consensus concept for thermostability engineering of proteins. *Biochimica et Biophysica Acta* **1543**, 408–415.

Lesuisse, E., Schanck, K. & Colson, C. (1993). Purification and preliminary characterization of the extracellular lipase of *Bacillus subtilis* 168, an extremely basic pH-tolerant enzyme. *European Journal of Biochemistry* **216**, 155–60.

Li, B., Li, Y., Bai, D., Zhang, X., Yang, H., Wang, J., Liu, G., Yue, J., Ling, Y. & other authors. **(2014).** Whole-cell biotransformation systems for reduction of prochiral carbonyl compounds to

chiral alcohol in *Escherichia coli*. *Scientific Reports* **4**, 6750.

Li, P., Beckwith, J. & Inouye, H. (1988). Alteration of the amino terminus of the mature sequence of a periplasmic protein can severely affect protein export in *Escherichia coli*. *Proceedings of the National Academy of Sciences of the United States of America* **85**, 7685–9.

Li, W., Zhou, X. & Lu, P. (2004). Bottlenecks in the expression and secretion of heterologous proteins in *Bacillus subtilis* . *Research in Microbiology* **155**, 605–10.

Liu, B., Deikus, G., Bree, A., Durand, S., Kearns, D. B. & David, H. (2015). Global analysis of mRNA decay intermediates in *Bacillus subtilis* and polynucleotide phosphorylase-deletion strains. *Molecular Microbiology* **94**, 41–55.

Liu, L., Liu, Y., Shin, H., Chen, R. R., Wang, N. S., Li, J., Du, G. & Chen, J. (2013). Developing *Bacillus* spp. as a cell factory for production of microbial enzymes and industrially important biochemicals in the context of systems and synthetic biology. *Applied Microbiology and Biotechnology* **14**, 6113–6127.

Le Loir, Y., Gruss, A., Ehrlich, S. D. & Langella, P. (1998). A nine-residue synthetic propeptide enhances secretion efficiency of heterologous proteins in *Lactococcus lactis*. *Journal of Bacteriology* **180**, 1895–903.

Luttinger, A., Hahn, J. & Dubnau, D. (1996). Polynucleotide phosphorylase is necessary for competence development in *Bacillus subtilis*. *Molecular Microbiology* **19**, 343–356.

Mallik, I., Smith, M. A. & Flower, A. M. (2002). Recognition of secretory proteins in *Escherichia coli* requires signals in addition to the signal sequence and slow folding. *BMC microbiology* **6**, 2–7.

Mar Carrio, M., Cubarsi, R. & Villaverde, A. (2000). Fine architecture of bacterial inclusion bodies. *FEBS letters* **471**, 7–11.

Maurer, K. H., Elleuche, S. & Antranikian, G. (2013). *Industrielle Mikrobiologie* (H. Sahm, G. Antranikian, K.-P. Stahmann & R. Takors, Eds.). Springer Spektrum.

Menoncin, S., Domingues, N. M., Freire, D. M. G., Toniazzo, G., Cansian, R. L., Oliveira, J. V., Di Luccio, M., De Oliveira, D. & Treichel, H. (2008). Study of the extraction, concentration, and partial characterization of lipases obtained from *Penicillium verrucosum* using solid-state fermentation of soybean bran. *Food and Bioprocess Technology* **3**, 537–544.

Moeller, B., Vetter, R., Wilke, D. & Foullois, B. (1995). Alkaline *Bacillus* lipases, coding DNA sequences therfor and *Bacilli*, which produce these lipases. *United States Patent* 5427936.

Mooney, R. A., Artsimovitch, I. & Landick, R. (1998). Information processing by RNA polymerase recognition of regulatory signals during RNA chain elongation. *Journal of Bacteriology* **180**, 3265–3275.

Murphy, C. D. (2012). The microbial cell factory. *Organic & Biomolecular Chemistry* **10**, 1949–57.

Müller, J. P., Bron, S., Venema, G. & Van Dijl, J. M. (2000a). Chaperone-like activities of the CsaA protein of *Bacillus subtilis*. *Microbiology* **146 Pt 1**, 77–88.

Müller, J. P., Ozegowski, J., Vettermann, S., Swaving, J., Van Wely, K. H. & Driessen, A. J. (2000b). Interaction of *Bacillus subtilis* CsaA with SecA and precursor proteins. *The Biochemical Journal* **348 Pt 2**, 367–73.

Nakamura, Y., Ito, K. & Isaksson, L. A. (1996). Emerging understanding of translation termination. *Cell* **87**, 147–150.

Nardini, M. & Dijkstra, B. W. (1999). α/β Hydrolase fold enzymes : the family keeps growing. *Current Opinion in Structural Biology* **9**, 732–737.

Nardini, M., Lang, D. A., Liebeton, K., Jaeger, K.-E. & Dijkstra, B. W. (2000). Crystal structure of *Pseudomonas aeruginosa* lipase in the open conformation. The prototype for family I.1 of bacterial lipases. *Journal of Biological Chemistry* **275**, 31219–31225.

Nicolas, P., Mäder, U., Dervyn, E., Rochat, T., Leduc, A., Pigeonneau, N., Bidnenko, E., Marchadier, E., Hoebeke, M. & other authors. **(2012).** Condition-dependent transcriptome architecture in *Bacillus subtilis*. *Science* **335**, 1103–1106.

Nijland, R. & Kuipers, O. P. (2008). Optimization of protein secretion by *Bacillus subtilis*. *Recent Patents on Biotechnology* **2**, 79–87.

Nijland, R., Heerlien, R., Hamoen, L. W. & Kuipers, O. P. (2007). Changing a single amino acid in *Clostridium perfringens* beta-toxin affects the efficiency of heterologous secretion by *Bacillus subtilis*. *Applied and Environmental Microbiology* **73**, 1586–93.

Noble, M. E., Cleasby, A., Johnson, L. N., Egmond, M. R. & Frenken, L. G. (1993). The crystal structure of triacylglycerol lipase from *Pseudomonas glumae* reveals a partially redundant catalytic aspartate. *FEBS letters* **331**, 123–8.

Nov, Y. (2012). When second best is good enough: another probabilistic look at saturation mutagenesis. *Applied and Environmental Microbiology* **78**, 258–62.

Nthangeni, M. B., Patterton, H.-G., Van Tonder, A., Vergeer, W. P. & Litthauer, D. (2001). Over-expression and properties of a purified recombinant *Bacillus licheniformis* lipase: a comparative report on *Bacillus* lipases. *Enzyme and Microbial Technology* **28**, 705–712.

Ollis, D. L., Cheah, E., Cygler, M., Dijkstra, B., Frolow, F., Franken, S. M., Harel, M., Remington, S. J., Silman, I. & other authors. **(1992).** The α/β hydrolase fold. *Protein Engineering, Design and Selection* **5**, 197–211.

Osawa, S. & Muto, A. (1987). The guanine and cytosine content of genomic DNA and bacterial evolution. *Proceedings of the National Academy of Sciences of the United States of America* **84**, 166–169.

Oussenko, I. A. & Bechhofer, D. H. (2000). The yvaJ gene of *Bacillus subtilis* encodes a 3`-to-5` exoribonuclease and is not essential in a strain lacking polynucleotide phosphorylase. *Journal of Bacteriology* **182**, 2639–2642.

Oussenko, I. A., Sanchez, R. & Bechhofer, D. H. (2002). *Bacillus subtilis* YhaM , a member of a new family of 3`-to-5` exonucleases in Gram-positive bacteria. *Journal of Bacteriology* **184**, 6250–6259.

Park, Y. C., Kim, S. G., Park, K., Lee, K. H. & Seo, J. H. (2004). Fed-batch production of D-ribose from sugar mixtures by transketolase-deficient *Bacillus subtilis* SPK1. *Applied Microbiology and Biotechnology* **66**, 297–302.

Pauwels, K., Lustig, A., Wyns, L., Tommassen, J., Savvides, S. N. & Van Gelder, P. (2006). Structure of a membrane-based steric chaperone in complex with its lipase substrate. *Nature Structural & Molecular Biology* **13**, 374–5.

Peterson, G. L. (1977). A simplification of the protein assay method of Lowry *et al.* which is more generally applicable. *Analytical Biochemistry* **83**, 346–356.

Phan, T. T. P., Nguyen, H. D. & Schumann, W. (2012). Development of a strong intracellular expression system for

Bacillus subtilis by optimizing promoter elements. *Journal of Biotechnology* **157**, 167–172.

Pool, M. R. (2005). Signal recognition particles in chloroplasts, bacteria, yeast and mammals. *Molecular Membrane Biology* **22**, 3–15.

Porter, J. L., Rusli, R. a & Ollis, D. L. (2016). Directed evolution of enzymes for industrial biocatalysis. *Chembiochem: a European Journal of Chemical Biology* **17**, 197–203.

Power, P. M., Jones, R. a, Beacham, I. R., Bucholtz, C. & Jennings, M. P. (2004). Whole genome analysis reveals a high incidence of non-optimal codons in secretory signal sequences of *Escherichia coli*. *Biochemical and Biophysical Research Communications* **322**, 1038–44.

Pribnow, D. (1975). Nucleotide sequence of an RNA polymerase binding site at an T7 promoter. *Proceedings of the National Academy of Sciences of the United States of America* **72**, 784–788.

Quentin, Y., Fichant, G. & Joseph, C. (1999). Inventory, assembly and analysis of *Bacillus subtilis* ABC transport systems. *Journal of Molecular Biology* **287**, 467–484.

Rahmen, N., Fulton, A., Ihling, N., Magni, M., Jaeger, K.-E. & Büchs, J. (2015a). Exchange of single amino acids at different positions of a recombinant protein affects metabolic burden in *Escherichia coli*. *Microbial Cell Factories* **14**, 10.

Rahmen, N., Schlupp, C. D., Mitsunaga, H., Fulton, A., Aryani, T., Esch, L., Schaffrath, U., Fukuzaki, E., Jaeger, K.-E. & Büchs, J. (2015b). A particular silent codon exchange in a recombinant gene greatly influences host cell metabolic activity. *Microbial Cell Factories* **14**, 156. BioMed Central.

Rasmussen, B. A. & Silhavy, T. J. (1987). The first 28 amino acids of mature LamB are required for rapid and efficient export from the cytoplasm. *Genes & Development* **1**, 185–196.

Rathi, P. C., Fulton, A., Jaeger, K.-E. & Gohlke, H. (2016). Application of rigidity theory to the thermostabilization of lipase A from *Bacillus subtilis*. *PLoS Computational Biology* **12**, e1004754 (S. Fleishman, Ed.).

Reetz, M. T., Kahakeaw, D. & Lohmer, R. (2008). Addressing the numbers problem in directed evolution. *Chembiochem: a European Journal of Chemical Biology* **9**, 1797–804.

Roblin, P., Lebrun, P., Rucktooa, P., Dewitte, F., Lens, Z., Receveur-Brechot, V., Raussens, V., Villeret, V. & Bompard, C. (2013). The structural organization of the N-terminus domain of SopB, a virulence factor of *Salmonella*, depends on the nature of its protein partners. *Biochimica et Biophysica Acta* **12**, 2564–2572. Elsevier B.V.

Rocha, E. P. C., Danchin, A. & Viari, A. (1999). Translation in *Bacillus subtilis* roles and trends of initiation and termination, insights from a genome analysis. *Nucleic Acids Research* **27**, 3567–3576.

Rosenau, F., Tommassen, J. & Jaeger, K.-E. (2004). Lipase-specific foldases. *Chembiochem: a European Journal of Chemical Biology* **5**, 152–61.

Röllen, K. (2012). Release of Bacillus subtilis lipase LipA upon heterologous expression in *Escherichia coli*. Masterarbeit, Heinrich-Heine-Universität Düsseldorf.

Rúa, M. L., Atomi, H., Schmidt-Dannert, C. & Schmid, R. D. (1998). High-level expression of the thermoalkalophilic lipase from Bacillus thermocatenulatus in

Escherichia coli. *Applied Microbiology and Biotechnology* **49**, 405–10.

Sambrook, J. & Russell, D. W. (2001). *Molecular cloning: a laboratory manual*, 3rd edn. Cold Spring Harbor: Cold Spring Harbor Laboratory Press.

Schallmey, M., Singh, A. & Ward, O. P. (2004). Developments in the use of *Bacillus* species for industrial production. *Canadian Journal of Microbiology* **17**, 1–17.

Schiebel, E., Driessen, A. J., Hartl, F. U. & Wickner, W. (1991). ΔμH+ and ATP function at different steps of the catalytic cycle of preprotein translocase. *Cell* **64**, 927–39.

Schmidt-Dannert, C., Sztajer, H., Stöcklein, W., Menge, U. & Schmid, R. D. (1994). Screening, purification and properties of a thermophilic lipase from *Bacillus thermocatenulatus*. *Biochimica et Biophysica Acta* **1214**, 43–53.

Schrag, J. D., Li, Y., Cygler, M., Lang, D., Burgdorf, T., Hecht, H. J., Schmid, R., Schomburg, D., Rydel, T. J. & other authors. **(1997).** The open conformation of a *Pseudomonas* lipase. *Structure* **5**, 187–202.

Shahbabian, K., Jamalli, A., Zig, L. & Putzer, H. (2009). RNase Y, a novel endoribonuclease, initiates riboswitch turnover in *Bacillus subtilis*. *The EMBO Journal* **28**, 3523–33.

Shank, E. A. & Kolter, R. (2011). Extracellular signaling and multicellularity in *Bacillus subtilis*. *Current Opinion in Microbiology* **14**, 741–7. Elsevier Ltd.

Sharp, P. M., Cowe, E., Higgins, D. G., Shields, D. C., Wolfe, K. H. & Wright, F. (1988). Codon usage patterns in *Escherichia coli*, *Bacillus subtilis*, *Saccharomyces cerevisiae*, *Schizosaccharomyces pombe*, *Drosophila melanogaster* and *Homo sapiens*; a review of the considerable within-species diversity. *Nucleic Acids Research* **16**, 8207–8211.

Sievers, F., Wilm, A., Dineen, D., Gibson, T. J., Karplus, K., Li, W., Lopez, R., McWilliam, H., Remmert, M. & other authors. **(2011).** Fast, scalable generation of high-quality protein multiple sequence alignments using Clustal Omega. *Molecular Systems Bology* **7**, 539.

Sinchaikul, S., Sookkheo, B., Phutrakul, S., Wu, Y. T., Pan, F. M. & Chen, S. T. (2001). Structural modeling and characterization of a thermostable lipase from *Bacillus stearothermophilus* P1. *Biochemical and Biophysical Research Communications* **283**, 868–75.

Skoczinski, P. (2012). Site-saturation mutagenesis of *Bacillus subtilis* lipase LipA to identify amino acids essential for secretion. Masterarbeit, Heinrich-Heine-Universität Düsseldorf.

Smensen, M. A., Kurland, C. G. & Pedersen, S. (1989). Codon usage determines translation rate in *Escherichia coli*. *Journal of Molecular Biology* **207**, 365–377.

Smith, H., Birnstiel, M. L., Ii, M. & Zurich, D. U. (1976). A simple method for DNA restriction site mapping. *Nucleic Acids Research* **3**, 2387–2398.

Song, Y., Nikoloff, J. M. & Zhang, D. (2015). Improving protein production on the level of regulation of both expression and secretion pathways in *Bacillus subtilis*. *Journal of Microbiology and Biotechnology* **25**, 963–77.

Spencer, P. S., Siller, E., Anderson, J. F. & Barral, J. M. (2012). Silent substitutions predictably alter translation elongation rates and protein folding efficiencies. *Journal of Molecular Biology* **422**, 328–35. Elsevier Ltd.

Steipe, B., Schiller, B., Plückthun, A. & Steinbacher, S. (1994). Sequence statistics reliably predict stabilizing mutations in a protein domain. *Journal of Molecular Biology* **240**, 188–192.

Tjalsma, H., Bolhuis, A., Jongbloed, J. D., Bron, S. & Van Dijl, J. M. (2000). Signal peptide-dependent protein transport in *Bacillus subtilis*: a genome-based survey of the secretome. *Microbiology and Molecular Biology Reviews* **64**, 515–47.

Tjalsma, H., Antelmann, H., Jongbloed, J. D. H., Braun, P. G., Darmon, E., Dorenbos, R., Dubois, J. F., Westers, H., Zanen, G. & other authors. **(2004).** Proteomics of protein secretion by *Bacillus subtilis*: separating the " secrets " of the secretome. *Microbiology and Molecular Biology Reviews* **68**, 207–233.

Ton-That, H., Marraffini, L. A. & Schneewind, O. (2004). Protein sorting to the cell wall envelope of Gram-positive bacteria. *Biochimica et Biophysica Acta* **1694**, 269–78.

Treichel, H., De Oliveira, D., Mazutti, M. A., Di Luccio, M. & Oliveira, J. V. (2009). A review on microbial lipases production. *Food and Bioprocess Technology* **3**, 182–196.

Untergasser, A., Cutcutache, I., Koressaar, T., Ye, J., Faircloth, B. C., Remm, M. & Rozen, S. G. (2012). Primer3--new capabilities and interfaces. *Nucleic Acids Research* **40**, e115.

Uptain, S. M., Kane, C. M. & Chamberlin, M. J. (1997). Basic mechanisms of transcript elongation and its regulation. *Annual Review of Biochemistry* **66**, 117–172.

Van Pouderoyen, G., Eggert, T., Jaeger, K.-E. & Dijkstra, B. W. (2001). The crystal structure of *Bacillus subtilis* lipase: a minimal α/β hydrolase fold enzyme. *Journal of Molecular Biology* **309**, 215–226.

Van Roosmalen, M. L., Geukens, N., Jongbloed, J. D. H., Tjalsma, H., Dubois, J.-Y. F., Bron, S., Van Dijl, J. M. & Anné, J. (2004). Type I signal peptidases of Gram-positive bacteria. *Biochimica et Biophysica Acta* **1694**, 279–97.

Varenne, S., Baty, D., Verheij, H., Shire, D. & Lazdunski, C. (1989). The maximum rate of gene expression is dependent on the downstream context of unfavourable codons. *Biochimie* **71**, 1221–1229.

Verger, R. (1997). "Interfacial activation"of lipases: facts and artifacts. *Trends in Biotechnology* **15**, 32–38.

Vogelstein, B. & Gillespie, D. (1979). Preparative and analytical purification of DNA from agarose. *Proceedings of the National Academy of Sciences of the United States of America* **76**, 615–9.

Wang, P. Z. & Roy, H. . (1984). Overlapping promoters transcribed by *Bacillus subtilis* σ 55 and σ 37 RNA polymerase holoenzymes during growth and stationary phases. *Journal of Biological Chemistry* **259**, 8619–8625.

Van Wely, K. H., Swaving, J., Freudl, R. & Driessen, A. J. (2001). Translocation of proteins across the cell envelope of Gram-positive bacteria. *FEMS Microbiology Reviews* **25**, 437–54.

Wenzel, M., Müller, A., Siemann-Herzberg, M. & Altenbuchner, J. (2011). Self-inducible *Bacillus subtilis* expression system for reliable and inexpensive protein production by high-cell-density fermentation. *Applied and Environmental Microbiology* **77**, 6419–25.

Westers, H., Darmon, E., Zanen, G., Veening, J.-W., Kuipers, O. P., Bron, S., Quax, W. J. & Van Dijl, J. M. (2004a). The *Bacillus* secretion stress response is an indicator for alpha-amylase production levels.

Letters in Applied Microbiology **39**, 65–73.

Westers, L., Westers, H. & Quax, W. J. (2004b). *Bacillus subtilis* as cell factory for pharmaceutical proteins: a biotechnological approach to optimize the host organism. *Biochimica et Biophysica Acta* **1694**, 299–310.

Wi, A. R., Jeon, S.-J., Kim, S., Park, H. J., Kim, D., Han, S. J., Yim, J. H. & Kim, H.-W. (2014). Characterization and a point mutational approach of a psychrophilic lipase from an arctic bacterium, *Bacillus pumilus*. *Biotechnology Letters* **36**, 1295–302.

Widner, B., Thomas, M., Sternberg, D., Lammon, D., Behr, R. & Sloma, A. (2000). Development of marker-free strains of *Bacillus subtilis* capable of secreting high levels of industrial enzymes. *Journal of Industrial Mcrobiology &i Biotechnology* **25**, 204–212.

Wilson, C. & Agard, D. (1991). Engineering substrate specificity. *Current Opinion in Structural Biology* **1**, 617–623.

Winkler, F., D'Arcy, A. & Hunziker, W. (1990). Structure of human pancreatic lipase. *Nature* **343**, 771–774.

Winkler, U. K. & Stuckmann, M. (1979). Glycogen, hyaluronate, and some other polysaccharides greatly enhance the formation of exolipase by *Serratia marcescens*. *Journal of Bacteriology* **138**, 663–70.

Van der Wolk, J. P., De Wit, J. G. & Driessen, A. J. (1997). The catalytic cycle of the *Escherichia coli* SecA ATPase comprises two distinct preprotein translocation events. *The EMBO Journal* **16**, 7297–304.

Woodcock, D., Crowther, P., Doherty, J., Jefferson, S., DeCruz, E., Noyer-Weidner, M., Smith, S., Michael, M. & Graham, M. (1989). Quantitative evaluation of *Escherichia coli* host strains for tolerance to cytosine methylation in plasmid and phage recombinants. *Nucleic Acids Research* **17**, 3469–3478.

Yamane, K., Bunai, K. & Kakeshita, H. (2004). Protein traffic for secretion and related machinery of *Bacillus subtilis* . *Bioscience, Biotechnology, and Biochemistry* **68**, 2007–23.

Zanen, G., Antelmann, H., Meima, R., Jongbloed, J. D. H., Kolkman, M., Hecker, M., Van Dijl, J. M. & Quax, W. J. (2006). Proteomic dissection of potential signal recognition particle dependence in protein secretion by *Bacillus subtilis*. *Proteomics* **6**, 3636–48.

Öztürk, S., Calik, P. & Özdamar, T. H. (2015). Fed Batch biomolecule production by *Bacillus subtilis* a state of the art review. *Trends in Biotechnology* **34**, 329–345.

8. Appendix

Tab. 8.1 Oligonucleotide sequences for generation of *lipA* site saturation mutagenesis library

The forward and reverse oligonucleotide sequence is shown for each mutated codon positions. Codon positions highlighted in light grey code for amino acids with a conservation ≥ 95 % (among the *Firmicutes*) and were not considered for mutagenesis.

position	forward primer	reverse primer
1	GACTGGATTGTGTTCSNNGGCTTTTGCTGACGG	CCGTCAGCAAAAGCCNNSGAACACAATCCAGTC
2	AACGACTGGATTGTGSNNAGCGGCTTTTGCTGA	TCAGCAAAAGCCGCTNNSCACAATCCAGTCGTT
3	CATAACGACTGGATTSNNTTCAGCGGCTTTTGC	GCAAAAGCCGCTGAANNSAATCCAGTCGTTATG
4	AACCATAACGACTGGSNNGTGTTCAGCGGCTTT	AAAGCCGCTGAACACNNSCCAGTCGTTATGGTT
5	-	-
6	-	-
7	AATACCGTGAACCATSNNGACTGGATTGTGTTC	GAACACAATCCAGTCNNSATGGTTCACGGTATT
8	TCCAATACCGTGAACSNNAACGACTGGATTGTG	CACAATCCAGTCGTTNNSGTTCACGGTATTGGA
9	-	-
10	-	-
11	-	-
12	GAATGATGCCCCTCCSNNACCGTGAACCATAAC	GTTATGGTTCACGGTNNSGGAGGGGCATCATTC
13	ATTGAATGATGCCCCSNNAATACCGTGAACCATAAC	GTTATGGTTCACGGTATTNNSGGGGCATCATTCAAT
14	AAAATTGAATGATGCSNNTCCAATACCGTGAAC	GTTCACGGTATTGGANNSGCATCATTCAATTTT
15	CGCAAAATTGAATGASNNCCCTCCAATACCGTG	CACGGTATTGGAGGGNNSTCATTCAATTTTGCG
16	TCCCGCAAAATTGAASNNTGCCCCTCCAATACC	GGTATTGGAGGGGCANNSTTCAATTTTGCGGGA
17	AATTCCCGCAAAATTSNNTGATGCCCCTCCAATAC	GTATTGGAGGGGCATCANNSAATTTTGCGGGAATT
18	CTTAATTCCCGCAAASNNGAATGATGCCCCTCC	GGAGGGGCATCATTCNNSTTTGCGGGAATTAAG
19	GCTCTTAATTCCCGCSNNATTGAATGATGCCCC	GGGGCATCATTCAATNNSGCGGGAATTAAGAGC
20	GCTCTTAATTCCSNNAAAATTGAATGATGC	GCATCATTCAATTTTNNSGGAATTAAGAGC
21	ATAGCTCTTAATSNNCGCAAAATTGAATGATGC	GCATCATTCAATTTTGCGNNSATTAAGAGCTAT
22	-	-
23	AGATACGAGATAGCTSNNAATTCCCGCAAAATTG	CAATTTTGCGGGAATTNNSAGCTATCTCGTATCT
24	CTGAGATACGAGATASNNCTTAATTCCCGC	GCGGGAATTAAGNNSTATCTCGTATCTCAG
25	GCCCTGAGATACGAGSNNGCTCTTAATTCCCGC	GCGGGAATTAAGAGCNNSCTCGTATCTCAGGGC
26	CCAGCCCTGAGATACSNNATAGCTCTTAATTCC	GGAATTAAGAGCTATNNSGTATCTCAGGGCTGG
27	CGACCAGCCCTGAGASNNGAGATAGCTCTTAATTC	GAATTAAGAGCTATCTCNNSTCTCAGGGCTGGTCG
28	CCGCGACCAGCCCTGSNNTACGAGATAGCTC	GAGCTATCTCGTANNSCAGGGCTGGTCGCGG
29	GTCCCGCGACCAGCCSNNAGATACGAGATAGCT	AGCTATCTCGTATCTNNSGGCTGGTCGCGGGAC
30	CTTGTCCCTCGACCASNNCTGAGATACGAGATAG	CTATCTCGTATCTCAGNNSTGGTCGAGGGACAAG
31	CAGCTTGTCCCGCGASNNGCCCTGAGATACGAG	CTCGTATCTCAGGGCNNSTCGCGGGACAAGCTG
32	ATACAGCTTGTCCCGSNNCCAGCCCTGAGATAC	GTATCTCAGGGCTGGNNSCGGGACAAGCTGTAT
33	TGCATACAGCTTGTCSNNCGACCAGCCCTGAG	CTCAGGGCTGGTCGNNSGACAAGCTGTATGCA
34	AACTGCATACAGCTTSNNCCGCGACCAGCCCTG	CAGGGCTGGTCGCGGNNSAAGCTGTATGCAGTT
35	ATCAACTGCATACAGSNNGTCCCGCGACCAGCC	GGCTGGTCGCGGGACNNSCTGTATGCAGTTGAT
36	AAAATCAACTGCATASNNCTTGTCCCGCGACCAG	CTGGTCGCGGGACAAGNNSTATGCAGTTGATTTT
37	CCAAAAATCAACTGCSNNCAGCTTGTCCCGCGAC	GTCGCGGGACAAGCTGNNSGCAGTTGATTTTTGG
38	-	-
39	CTTGTCCCAAAAATCSNNTGCATACAGCTTGTC	GACAAGCTGTATGCANNSGATTTTTGGGACAAG
40	TGTCTTGTCCCAAAASNNAACTGCATACAGCTT	AAGCTGTATGCAGTTNNSTTTTGGGACAAGACA
41	GCCTGTCTTGTCCCSNNATCAACTGCATACAG	CTGTATGCAGTTGATNNSGGGACAAGACAGGC
42	TGTGCCTGTCTTGTCSNNAAAATCAACTGCATA	TATGCAGTTGATTTTNNSGACAAGACAGGCACA
43	ATTTGTGCCTGTCTTSNNCCAAAAATCAACTGC	GCAGTTGATTTTTGGNNSAAGACAGGCACAAAT
44	ATAATTTGTGCCTGTSNNGTCCCAAAAATCAAC	GTTGATTTTTGGGACNNSACAGGCACAAATTAT
45	GTTATAATTTGTGCCSNNCTTGTCCCAAAAATC	GATTTTTGGGACAAGNNSGGCACAAATTATAAC

position	forward primer	reverse primer
46	-	-
47	TCCATTGTTATAATTSNNGCCTGTCTTGTCCCAAAAATC	GATTTTTGGGACAAGACAGGCNNSAATTATAACAATGGA
48	CGGTCCATTGTTATASNNTGTGCCTGTCTTGTC	GACAAGACAGGCACANNSTATAACAATGGACCG
49	TACCGGTCCATTGTTSNNATTTTGTGCCTGTCTT	AAGACAGGCACAAAATNNSAACAATGGACCGGTA
50	TAATACCGGTCCATTSNNATAATTTGTGCCTGT	ACAGGCACAAATTATNNSAATGGACCGGTATTA
51	TGATAATACCGGTCCSNNGTTATAATTTGTGCC	GGCACAAATTATAACNNSGGACCGGTATTATCA
52	TCGTGATAATACCGGSNNATTGTTATAATTTGTG	CACAAATTATAACAATNNSCCGGTATTATCACGA
53	AAATCGTGATAATACSNNTCCATTGTTATAATT	AATTATAACAATGGANNSGTATTATCACGATTT
54	CACAAATCGTGATAASNNCGGTCCATTGTTATA	TATAACAATGGACCGNNSTTATCACGATTTGTG
55	TTGCACAAATCGTGASNNTACCGGTCCATTG	CAATGGACCGGTANNSTCACGATTTGTGCAA
56	CTTTTGCACAAATCGSNNTAATACCGGTCCATTG	CAATGGACCGGTATTANNSCGATTTGTGCAAAAG
57	AACCTTTTGCACAAASNNTGATAATACCGGTCC	GGACCGGTATTATCANNSTTTGTGCAAAAGGTT
58	TAAAACCTTTTGCACSNNTCGTGATAATACCGG	CCGGTATTATCACGANNSGTGCAAAAGGTTTTA
59	ATCTAAAACCTTTTGSNNAAATCGTGATAATAC	GTATTATCACGATTTNNSCAAAAGGTTTTAGAT
60	TTCATCTAAAACCTTSNNCACAAATCGATAA	TTATCGATTTGTGNNSAAGGTTTTAGATGAA
61	CGTTCCATCTAAAACSNNTTGCACAAATCGTG	CACGATTTGTGCAANNSGTTTTAGATGGAACG
62	-	-
63	CGCACCCGTTTCATCSNNAACCTTTTGCACAAATC	GATTTGTGCAAAAGGTTNNSGATGAAACGGGTGCG
64	TTTCGCACCCGTTTCSNNTAAAACCTTTTGCAC	GTGCAAAAGGTTTTANNSGAAACGGGTGCGAAA
65	TTTTTTCGCACCCGTSNNATCTAAAACCTTTTG	CAAAAGGTTTTAGATNNSACGGGTGCGAAAAAA
66	-	-
67	-	-
68	AATATCCACTTTTTTSNNACCCGTTTCATCTAAAAC	GTTTTAGATGAAACGGGTNNSAAAAAAGTGGATATT
69	GACAATATCCACTTTSNNCGCACCCGTTTCATC	GATGAAACGGGTGCGNNSAAAGTGGATATTGTC
70	-	-
71	-	-
72	GCTGTGAGCGACAATSNNCACTTTTTTCGCACC	GGTGCGAAAAAAGTGNNSATTGTCGCTCACAGC
73	-	-
74	CCCCATGCTGTGAGCSNNAATATCCACTTTTTTC	GAAAAAAGTGGATATTNNSGCTCACAGCATGGGG
75	-	-
76	-	-
77	-	-
78	TGTGTTCGCGCCCCCSNNGCTGTGAGCGACAATATC	GATATTGTCGCTCACAGCNNSGGGGGCGCGAACACA
79	-	-
80	GTAAAGTGTGTTCGCSNNCCCCATGCTGTGAGC	GCTCACAGCATGGGGNNSGCGAACACACTTTAC
81	GTAGTAAAGTGTGTTSNNGCCCCCCATGCTGTG	CACAGCATGGGGGGCNNSAACACACTTTACTAC
82	TATGTAGTAAAGTGTSNNCGCGCCCCCCATGCTG	CAGCATGGGGGGCGCGNNSACACTTTACTACATA
83	TTTTATGTAGTAAAGSNNGTTCGCGCCCCCCATG	CATGGGGGGCGCGAACNNSCTTTACTACATAAAA
84	ATTTTTTATGTAGTASNNTATGTTCGCGCCCCC	GGGGGCGCGAACATANNSTACTACATAAAAAAT
85	CAGATTTTTTATGTASNNAAGTGTGTTCGCGCC	GGCGCGAACACACTTNNSTACATAAAAAATCTG
86	-	-
87	GCCGTCCAGATTTTTSNNGTAGTAAAGTGTGTTC	GAACACACTTTACTACNNSAAAAATCTGGACGGC
88	TCCGCCGTCCAGATTSNNTATGTAGTAAAGTGTG	CACACTTTACTACATANNSAATCTGGACGGCGGA
89	ATTTCCGCCGTCCAGSNNTTTTATGTAGTAAAG	CTTTACTACATAAAANNSCTGGACGGCGGAAAT
90	TTTATTTCCGCCGTCSNNATTTTTTATGTAGTAAAG	CTTTACTACATAAAAAATNNSGACGGCGGAAATAAA
91	AACTTTATTTCCGCCSNNCAGATTTTTTATGTAG	CTACATAAAAAATCTGNNSGGCGGAAATAAAGTT
92	TGCAACTTTATTTCCSNNGTCCAGATTTTTTATG	CATAAAAAATCTGGACNNSGGAAATAAAGTTGCA
93	GTTTGCAACTTTATTSNNGCCGTCCAGATTTTTTATG	CATAAAAAATCTGGACGGCNNSAATAAAGTTGCAAAC
94	GACGTTTGCAACTTTSNNTCCGCCGTCCAGATTTTTTATG	CATAAAAAATCTGGACGGCGGANNSAAAGTTGCAAACGTC
95	CACGACGTTTGCAACSNNATTTCCGCCGTCCAG	CTGGACGGCGGAAATNNSGTTGCAAACGTCGTG

position	forward primer	reverse primer
96	CGTCACGACGTTTGCSNNTTTATTTCCGCCGTC	GACGGCGGAAATAAANNSGCAAACGTCGTGACG
97	AAGCGTCACGACGTTSNNAACTTTATTCCTGCC	GGCAGGAATAAAGTTNNSAACGTCGTGACGCTT
98	GCCAAGCGTCACGACSNNTGCAACTTTATTTCC	GGAAATAAAGTTGCANNSGTCGTGACGCTTGGC
99	GCCGCCAAGCGTCACSNNGTTTGCAACTTTATTTC	GAAATAAAGTTGCAAACNNSGTGACGCTTGGCGGC
100	CGCGCCGCCAAGCGTSNNGACGTTTGCAAC	GTTGCAAACGTCNNSACGCTTGGCGGCGCG
101	GTTCGCGCCGCCAAGSNNCACGACGTTTGCAAC	GTTGCAAACGTCGTGNNSCTTGGCGGCGCGAAC
102	ACGGTTCGCGCCGCCSNNCGTCACGACGTTTGC	GCAAACGTCGTGACGNNSGGCGGCGCGAACCGT
103	-	-
104	CGTTAAACGGTTCGCSNNGCCAAGCGTCACGAC	GTCGTGACGCTTGGCNNSGCGAACCGTTTAACG
105	TGTCGTTAAACGGTTSNNGCCGCCAAGCGTCAC	GTGACGCTTGGCGGCNNSAACCGTTTAACGACA
106	-	-
107	CTTGCCTGTCGTCAASNNGTTCGCGCCGCCAGG	CCTGGCGGCGCGAACNNSTTGACGACAGGCAAG
108	CGCCTTGCCTGTCGTSNNACGGTTCGCGCCGCC	GGCGGCGCGAACCGTNNSACGACAGGCAAGGCG
109	AAGCGCCTTGCCTGTSNNCAAACGGTTCGCGCC	GGCGCGAACCGTTTGNNSACAGGCAAGGCGCTT
110	CCGAAGCGCCTTGCCSNNCGTCAAACGGTTCGC	GCGAACCGTTTGACGNNSGGCAAGGCGCTTCGG
111	CCCGGAAGCGCCTTSNNTGTCGTCAAACGGTTC	GAACCGTTTGACGACANNSAAGGCGCTTCCGGG
112	TGTTCCCCGAAGCGCSNNGCCTGTCGTCAAACG	CGTTTGACGACAGGCNNSGCGCTTCGGGGAACA
113	ATCTGTTCCCGGAAGSNNCTTGCCTGTCGTTAAAC	GTTTAACGACAGGCAAGNNSCTTCCGGGAACAGAT
114	TGGATCTGTTCCCGGSNNCGCCTTGCCTGTCG	CGACAGGCAAGGCGNNSCCGGGAACAGATCCA
115	ATTTGGATCTGTTCCSNNAAGCGCCTTGCCTGTC	GACAGGCAAGGCGCTTNNSGGAACAGATCCAAAT
116	TTGATTTGGATCTGTSNNCGGAAGCGCCTTGCC	GGCAAGGCGCTTCCGNNSACAGATCCAAATCAA
117	CTTTTGATTTGGATCSNNTCCCGGAAGCGCCTTG	CAAGGCGCTTCCGGGANNSGATCCAAATCAAAAG
118	AATCTTTTGATTTGGSNNTGTTCCCGGAAGCGC	GCGCTTCCGGGAACANNSCCAAATCAAAAGATT
119	TAAAATCTTTTGATTSNNATCTGTTCCCGGAAG	CTTCCGGGAACAGATNNSAATCAAAAGATTTTA
120	GTATAAAATCTTTTGSNNTGGATCTGTTCCCGG	CCGGGAACAGATCCANNSCAAAAGATTTTATAC
121	TGTGTATAAAATCTTSNNATTTGGATCTGTTCC	GGAACAGATCCAAATNNSAAGATTTTATACACA
122	GGATGTGTATAAAATSNNTTGATTTGGATCTG	CAGATCCAAATCAANNSATTTTATACACATCC
123	AATGGATGTGTATAASNNCTTTTGATTTGGATC	GATCCAAATCAAAAGNNSTTATACACATCCATT
124	GTAAATGGATGTGTASNNATTCTTTTGATTTGG	CCAAATCAAAAGAATNNSTACACATCCATTTAC
125	GCTGTAAATGGATGTSNNTAAAATCTTTTGATTTG	CAAATCAAAAGATTTTANNSACATCCATTTACAGC
126	ACTGCTGTAAATGGASNNGTATAAAATCTTTTG	CAAAAGATTTTATACNNSTCCATTTACAGCAGT
127	GGCACTGCTGTAAATSNNTGTGTATAAAATCTT	AAGATTTTATACACANNSATTTACAGCAGTGCC
128	ATCGGCACTGCTGTASNNGGATGTGTATAAAATC	GATTTTATACACATCCNNSTACAGCAGTGCCGAT
129	-	-
130	AATCATATCGGCACTSNNGTAAATGGATGTG	CACATCCATTTACNNSAGTGCCGATATGATT
131	GACAATCATATCGGCSNNGCTGTAAATGGATG	CATCCATTTACAGCNNSGCCGATATGATTGTC
132	CATGACAATCATATCSNNACTGCTGTAAATGG	CCATTTACAGCAGTNNSGATATGATTGTCATG
133	ATTCATGACAATCATSNNGGCACTGCTGTAAATG	CATTTACAGCAGTGCCNNSATGATTGTCATGAAT
134	GTAATTCATGACAATSNNATCGGCACTGCTGTAAATG	CATTTACAGCAGTGCCGATNNSATTGTCATGAATTAC
135	TAAGTAATTCATGACSNNCATATCGGCACTGCTG	CAGCAGTGCCGATATGNNSGTCATGAATTACTTA
136	TGATAAGTAATTCATSNNAATCATATCGGCACTG	CAGTGCCGATATGATTNNSATGAATTACTTATCA
137	TCTTGATAAGTAATTSNNGACAATCATATCGGC	GCCGATATGATTGTCNNSAATTACTTATCAAGA
138	TAATCTTGATAAGTASNNCATGACAATCATATC	GATATGATTGTCATGNNSTACTTATCAAGATTA
139	ATCTAATCTTGATAASNNATTCATGACAATCATATCGGC	GCCGATATGATTGTCATGAATNNSTTATCAAGATTAGAT
140	ACCATCTAATCTTGASNNGTAATTCATGACAATC	GATTGTCATGAATTACNNSTCAAGATTAGATGGT
141	-	-
142	TCTAGCACCATCTAASNNTGATAAGTAATTCATG	CATGAATTACTTATCANNSTTAGATGGTGCTAGA
143	GTTTCTAGCACCATCSNNTCTTGATAAGTAATTC	GAATTACTTATCAAGANNSGATGGTGCTAGAAAC
144	AACGTTTCTAGCACCSNNTAATCTTGATAAGTAATT	AATTACTTATCAAGATTANNSGGTGCTAGAAACGTT
145	-	-

position	forward primer	reverse primer
146	GATTTGAACGTTTCTSNNACCATCTAATCTTG	CAAGATTAGATGGTNNSAGAAACGTTCAAATC
147	ATGGATTTGAACGTTSNNAGCACCATCTAATCTTG	CAAGATTAGATGGTGCTNNSAACGTTCAAATCCAT
148	GCCATGGATTTGAACSNNTCTAGCACCATCTAATC	GATTAGATGGTGCTAGANNSGTTCAAATCCATGGC
149	AACGCCATCGATTTGSNNGTTTCTAGCACCATC	GATGGTGCTAGAAACNNSCAAATCGATGGCGTT
150	TCCAACGCCATGGATSNNAACGTTTCTAGCACC	GGTGCTAGAAACGTTNNSATCCATGGCGTTGGA
151	GTGTCCAACGCCATGSNNTTGAACGTTTCTAGC	GCTAGAAACGTTCAANNSCATGGCGTTGGACAC
152	GATGTGTCCAACGCCSNNGATTTGAACGTTTCTAG	CTAGAAACGTTCAAATCNNSGGCGTTGGACACATC
153	-	-
154	AAGGCCGATGTGTCCSNNGCCATGGATTTGAAC	GTTCAAATCCATGGCNNSGGACACATCGGCCTT
155	CAGAAGGCCGATGTGSNNAACGCCATGGATTTG	CAAATCCATGGCGTTNNSCACATCGGCCTTCTG
156	GTACAGAAGGCCGATSNNTCCAACGCCATGGATTTG	CAAATCCATGGCGTTGGANNSATCGGCCTTCTGTAC
157	GCTGTACAGAAGGCCSNNGTGTCCAACGCCATG	CATGGCGTTGGACACNNSGGCCTTCTGTACAGC
158	GCTGCTGTACAGAAGSNNGATGTGTCCAACGCC	GGCGTTGGACACATCNNSCTTCTGTACAGCAGC
159	TTGGCTGCTGTACAGSNNGCCGATGTGTCCAAC	GTTGGACACATCGGCNNSCTGTACAGCAGCCAA
160	GACTTGGCTGCTGTASNNAAGGCCGATGTGTCC	GGACACATCGGCCTTNNSTACAGCAGCCAAGTC
161	GTTGACTTGGCTGCTSNNCAGAAGGCCGATGTG	CACATCGGCCTTCTGNNSAGCAGCCAAGTCAAC
162	GCTGTTGACTTGGCTSNNGTACAGAAGGCCGATG	CATCGGCCTTCTGTACNNSAGCCAAGTCAACAGC
163	CAGGCTGTTGACTTGSNNGCTGTACAGAAGGCC	GGCCTTCTGTACAGCNNSCAAGTCAACAGCCTG
164	AATCAGGCTGTTGACSNNGCTGCTGTACAGAAG	CTTCTGTACAGCAGCNNSGTCAACAGCCTGATT
165	-	-
166	TTCTTTAATCAGGCTSNNGACTTGGCTGCTGTAC	GTACAGCAGCCAAGTCNNSAGCCTGATTAAAGAA
167	CCCTCCTTTAATCAGSNNGTTGACTTGGCTGCTG	CAGCAGCCAAGTCAACNNSCTGATTAAAGGAGGG
168	CAGCCCTTCTTTAATSNNGCTGTTGACTTGGCTGCTG	CAGCAGCCAAGTCAACAGCNNSATTAAAGAAGGGCTG
169	GTTCAGCCCTTCTTTSNNCAGGCTGTTGACTTG	CAAGTCAACAGCCTGNNSAAAGAAGGGCTGAAC
170	GCCGTTCAGCCCTTCSNNAATCAGGCTGTTGAC	GTCAACAGCCTGATTNNSGAAGGGCTGAACGGC
171	CCCGCCGTTCAGCCCSNNTTTAATCAGGCTGTT	AACAGCCTGATTAAANNSGGGCTGAACGGCGGG
172	GCCCCCGCCGTTCAGSNNTTCTTTAATCAGGCT	AGCCTGATTAAAGAANNSCTGAACGGCGGGGGC
173	CTGGCCCCCGCCGTTSNNCCCTTCTTTAATCAG	CTGATTAAAGAAGGGNNSAACGGCGGGGGCCAG
174	TTCTGGCCCCCGCCSNNCAGCCCTTCTTTAATC	GATTAAAGAAGGGCTGNNSGGCGGGGGCCAGAA
175	CGTATTCTGGCCCCCSNNGTTCAGCCCTTCTTT	AAAGAAGGGCTGAACNNSGGGGGCCAGAATACG
176	ATTCGTATTCTGGCCSNNGCCGTTCAGCCCTTC	GAAGGGCTGAACGGCNNSGGCCAGAATACGAAT
177	TTAATTCGTATTCTGSNNCCCGCCGTTCAGCCC	GGGCTGAACGGCGGGNNSCAGAATACGAATTAA
178	GCTTGTCGACGGAGCTCTCATTAATTCGTATTSNNGCC	GGCNNSAATACGAATTAATGAGAGCTCCGTCGACAAGC
179	GCTTGTCGACGGAGCTCTCATTAATTCGTSNNCTC	GAGNNSACGAATTAATGAGAGCTCCGTCGACAAGC
180	GCTTGTCGACGGAGCTCTCATTAATTSNNATT	AATNNSAATTAATGAGAGCTCCGTCGACAAGC
181	GCTTGTCGACGGAGCTCTCATTASNNCGT	ACGNNSTAATGAGAGCTCCGTCGACAAGC

Tab. 8.2 LipA amino acid sequence conservation

64 lipase sequences out of 41 species from the *Firmicutes* phylum were aligned. The number of identical amino acids in this alignment like in *B. subtilis* LipA was counted and calculated in percentage frequency for each position to determine the conservation of this amino acid within the *Firmicutes* phylum. The amino acid position (pos.), the amino acid (aa) and the percentaged conservation (%), as well as the structural motif (struc.) are shown.

pos.	aa	%	struc.	pos.	aa	%	struc.	pos.	aa	%	struc.	pos.	aa	%	struc.
1	A	55	c	52	G	66	αB	103	G	97	c	154	V	69	c
2	E	43	c	53	P	85	αB	104	G	91	c	155	G	78	c
3	H	83	c	54	V	20	αB	105	A	91	c	156	H	92	t
4	N	83	c	55	L	92	αB	106	N	98	αD	157	I	85	t
5	P	97	β3	56	S	65	αB	107	R	29	αD	158	G	91	3_{10}
6	V	95	β3	57	R	48	αB	108	L	91	αD	159	L	91	3_{10}
7	V	89	β3	58	F	52	αB	109	T	23	t	160	L	92	3_{10}
8	M	65	β3	59	V	80	αB	110	T	49	c	161	Y	11	3_{10}
9	V	98	β3	60	Q	28	αB	111	G	15	c	162	S	49	c
10	H	97	c	61	K	38	αB	112	K	23	c	163	S	94	αF
11	G	100	c	62	V	98	αB	113	A	89	c	164	Q	80	αF
12	I	74	t	63	L	92	αB	114	L	78	c	165	V	97	αF
13	G	72	t	64	D	35	αB	115	P	77	c	166	N	62	αF
14	G	91	c	65	E	52	αB	116	G	86	c	167	S	22	αF
15	A	86	c	66	T	97	αB	117	T	78	c	168	L	43	αF
16	S	77	3_{10}	67	G	98	c	118	D	78	c	169	I	80	αF
17	F	28	3_{10}	68	A	94	c	119	P	75	t	170	K	85	αF
18	N	92	3_{10}	69	K	72	c	120	N	80	t	171	E	78	αF
19	F	94	αA	70	K	97	c	121	Q	78	c	172	G	85	αF
20	A	62	αA	71	V	100	β5	122	K	85	c	173	L	92	αF
21	G	38	αA	72	D	92	β5	123	I	85	c	174	N	75	t
22	I	97	αA	73	I	100	β5	124	L	78	β7	175	G	75	t
23	K	89	αA	74	V	92	β5	125	Y	92	β7	176	G	83	t
24	S	45	αA	75	A	95	β5	126	T	92	β7	177	G	86	c
25	Y	89	αA	76	H	98	β5	127	S	91	β7	178	Q	55	c
26	L	94	αA	77	S	98	t	128	I	63	β7	179	N	78	c
27	V	48	αA	78	M	91	αC	129	Y	97	β7	180	T	71	c
28	S	65	αA	79	G	98	αC	130	S	91	β7	181	N	71	c
29	Q	88	t	80	G	94	αC	131	S	60	t				
30	G	92	t	81	A	91	αC	132	A	57	t				
31	W	89	c	82	N	91	αC	133	D	92	c				
32	S	32	c	83	T	86	αC	134	M	22	c				
33	R	52	3_{10}	84	L	91	αC	135	I	91	c				
34	D	22	3_{10}	85	Y	89	αC	136	V	91	c				
35	K	43	3_{10}	86	Y	97	αC	137	M	26	c				
36	L	78	β4	87	I	89	αC	138	N	91	αE				
37	Y	77	β4	88	K	85	αC	139	Y	26	αE				
38	A	97	β4	89	N	75	t	140	L	91	αE				
39	V	26	c	90	L	89	c	141	S	98	αE				
40	D	83	c	91	D	69	c	142	R	77	c				
41	F	92	c	92	G	91	3_{10}	143	L	89	c				
42	W	20	c	93	G	86	3_{10}	144	D	28	t				
43	D	85	c	94	N	38	3_{10}	145	G	97	t				
44	K	88	t	95	K	89	t	146	A	83	c				
45	T	85	t	96	V	34	β6	147	R	58	β8				
46	G	98	c	97	A	25	β6	148	N	89	β8				
47	T	20	c	98	N	78	β6	149	V	65	β8				
48	N	92	αB	99	V	86	β6	150	Q	60	β8				
49	Y	28	αB	100	V	83	β6	151	I	69	β8				
50	N	74	αB	101	T	89	β6	152	H	58	c				
51	N	91	αB	102	L	80	β6	153	G	97	c				

Tab. 8.3 LipA amino acid positions with the highest number of identified inactive LipA clones.
The table shows the amino acid position, the structural motif and its orientation (b: buried; s: surface), as well as the amino acid conservation in % at the respective position, the conservation of the neighbor residue (red < 95 %; green ≥ 95 %) and the orientation towards the active center (active cleft).

position	structural motif	orientation	conservation %	neighbour residue conservation	active cleft orientation
26	αA	b	94		no
35	αA	s	43		no
41	coil	s	92		no
49	αB	s	28		no
101	β6	b	89		no
102	β6	b	80		no
104	coil	b	91		no
156	turn	s	92		yes
160	αF	b	92		yes
181	coil	s	71		no

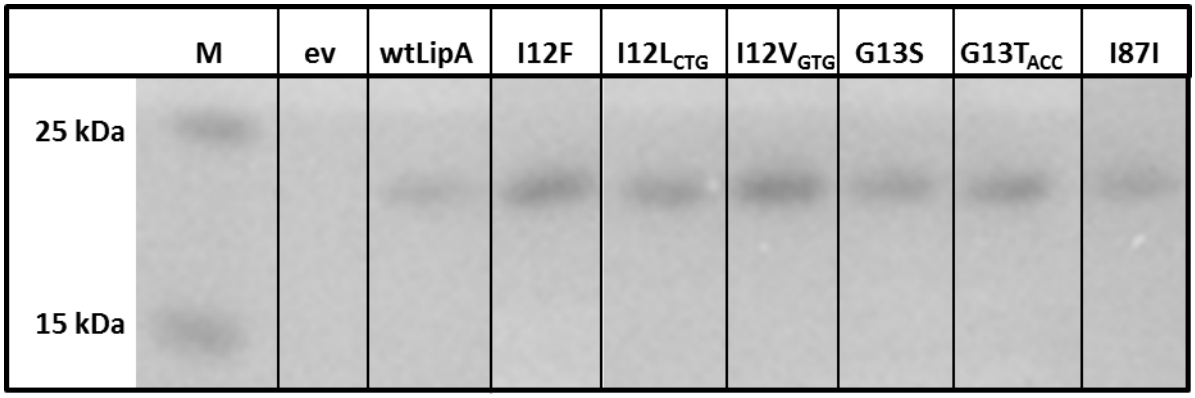

Fig. 8.1 Immunodetection of six LipA variants with increased extracellular lipase activity.
B. subtilis TEB1030 producing each of the six more active LipA variants was cultivated as three biological replicates in a 48-well Flowerplate® for 6 h. The proteins in the culture supernatant were precipitated via TCA-NaDoc precipitation, resuspended to an $O.D._{580\ nm}$ = 1.25 and applied on a NuPAGE® Novex® 4-12 % Bis-Tris Protein Gel. LipA was detected with a specific polyclonal LipA antibody. ev: empty vector; wtLipA: wild-type LipA.

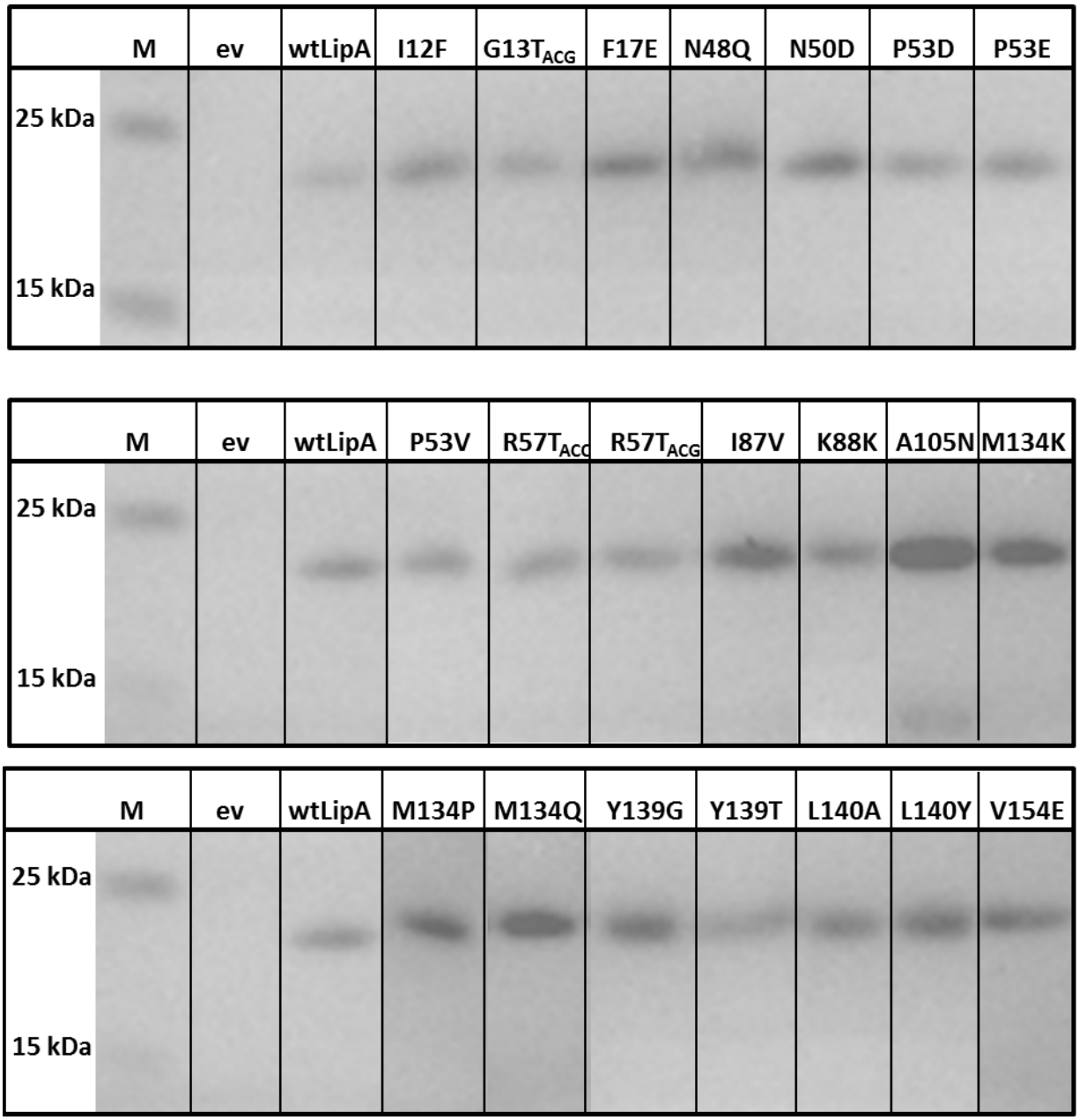

Fig. 8.2 Immunodetection of 21 LipA variants with higher extracellular lipase amount.
B. subtilis TEB1030 producing each of the 21 LipA variants with higher extracellular lipase amount was cultivated as three biological replicates in a 48-well Flowerplate® for 6 h. The proteins in the culture supernatant were precipitated via TCA-NaDoc precipitation, resuspended to an $O.D._{580\ nm}$ = 1.25 and applied on a NuPAGE® Novex® 4-12 % Bis-Tris Protein Gel. LipA was detected with a specific polyclonal LipA antibody. ev: empty vector; wtLipA: wild-type LipA.